EXHAUST SYSTEM INTERACTION PROGRAM

John E. Postlewaite, et al

Boeing Aerospace Company

Prepared for:

Air Force Aero Propulsion Laboratory

June 1973

UNCLASSIFIED
Security Classification

AD-769086

DOCUMENT CONTROL DATA - R&D

(Security classification of title, body of abstract and indexing annotation must be entered when the overall report is classified).

1. ORIGINATING ACTIVITY (Corporate author)
The Boeing Company

2a. REPORT SECURITY CLASSIFICATION
UNCLASSIFIED

2b. GROUP

3. REPORT TITLE
Exhaust System Interaction Program

4. DESCRIPTIVE NOTES (Types of report and inclusive dates)
Technical Report Final

5. AUTHORS (First name, middle initial, last name)
John E. Postlewaite, Victor Salemann

6. REPORT DATE
June 1973

7a. TOTAL NO. OF PAGES
~~161~~ 178

7b. NO. OF REFS

8a. CONTRACT OR GRANT NO.
F33615-70-C-1450

b. Project No. 3066

c.

d.

9a. ORIGINATOR'S REPORT NUMBERS
AFAPL-TR-73-59

9b. OTHER REPORT NO(S) (Any other numbers that may be assigned this report)
D162-10467-13

10. DISTRIBUTION STATEMENT
Approved for public release; distribution unlimited.

11. SUPPLEMENTARY NOTES

12. SPONSORING MILITARY ACTIVITY
Air Force Aero Propulsion Labortory
Wright-Patterson AFB, OH 45433

13. ABSTRACT

The program consisted of two phases. The purpose of Phase I was to define what needs to be known, and when, and with what accuracy to define the engine cycle and thrust required by a proposed airplane, and to develop methods to obtain the required information -- particularly in the engine-exhaust system area. The second phase simulated the preliminary design and engine airframe matching portions of an airplane system development, stressing the evaluation of exhaust system installation losses at several levels of validity. This final report presents a summary of the work. The individual tasks are documented in seven volumes from Phase I (Vols. I - VII), ten volumes from Phase II (Vols. VIII - XVII) of Ancilliary Reports (including D162-10467-12).

14. KEY WORDS	LINK A ROLE	LINK A WT	LINK B ROLE	LINK B WT	LINK C ROLE	LINK C 2T
Airplane System Development Process						
Performance Integration						
Element Performance Prediction						
Installation Losses						
Sensitivity of Engine Cycle						
Derivative Engine Study						
Concurrent Engine - Airframe Development						
Thrust-Drag Accounting System						
Wind Tunnel Testing Techniques						
Support System Interference						
Wind Tunnel Blockage						
Parametric Afterbody Study						
Integral Mean Slope						
Data Exchange						

AD-769086

EXHAUST SYSTEM INTERACTION PROGRAM

FINAL REPORT

AFAPL-TR-73-59

THE BOEING COMPANY
BOEING AEROSPACE COMPANY
RESEARCH AND ENGINEERING DIVISION
SEATTLE, WASHINGTON

Contract No. F33615-70-C-1450

Project 3066

JUNE 1973

UNITED STATES AIR FORCE
AERO PROPULSION LABORATORY
AIR FORCE SYSTEMS COMMAND
WRIGHT-PATTERSON AFB, OHIO 45433

FOREWORD

The effort summarized in this report was conducted under the Exhaust System Interaction Program. The report is submitted to the Air Force Aero Propulsion Laboratory by The Boeing Company under provisions of Contract #F33615-70-C-1450.

Phase I work defined the information requirements for concurrent engine-airframe development using a strategic multimission bomber type aircraft as an example in the airplane system development plan and in a sensitivity study of the engine selection to possible errors in exhaust performance estimates. Parametric aft body drag wind tunnel test data from measurements conducted in the Boeing 8' x 12' transonic wind tunnel are presented to fill some of the data voids for twin buried exhaust system installations.

Phase II applied the developed information and methodology to the integration of a high-q, high-maneuverability supersonic fighter-bomber. Fixed and variable-turbine engines were combined with several installation concepts and tailored to develop the lowest weight airplane for the mission. Parametric and systematic cycle variations were explored. Analytical methods were adjusted to improve integration realism and provide output visibility. Large-scale models of three designs were built to demonstrate improved test techniques and provide more accurate performance predictions.

The program has been directed and supported by AFAPL project engineers Capt. R. McTasney, Squadron Leader A. Rowlands, H. Gratz, and I. Bush. Within The Boeing Company, overall program management was under J. Postlewaite. The principal investigator for this program was V. Salemann. Chief contributors in the engineering disciplines were R. Woodling and G. Eckard, aerodynamic performance; J. Ramsay, propulsion system performance; Dr. F. Marshall, inlet performance and performance integration methods; S. Miller, exhaust system performance; and C. Pecoraro, wind tunnel testing. Principal members of the subcontractor's team supporting this contract were J. Kutney, D. Dusa, and H. Brown of the General Electric Company; and W. Usab, C. Swavely, and J. Soileau of Pratt & Whitney Aircraft.

Publication of this report does not constitute Air Force approval of the report's findings or conclusions. It is published only for the exchange and stimulation of ideas.

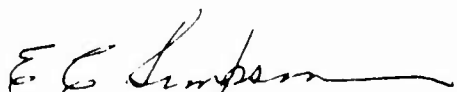

E. C. Simpson, Director
Turbine Engine Division
AF Aero Propulsion Laboratory

ABSTRACT

The program consisted of two phases. The purpose of Phase I was to define what needs to be known, and when, and with what accuracy to define the engine cycle and thrust required by a proposed airplane, and to develop methods to obtain the required information - particularly in the engine-exhaust system area. The second phase simulated the preliminary design and engine airframe matching portions of an airplane system development, stressing the evaluation of exhaust system installation losses at several levels of validity. This final report presents a summary of the work. The individual tasks are documented in seven volumes from Phase I (Vols. I - VII), ten volumes from Phase II (Vols. VIII - XVII) of Ancilliary Reports (including D162-10467-12).

NOTICE

When Government drawings, specifications, or other data are used for any purpose other than in connection with a definitely related Government procurement operation, the United States Government thereby incurs no responsibility nor any obligation whatsoever; and the fact that the Government may have formulated, furnished, or in any way supplied the said drawings, specifications, or other data, is not to be regarded by implication or otherwise as in any manner licensing the holder or any other person or corporation, or conveying any rights or permission to manufacture, use, or sell any patented invention that may in any way be related hereto.

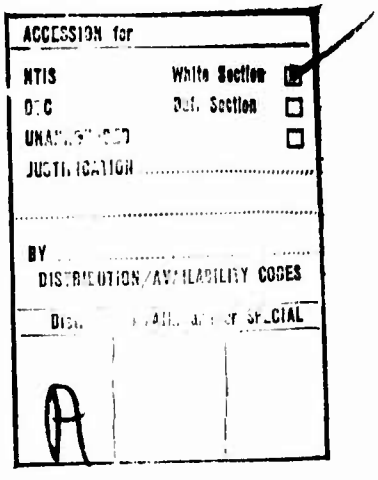

Copies of this report should not be returned unless return is required by security considerations, contractual obligations, or notice on a specific document.

TABLE OF CONTENTS

TABLE OF CONTENTS (Concluded)

LIST OF FIGURES

LIST OF FIGURES (Continued)

LIST OF FIGURES (Continued)

LIST OF FIGURES (Continued)

LIST OF FIGURES (Concluded)

LIST OF TABLES

1.0 ESIP FINAL REPORT

This final report is a combination of the Phase I Summary (Volume I) and the Phase II Summary (Volume VIII). The contents of the complete ESIP Phase I and II report is listed below by volume.

ESIP PHASE I AND II REPORT (D162-10467-11)

Phase I Report

Volume I - Summary

Volume II - Introduction and Review of Airplane System Development Process

Volume III - Performance Integration Methods

Volume IV - Element Performance Prediction Methods

Volume V - Effect of Installation Losses on Engine Selection

- Sensitivity of Engine Cycle Selection to Element Performance Prediction Errors

Volume VI - Effect of Installation Losses on Engine Selection

- Derivative Engine Study
- Phasing and Performance Data Requirements for Concurrent Engine-Airframe Development

Volume VII - Phase I Test

Phase II Report

Volume VIII - Summary

Volume IX - Obtaining the Fighter/Bomber Baseline

Volume X - Configuring the Fighter/Bomber

Volume XI	- Boeing Engine-Airplane Matching Program - TEM 129C
Volume XII	- Engine Selection and Airframe-Engine Company Data Exchange
Volume XIII	- Results of Phase II Fighter/Bomber System Defintion and Performance Analysis
Volume XIV	- Phase II Pretest
Volume XV	- Phase I Drag Correlations
Volume XVI	- Model Strut Evaluation Pretest Report and Test Plan
Volume XVII	- Input tc the Phase II System Analyses

1.1 PHASE I SUMMARY

1.1.1 Introduction

Performance predictions for military aircraft have not been accurate. It is not easy to substantiate this claim in general. The actual performance of most airplanes is only known to their respective manufacturers, and the initial mission performance specifications have often been revised prior to introduction of the airplane into service, making it difficult to distinguish between desired changes and inability to meet the original specification. In one case there are sufficient data in the congressional record: The F111A achieved only 55% of guaranteed ferry range and 15% of the guaranteed M=1.2 sea level dash range. Other examples may be more controversial: The B-58 and the B-70 did not meet the required range. In most cases off-design (part power) performance of the propulsion system or off-design (transient, transonic) performance of the airframe system were lower than predicted. Propulsion system installation losses seem to have been higher than expected. The uninstalled fuel consumption rate of the engine in the F4K is 15% better than that of the F4J, yet no significant improvement in actual airplane performance was measured. Another reason for suspecting installation losses is the fact that transport type airplanes generally perform very close to their predictions - within 10-15%. The engines in subsonic transports operate at relatively high power settings over most of the mission.

Another reason for poor performance of initial models of some airplanes is insufficient thrust. This is generally not due to maximum thrust being less than originally specified for the engine, but due to higher weight or drag of the airplane, requiring more thrust than originally predicted.

As part-power losses increase, some engine cycles are penalized more than others. This is true because some losses are a function of airflow, others are a function of nozzle exit area and others yet of gross thrust. At equal net thrust the airflow, nozzle exit and gross thrust of engines of various cycles varies, thus causing a variation in losses. Thus, some cycles are penalized more than others by a given magnitude of installation losses. It is therefore likely that if the extent of the off-design installation losses were

known earlier in the program, a different engine cycle may have been selected.

1.1.2 Purpose

The purpose of this program is to define what needs to be known and when, and with what accuracy, to define the engine cycle and thrust required by a proposed airplane, and to develop methods to obtain the required information, particularly in the engine-exhaust system area.

1.1.3 Objectives of Phase I

This report covers the work conducted as part of Phase I of the program. The objectives of Phase I are to identify, evaluate and improve the military airplane development process in respect to the engine and exhaust system selection and development. This involves identifying the methods used to evaluate and select engine cycles and exhaust systems for various missions, identifying and evaluating element performance data or prediction methods required as input to the system evaluation methods, and the timing when these data are required to support critical decisions in the airplane development process. If the work shows that the available data or performance prediction methods in the aft end area are deficient, a program should be defined and executed to improve the data and the methods.

1.1.4 Approach

The general approach was to first review a number of recent engine-airframe development programs to identify the methods, timing and data used to make the engine cycle and size selection. The Boeing Company as prime contractor on this program could draw on first-hand experience in its commercial programs, as well as on work on AMSA and B-1 programs up to the proposal stage, which is right up to the time of the final engine selection. The General Electric Company and Pratt and Whitney Aircraft Company, as sub-contractors in this program, reviewed their experience in the B-1 and F-15 engine-nozzle selection process.

A survey was conducted to collect performance data of various exhaust system and afterbody types on recent multi-mission airplanes. Performance prediction techniques that could be used to assess the performance of various elements of an airplane were also reviewed. The data and methods were

arranged in a number of levels as a function of input requirement to apply the methods or the method used to obtain the data. A system performance integration method, as well as system and mission performance optimization methods were defined as would be used during an actual engine selection process.

The accuracy of data inputs into the selection procedure was estimated and evaluated by inputting large, but probable errors in performance prediction into the analysis program and observing the effect on the ranking of engines of different cycles. The impact of probable data accuracy on the relative timing of initial engine and airframe decisions in a concurrent development was evaluated. This work plus the preceding survey of aft end data showed that additional tests should be run to obtain twin-model aft end data for a large number of models in which design and operating features, such as nozzle spacing, nozzle type and size and pressure ratio are varied parametrically. The data would serve as a basis for empirical correlations to predict the pressure drag of twin afterbodies as a function of physically significant parameters.

1.1.5 The Airplane Development Problem

The airplane and engine development processes are summarized on Figure 1-1. The most significant engine milestones are shown in relation to some of the airplane milestones. The curves along the bottom of the figure illustrate the typical error in two pieces of required information at any given time. It is seen that the engine design freeze occurs at a time where substantial possibility for error exist in the information needed to define the required engine thrust and type.

The airplane system was first broken down into four major elements and two subsystems as shown below.

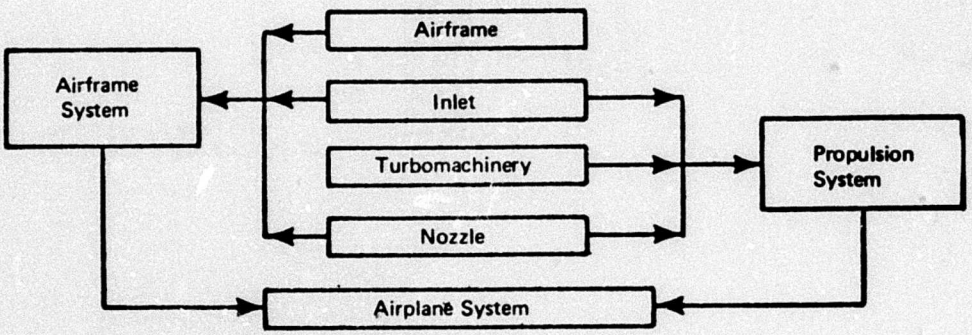

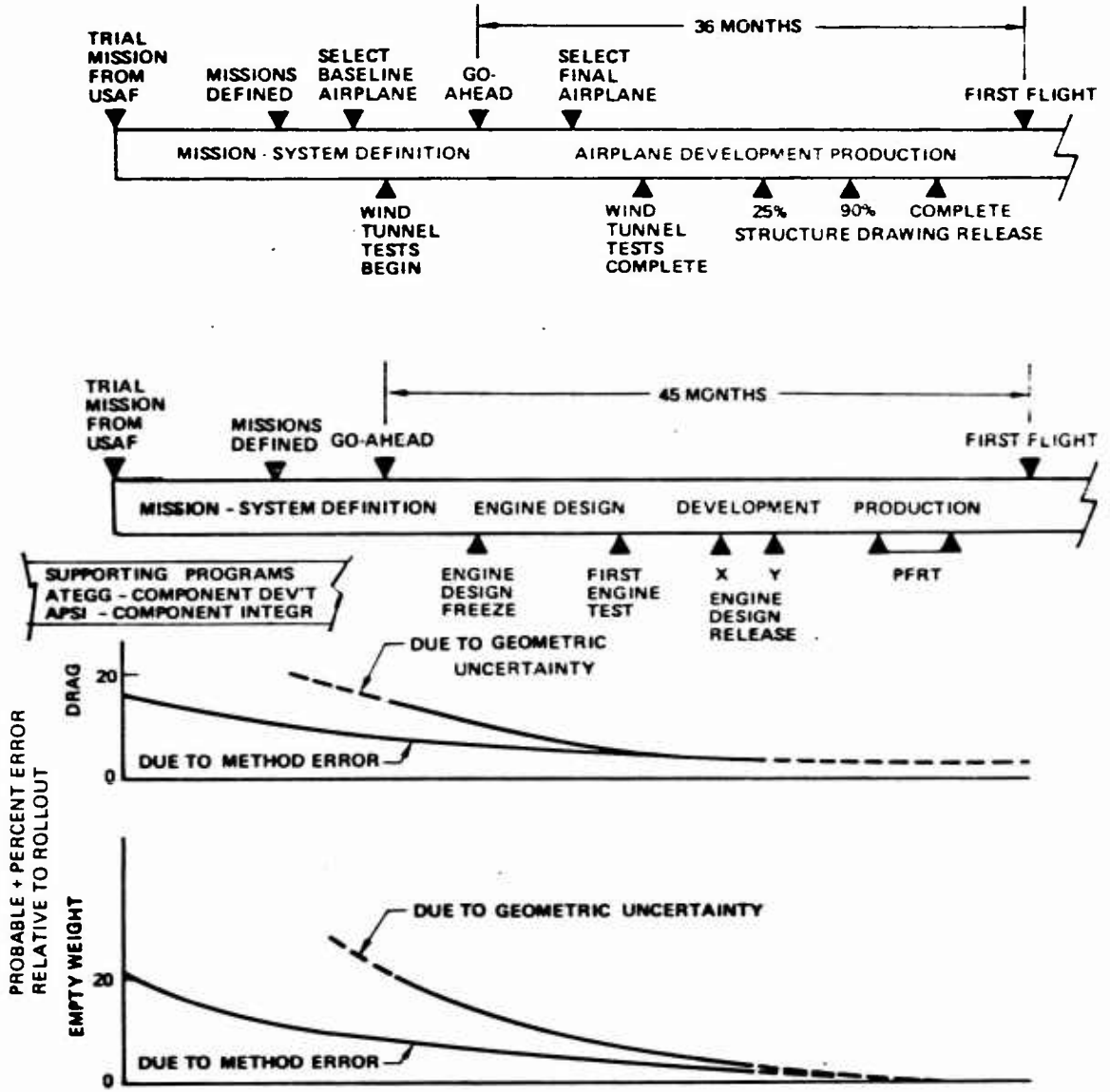

Figure 1-1: Typical Engine – Airframe Development Schedule

Information requirements for each element were then identified and a method to integrate the performance of elements and subsystems into system mission performance was defined.

1.1.6 Element Performance Integration Techniques

The need for an element performance integration system in an airplane development program arises largely from the inability to determine the performance of the complete airplane system in a single test or computation. Thus, a performance integration system is required to insure that the performance estimates for the various elements of the airplane system are properly integrated to yield an accurate prediction of overall system performance.

The emphasis here is placed on problems associated with airplane configurations having highly integrated propulsion system installations. In addition, problems associated with exhaust system performance are emphasized, consistent with the overall emphasis of the Exhaust System Interaction Program.

The element performance integration techniques recommended here apply specifically to systems utilizing flow-through propulsion simulation for the general aerodynamic drag testing and inlet drag testing, and blowing models for exhaust system drag testing.

Three criteria are used to judge the effectiveness of a performance integration system. First, and most important, is the requirement for accuracy in predicting the overall thrust-minus-drag performance of an airplane system. Secondly, the performance integration procedures should afford as much visibility as feasible to the performance of the individual elements of the airplane system. Finally, the element performance integration system should be applicable throughout an entire airplane development program.

The approach recommended here is based on the premise that the reference propulsion system conditions (inlet mass flow ratio and geometry and exhaust system pressure ratio and geometry), of the flow-through wind tunnel models used for the general aerodynamic drag testing, should be selected solely on the basis of overall experimental accuracy. Thus, small (often unrealistic) aft-end boattail angles are recommended for the reference exhaust system configuration to minimize the probability of aft-end flow separation. The objective here is to obtain reference flow conditions which can be precisely reproduced in an exhaust system blowing test with faired-over, plugged inlets.

A consequence of the above procedure is that the wind tunnel drag polar corresponding to reference exhaust system conditions may differ considerably from that associated with any realistic exhaust system operating conditions. However, it is also recommended that part of the drag increments measured in the blowing tests be used to correct the wind tunnel drag polar to a realistic "baseline" exhaust system geometry and pressure ratio. This baseline geometry and pressure ratio combination would correspond to a specified engine throttle setting. All remaining drag increments due to throttle setting changes relative to the baseline conditions would be charged to engine net thrust, not affecting the drag polar. This approach is shown on Figure 1-2, and does not require additional testing relative to conventional performance integration schemes.

The use of a static thrust measurement to define the internal force and thereby isolate the external force on a blowing model, when real exhaust system operation is being simulated, is also recommended.

It is also suggested that the element performance integration system not deal with the absolute force acting on any arbitrarily specified (metric) section of the external surfaces.

The approach recommended here satisfies all the previously described criteria for evaluating element performance integration systems. It allows for an accurate evaluation of airplane system performance, insuring that all force components acting on an airplane are counted once, and only once, in the overall thrust-minus-drag build-up.

It is shown that meaningful element-to-element performance comparisons between airplanes of different configuration types are generally not physically possible (except for internal performance parameters). However, using the concept of baseline exhaust system conditions, the techniques recommended here will produce airplane drag polars with which meaningful comparisons can be made between competing airplane configurations.

The use of static thrust measurements to isolate the external force on blowing models, combined with the use of baseline exhaust system conditions, renders the recommended techniques applicable over an entire airplane development program. Thus, drag polar predictions based on theoretical calculations, wind tunnel measurements, or flight test results, may all be developed on a common basis and meaningfully compared.

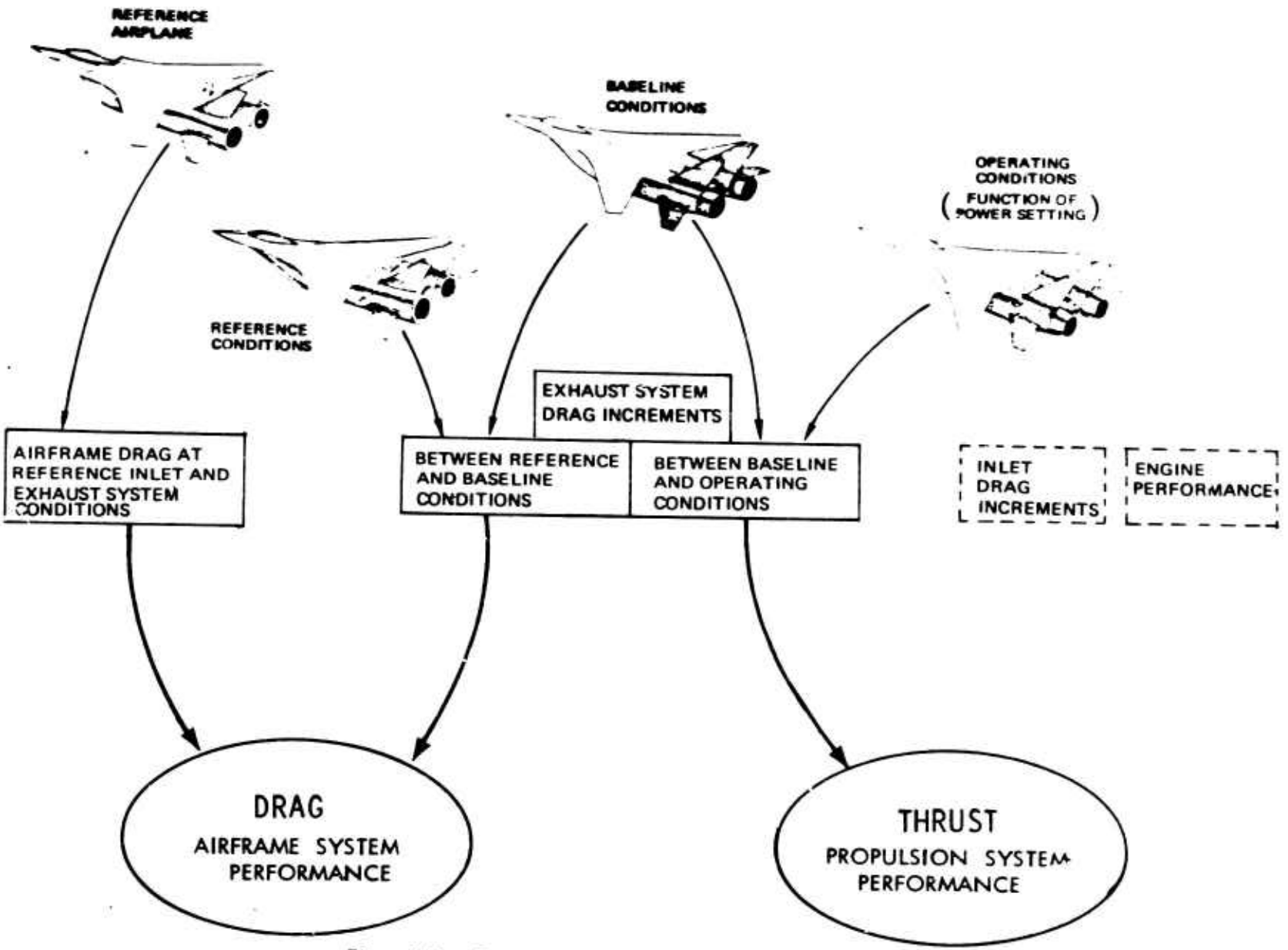

Figure 1-2: Recommended Definition of Thrust and Drag

1.1.7 Parametric and Derivative Methods for Engine Cycle Selection

The most direct method to evaluate and select engine cycles for various missions is to design a number of airframes around a parametric series of engine types and select the combination which produces the best figure of merit. This method requires a large number of computer runs to generate engine data and airplane data.

For this program, an alternate method was developed by General Electric under subcontract, using engine and airplane performance derivatives. One engine-airframe combination is optimized, then the effect of changes in engine performance parameters, such as maximum thrust, fuel consumption, diameter etc., on airplane performance are computed leg-by-leg for the entire mission. Engine derivatives, which give engine performance changes as a function of design parameter changes, such as bypass ratio for speed etc. are also computed. The two sets of data are combined in a linear optimization program which identifies the desired combination of engine design parameters which will optimize the airplane figure of merit. The process was tested on a bomber mission and appears promising.

1.1.8 Element Performance Prediction

A survey was made of the available empirical data and experimental and analytical methods to predict the performance of the propulsion systems, with emphasis on the external and internal performance of exhaust systems. Results showed that simplified, approximate methods could result in large errors, and that very little information is freely available on the accuracy of even the most sophisticated methods due to lack of accurate pairs of flight data and predictions.

The various available methods to predict element performance were grouped into four levels, according to their probable accuracy, the amount of work necessary to obtain an answer, and their historical time period of application. The methods are summarized on Figure 1-3. The accuracy of lower level methods was estimated by comparison to higher level tasks. Figure 1-4 illustrates the estimated magnitude of Level I errors in drag estimates, including the aft end drag. It is seen that errors could be as high as 20 percent.

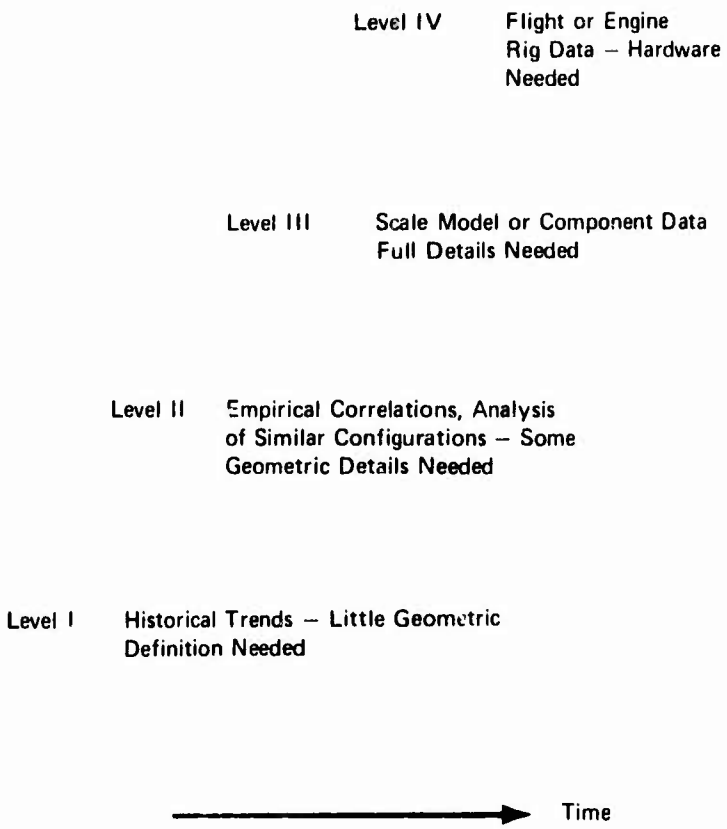

Figure 1-3: Definition of Performance Prediction Methods

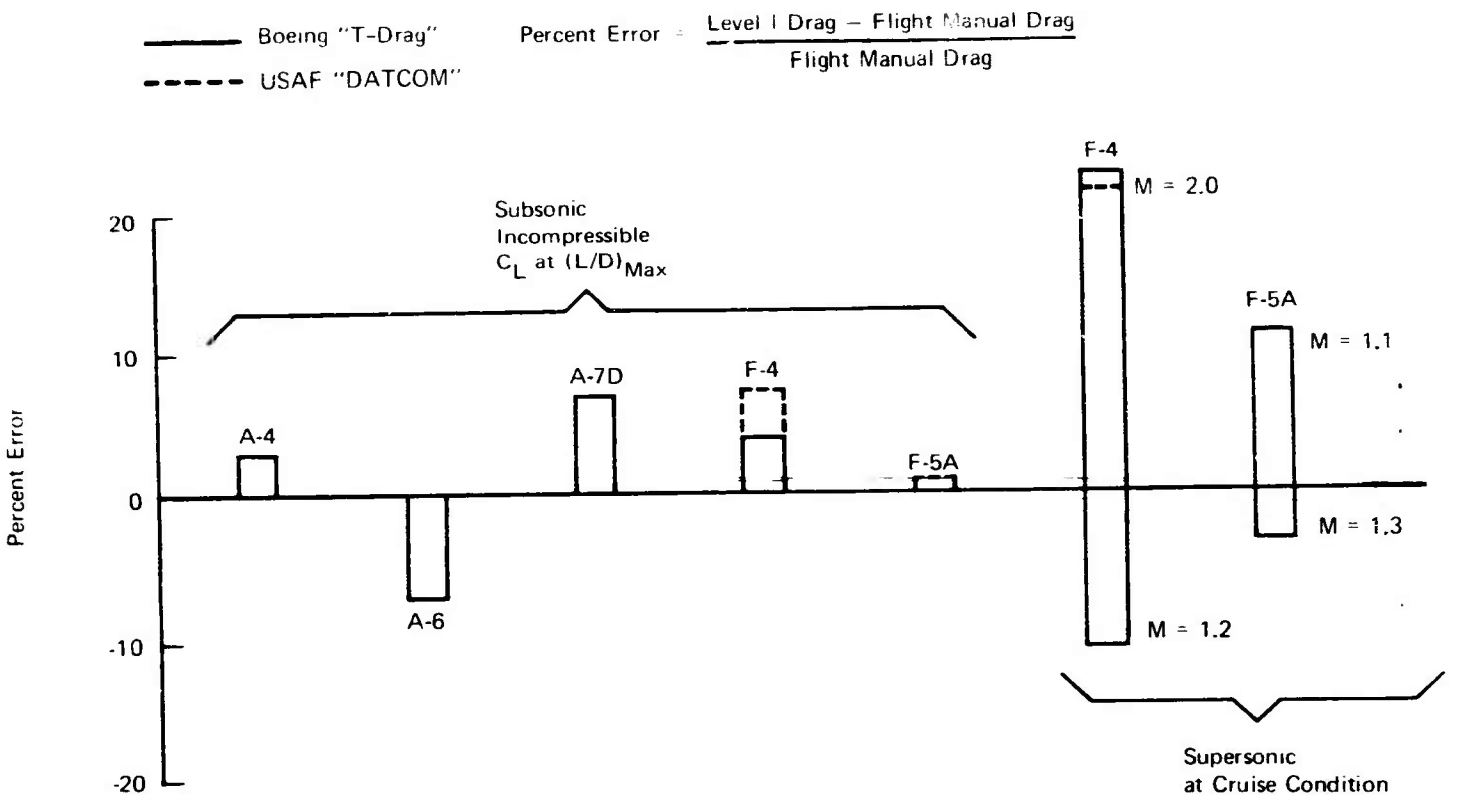

Figure 1-4: Typical Errors in Predicted Airframe Plus Propulsion System Drag Using Level I Methods

In general, the errors are due to the basic inaccuracy of lower level methods and due to incomplete or erroreous knowledge of the size and shape of the element at the time the performance predictions are made.

In the case of aft end performance prediction, even Level III methods do not enjoy a high degree of accuracy. Figure 1-5 illustrates results of a 5% scale model test and flight test from the NASA-Lewis F106-J85 nacelle program. It is seen that the Reynolds number has a significant effect over the range flown, but model data is far below what one would expect by extrapolation back from flight test. Another example (Fig. 1-6) from the same program, shows significant performance variation due to slight geometric changes as well as Reynolds number. Based on these examples, the maximum error assumed for the exhaust system drag corresponded to the case where the drag was predicted based on attached flow around low-angle, radiused boattails from isolated boattail data, but the actual configuration was such that the boattail was entirely separated.

1.1.9 Sensitivity of Cycle Selection to Element Performance Prediction Errors

Maximum errors in the performance predictions of the four major elements that could be reasonably expected on the basis of past evidence were estimated and the effect on the engine type selection, as exemplified by the bypass ratio, was derived.

A multimission bomber was optimized with each of three engine types (Bypass 1, 2 and 3), using the low and high estimates for aft end drags. Results were plotted in terms of range for a fixed weight airplane. Figure 1-7 shows that, when low aft end drags are assumed the optimum bypass ratio would be between 1.4 and 2. However, if the aft end drag was increased by the amount corresponding to the effect of a completely separated aft end, the choice would move back to about 1.1, and a bypass 3 engine would result in totally unworkable engine-airframe combination.

Similar effects were noted for large changes in inlet drag, engine performance and some airplane drag components. In each case, the changes corresponded to the difference between a typical optimistic prediction and model or full scale data or final design which demonstrated low performance. As a result it was concluded that major decisions as to the required engine type and size cannot be made on the strength of lower levels of element definition and performance prediction.

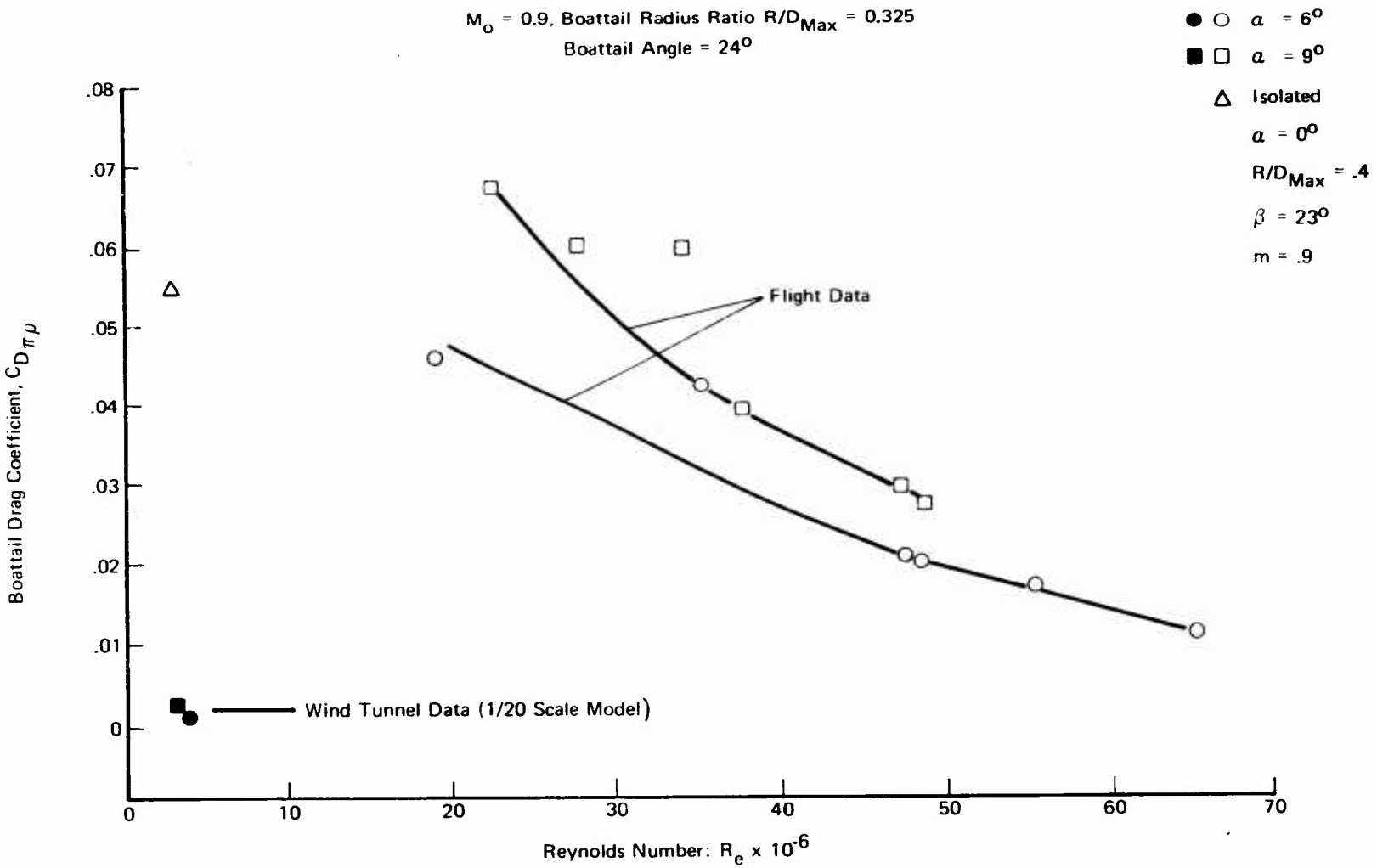

Figure 1-5: Reynolds Number Effect on Boattail Drag

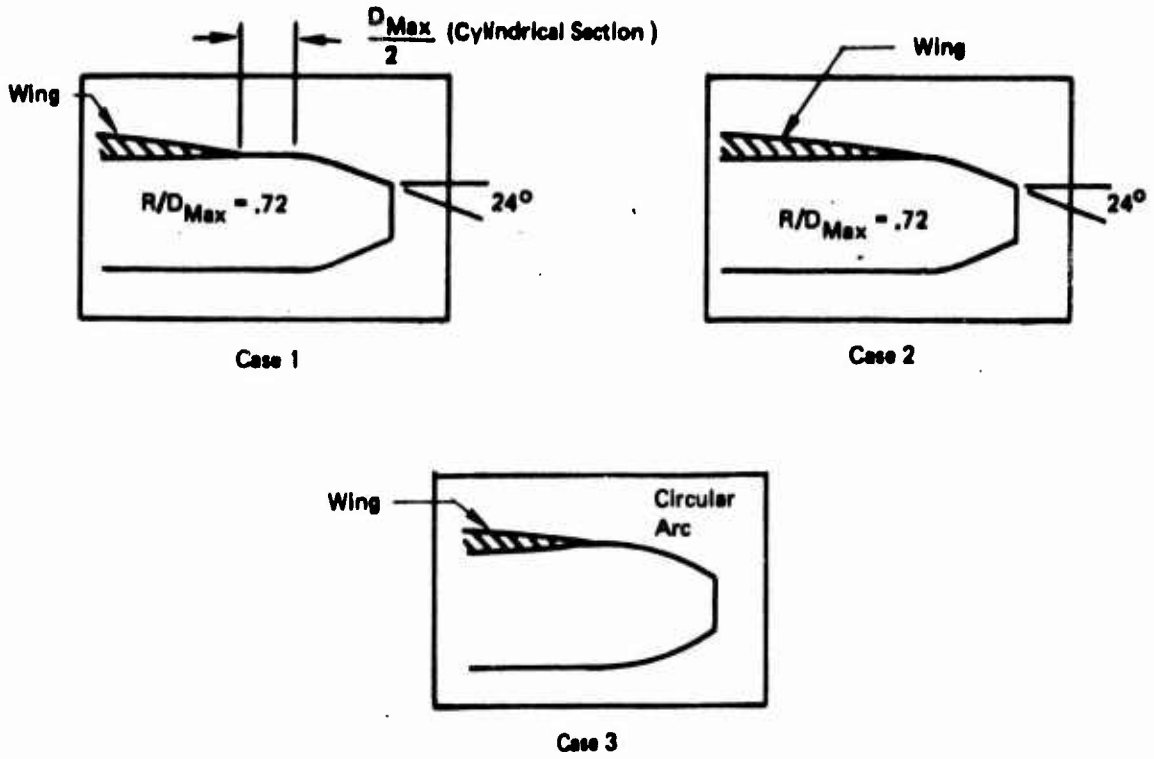

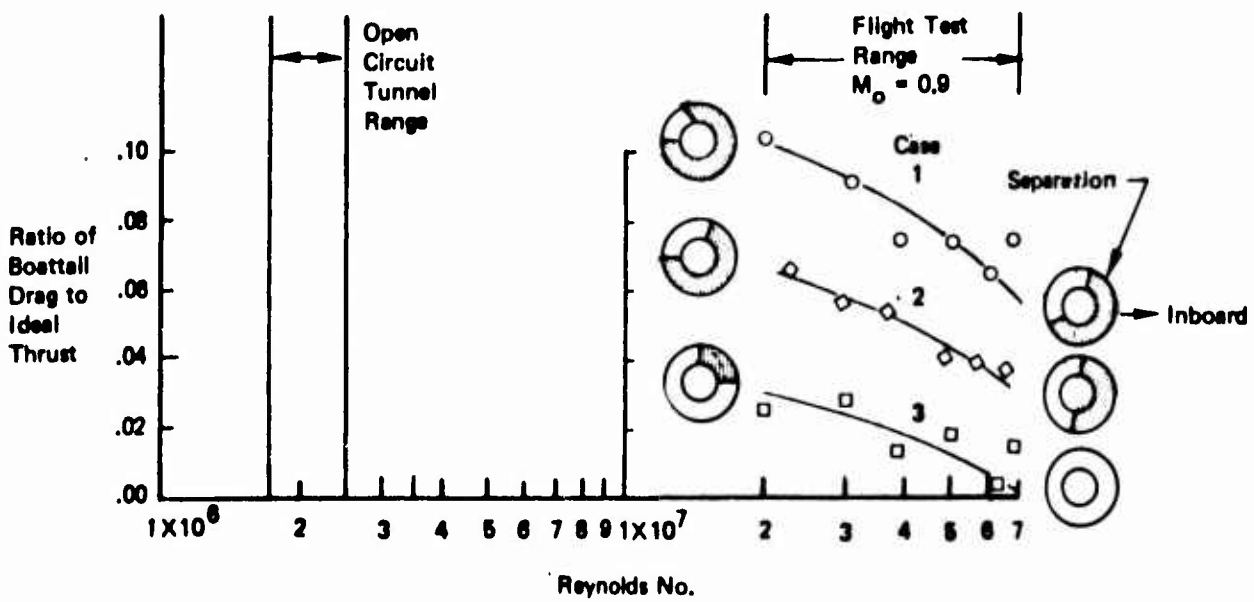

Figure 1-6: Effects of Geometry and Reynolds Number on Separation and Drag

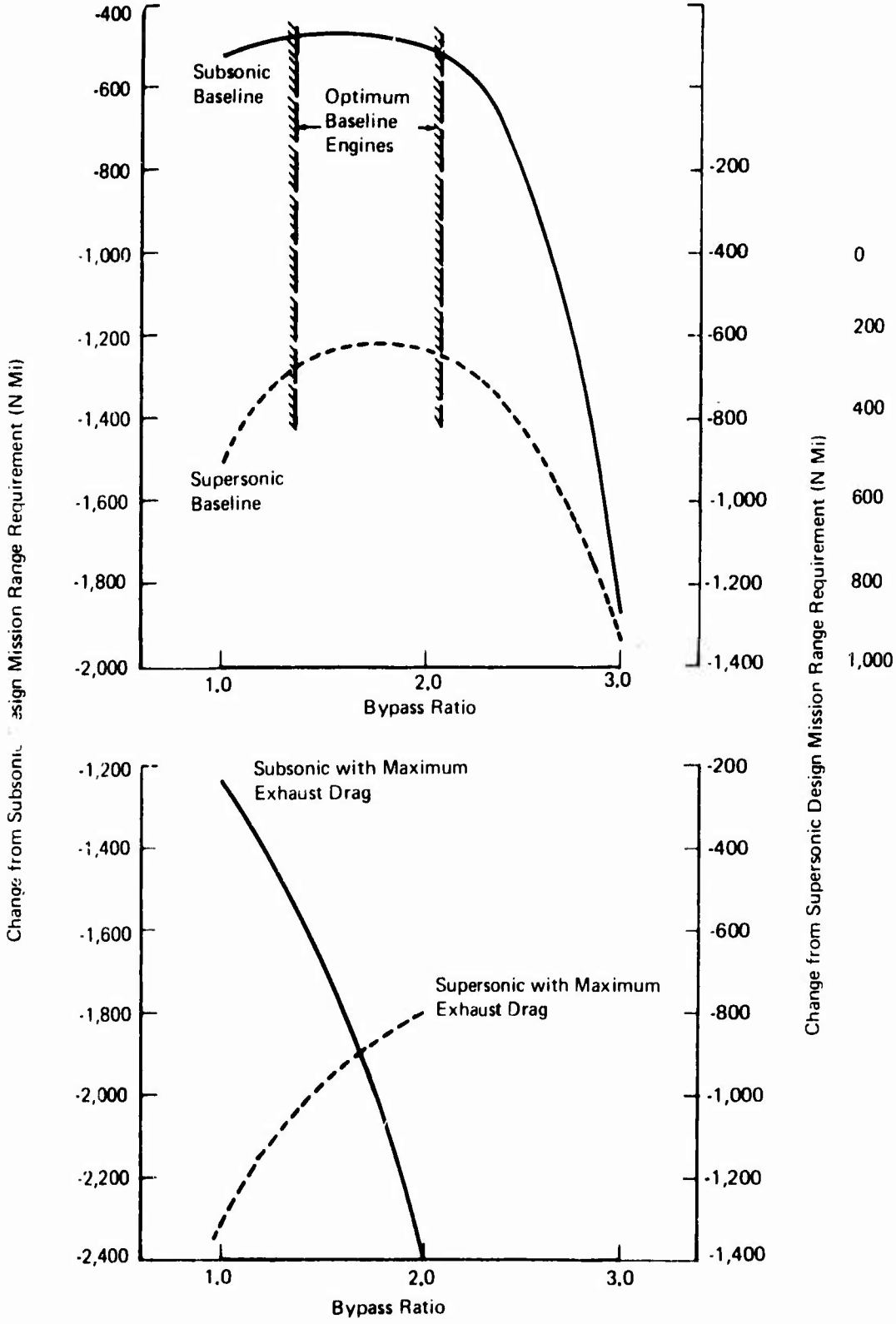

Figure 1-7: Effect of Exhaust System Drag on the Engine Cycle Selection

1.1.10 Recommendations

A survey of Level II methods and empirical data to predict exhaust system performance showed that no satisfactory data are available to predict the drag of practical aft ends of integrated engine-airframe configurations. Potential flow and boundary layer theory cannot satisfactorily handle typical 3-dimensional afterbody problems and empirical correlations do not recognize some of the most important parameters due to lack of data on their effects. A test program was therefore initiated to begin a systematic collection of such data and hopefully develop a general prediction method.

In the light of demonstrated errors in wind tunnel test predictions compared to flight test data for identical configurations, it is questionable whether satisfactory installation drag predictions can be made on the basis of present test procedures. Additional programs to define sources of errors in both wind tunnel test data and flight test data are needed. Reynolds number, support, blockage and improper simulation effects should be investigated. Methods to define and reduce bias and random errors in both wind tunnel and flight test data should be investigated.

Since the engine cycle choice has been shown to be strongly affected by external installation losses, it is proposed to slide the airplane schedule of future programs to the left relative to the engine schedule on Figure 1-8 allowing more time to define element geometry and performance prior to engine design freeze.

The cycle freeze has been set six months before completion of the Configuration Development Phase. At this time, all aft-end testing and about half of the inlet and airframe testing have been completed.

The thrust freeze could then occur six months later, at the end of the Configuration Development Phase. At this time the final airplane configuration has been selected and the geometric uncertainties have been nearly eliminated. Figure 1-1 shows that very little improvement in drag prediction errors can be expected after that date. However, a sizeable uncertainty remains, approximately ±7% in drag and ±10% in weight.

It is therefore proposed that the probable uncertainty in the predicted performance and weight of each major element of the airplane be kept visible in future development programs and that the cycle and thrust freeze be preceded by an

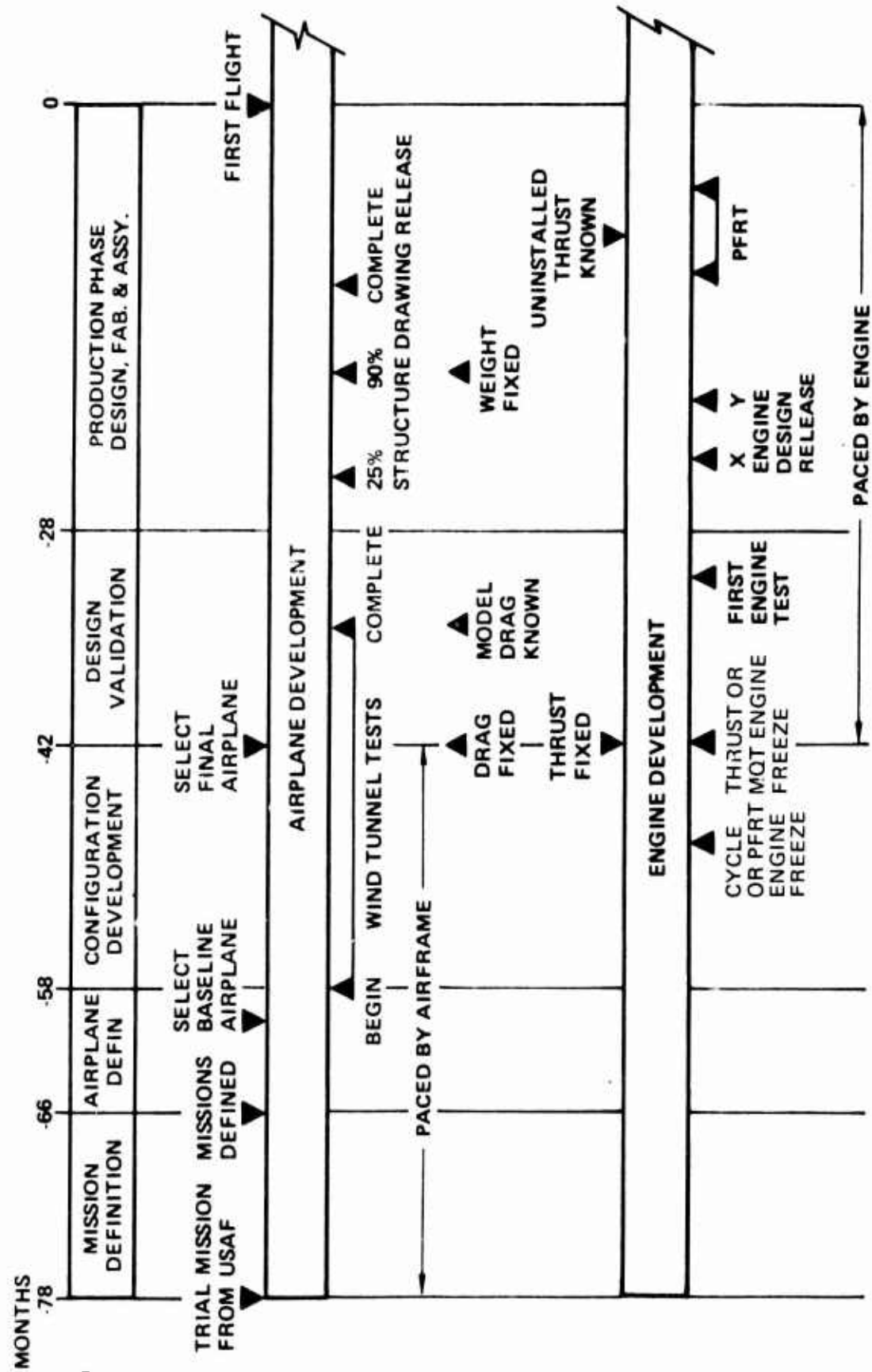

Figure 1-8: Proposed Engine – Airframe Development Schedule

analysis of the consequences of a positive and negative error in predicted thrust requirements. It is expected that a prudent trade of risk versus airplane performance or cost can then be made, and the cycle and thrust size chosen accordingly.

A similar reassessment should be conducted around the 90% drawing release date, when weight prediction errors should be reduced to a minimum. At this time, the only remaining option is to slide the program if an engine change is indicated.

1.1.11 Phase I Test Results

The Phase I test program consisted of a preliminary test to investigate the blockage and strut interference effects and define the range of Mach numbers over which data would be free from or correctible for tunnel and support effects. All tests were conducted in the Boeing 8 x 12 foot transonic wind tunnel.

The results of the blockage test are summarized on Figure 1-9. Integrated pressure drag for the .1%, .5% and .75% blockage models are plotted against Mach number. The blockage model was axisymmetric and its area distribution corresponded to the sum of the areas of the forebody and strut and of one short afterbody. Afterbody pressure drags for all three sizes did not diverge below M=.9 indicating no measureable blockage effects on the afterbody. Up to M=.975 the drag of the large model diverges from the other two, then the curves begin intersecting. It is felt that drag data is correctable up to M=.975. This will be the limit of future testing using the subject forebody and strut.

The effectiveness of the slotted walls to cancel shock waves was investigated with the shock reflection model as shown on Figure 1-10. The pressure distribution along the top of the strut mounted forebody is plotted on Figure 1-11 for Mach numbers up to .925 and shows a much weaker influence due to the strut area than the blockage model data. Above M=.925, as shown on Figure 1-12, the strut influence is strong, but still tends to dissipate upstream of the split plane. The pressure at the split plane, however, gradually increases with Mach number. Reflected disturbances appear at M=1.05 and 1.07. These shocks would invalidate data on longer afterbodies. This part of the test confirms M=.900 as a limit of interference-free testing.

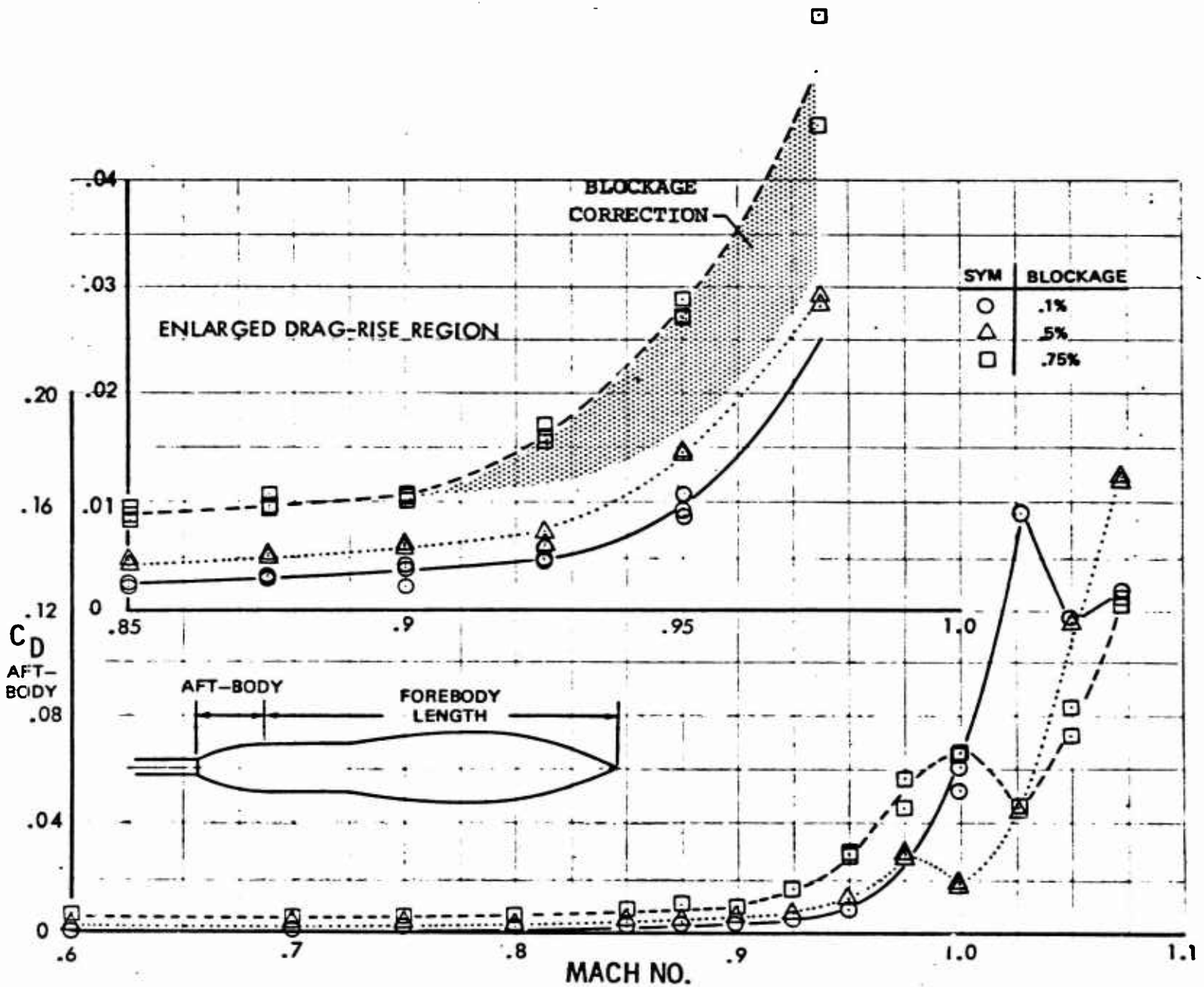

Figure 1-9: Blockage Effect

Blockage Model

Shock Reflection and Tare Model

Figure 1 – 10

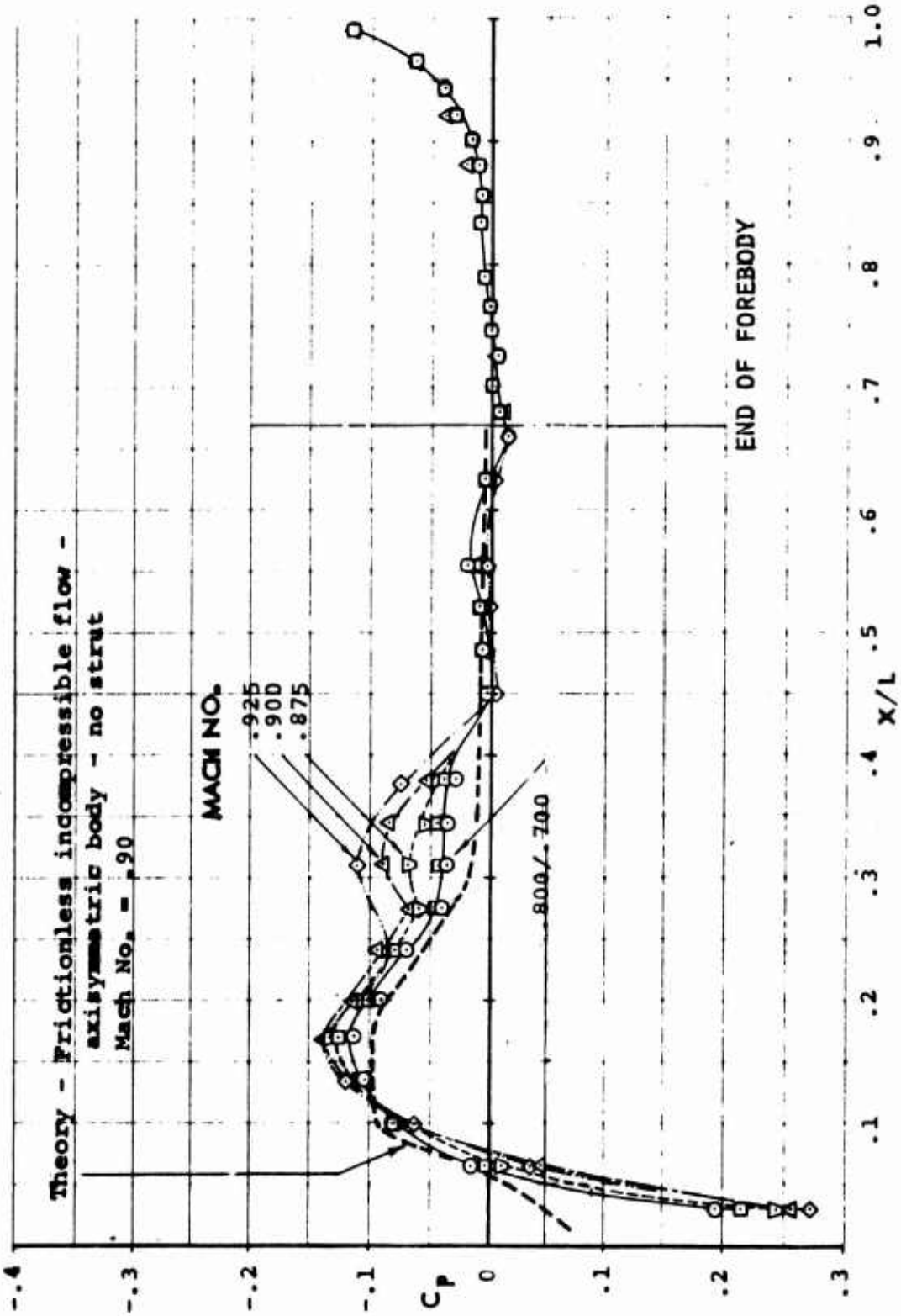

Figure 1-11: Pressure Distribution Shock Reflection Test – Mach No. ⩽ .925

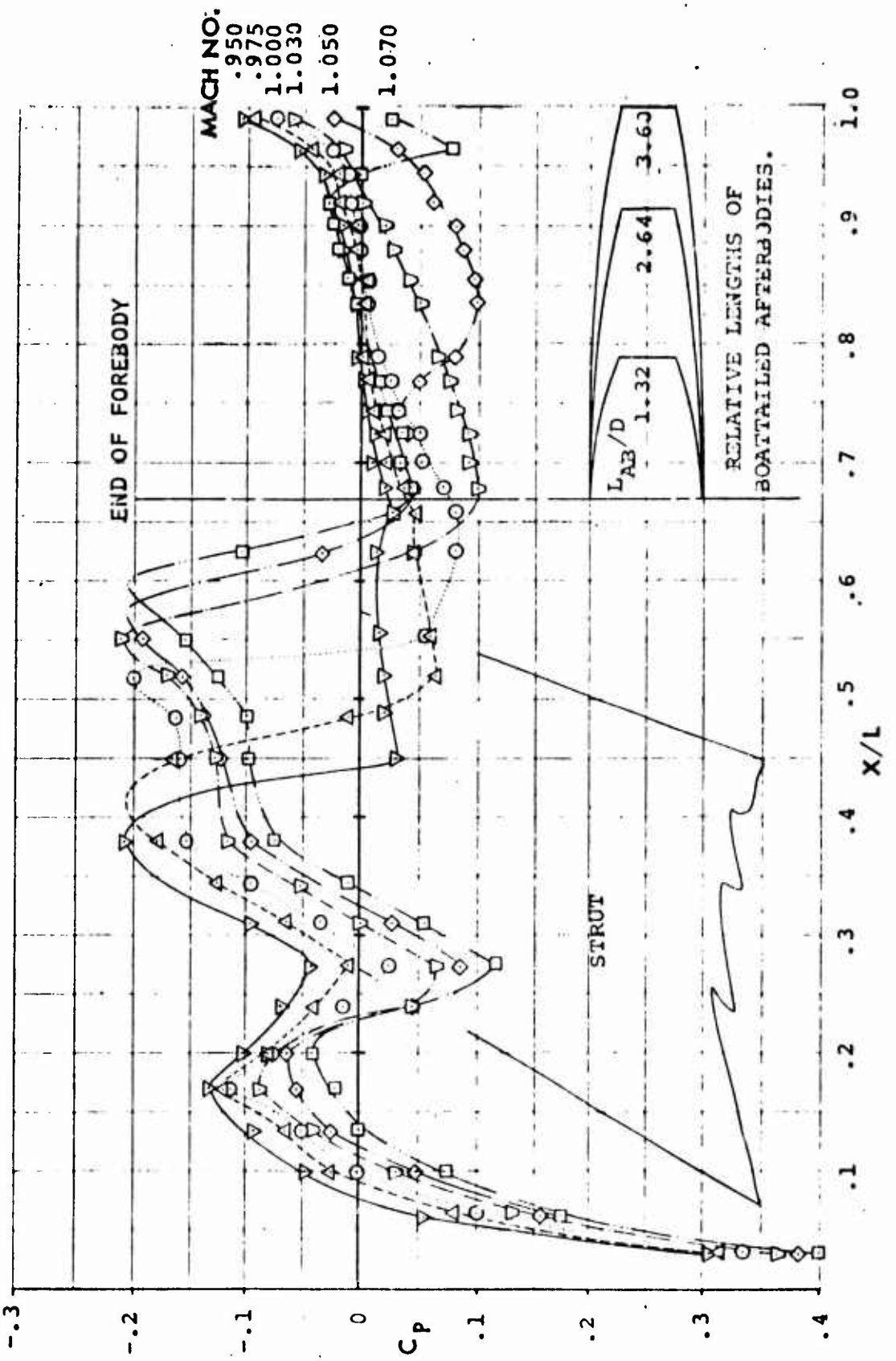

Figure 1-12: Pressure Distribution Shock Reflection Test – Mach No. ≥ .950

To measure the effect of the support system, in this case a strut, two twin-nozzle afterbodies were tested on an internal balance cantilevered off the forebody. The forebody was either sting mounted through the nozzles or strut mounted with dummy stings in place. Forebody pressure distributions and force measurements were made.

The results show negligible strut interference on the N_7 model at all Mach numbers (Figure 1-13) and slight interference ($\Delta C_{D\pi}$ .005) on the N_3 model up to M=.9, increasing to $\Delta C_{D\pi}$ = .03 at M=.975, Figure 1-14. The N_3 afterbody is shorter than the N_7 afterbody. The pressure disturbance due to the strut has been shown to decrease with increasing distance in the previously described test using a cylindrical afterbody. It therefore appears plausible that shorter afterbodies would be more strongly affected.

During the parametric afterbody drag tests the model included an internal balance to measure the afterbody thrust-minus-drag, see Figure 1-15. Total thrust-minus-drag, including the forebody and strut, were measured on the floor balance. Static tests were performed to define the nozzle velocity coefficients and the results used with wind-on nozzle total pressure and airflow measurements to compute thrust.

The total number of model variations tested was 75. This included area plot variations, vertical tail location effects, convergent, convergent-divergent and plug nozzle effects and spacing effects. Afterbody drag data from the main balance agreed with data from the internal balance, although the internal balance data showed more scatter.

The flow meter in use was an ASME type nozzle. The nozzle was preceded by throttling plates and swirl straighteners and an 80-inch section of 4-inch pipe.

This unit has been shown to be insensitive to upstream conditions in the calibration laboratory. With this unit, the flow coefficients fell within the band of available data for the N_{22} nozzle-afterbody as shown on Figure 1-16. The internal lines of this nozzle were identical to the lines of a Boeing thrust and airflow reference model in use since 1960.

Throughout all three blowing entries the N_7 afterbody with twin verticals on nacelle centerline was used as a reference model. This configuration was tested eleven separate times

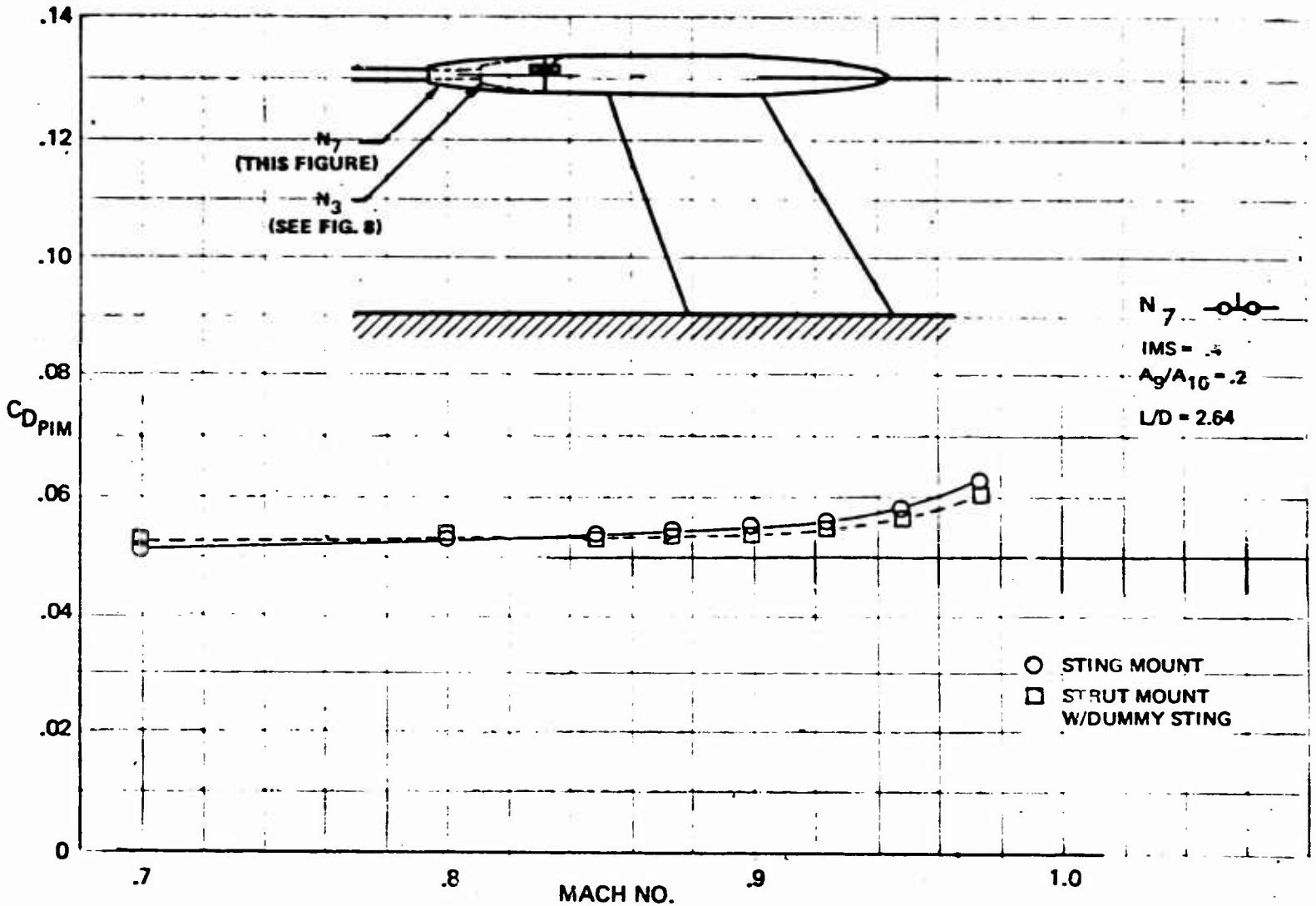

Figure 1-13: Effect of Strut Mount on Low Drag Afterbody

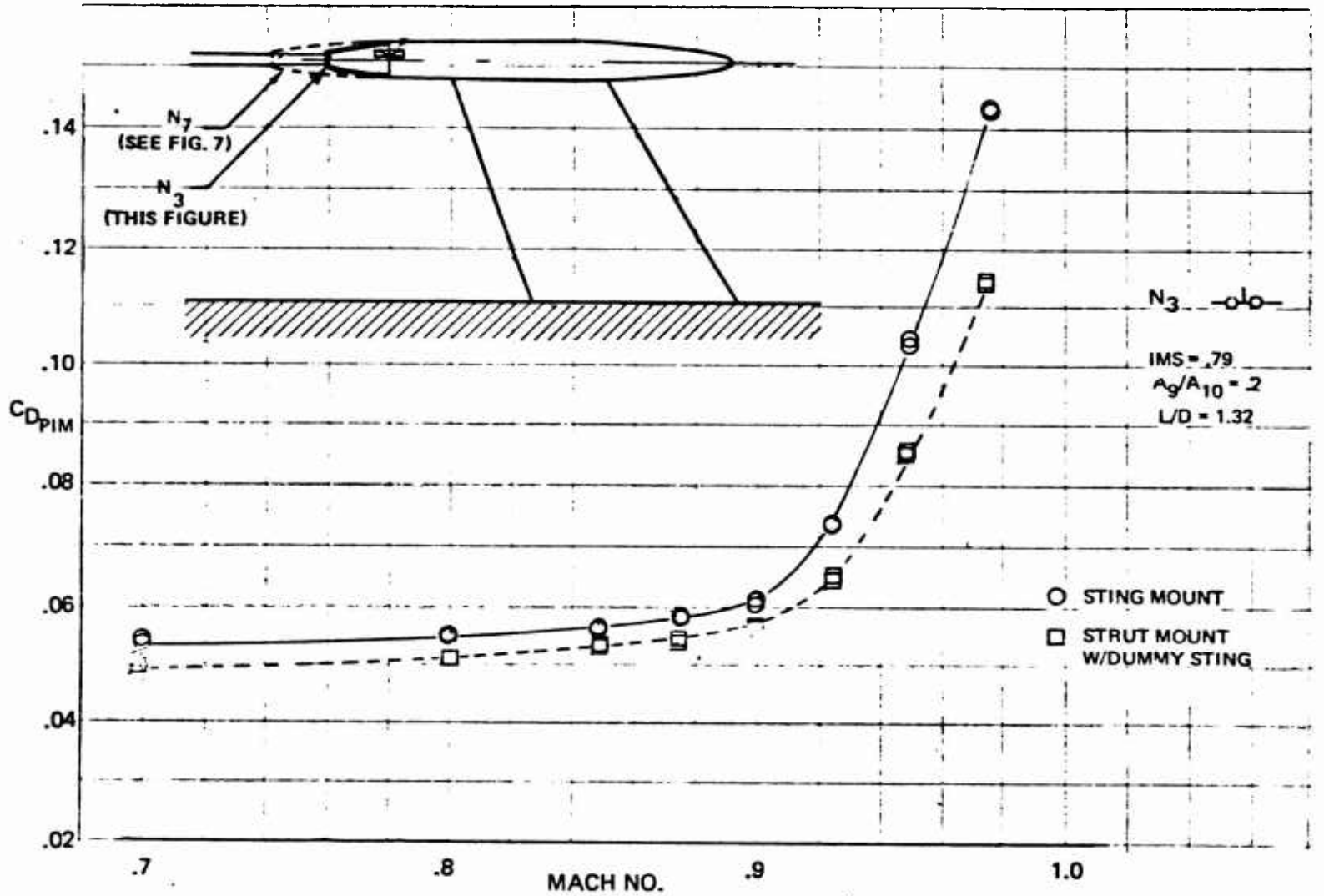

Figure 1-14: Effect of Strut Mount on High Drag Afterbody

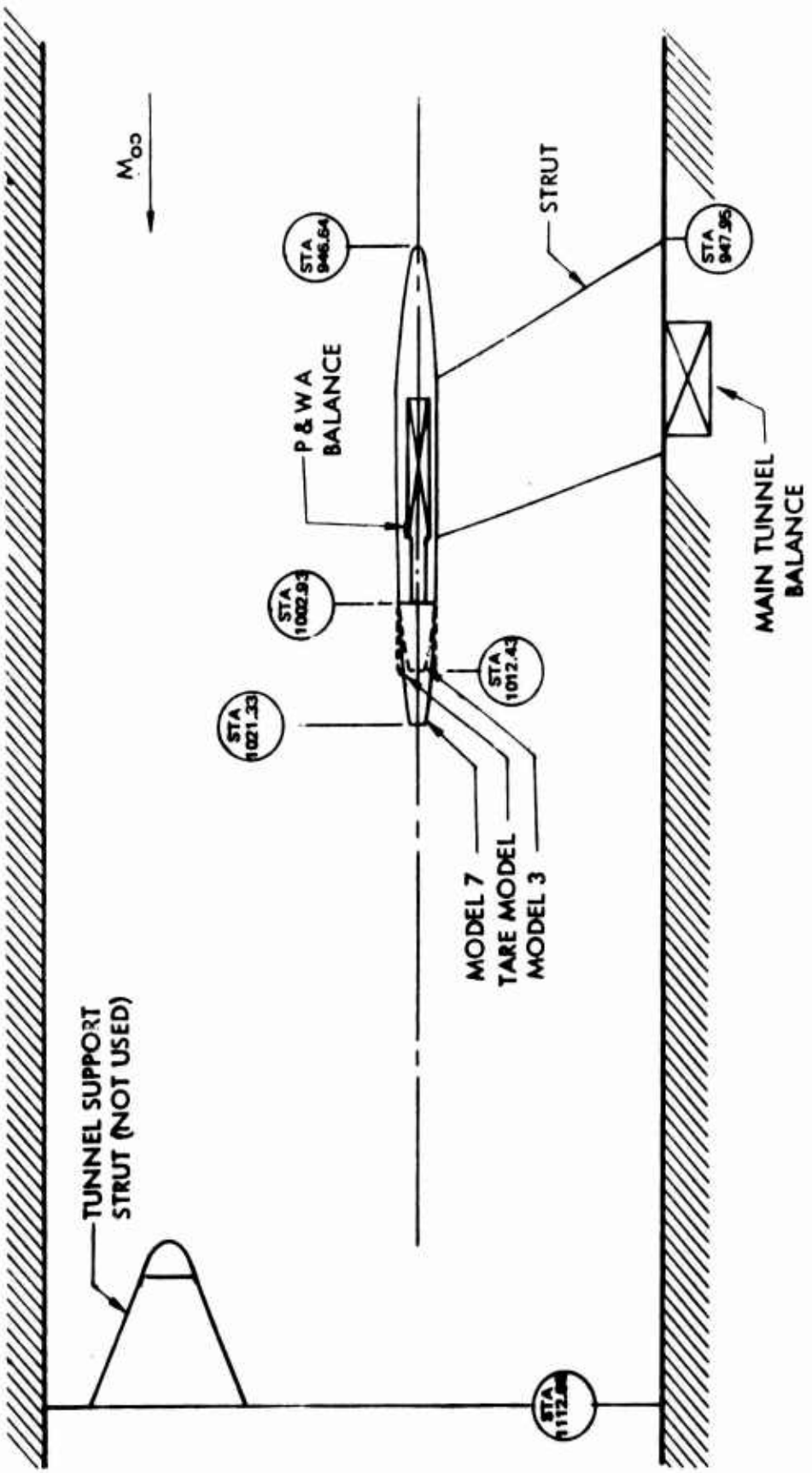

Figure 1-15: Parametric Test Configuration

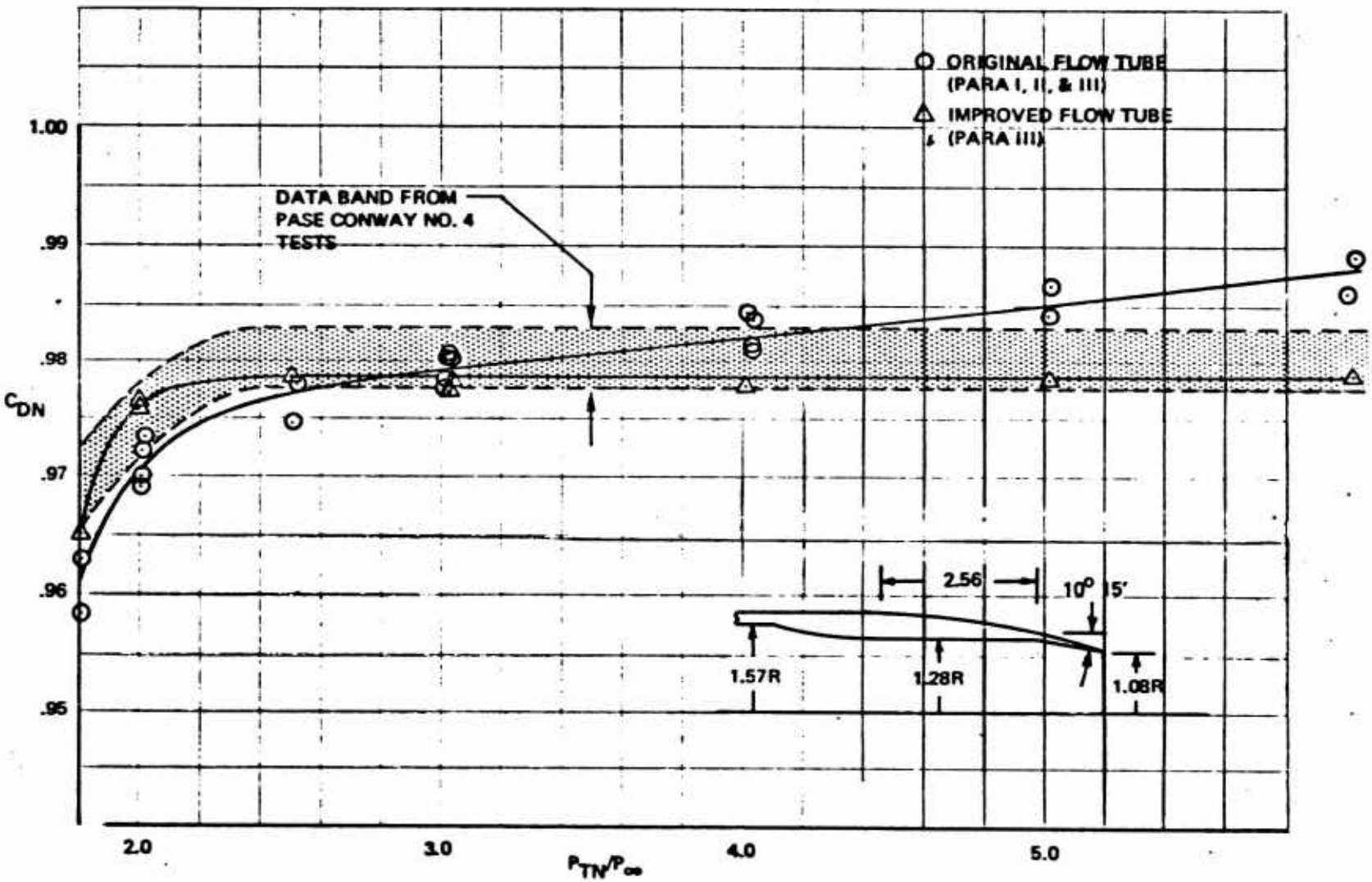

Figure 1-16: Discharge Coefficient for Conway No. 4 Nozzles

during the three entries. Figure 1-17 presents all these data. The band of data scatter is ±.005 $\Delta C_{D_{PIM}}$ at all pressure ratios except 3.0 which shows more scatter due to a much higher level of thrust.

The data presented have been corrected for blockage and strut interference, but still include skin friction and pressure drag on the afterbody, including tail fins, as measured in the tunnel at model Reynolds numbers.

Data for N_3, a short afterbody with a medium value of integral mean slope (IMS=.79) and nozzle exit to maximum cross sectional area ratio of 0.2 are shown on Figure 1-18 as an example. The data for N_7, a medium length, low IMS afterbody are shown on Figure 1-17. These bodies represent low total drag examples, with one having predominantly skin friction drag, and the other a more balanced split between skin friction and pressure drag up to M=.9 and an earlier drag rise. The test series included a range of lengths, area ratios, IMS values, shapes and model types. Two spacings and several tail locations were investigated on many models. The entire test matrix is shown on Figure 1-19.

Boundary layer flow visualization photos by means of oilflows were taken for most models. Configuration photos on Figure 1-20 and 1-21 show the tail locations investigated, and oilflow patterns are shown on Figure 1-22. Separated flow areas on the boattails and interfairing vary in size and shape as a function of tail location. In addition, force measurements showed corresponding large changes in drag.

The force data are presently being analyzed by Boeing and Pratt and Whitney Aircraft with the aim of developing a correlation for the pressure drag as a function of afterbody shape parameters and plume parameters.

1.1.12 Conclusions

Present methods to predict airplane element performance from emperical correlations and model data are often not sufficiently accurate to select optimum engine cycles and sizes for various missions. Engine-airframe development programs should be rearranged to provide more time for inlet airframe and exhaust system performance predictions. Better methods must also be developed, particularly in wind tunnel and flight testing, to improve the accuracy of predictions.

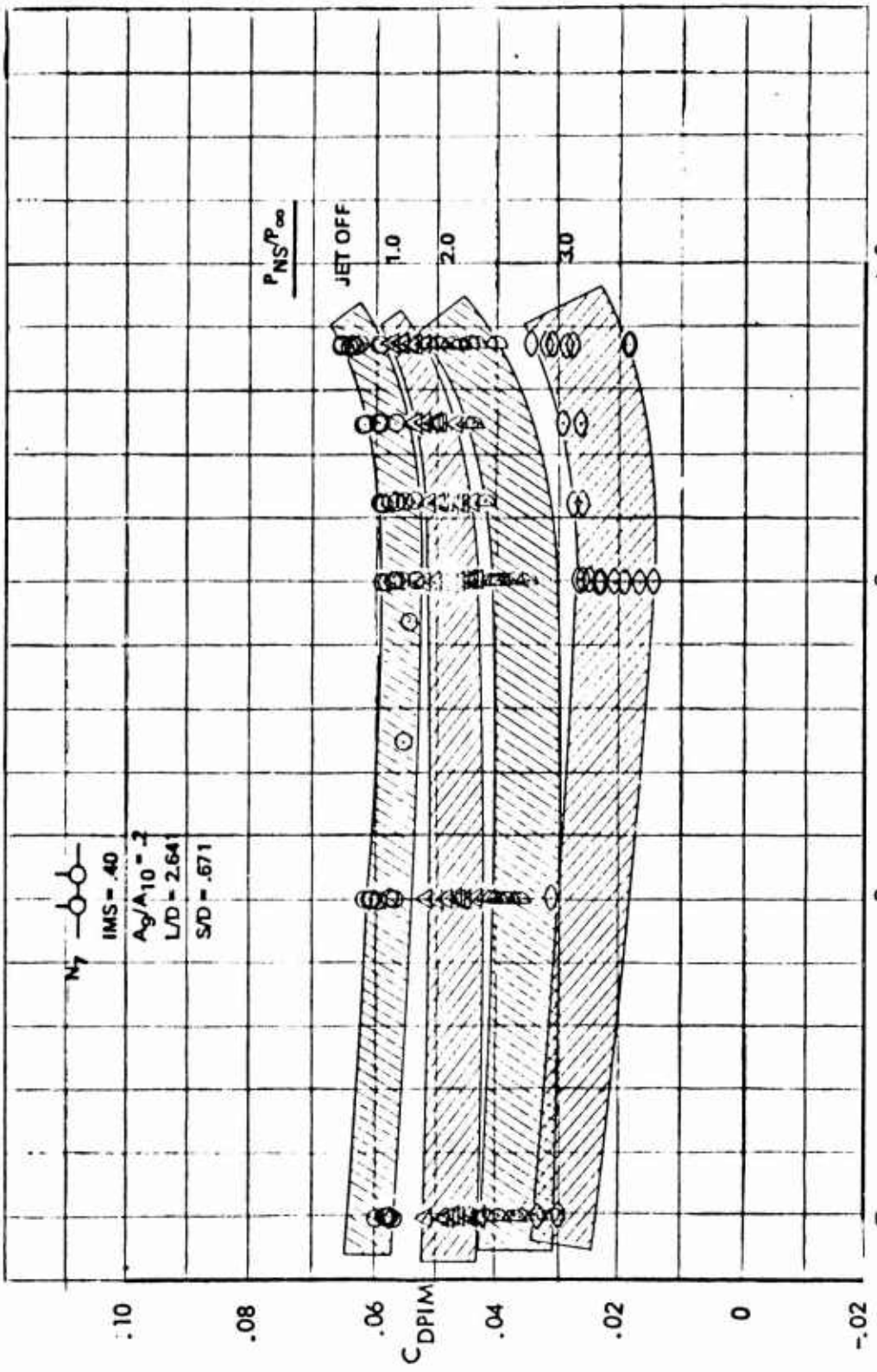

Figure 1-17: Drag Map for N_7 Afterbody – Twin Vertical Tails

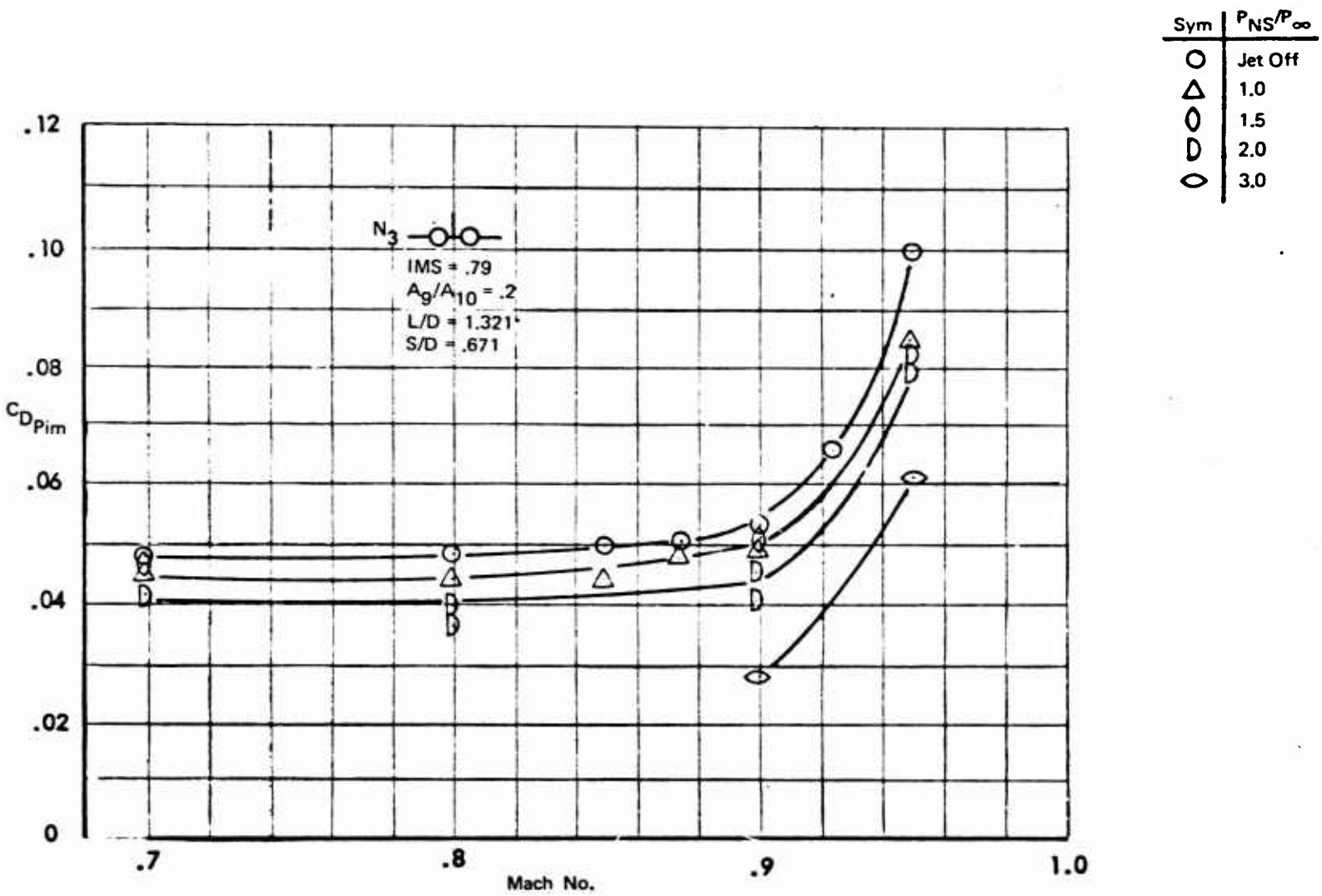

Figure 1-18: Drag Map for N_3 Afterbody – Single Vertical Tail

CONFIGURATION				GEOMETRY			TEST CONDITIONS		TEST ENTRY	RUN NO'S
AFTER-BODY DESIG-NATION	TAIL TYPE	NOZZLE TYPE	IMS	A_9/A_{10}	$L/_{DEQ}$	$S/_{DEQ}$	MACH NO.	PNS/P_∞	PARA	
N_1		Con.	.9	.1	1.321	.671	.7 to .95	1.0 to 3.0	I	240-278
		Con.					.7 to .95	1.0 to 3.0	II	533-550
		2/1,6°,C-D					.7 to .95	1.0 to 4.0	II	130-148
		1.4/1,6°,C-D					.7 to .95	.8 to 2.0	III	75-93
		1.4/1,12°,C-D					.7 to .95	.8 to 2.0	III	94-111&305 -311
N_2		Con.	1.12	.1	1.321	.671	.7 to .95	1.0 to 3.0	II	498-519
		Con.					.7 to .95	1.0 to 3.0	I	279-327
		Con.					.7 to .95	1.0 to 3.0	II	466-476
		2/1,6°,C-D					Static	1.0 to 3.0	II	465
		2/1,12°,C-D					.7 to .95	1.0 to 3.0	II	445-464
		1.4/1,6°,C-D					.7 to .95	.8 to 2.0	III	112-131
		1.4/1,12°,C-D					.7 to .95	.8 to 2.0	III	132-149
		Con.					.7 to .95	1.0 to 3.0	II	477-496
N_3		Con.	.79	.2	1.321	.671	.7 to .95	1.0 to 3.0	I	328-363
		Con.					.7 to .95	1.0 to 3.0	II	111-129
		Con.					.7 to .95	1.0 to 3.0	III	35-62
		Con.					.7 to .95	1.0 to 3.0	II	63-85,108+ +110
		Con.					.7 to .95	1.0 to 3.0	II	86-107
		1.4/1,6°,C-D					.7 to .95	.8 to 2.0	III	163-176
		1.4/1,12°,C-D					.7 to .95	.8 to 2.0	III	177-197
	*	Con.					.7 to .95	1.0 to 3.0	III	330-355
	*	Con.					.7 to .95	1.0 to 3.0	III	356-371
	*	Con.					.7 to .95	1.0 to 3.0	III	372-388

* LARGE TAIL

Figure 1-19: Parametric Test Configuration Geometry

CONFIGURATION		GEOMETRY					TEST CONDITIONS		TEST ENTRY	RUN NO'S
AFTER-BODY DESIG-NATIONS	TAIL TYPE	NOZZLE TYPE	IMS	A_9/A_{10}	$L/_{DEQ}$	$S/_{DEQ}$	MACH NO.	PNS/P_∞	PARA	
N_4	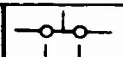	Con Con	.99	.2	1.321	.671	.7 to .950 .7 to .950	1.0 to 3.0 1.0 to 3.0	II II	213-231 271-291
N_5	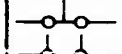	Con Con	.45	.1	2.641	.671	.7 to .975 .7 to .975	1.0 to 3.0 1.0 to 3.0	I II	364-391 232-251
N_6	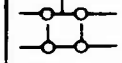	Con Con	.56	.1	2.641	.671	.7 to .975 .7 to .975	1.0 to 3.0 1.0 to 3.0	II II	252-270 298-317
N_7	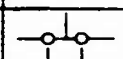	Con Con	.40	.2	2.641	.671	.7 to .975 .7 to .975	1.0 to 3.0 1.0 to 3.0	I I,II III	119-187 *
	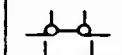	Con					.7 to .975	1.0 to 3.0	II	375-384
	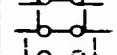	Con					.7 to .975	1.0 to 3.0	II	150-174
	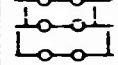	Con					.7 to .975	OFF	II	175-189
		Con					.9 to .975	OFF	II	185-187
	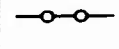	Con					.7 to .975	OFF	II	527-532
*N_7		Para I 188-217 392-406	Para II 1-34 189-212 292-297 358-374 520-526		Para III 1-24 150-162 389-401 420-423					
N_8	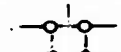	Con Con	.40	.2	2.641	.671	.7 to .975 .7 to .975	1.0 to 3.0 1.0 to 3.0	II II	318-335 341-357
N_9	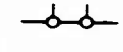	Con	.67	.4	1.321	.671	.7 to .95	1.0 to 3.0	II & III	336-340 55-74

Figure 1-19 (Cont.) Parametric Test Configuration Geometry

CONFIGURATION		GEOMETRY					TEST CONDITIONS		TEST ENTRY	RUN NO'S
AFTER-BODY DESIG-NATIONS	TAIL TYPE	NOZZLE TYPE	IMS	A_9/A_{10}	$L/_{DEQ}$	$S/_{DEQ}$	MACH NO.	PNS/P_∞	PARA	
N_{10}	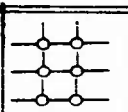	Con 2/1,Plug 4/1,Plug	.36	.4	1.321	.671	.7 to .975 .7 to .975 .7 to .975	1.0 to 3.0 1.0 to 3.0 1.0 to 3.0	III III III	198-222 243-260 261-283
N_{11}	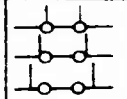	Con Con Con	.34	.1	3.60	.671	.7 to .975 .7 to .975 .7 to .975	1.0 to 3.0 1.0 to 3.0 OFF	II II II	385-401 402-418 419-426
N_{12}	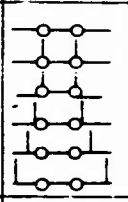	Con Con Con Con Con Con	.68	1.	3.61	.671	.7 to .975 .7 to .975 .7 to .975 .7 to .975 .7 to .975 .7 to .975	1.0 to 3.0 1.0 to 3.0 1.0 to 3.0 1.0 to 3.0 1.0 to 3.0 OFF	II II II II II II	603-615 427-444 588-602 551-569 570-581 582-587
N_{13}	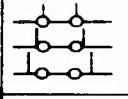	Con Con Con	1.07	.1	3.60	.671	.7 to .975 .7 to .975 .7 to .975	1.0 to 3.0 1.0 to 3.0 1.0 to 3.0	II II II	619-632 633-644 645-665
N_{14}	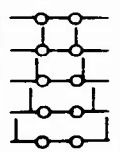	Con Con Con Con Con	.91	.1	1.321	1.28	.7 to .975 .7 to .975 .7 to .975 .7 to .975 .7 to .975	1.0 to 3.0 1.0 to 3.0 1.0 to 3.0 1.0 to 3.0 1.0 to 3.0	III III III III III	526-544 * 545-561 562-577 578-595

*N_{14} Para III
509-526
674-686
763-775

Figure 1-19: (Cont.) Parametric Test Configuration Geometry

CONFIGURATION		GEOMETRY					TEST CONDITIONS		TEST ENTRY	RUN NO'S
AFTER-BODY DESIG-NATIONS	TAIL TYPE	NOZZLE TYPE	IMS	A_9/A_{10}	$L/_{DEQ}$	$S/_{DEQ}$	MACH NO.	PNS/P_∞	PARA	
N_{15}	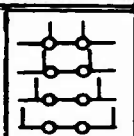	Con Con Con Con	.66	.1	2.641	1.28	.7 to .975 .7 to .975 .7 to .975 .7 to .975	1.0 to 3.0 1.0 to 3.0 1.0 to 3.0 1.0 to 3.0	III III III III	596-621 622-638 639-656 657-673
N_{16}		Con		.1	2.641	1.28	.7 to .975	1.0 to 3.0	III	687-706
N_{17}	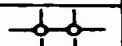	Con 1.4/1,6°, C-D	.65	.2	2.641	1.28	.7 to .975 .7 to .975	1.0 to 2.0 .8 to 2.0	III III	707-726 727-735
N_{18}	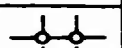	Con 1.4/1,6°, C-D		.2	2.641	1.28	.7 to .975 .7 to .975	1.0 to 2.0 .8 to 2.0	III III	736-753 754-762
N_{19}	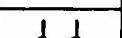	Con	.454	.4	1.321	.671	.7 to .950	1.0 to 3.0	III	312-329
N_{20}	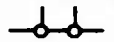	I.4/1,6°, C-D	1.03	.4	2.641	.671	.7 to .975	.8 to 2.0	III	224-242
N_{21}	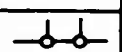	1.4/1,6°, C-D	.66	.4	3.60	.671	.7 to .975	.8 to 2.0	III	286-304
N_{22}	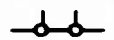	Con	1.05	.2	3.60	.671	.7 to .975	1.0 to 3.0	III	25-54 402-419

Figure 1-19: Concluded Parametric Test Configuration Geometry

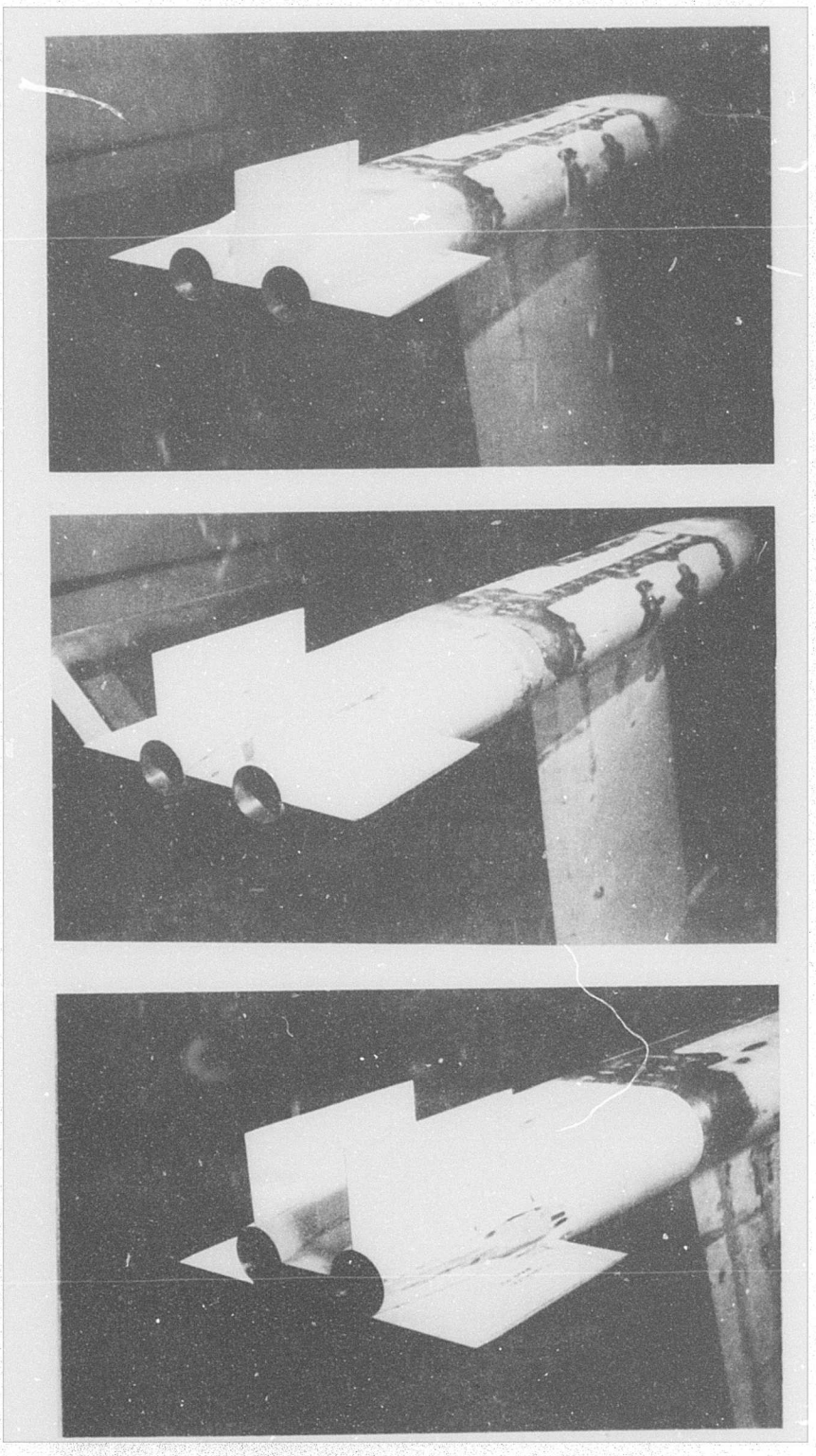

SINGLE TAIL

TWIN VERTICAL
ON NACELLE

TWIN VERTICAL
WITH LOWERED
HORIZONTALS

TAIL TYPES

Figure 1-20

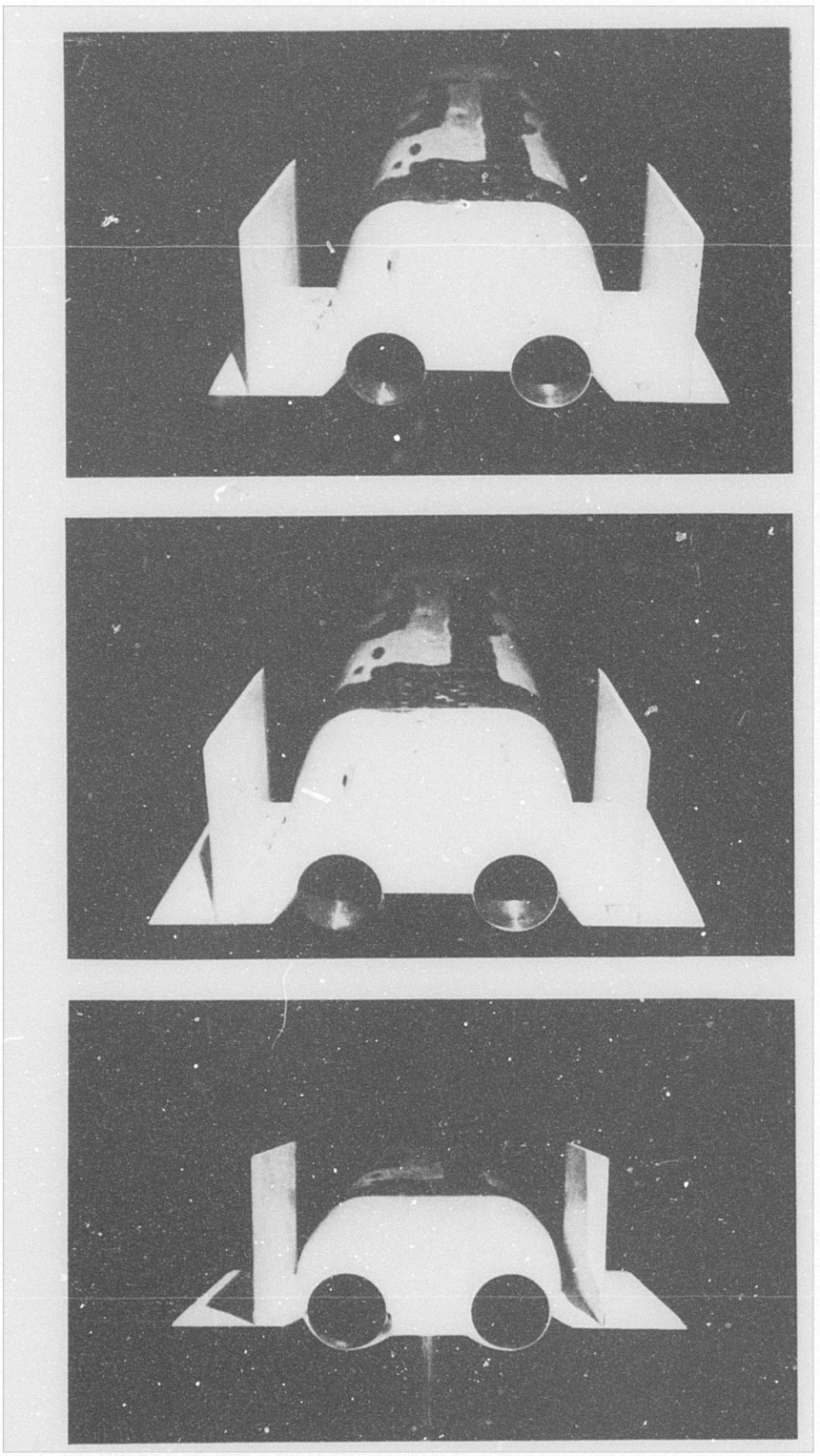

1.20-In. Spacing Between LE of Vertical and Body

.60-In. Spacing

.00-In. Spacing

Figure 1-21: N_3 With Twin Boom Tails

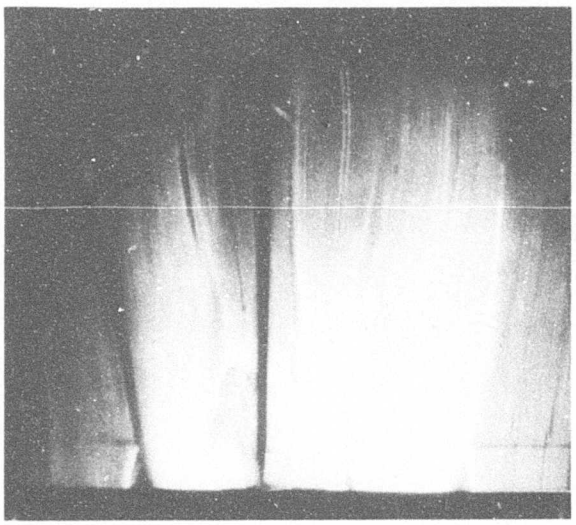

SINGLE TAIL

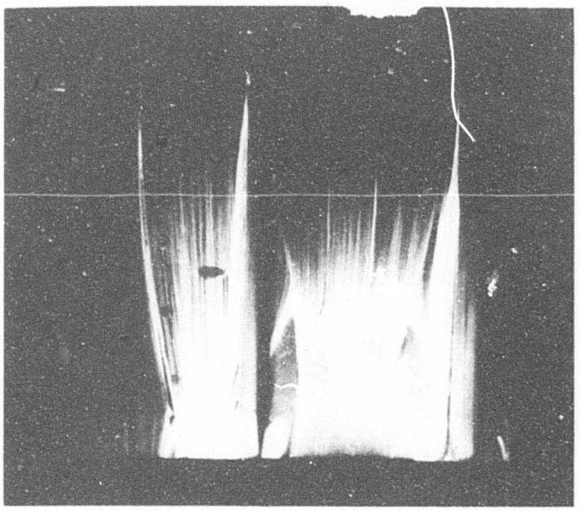

TWIN VERTICAL ON NACELLE $\mathbb{Q}_L$

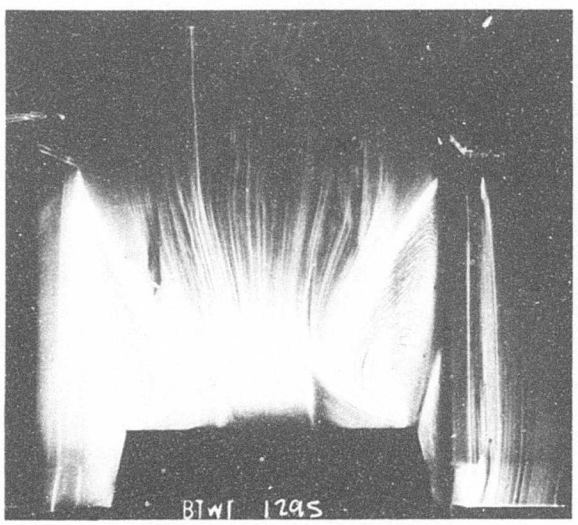

TWIN BOOM VERTICAL
.00" SPACING BETWEEN
TAIL AND BODY

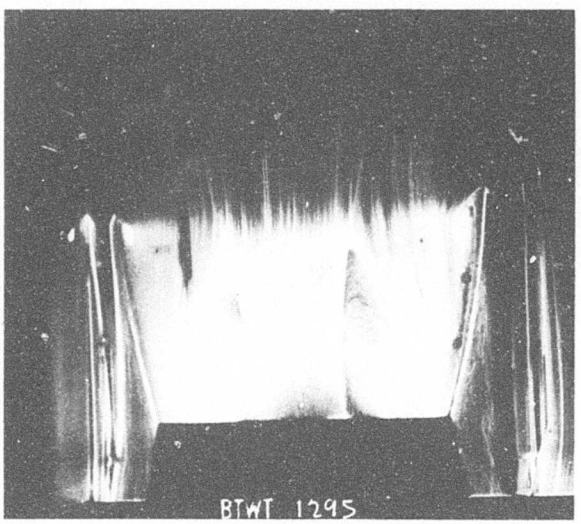

TWIN BOOM VERTICAL
.60" SPACING BETWEEN
TAIL AND BODY

Figure 1-22: N_3 Tail Type Effects Mach = .90 Oilflows

Evaluations of competing configurations, both in-house and by the government, and tracking of performance throughout the life of a program, would be facilitated by an industry-wide common element performance integration method. Such a method is proposed.

A common set of Level II element performance prediction methods would also improve and facilitate industry-side prediction work and comparisons. The result of the Phase I wind tunnel test and correlations of this data are offered as a start.

1.2 PHASE II SUMMARY

1.2.1 Introduction

The first phases in development of a weapon system were simulated in the second phase of the Exhaust System Interaction Program (ESIP). The development simulation was intended to employ some of the procedures, phasing and methodology identified in Phase I investigations. Attention was directed toward selection of propulsion system components, proper integration of those components into the weapon system and evaluation of component and system performance. Propulsion system installation losses, particularly in the exhaust area, would receive careful scrutiny. Exhaust system installation losses would be evaluated at several levels of validity.

System definition and performance analyses conducted in Phase II was directed toward satisfaction of the following goals:

- Determination of engine company/airframer communication requirements for selection of an optimum engine/airframe combination.
- Improvement of system integration and analysis processes with provision for element performance visibility and interactive engine/airframe integration capabilities.
- Identification of good combinations of engines and airframes for the Phase II system with eventual definition of engine/airframe combinations for Phase II/III wind tunnel models.
- Determination of data requirements to allow accurate prediction of engine/exhaust system installation losses and, therefore, selection of proper propulsion system components.

The weapon system development was initiated with specification of operational requirements. Preliminary analyses led to establishment of baseline system concepts and design criteria. Engines were selected and airframes were configured about them. Element performance was estimated and programmed for

evaluation of integrated system performance. Finally, superior engines, airframes and systems, as well as integration and analysis methods, were identified in comparisons of their relative merits.

The following section describes the major technological areas that were encountered in the Phase II analyses. The purpose of this particular section is to present an overall picture of the complete system development process that was followed. The reader is referred to succeeding sections for detailed discussions of Phase II efforts in the following areas:

- Section 9.0 - Obtaining the Fighter/Bomber Baseline:
  This section covers the very conceptual design stage between specification of mission requirements and first configuration of a feasible, properly integrated system.

- Section 10.0 - Configuring the Fighter/Bomber:
  This section discusses the configuration processes and design criteria which governed evolution of a wide variety of fighter/bomber configurations designed for analysis in Phase II.

- Section 11.0 - The Boeing Engine-Airplane Matching Program (BEAM), TEM 129C:
  This section describes the performance analysis computer program that was used for Phase II mission analyses and analytical system integration.

- Section 12.0 - Engine Selection and Airframe-Engine Company Data Exchange:
  Procedures and communications that led to identification of optimum engine characteristics in the Phase II development simulation are discussed in this section.

- Section 13.0 - Results of Phase II Fighter/Bomber System Definition and Performance Analysis:
  Development simulation results are presented and discussed in this section.

- Section 14.0 - Phase II and III Test Program Description:
  The ESIP Phase II and III wind tunnel test programs to be conducted in the AEDC PWT 16-foot facilities are described. Program objectives are specified and the technical approach to attain these objectives is outlined. Applications of test program results to the overall ESIP program objectives are discussed. Brief descriptions of test model and support system hardware, data system requirements, and test operating conditions are given. The test was not conducted under ESIP because of excessive slides in the AEDC 16T and 16S schedules.

- Section 15.0 - Phase I Data Correlation:
  Afterbody pressure drag data obtained during the Phase I parametric afterbody drag test were correlated and a simple, fast pressure drag prediction method for twin, faired afterbodies was developed.

- Section 16.0 - ESIP Phase II Model Strut Evaluation:
  A mounting strut interference study is proposed for the AEDC 1T facility. The primary purpose of the test program is to determine in a qualitative manner the effects on model afterbody pressure data of boundary layer removal (suction) along the trailing edge of a mounting strut similar to the strut for the Phase II model for the 16-foot tunnel. The test was not conducted under ESIP because of excessive slides in the AEDC 1T schedule.

- Section 17.0 - Inputs to the Phase II Analysis:
  This section contains collective inputs of afterbody drag, airframe drag, inlet performance and structural weight relationships used in the Phase II analyses.

The Air Force Aero/Propulsion Laboratory specified the mission requirements and a technology level for a system to serve as an example on which to develop and demonstrate techniques identified in Phase I. Engine cycle concepts were suggested for investigation. These were originally mixed and separate flow turbofans and turbojets with high turbine inlet temperatures approaching the stoichiometric limit.

Subsequently, variable area turbine engines were added. This engine type offers the potential to maintain a large nozzle area throughout the power setting range, eliminating the steep closure characteristic of afterburning type engines at low power settings. A possibility also exists that inlet spillage rates can be reduced by controlling the mass flow of the engine to match the characteristics of the inlet. If such an engine were feasible, much of the early integration testing could be reduced or delayed, for several reasons:

1. Low installation losses over the entire operating envelope may permit cycle selection without exact knowledge of their magnitude.

2. It is usually easier to predict the performance of low-loss devices than it is of devices operating on the edge of a "tolerable" performance level.

3. The additional degree of freedom within the engine may permit matching an existing engine to peculiar characteristics of an inlet or exhaust system that were not known when the engine design was frozen.

Thus, it appears that recommendations may differ considerably regarding the type and timing of the data and testing required to predict the total propulsion system performance of specific configurations, for the purpose of cycle and exhaust system selection, depending on the type of engine involved.

As a result of the above considerations, the following guidelines for Phase II were proposed:

1. Configure a number of airplanes, including a wide variety of engine and afterbody types.

2. All engines will be of the same advanced technology, consistent with the technology used in APSI studies. The engine types will include:

a) mixed flow fixed geometry turbofan
b) separate flow fixed geometry turbofan
c) turbojet
d) variable geometry turbofan
e) variable geometry turbojet

3. Nozzles will include convergent, convergent-divergent and plug types.

4. An inlet matrix is not planned. A mixed compression, two-dimensional inlet will be used. However, an external compression inlet would be considered.

5. No matrix of airframe types, other than implied by the aft-end type, was contemplated.

6. Optimizations of the various engine/airframe combinations will be limited to sizing the wing, engine and airplane for Level I estimates. Engine cycle optimization of General Electric engines would be severely limited because level of funding was not established with a requirement for advanced technology or variable geometry engines. Pratt & Whitney Aircraft would provide a matrix of fixed geometry fans and jets and a matrix of variable geometry engines.

7. Gross weight required to perform the given mission will be computed for each configuration using various levels of data for afterbody drag. These configurations will be ranked each time. Changes in ranking as a function of afterbody drag data level will be considered evidence that the higher level data is necessary before any one of the configurations can be selected as best.

It is felt that gross weight or range comparisons among configurations employing fixed and variable area turbine engines will not be meaningful unless all airplane elements are optimized for each engine and at each level of comparison. The cost of higher level data for elements other than the afterbody was beyond the funding of the program.

8. The three different levels of afterbody drag data are defined as:

a) presently available - Level I
b) parametric data to be obtained in Phase II tests - Level II
c) configuration data to be obtained in Phase II/III tests - Level III

9. The Phase I and II tests will also include studies of test techniques necessary to ensure that the data is valid.

10. A study will be conducted to explore how afterbody design features and details develop as the airplane definition progresses from (a) a general arrangement drawing configured during the mission analysis phase, (b) to drawings which serve as the basis for Level II studies and parametric testing, and (c) then to drawings from which Level III configuration models are built. The impact of changes in design detail on afterbody drag will be estimated. Testing may be required to demonstrate the danger of afterbody/cycle selection on the basis of test data obtained from "immature" configurations.

A total of 20 engines, 12 from Pratt & Whitney Aircraft and 8 from General Electric, were partially matrixed with 7 airframe configuration types and analyzed with several levels of afterbody drag before the Phase II development simulation was concluded.

1.2.2 Mission Definition

The mission profile was selected under the following ground rules:

1. The mission must be operationally realistic.

2. The mission requirements must be such that the required technology is now available or will be available within the near future.

3. The mission profile must consist of a wide range of propulsion system operating points and must be such that roughly equal priority is given to both supersonic and subsonic operation.

4. The mission must be unclassified.

Airframe/engine combinations will be processed through mission analysis using the same specified mission. The propulsion system will be sized at the critical mission points. The resulting thrust requirement will control the amount of resizing of the baseline airframe to meet the mission constraints. After completing the mission studies, the

relative merits of each configuration for the designated mission should become apparent. Each configuration should be ranked with respect to the others according to the ground rules of the mission study.

Mission requirements were patterned after those of an advanced tactical fighter or fighter/bomber. The specified mission profile is illustrated in Figure 1-23. Mission requirements, described by segment, are:

1. Warm-Up and Takeoff: Fuel allowance for starting engines, taxi, takeoff, and accelerate to climb speed is the sum of the fuel used in 6 minutes with sea level installed thrust loading of 0.2 and 0.2 minutes of sea level maximum A/B power.

2. Climb: Climb on course, to the best cruise altitude and speed at military power.

3. Cruise: Cruise 250 n.mi. (including climb distance) at altitude and speed for best range.

4. Descent: Descend to 25,000 ft (no fuel consumed, no distance gained).

5. Acceleration: Accelerate at constant altitude (25,000 ft) to M_{PEN} (2.3) at maximum A/B power.

6. Cruise: Cruise at 25,000 ft for 50 n.mi. (including acceleration distance) at M_{PEN}.

7. Drop Payload: Drop payload of 2000 lbs.

8. Cruise: Cruise at 25,000 ft for 50 n.mi. at M_{PEN}.

9. Combat: Combat for 2 minutes at maximum power at 25,000 ft, M = 0.9. Expend gun ammunition (548 lbs).

   Maximum Sustained Level Flight "G" Loading - 4.25
   P_S @ 1 g - 600 ft/sec

10. Acceleration: Accelerate at constant altitude (25,000 ft) from combat Mach number (0.9) to M_{MAX} (2.7) at maximum A/B power. The maximum allowable time for the acceleration is 1.0 minutes.

11. Deceleration: Decelerate from 25,000 ft, M_{MAX} to best cruise altitude and speed (no fuel consumed).

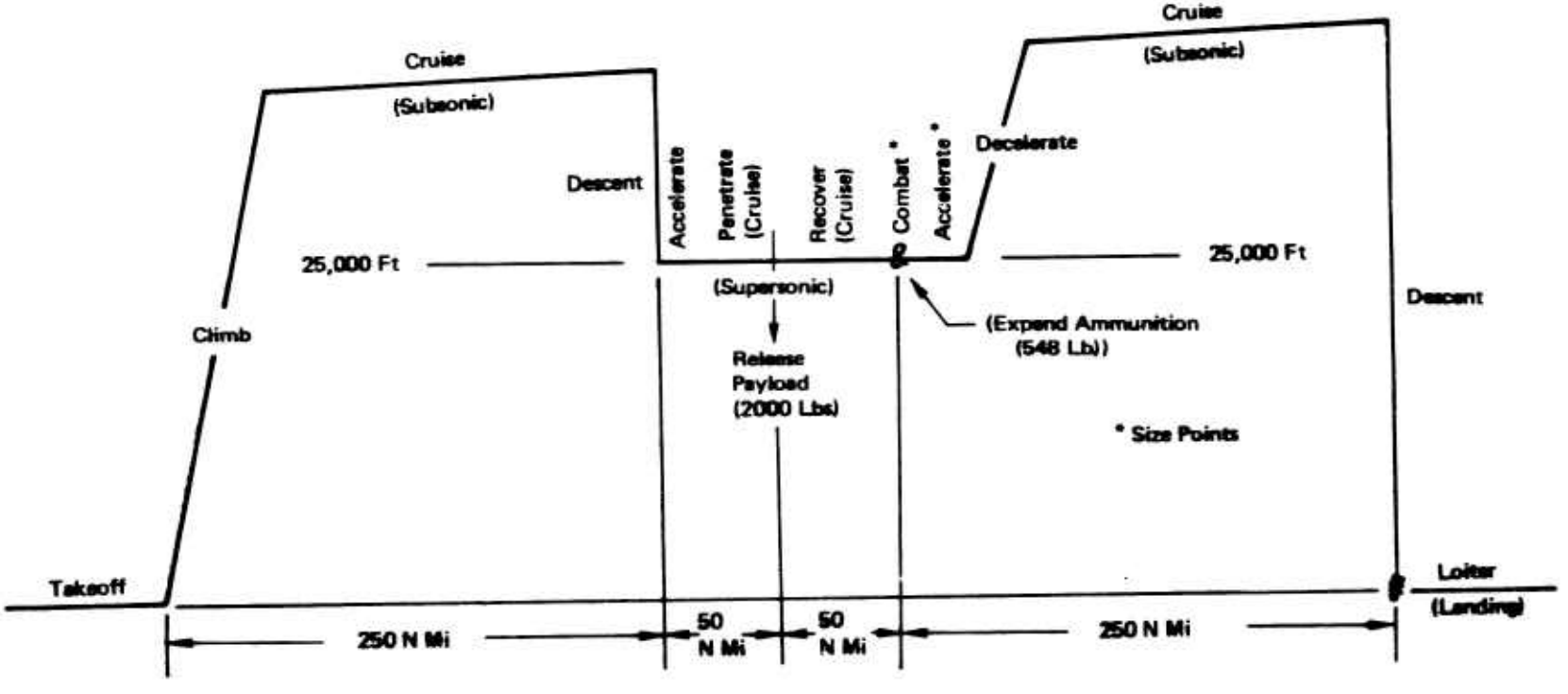

Figure 1-23: ESIP Fighter/Bomber Mission

12. Cruise: Cruise 250 n.mi. (including acceleration and deceleration distances) at altitude and speed for best range.

13. Descent: Descend to sea level (no fuel consumed, no distance gained).

14. Landing: Fuel allowance for landing and reserves is the sum of 5 percent of initial fuel and 20 minutes at speed for maximum endurance at sea level with all engines operating.

Review of mission requirements leads to formulation of design and analysis criteria. Engine size points in the acceleration and combat segments can be identified. Requirements for substantial supersonic capability, efficient subsonic cruise capability and high dynamic pressure tolerance are notable.

Following detailed examination of system requirements, the development simulation passed into the conceptual stage in which a baseline configuration is established.

1.2.3 Obtaining the Fighter/Bomber Baseline

The process in which airframe and propulsion system element concepts are selected, integrated and evaluated can be simply stated. Based on requirements, component concepts are selected using engineering judgement and experience. Component sizes are estimated. Selected component types, at the sizes estimated for them, are assembled into a system. The system's definition and the performance of its elements are used to predict the performance capability of the design.

The process is an iterative one. In the beginning it is not known which of a variety of airframe and engine cycle concepts or which variables within those concepts should be combined to form the weapon system. By its inherently iterative nature, however, the system definition process eventually converges on a near optimum system as more and more element and system performance data are made available at higher and higher levels of validity.

Following review of requirements, a conceptual fighter/bomber system was fisualized. It was a streamlined design with variable sweep wings. Horizontal ramp, two-dimensional, side mounted, mixed compression inlets would be used. Two engines would be located side-by-side, in the afterbody. A two man crew would be seated in tandem. Empennage would be conventionally arranged.

System and component performance levels were estimated grossly. Using an assumed maximum combat lift capability, wing and thrust loadings required for combat were estimated. Rough mission performance calculations, using available, representative engine data, yielded a credible first guess takeoff gross weight (80,000 lbs) and structural weight fraction. These estimated weights, along with approximated wing, inlet, and engine sizes were communicated to the designer.

The first configuration representation was assembled. Using this common focal point, element performance control disciplines (Aerodynamics, Propulsion and Structures-Weights) made detailed Level I estimates of element performance. These estimates were assembled and programmed for computerized determination of system performance.

Resultant performance levels were inappropriate to the specified requirements. The system was excessively heavy at 80,000 lbs and exceeded the mission range requirement substantially.

Successive iterations which also included configuration and element and system performance determinations, led to reduced takeoff gross weight. Wing sizing criteria was adjusted to reduce weight still further.

As has been stated, a maximum lift capability in combat had been used in determination of the fighter/bomber wing size. Satisfaction of the 4.25 "g" load factor requirement with high levels of lift (C_L) caused high wing loadings or relatively small wing sizes. However, engine sizes required to overcome the high level of drag experienced at maximum lift levels were excessive.

An alternate approach was examined. Wing loading was lowered, wing sizes increased and, consequently, the combat lift requirement reduced. Lower drag levels at the lower lift coefficients could be overcome with a smaller propulsion system. Structural weight studies eventually revealed that the trade of propulsion system weight for wing weight was a favorable one (see Figure 1-24). A more efficient system could be configured by the alternate criteria.

Eventually a feasible fighter/bomber system was determined. Mission requirements could be satisfied at takeoff gross weights near 50,000 lbs. All mission sized components could be assembled logically and efficiently within that gross weight limitation and the selected configuration concept. System and element design criteria, specified by all involved technologies, were satisfied. The baseline configuration concept was established.

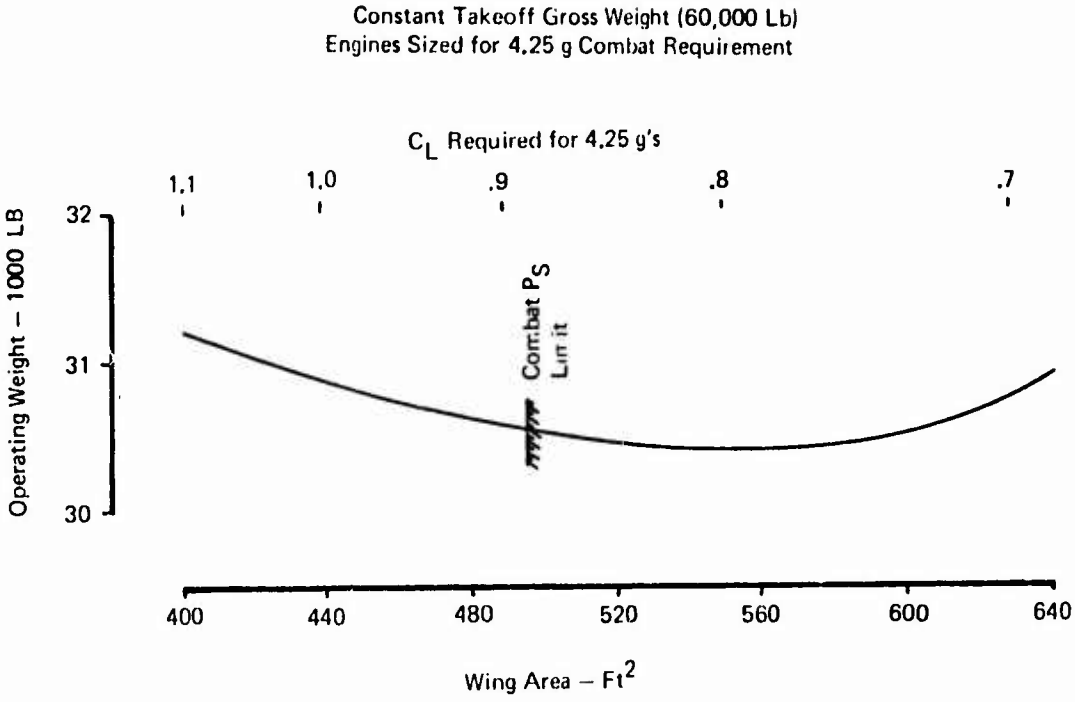

Figure 1-24: Wing Area/Weight Trade

Much of the baseline configuration concept would not vary throughout the Phase II development simulation. Other than inlet size, definition of the system forward of body maximum cross-sectional area would remain essentially fixed. Reference airplane wing concept and size would not vary. Engine, empennage, and gear sizing criteria would be applicable to all Phase II configurations.

On the other hand, many different engine signatures would be examined. A variety of afterbody arrangements would be configured about them. Engine shape would be exploited by adjustments to body cross-sectional area distribution philosophy.

1.2.4 Engines and Engine Company/Airframer Communication

Following establishment of the baseline concept, system engine requirements and installation considerations were assembled and transmitted to Pratt & Whitney Aircraft and General Electric. These two companies, subcontracting to Boeing on ESIP, would use that information to define candidate engines for analysis in Phase II engine/airplane matching.

A total of 20 candidate engines were examined before Phase II analyses were concluded. Twelve of these came from Pratt & Whitney, while the remaining 8 were supplied by General Electric. Pratt & Whitney offerings were generally supplied in parametric families. General Electric supplied engine data in more of a series approach. All engines were advanced technology, high turbine inlet temperature designs.

1.2.4.1 Pratt & Whitney Aircraft Support

Pratt & Whitney engines were offered in three, generally parametric, groups. All Pratt & Whitney offerings were designed for, and used in, APSI studies.

The first parametric engine family received for analysis, consisted of a group of conventionally shaped, high performance turbofans (a turbojet included) with convergent-divergent nozzles. Following analysis of these designs which led to identification of cycle characteristics yielding optimum fighter/bomber performance, a data package was assembled and transmitted to Pratt & Whitney.

These data, typified by those tabulated on Table 1-I, led to definition of several improved turbofan designs.

CONFIG 908-351-11 TOGW 53492 OW 32648

ENGINE P&WA MF F208 T/W .862 AFT DRAG DATA LEVEL I

AFTERBODY 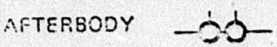 $D_{APL} = C_D q_\infty S_{REF}$ *FUEL CONSERV 5%

ENG SIZE PT ACCEL; REQMT = 1 MIN, ACTUAL = .84 MIN
COMBAT; P_S = 600 ft/sec & n = 4.25g COMBAT WT 41356

MISSION SEGMENT	ALT	M_∞	POWER SET	INSTALL FN/ENG	INSTALL SFC •	W_o/ENG	% FUEL	C_D	S_{REF}
TAKEOFF	0	0	MAX	23067	2.17	203.7	8.4	--	--
CLIMB	0	.54	MIL	17480	.98	260	5.2	.0240	487.6
CRUISE (1)	36560	.82	.44 MIL	2090	1.05	62.5	13.1	.0394	487.6
ACCEL (1)	25000	.82	MAX	15984	2.10	144.1	11.9	.0213	750
PENETR	25000	2.3	.07 AUG	19274	1.45	491.8	8.1	.0185	750
RECOVER	25000	2.3	.07 AUG	19236	1.45	491.8	11.6	.0184	750
COMBAT	25000	.90	MAX	16311	2.12	148.2	13.2	.0245	505
ACCEL (2)	25000	.90	MAX	--	--	--	11.8	.0165	750
CRUISE (2)	43554	.82	.44 MIL	1535	1.06	44.7	8.9	.0404	487.6
LOITER	0	.32	.07 MIL	1378	1.49	90.5	7.8	.0373	487.6

Table 1-I: ESIP Propulsion System Installed Performance Summary

Analysis of both the original and improved turbofans and continuous data transmittals directed definition of a parametric family of variable geometry turbine (VGT) turbofans and a variable geometry turbine turbojet.

These engines were characteristically short, separate flow machines with plug nozzles. Once again analysis led to definition of optimum cycle characteristics within this parametric family. Another data package was assembled and transmitted to Pratt & Whitney.

The final engine offering from Pratt & Whitney was an improved variable geometry turbine engine. It used cycle characteristics identified as optimum for fighter/bomber performance and included core flow augmentation capability to augment fan flow augmentation.

Non-proprietary characteristics of all Pratt & Whitney offerings are presented on Table 1-II. Note the vast difference in fineness ratio between the fixed geometry turbine designs and the variable geometry turbine engines.

Analysis revealed that many of the cycles offered for ESIP by Pratt & Whitney yielded about the same high level of installed performance. A few of the cycles offered, including the turbojets, were non-competitive. This result indicates the level of screening and cycle tuning which Pratt & Whitney performed prior to transmittal of engine data to Boeing.

The parametric approach to engine selection is felt to be a fast and efficient way to determine optimum cycle characteristics within a selected cycle concept. It does not indicate, however, whether or not a cycle concept outside of parametric families examined in analyses might not lead to a more optimum system.

1.2.4.2 General Electric Support

ESIP Phase II analyses were initiated with a single General Electric engine offering. That engine, the GE16/1382-1 turbofan, was a short, low fineness ratio, separate flow "duct burner" with a sliding shroud, plug nozzle. The cycle, as originally offered, proved to be totally inappropriate for the ESIP fighter/bomber.

Airframer/engine company communications led to modification of the GE-1 airflow schedules and definition of the GE-1A cycle. This engine was a definite improvement over the initial offering but, still, below expectations.

ENGINE	F 0.0	F 0.4	F 0.8	F 1.4	F 2.1	S 1.0	S 1.6	V 0.0	V 0.9	V 1.7	V .21	A 1.7*
CYCLE TYPE	FG JET	FG FAN	———	———	———	———	FG FAN	VG JET	VG FAN	———	———	VG FAN
BYPASS RATIO	0.0	0.4	0.8	1.4	2.1	1.0	1.6	0.0	0.9	1.7	2.1	1.7
OA LENGTH/MAX DIAMETER	3.45	3.89	4.14	4.05	4.05	4.14	4.05	4.08	2.78	2.48	2.39	2.40
COMBAT MAX THRUST/WEIGHT	4.53	5.50	5.74	5.99	6.06	6.01	6.19	4.64	4.79	5.68	5.35	6.15
SLS MAX THRUST/W_0	125	126	119	111	103	120	111	129	103	99	93	109

*WITH CORE FLOW AUGMENTATION

Table 1-II: Uninstalled Pratt & Whitney Aircraft Engine Characteristics

Derivatives were calculated for the system powered by the GE-1A engine. These derivatives are the step changes in system figure of merit resulting from step changes in engine physical and performance characteristics. Engine weight, diameter, airflow, thrusts, specific fuel consumptions, etc., were varied and the effect of those variations on takeoff gross weight, system figure-of-merit were determined. These derivatives were communicated to General Electric and applied in the "derivative process," to define a succeeding, improved cycle.

General Electric 16/1382-1A derivatives led to definition of the GE-3 turbofan cycle. The GE-4, "leaky" turbojet cycle was defined in the same time period.

Derivatives determined on GE-3 powered system led eventually to definition of the GE-5 and GE-6 engines. Derivatives calculated for the GE-4 system led to the GE-2 turbojet cycle. All of these systems were similar in shape to the original General Electric offering; short, separate flow designs with plug nozzles.

A list of derivatives, typical of these transmitted regularly from Boeing to General Electric during the Phase II analyses, is illustrated in Table 1-III.

A list of non-proprietary characteristics of General Electric engines offered for ESIP Phase II analyses is presented in Table 1-IV. Included in the list are characteristics of the GE16/1382-7 engine; a mixed flow, conventionally shaped turbofan with a convergent-divergent nozzle.

Application of system derivatives; system changes resulting from perturbations of engine signature, and engine derivatives; engine performance variations caused by cycle parameter adjustments, led to eventual definition of competitive engine cycles with the derivative approach to engine cycle selection. Vast improvements in system performance at initial stages of engine/airplane matching were followed by more subtle improvements as cycle selection converged on an optimum.

Substantial amounts of data were interchanged between engine company and airframer in the process. With continual exchange of data both companies learned more of overall system requirements. The airframer saw engine signature affecting definition of the optimum derivative airframe. The engine company saw how the signature of his engines affected system performance. Opportunities were made available in which both companies could adjust their respective positions such that system performance might be optimized.

CONFIG 908-352-10 ENGINE CF16/1322-1(#2)

BASELINE DATA

TOGW 107133 W/S 114.5 T/W --

DERIVATIVE SIZING CONSTRAINTS

Ps 603.22 ft/sec n 4.25g t ≤ .0167 hr

WING LOADING HAS BEEN REOPTIMIZED AND THE ENGINES SCALED TO MEET THE SIZING CONSTRAINTS AT MINIMUM TOGW.

* LIMITING SIZE CONSTRAINT

PROPULSION INDEPENDENT VARIABLE	DELTA (%)	Δ TOGW (LB)	Δ TOGW / TOGW (%)	MISSION CONSTRAINTS		
				P_s (ft/sec)	n (g)	t (hr)
ENGINE DIA	-10	- 6466	-6.0	* 603.22	* 4.25	.0159
ENGINE WEIGHT	-10	-10231	-9.6	↑	↑	.0160
ENGINE LENGTH	+10	+1229	+1.2			.0160
AIRFLOW @ INLET SIZE POINT	-10	- 4760	-4.4			.0157
SFC @						
CRUISE 1 & 2	-10	- 5872	-5.5			.0161
ACCEL 1 & 2	-10	- 5361	-5.0			.0161
PEN & REC	-10	- 3587	-3.3			.0161
COMBAT	-10	- 3424	-3.2			.0161
LOITER	-10	- 2947	-2.8			.0160
FN @				↓		
ACCEL 1 & 2	+10	- 1137	-1.1	* 603.22	↓	.0137
COMBAT	+10	-10060	-9.4	645.9	* 4.25	* .0167

Table 1-III: ESIP Propulsion System Installed Performance Summary

ENGINE DESIGNATION, GE 16/1382	-1	-1A	-2	-3	-4	-5	-6	-7
CYCLE TYPE	SFTF	SFTF	SFTJ	SFTF	SFTJ	SFTF	SFTF	MFTF
BYPASS RATIO	1.24	1.24	.30	1.25	.30	1.23	1.23	.96
OA LENGTH/MAX DIAMETER	2.23	2.23	2.80	2.23	2.84	2.36	2.33	3.48
COMBAT MAX THRUST/WEIGHT	4.40	4.20	4.90	4.55	4.59	5.10	5.77	3.93
SLS MAX THRUST/W_0	97	74	129	80	105	83	105	108

Table 1-IV: Uninstalled General Electric Engine Characteristics

1.2.5 Afterbody Arrangements

A variety of afterbody arrangements were configured about the engines discussed in the previous section. The total afterbody/engine matrix examined in the Phase II development simulation is illustrated in Figure 1-25. The boxes marked with an X were the engine/airframe combinations actually evaluated.

Afterbody arrangements were selected from designs in use on current technology aircraft. Some of these aircraft are in operation. Other than physical appearance, the arrangements differ in structural concept.

Principal characteristics of the five basic afterbody arrangements are listed below:

Radially mounted twin vertical and horizontal tails and widely spaced engines are supported by cowl structure. Engines are separated by a wide, horizontal interfairing.

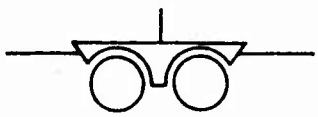

Twin vertical and horizontal tails are supported by outboard tail booms. Engines are less widely spaced and separated by a horizontal interfairing.

Single vertical, horizontal tails and narrowly spaced engines are supported by a structural yoke.

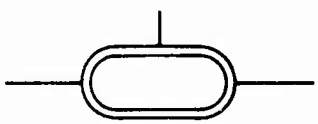

Single vertical, horizontal tails and very narrowly spaced engines are supported by a single structural ring. A base area separates the engines.

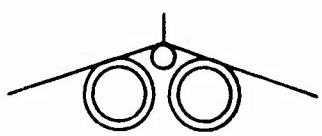

Single vertical and horizontal tails are supported by a single, central tail boom. Narrowly spaced engines are located forward and under the body.

Unique aerodynamic flow problem areas were expected to exist on each of the five afterbody types. Potentially separated flow areas on bases, booms and interfairings can be

903-351 906-352		-11	-12	-13	-14	-14A	-14B&C	-15
P&WA ENGINES								
	F00	X						
	F0.4	X	X		X			
	F0.8	X	X	X	X			X
	S1.0				X			
	F1.4	X	X		X			
	S1.6				X			
	F2.1				X			
	V0.0					X		
	V0.9					X		
	V1.7	X				X		
	A1.7					X		
	V2.1					X		
GE ENGINES 16/1382								
	-1	X						
	-1A	X						
	-2						X	
	-3						X	
	-4						X	
	-5						X	
	-6						X	
	-7				X			

Figure 1-25. ESIP Fighter/Bomber Engine/Airframe Matrix

identified. Channeled flow can be expected in some areas on some of the arrangements. These effects would be reflected in the afterbody drag levels estimated for each arrangement.

No direct effect of afterbody structural concept on structural weight can be identified with the Class I weight methods used in the second phase. Afterbody arrangement characteristics, like engine spacing, do affect parameters used in the Class I method and, therefore, the different afterbody arrangements indirectly affected structural weight. Of course, obvious distinctions, like twin as opposed to single vertical tails, impacted operating weight.

1.2.6 Configuring the Fighter/Bomber

Matrixed engines and afterbodies were integrated with the relatively fixed forebody and wing definitions to form fighter/bomber configurations for Phase II analyses. Initial, reference configurations were assembled by a designer.

The configuration process followed by the designer is illustrated in Figure 1-26. The illustration shows how the configuration effort proceeds from collection of requirements, criteria, component types and size selection, through a volume buildup, length and shape definition, to validation of the configuration in a design layout.

The first step in the process, Requirements and Data Collection, is essentially completed with establishment of the baseline concept.

The next three steps, Volume Buildup, Length and Shape Definition, are iterative for the fighter/bomber. Total system volume requirement cannot be determined until length is established since length affects diffuser volume. As length varies, changing distribution of the eventual total system volume requirement will affect shape of the fighter/bomber.

Shape or body cross-section area distribution of the fighter/bomber is extremely important. Body pressure drag, particularly wave drag at supersonic speeds, is strongly affected by shape. Interactive relationships between length and shape impact structural weight substantially. Both weight and drag are prime parameters affecting system performance, of course.

A

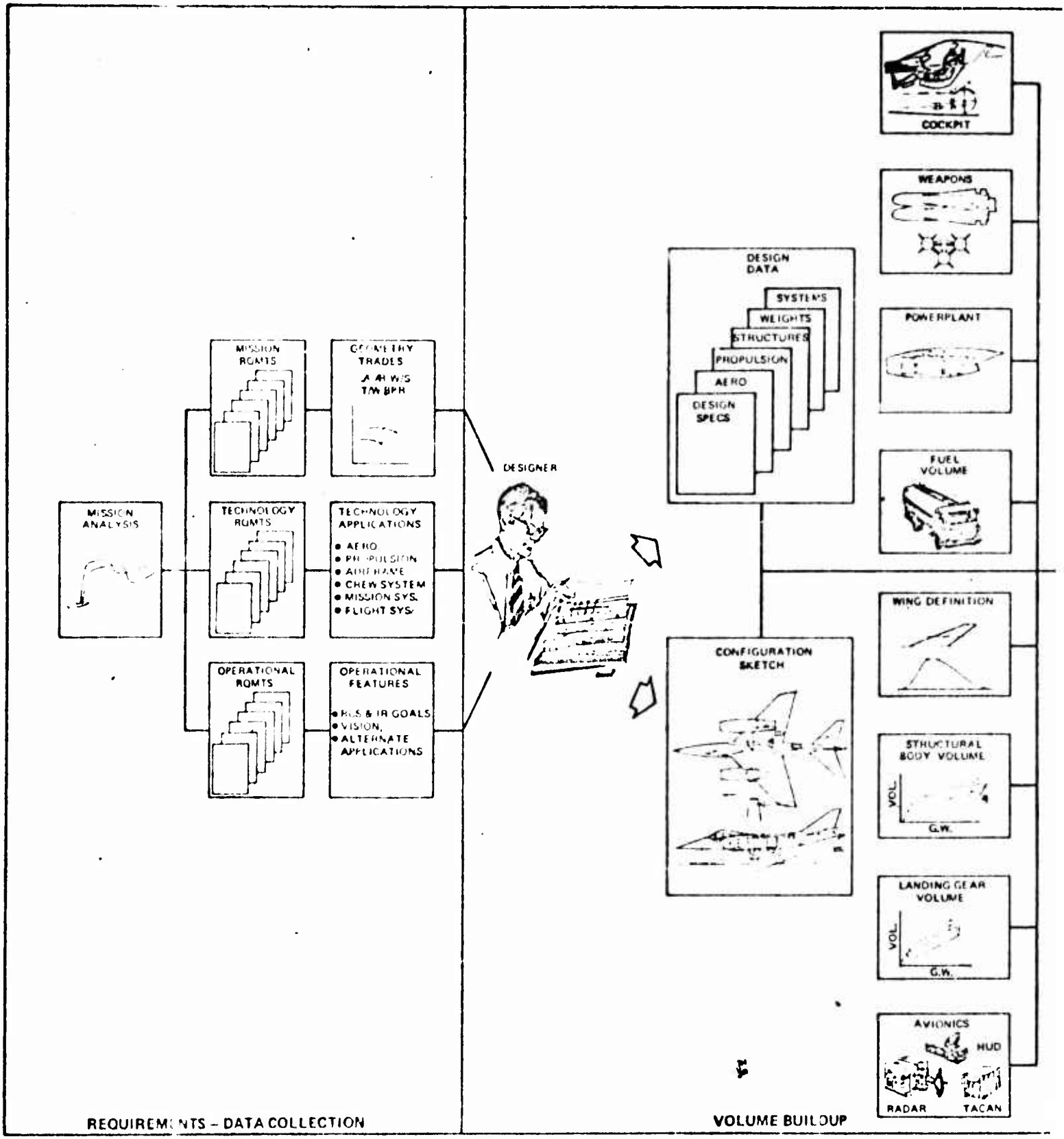
MISSION ANALYSIS
MISSION RQMTS
GEOMETRY TRADES
A/R W/S T/W BPR
TECHNOLOGY RQMTS
TECHNOLOGY APPLICATIONS
• AERO
• PROPULSION
• ADVANCE
• CREW SYSTEM
• MISSION SYS.
• FLIGHT SYS.
OPERATIONAL RQMTS
OPERATIONAL FEATURES
• R.S. & IR GOALS
• VISION,
• ALTERNATE APPLICATIONS
DESIGNER
DESIGN DATA
SYSTEMS
WEIGHTS
STRUCTURES
PROPULSION
AERO
DESIGN SPECS
CONFIGURATION SKETCH
COCKPIT
WEAPONS
POWERPLANT
FUEL VOLUME
WING DEFINITION
STRUCTURAL BODY VOLUME
VOL
G.W.
LANDING GEAR VOLUME
VOL
G.W.
AVIONICS
HUD
RADAR
TACAN
REQUIREMENTS – DATA COLLECTION
VOLUME BUILDUP

B

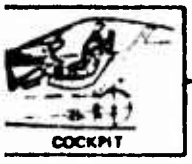

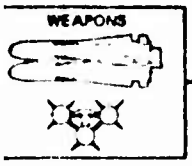

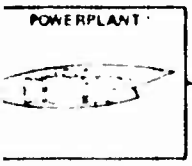

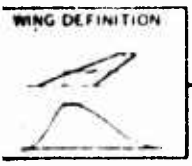

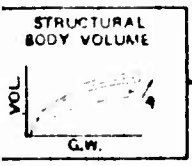

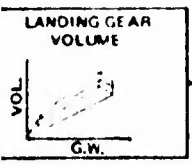

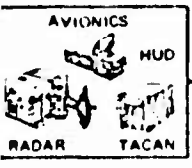

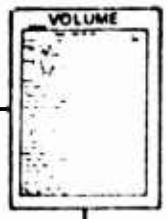

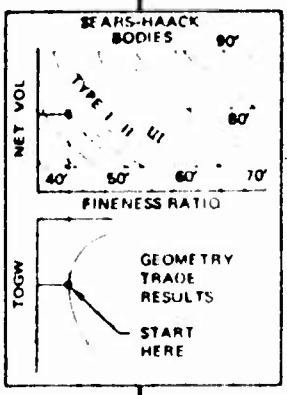

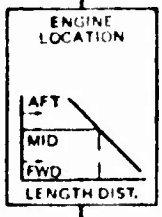

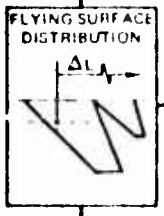

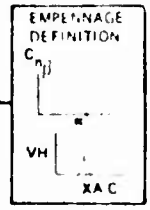

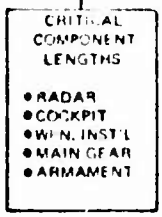

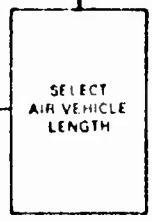

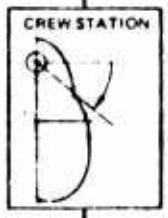

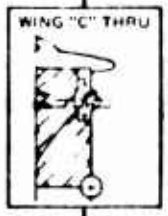

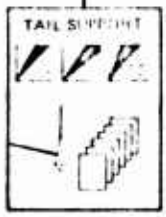

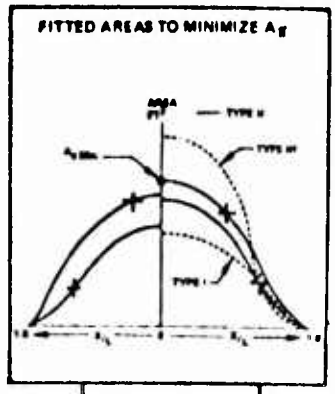

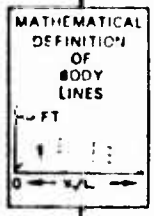

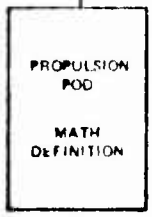

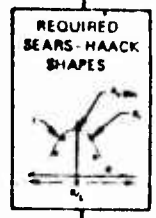

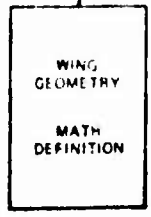

LENGTH DEFINITION

CRITICAL CONTROL POINTS

SHAPE DEFINITION

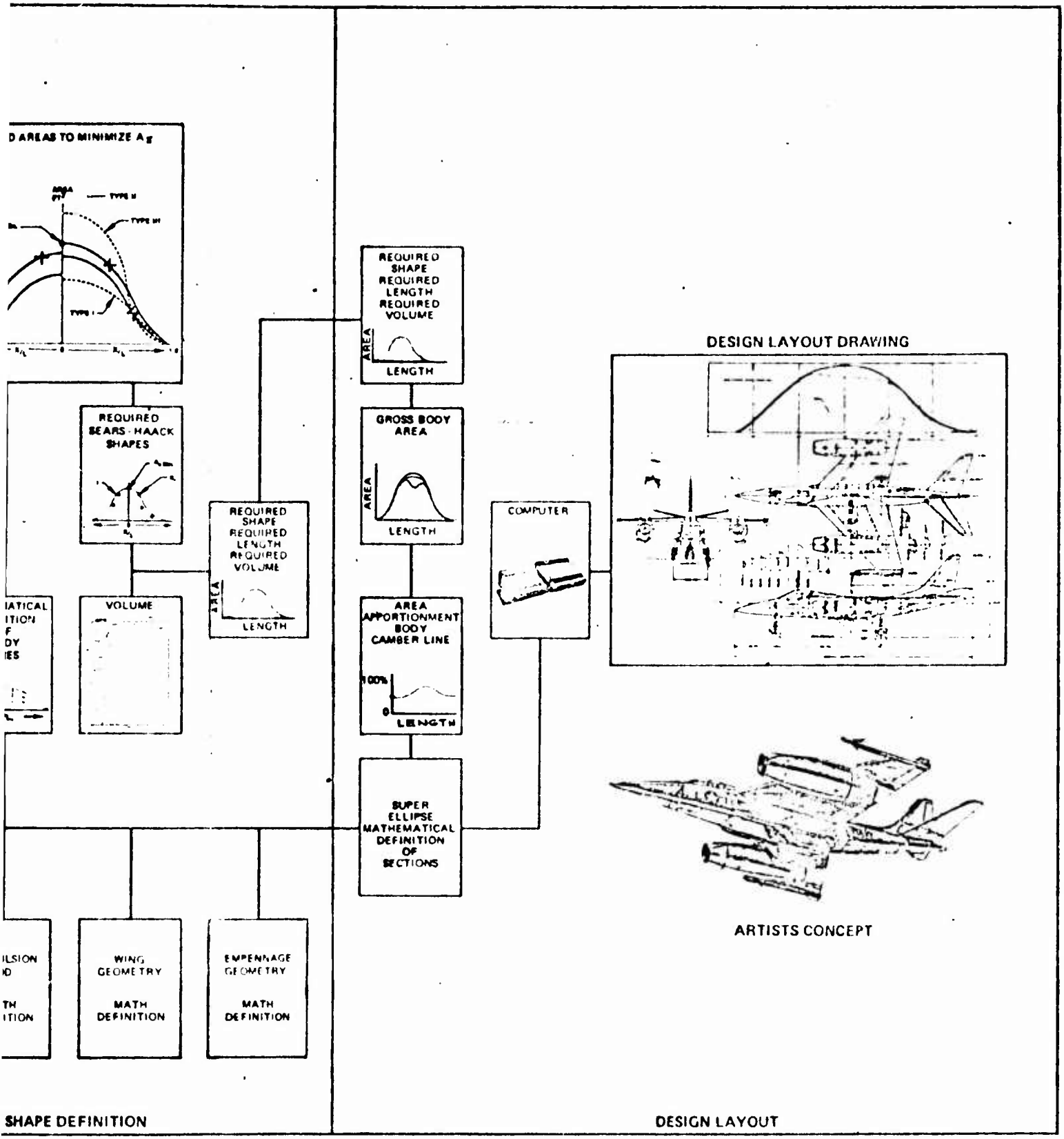

Figure 1-25: General Configuration Process

Shape is monitored and controlled with the plots of body cross-sectional area distribution. An illustrative example of such a plot is presented in Figure 1-27.

Body area distribution is designed to yield low levels of drag in the presence of the wing at design Mach numbers. Supersonic wave drag was examined in the conceptual design phase to determine fighter/bomber design Mach number. The specified supersonic cruise Mach number of 2.3 was selected for design. Comparisons showed little degradation in performance at off-design Mach numbers for a system designed at Mach 2.3.

Distribution of body cross-sectional area is influenced by location and makeup of "critical cross-sections" or "control points." These are specific cross-sectional area requirements which cannot be violated without a major change in design criteria or configuration concept. Six have been identified for the fighter/bomber and are shown as closed symbols on the area distribution presented in Figure 1-27. They are in the areas of:

- crew space
- wing pivot station
- main landing gear spaces
- empennage structural support station
- "customer connect" station
- end of the fuselage

Open symbols shown on the area plot are those programmed for system performance analysis (TEM 129C).

The configuration process is finalized with validation of an arrangement by Design Layout. This function checks the feasibility and logic of component arrangement. Aerodynamic/structural weight relationship is qualitatively assessed at this step.

Two of the ESIP fighter/bomber designs carried through Design Layout are presented in Figures 1-28 and 1-29. The first of these is relatively long and contains long, conventionally shaped engines. The second design is shorter. To satisfy a similar total system volume requirement in the shorter length, the area distribution of this body must bulge. A higher drag level results. However, higher drag is somewhat balanced by a reduction in structural weight for the shorter design.

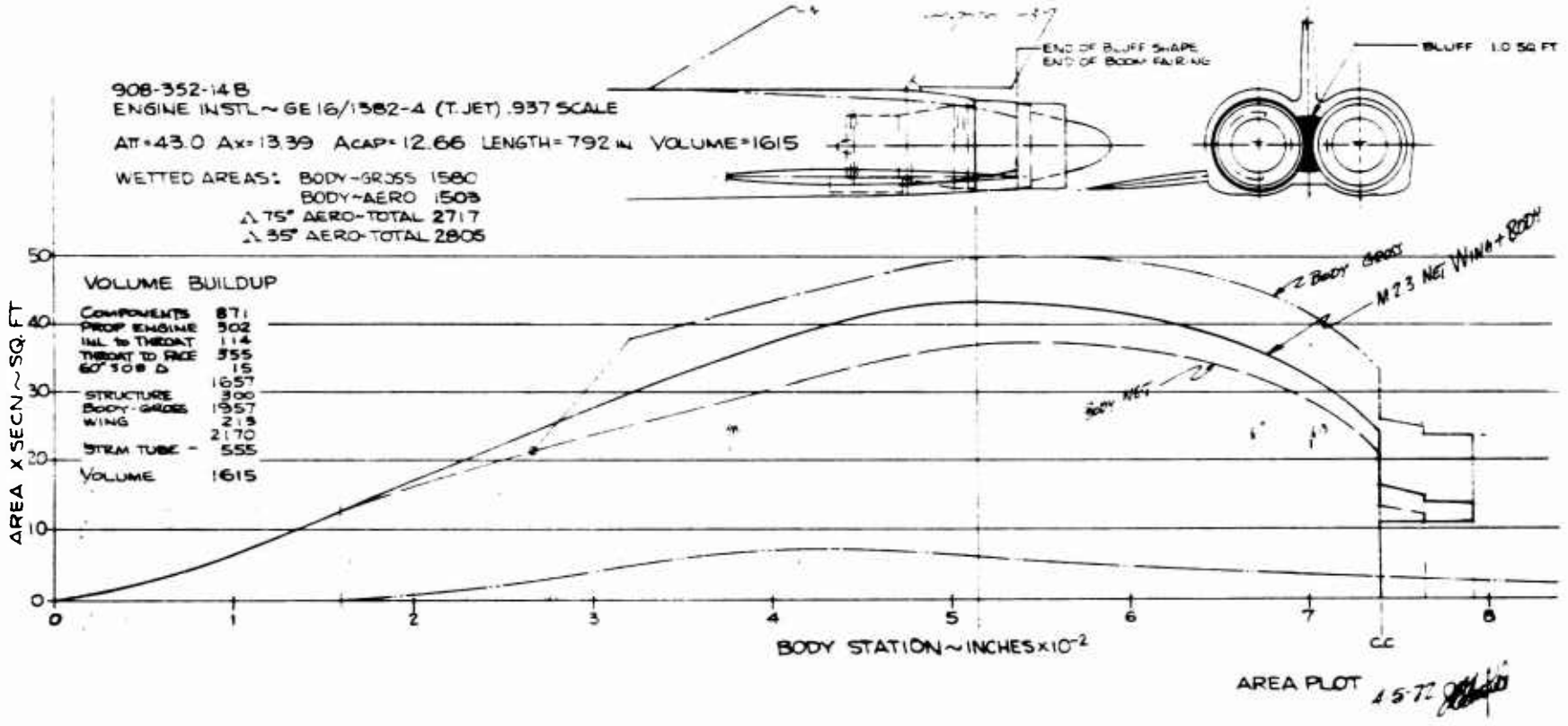

Figure 1-27: ESIP Model 908-352-14B Area Distribution

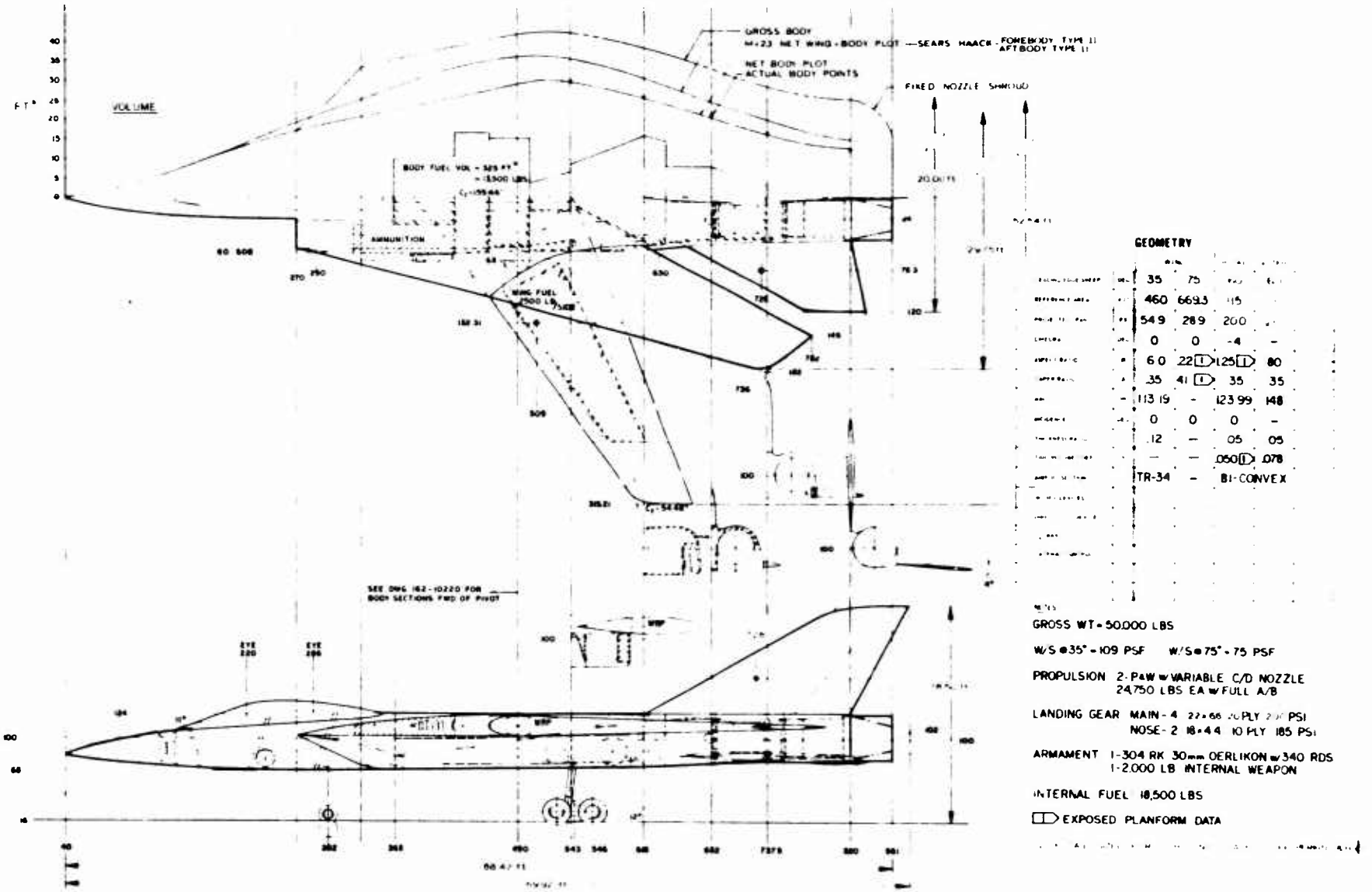

Figure 1-28: ESIP Model 908-351-14 General Arrangement

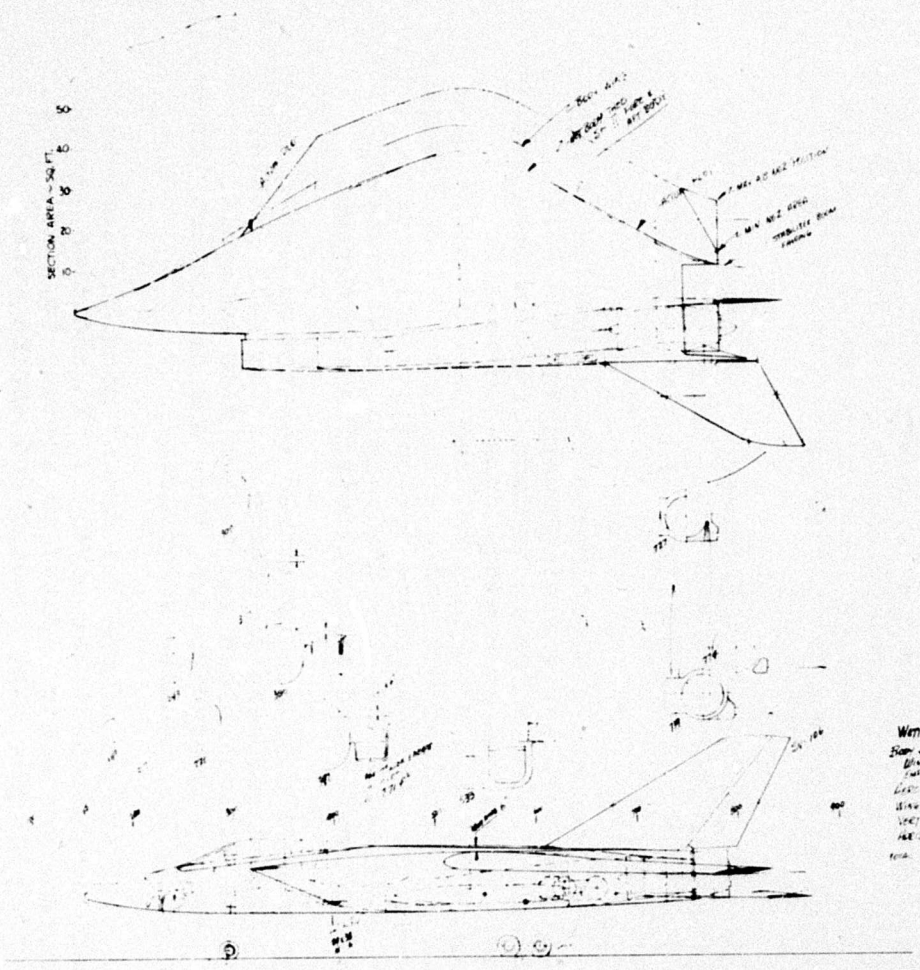

Figure 1-29: ESIP Model 908-351-14A General Arrangement

DRAWN		DATE	THE BOEING COMPANY
CHECKED			GENERAL ARRANGEMENT E.S.I.P. MODEL 908-351-14-A
STRESS			
ENGR APPR			
GROUP			
PD			CODE IDENT NO. 81205 J 162 10226
2-2555			SCALE 1/40 SHT 2

Note that relatively short, low fineness ratio engines are configured in the short fuselage. Performance analyses revealed that short engines are most efficiently configured in relatively short airframes; a fact that influenced analysis methodology in later stages of Phase II.

1.2.7 Element Performance

Following release of a configuration representation, the performance of system components or elements is estimated and mapped. These estimates will be programmed for system performance analysis. The estimates are made by element performance control technologies. These were Aero/Propulsion and Structures (Weights). Aerodynamics estimates the drag elements for the airframe. Propulsion determines inlet and exhaust system performance and assembles engine performance data in a form usable in analysis. Structures estimates the structural weight of the "as drawn" reference airplane and determines weight scaling parameters used in definition of an optimum derivative of the reference airplane.

Typical examples of element performance maps are presented in Section 17.0, "Inputs to the Phase II System Analysis," for airframe drag, afterbody drag, inlet performance, and structural weight.

Airframe drag elements are estimated as a function of Mach number, lift coefficient and wing sweep for the ESIP fighter/bomber. Drag elements include pressure drag factors for the body, wing and empennage, drag-due-to-lift parameters, roughness drag factors, and miscellaneous drag increments for interference and non-axisymmetric configuration characteristics. Drag elements for optimum derivative airplanes, defined within the analysis process, are scaled from these estimates and drag calculation subroutines.

Inlet performance maps are estimated for the selected inlet concept; a mixed compression design for the ESIP fighter/bomber. Maps include bleed and bypass flow schedules, spillage drag, recovery factors, buzz and distortion limits, and inlet entry Mach number schedule.

The structural weight of the "as drawn" configuration is determined, by component, at Level I. In addition, weight scaling parameters are estimated to account for changes in takeoff gross weight, wing loading and engine size. Structural weight of optimum derivatives with takeoff gross

weights, wing loadings and engine sizes different from those of the "as drawn" reference airplane are determined using the scaling parameters.

Exhaust system or afterbody drag maps are estimated for each of the different configurations. Afterbody drag varies with Mach number and throttle setting and is developed in terms of nozzle exit area and body maximum cross-sectional area. Several sources of afterbody drag were used in the Phase II analyses.

1.2.8 Afterbody Drag

Afterbody drag, estimated at several levels of validity, was a performance parameter of primary interest in ESIP. In Phase II, afterbody drag estimated at two levels of validity by Boeing and at a third level by the subcontracting engine companies were used in fighter/bomber analyses.

Original estimates, made by Boeing at Level I, applied Boeing-EWR test data to base, boom, boattail and interfairing areas assumed to be separated or problem flow areas. Axisymmetric body pressure drag was an additional increment calculated for inclusion in reference throttle setting afterbody drag. The latter increment is calculated internally in the analysis process. The former increment is estimated and mapped externally.

Afterbody drag of configurations with General Electric engines was estimated by that subcontractor. Pratt & Whitney Aircraft estimated the afterbody drag of configurations powered by their engines. Both companies used a similar estimation technique.

The technique involves the application of test data acquired on "blown" models of twin nozzle afterbodies. These data are correlated with parameters which account for average slope or afterbody closure angle and projected area.

Neither engine company had much supersonic test data with which to work. Theoretical interpolation and extrapolation was used to develop drag levels where data were unacceptable. This "hole" in the afterbody drag data bank yielded discrepancies which eventually affected analysis results.

Using a technique similar to those used by the engine companies, Boeing correlated a large amount of data acquired in subsonic ESIP Phase I parametric tests of blown, twin afterbodies. These correlations were then used to develop afterbody drag maps for fighter/bomber configurations at a third level of validity. These drag estimates fell into the Level II category. Supersonic afterbody drag this case, would be estimated in the same way as it was for the original Boeing estimates.

Four different estimates of subsonic afterbody drag, each for a single configuration at two throttle settings (A_9/A_{10} ratios with A_9, nozzle exit area, varying with throttle setting) are presented in Figure 1-30. In all four cases, drag levels at the higher A_9/A_{10} ratio are low. This area ratio or power setting is representative of a maximum power or reference condition.

At the other area ratio, representative of a minimum power setting, the estimates are substantially different in some cases. Even so, drag levels are relatively low.

1.2.9 System Performance Analysis

The configuration or design function provides a definition of a reference airframe. That definition, along with estimates of element performance for components of that system, are programmed for analysis of performance of the system. This process leads to definition of an optimum derivative system.

Takeoff gross weight was selected as the Phase II analysis figure-of-merit. The optimum derivative of a reference airplane is that scaled version of the reference vehicle which has minimum weight (figure-of-merit) and satisfies all mission requirements.

Optimum derivatives of combined airframe and engine concepts were determined in ESIP Phase II system performance analysis with the Boeing Engine-Airplane Matching Program (BEAM). An early version of this program, used in Phase II analyses, was designated TEM 129. A later, improved version which impacted the Phase II analyses to a substantial degree was designated TEM 129C. However, most of the Phase II analyses were derived using the earlier version.

Along with reference airplane definition, candidate engine performance, aerodynamic and propulsion element performance and structural weight parameters, the mission requirements are programmed for BEAM optimum derivative definition and performance analysis.

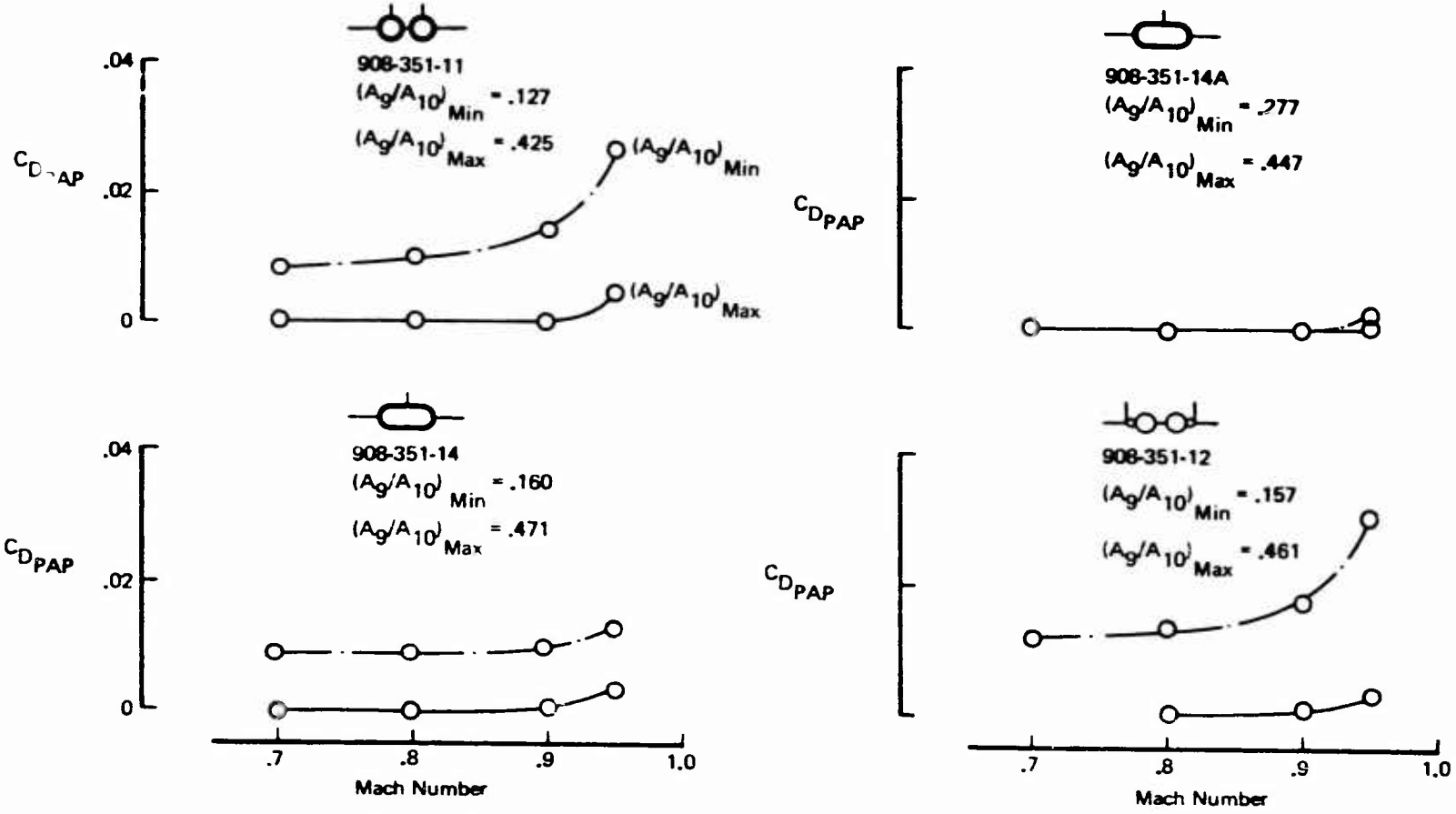

Figure 1-30: Comparison of Afterbody Pressure Drags Boeing Level II

Optimum derivative definition is obtained in an iterative computational process within the BEAM program. Aerodynamic and propulsion characteristics of the reference airframe and candidate engine are assembled and tested on the specified mission. Engine size is iteratively adjusted until specified mission thrust requirements are satisfied. Airframe physical characteristics and, therefore, drags, are adjusted to account for engine size effects on airplane shape. When propulsion thrust to airplane weight ratio satisfies mission requirements, structural weight remaining after completion of all mission requirements is compared against the actual structural weight computed for the mission sized system. Structural weight of a system at reference gross weight, specified wing loading and mission sized thrust loading is computed in a weight subroutine for comparison to "required" structural weight.

A growth factor is applied to any weight difference between required and available structural weight to project a next guess takeoff gross weight. This process is continued iteratively, with continuous attention to mission thrust requirements, until structural weight required and available converge within a specified tolerance.

A typical convergence is illustrated in Figure 1-31. The difference in weight between the lines of takeoff gross weight (TOGW) and operating weight (OW) required on the figure is a function of airframe aerodynamic characteristics and installed propulsion system performance. Operating weight available is a function of the physical makeup and structural weight of the system. The difference between the lines of operating weight available and required is a measure of system efficiency, that is, balance of the structural weight, drag and engine performance relationships. For the example shown, a minimum weight solution has been obtained for an engine size which just satisfies mission thrust requirements. Wing loading has not yet been optimized.

Alternate wing loadings are examined. Minimum takeoff gross weight solutions are obtained at several wing loadings, again, with thrust requirements just satisfied. A functional relationship between takeoff gross weight (figure-of-merit) and wing loading is established. Such a relationship is illustrated in Figure 1-32.

An optimum derivative system is identified where two mission thrust requirements have been satisfied simultaneously. The minimum gross weight system weighs approximately 50,000 lbs at a wing loading near 119 lb/ft^2. Systems at lower wing

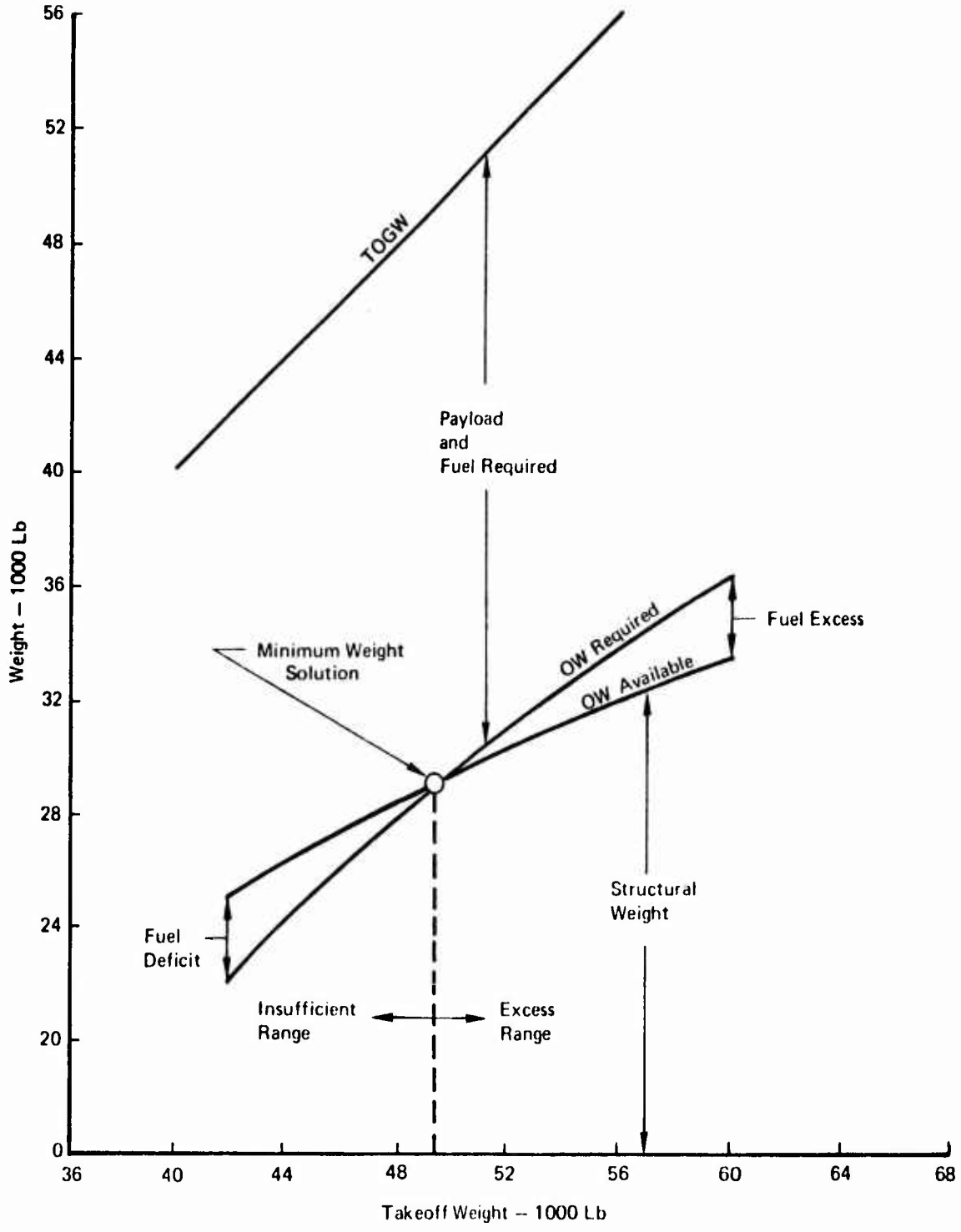

Figure 1-31: Gross Weight Iteration Procedure

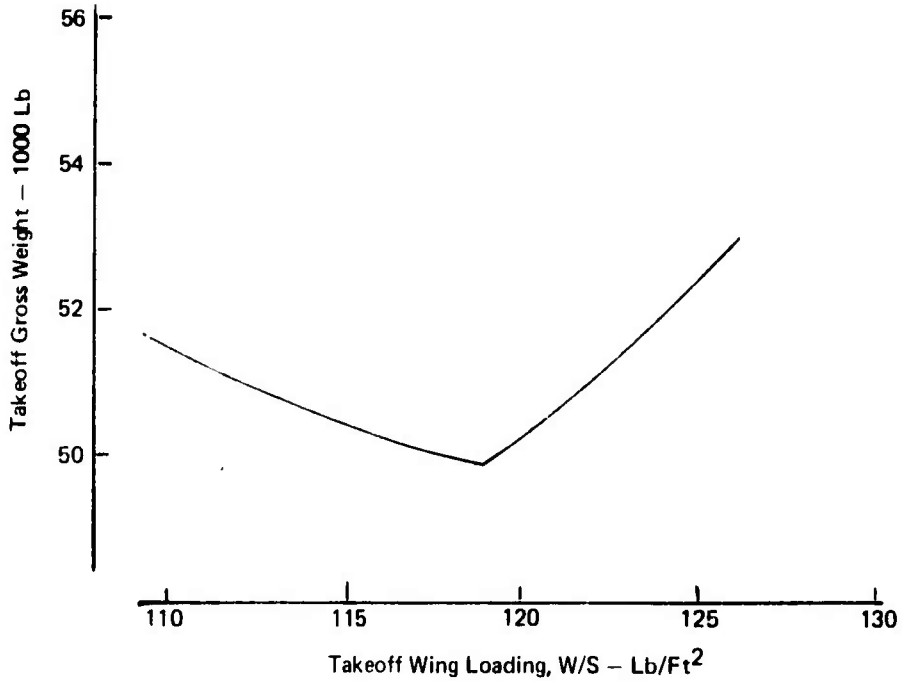

Figure 1-32: Effect of Wing Loading on Takeoff Gross Weight

loadings have engines sized by the time to accelerate following combat. Engines of systems at higher wing loadings are sized by the 4.25 g combat load factor requirement. Relationships of three engine sizing requirements and wing loading are shown in Figure 1-33.

Using these processes, then, optimum derivatives of reference airframe and candidate engine combinations were defined. Two variables, wing and engine size, were exercised within the TEM 129 program to minimize takeoff gross weight while just satisfying all specified mission requirements. The reference airframe was scaled to the proper weight and size to provide for wing, propulsion system, fuel and structural space requirements, as the airframe and engine scale, body maximum cross-sectional area (A_{10}) and engine exit area (A_9) change independently.

Change in the relationship between A_{10} and A_9 effects the performance of a propulsion system "installed" with afterbody drag defined in terms of those areas. Therefore, proper identification of an optimum derivative which is a scaled version of a reference airframe and candidate engine combination requires iterative "installation" of engine data, performance analysis and geometry adjustment.

Just such an iterative solution is illustrated in Figure 1-34. The data shown in the figure were obtained before automatic, interactive afterbody drag installation capability was made available in the BEAM program. At that time, engine data were pre-installed, external to BEAM, with an estimated A_{10}. The installed engine data was processed in BEAM and the A_{10} of the scaled system was output and compared to that used in the pre-installation. This procedure was repeated until A_{10} input in the pre-installation matched the A_{10} output from the BEAM program. It is obvious from the figure, that substantial errors can be incurred if afterbody drag data, dependent upon A_9 and A_{10}, are installed without careful tracking of, and adjustment for changes in those areas.

1.2.10 The Boeing Engine-Airplane Matching (BEAM) Program

BEAM is programmed for use on the CDC 6600 high speed digital computer at Boeing. The program requires approximately 100,000 (octal) words of central memory. A case can be processed in approximately half a minute. The program has also been converted for use on the AFAPL computer facilities at Wright-Patterson AFB. The BEAM program is documented in Section 11.0, "Boeing Engine-Airplane Matching Program - Version C."

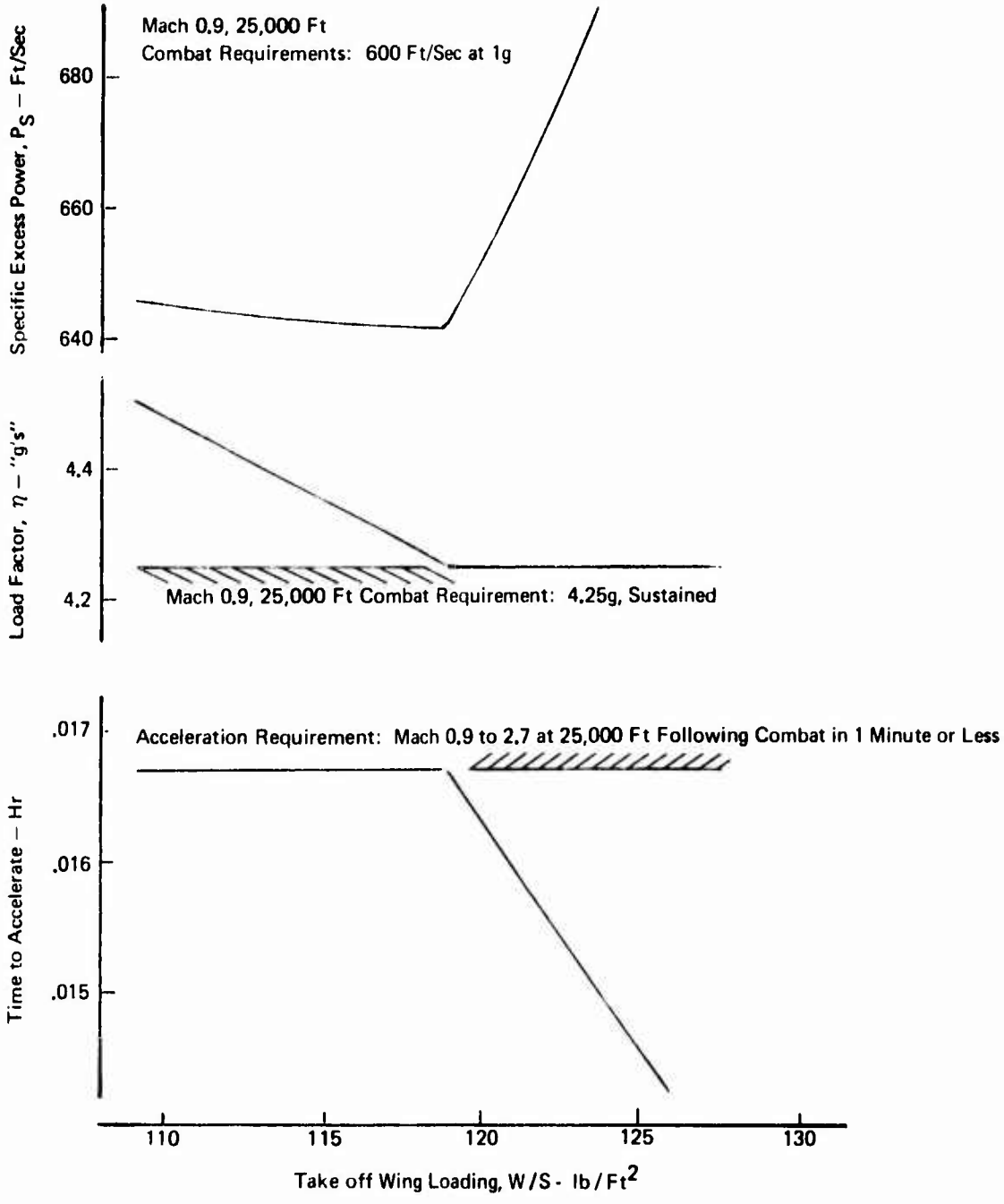

Figure 1-33: Effect of Wing Loading on Mission Maneuver Requirements

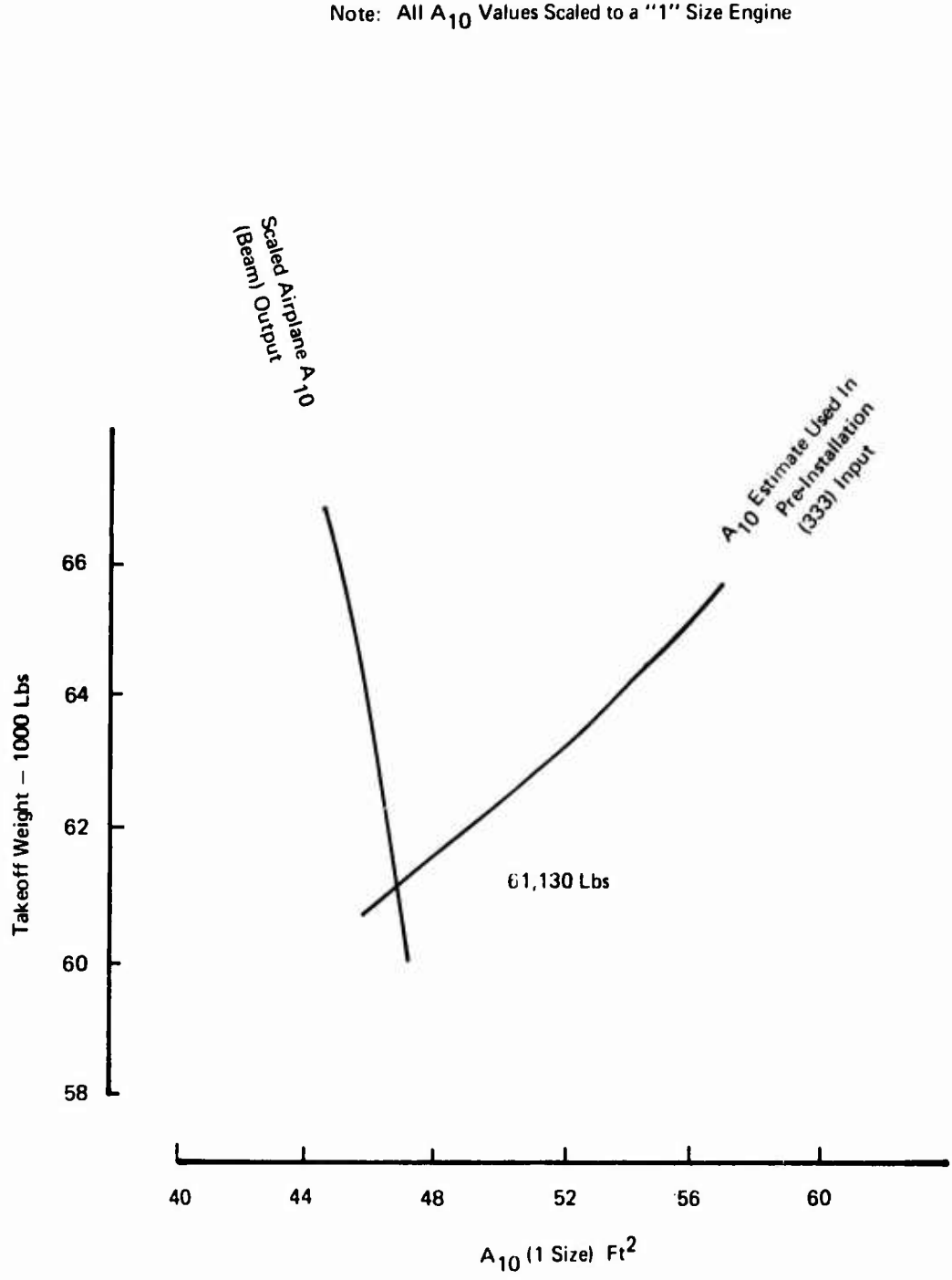

Figure 1-34: Iterative A_{10} Matching

The BEAM engine-airplane matching, mission analysis program is a collection of a main program and 123 subroutines. Some of these subroutines calculate geometry, aerodynamic performance, "installed" propulsion system performance, system structural weight and mission performance. Other subroutines regulate the computational processes and input/output formats.

A set of typical fighter/bomber inputs are illustrated on Tables 1-V through 1-IX. Aerodynamic, propulsion system, mission requirements, reference airframe description and uninstalled engine data inputs are represented.

A typical fighter/bomber mission summary output page is presented as Table 1-X. At the top of the table, physical characteristics of the scaled system are listed. Included are propulsion system shape characteristics, weight breakdown and airframe shape characteristics.

The rest of the summary page is devoted to a comprehensive listing of performance parameters particular to the individual segments in the specified mission. The listing includes flight conditions, segment range, time and fuel and aerodynamic and installed propulsion system performance parameters.

The BEAM program has been provided with the capability to provide element performance visibility by assembly of element performance components and outputting performance maps. Element performance maps can be developed for the airframe, inlet, afterbody and installed propulsion system. Representative examples of each of these maps are presented on Tables 1-XI through 1-XV. These sample element performance maps were calculated for a derivative of a reference airframe and candidate engine combination.

The airframe drag maps shown on Table 1-XI are developed for specified combinations of Mach number, altitude and wing sweep. In addition to total drag variation with lift, skin friction, pressure drag and drag-due-to-lift components are listed.

The inlet element performance maps shown on Tables 1-XII and 1-XIII are non-dimensional listings of recovery factor, inlet drag, distortion and buzz limits as a function of Mach number and airflow per unit capture area.

The afterbody element performance map is represented by Table 1-XIV. These maps are also developed for specified Mach number and altitude. Afterbody drags are listed as functions of A_{10}/A_9 or throttle setting. Total afterbody

INPUT GROUP A , AERO TABLES

DCDP

1.0	17.0	3.0	2.0		
0.0	0.	.25	.1	.15	.2
.25	.3	.35	.4	.45	.5
.6	.7	.8	.9	1.	1.1
35.	.00019	.00011	.00014	.00021	.0003
.0004	.00056	.00085	.00133	.00216	.00352
.00908	.02125	.04475	.07761	.09998	.12535
45.	.00014	.00009	.00014	.00023	.00037
.00046	.00069	.0011	.00179	.00296	.0048
.01289	.02818	.05798	.09362	.11984	.14945
75.	.00002	.00012	.00026	.00048	.00083
.00191	.00356	.00651	.01139	.01938	.03138
.07489	.1573	.2601	.335	.4178	.5106

SUPK

1.0	5.0	3.0	8.0		
0.0	1.0	1.5	2.0	2.5	3.0
45.	.19	.229	.34	.415	.465
60.	.208	.249	.368	.45	.505
75.	.259	.313	.464	.567	.635

DMAPS

2.0	4.0	6.0	9.0		
.2	10.	20.	30.	45.	2.
.0426	.025	.015	.001	3.	.007
.0105	.002	0.	4.	.0135	.001
0.	0.	5.	.002	0.	0.
0.	5.	0.	0.	0.	0.
7.	0.	0.	0.	0.	.4
10.	20.	30.	45.	2.	.0133
.0145	.007	.001	4.	.007	.0025
.0005	0.	4.	.0005	0.	0.
0.	6.	0.	0.	0.	0.
7.	0.	0.	0.	0.	0.
0.	0.	0.	0.		

DMCLT

1.0	11.0	9.0	10.0		
0.0	.1	.2	.3	.4	.5
.6	.7	.8	.9	1.0	1.1
0.	.03	.03	.03	.03	.03
.03	.03	.03	.05	.03	.03
.05	.078	.09	.102	.11	.113
.111	.113	.119	.122	.125	.13
.1	.034	.053	.074	.093	.104
.119	.12	.12	.15	.21	.26
.15	-.0093	.0162	.046	.0757	.1037
.1279	.15	.1721	.2411	.3169	.3996
.2	.025	.036	.047	.057	.062
.059	.13	.21	.24	.38	.47
.25	.0163	.0311	.0473	.0618	.078
.11	.15	.24	.33	.43	.52
.3	.0117	.0277	.0451	.0624	.0808
.11	.15	.24	.33	.43	.52
.35	.0062	.0217	.0391	.0592	.0802
.11	.15	.24	.33	.43	.52
.40	0.	.015	.03	.053	.077

Table 1-V: Airframe Drag Component Inputs

.11	.15	.24	.33	.43	.52	
						ORISHAP
1.	1.	17.	11.			
0.0	0.0	.95	0.	.96	0.	
.97	0.	.975	.0091	.98	.0033	
.385	.0006	.99	.001	.995	.0015	
1.0	.002	1.005	.0028	1.01	.0037	
1.02	.0047	1.04	.0174	1.06	.0236	
1.08	.0281	1.114	.0307	1.15	.0307	
1.0	4.0	7.0	12.0			KW-14A
0.0	35.	45.	60.	75.	1.0	KW-14A
.55	.87	.9	.21	1.2	.55	KW-14A
.87	.7	3.125	1.5	.55	.85	KW-14A
.94	2.93A	1.80	.65	.87	.95	KW-14A
2.51	2.10	.55	.97	.92	2.21	KW-14A
2.40	.95	.87	.88	1.940	2.70	KW-14A
.55	.87	.80	1.724			KW-14A
1.0	1.0	14.0	13.0	1.0	TAB TD13-3	1
0.	0.	.92	0.	.95	.06	
.98	.76	1.0	.60	1.03	.85	
1.36	.94	1.1	.99	1.15	1.0	
1.5	1.0	1.6	.99	1.8	.94	
2.2	.87	2.6	.77	3.0	.73	
1.0	1.0	7.0	14.0	2.0	TAB TD14-1	
		6.0	.15	7.0	.15	
8.0	.12	9.0	.10	10.0	.042	
11.0	.071	12.0	.063			
						DYNLOAFT
1.0	1.0	14.0	17.0			DINLOAFT
0.0	0.0	0.	0.	.6	0.	DINLOAFT
.8	.088	.9	.0299	1.0	.0698	DINLOAFT
1.1	.1449	1.2	.217	1.6	.2133	DINLOAFT
1.6	.1817	1.8	.1645	2.0	.1548	DINLOAFT
2.2	.1462	2.7	.1242	3.0	.1262	
						MISOF-11
1.0	1.0	14.0	20.0			-11 OAFT
0.0	0.0	0.	.48	.6	.48	-11 OAFT
.8	.61	.9	.67	1.0	.7	-11 OAFT
1.1	1.04	1.2	.65	1.4	.75	-11 OAFT
1.6	.78	1.8	.76	2.0	.75	
2.2	.75	2.7	.74	3.0	.74	
						DUM23
1.0	1.0	3.0	23.0			
0.0	0.0	0.	0.	1.	0.	
3.	0.					
1.0	1.0	3.0	24.0			EXFAC
0.0	0.0	35.	1.34	55.	1.34	
75.	1.17					
						AR/AR1
1.0	1.0	5.0	25.0			
0.0	0.0	35.	1.	40.	.9187	
45.	.8277	50.	.7293	75.	.2248	

Table 1-V: Airframe Drag Component Inputs (Continued)

1.0	1.0	5.0	26.0			SW/SW1
0.0	0.0	35.	1.	40.	1.0121	
45.	1.029	50.	1.0524	75.	1.4718	
1.0	1.0	5.0	27.0			CAVG/MAC
0.0	0.0	35.	.8432	40.	.8875	
45.	.9449	50.	1.3194	75.	2.2136	
1.0	1.0	5.0	28.0			T/C/T/C1
0.0	0.0	35.	1.	40.	.9502	
46.	.9924	50.	.8272	75.	.784	
1.	1.	2.	29.			GS
0.	0.	30.	0.	90.	0.	
1.0	1.0	5.0	30.0			AEXP/SWN
0.0	0.0	35.	.8449	40.	.8505	
45.	.81	50.	.7855	75.	.5142	
1.0	1.0	15.0	39.0	1.0	TAB	THP12
0.	0.	0.	1.0	.1	.999	
.2	.998	.3	.975	.4	.955	
.6	.898	.8	.838	1.0	.798	
1.2	.773	1.4	.745	1.6	.725	
1.8	.707	2.0	.692	2.5	.665	
3.0	.647					
1.0	1.0	15.0	40.0	1.0	TAB	THN12
0.	0.	-1.0	.25	0.	.25	
.01	.258	.02	.267	.03	.283	
.05	.327	.075	.410	.10	.498	
.15	.775	.20	.825	.25	.917	
.70	.978	.325	.992	.35	1.00	
.4	1.00					
1.0	1.0	9.0	41.0			KBF-14A
0.0	0.0	0.	.797	.1	.796	KBF-14A
.2	.8135	.5	.835	.8	.855	KBF-14A
1.1	.939	1.3	.955	1.5	.96	KBF-14A
1.0	1.0	9.0	42.0	1.0	TAB	TKD13
0.	0.	0.	1.0	.1	.333	
.2	.978	.3	.954	.4	.930	
.6	.880	.8	.831	1.0	.745	
1.0	1.0	13.0	43.0	1.0	TAB	TKP13
0.	0.	0.	1.0	.05	1.0	
.10	1.005	.15	1.023	.20	1.052	
.25	1.088	.30	1.133	.35	1.178	
.40	1.230	.45	1.290	.50	1.352	
.55	1.422	.60	1.500			
1.0	1.0	19.0	47.	1.0	TAB	TOT-1 1
0.	0.	0.	1.0	.1	.999	2
.2	.994	.3	.987	.4	.978	3
.5	.967	.6	.956	.7	.945	4
.8	.927	.9	.910	1.0	.898	5

Table 1-V: Airframe Drag Component Inputs (Continued)

1.2	.848	1.4	.803	1.6	.753	6
1.8	.702	2.0	.665	2.5	.564	7
3.0	.492	3.5	.412			
1.0	1.0	19.0	48.	1.0	YAB YW=1	1
0.	0.	0.	0.	.1	-.001	2
.2	-.004	.3	-.010	.4	-.018	3
.5	-.026	.6	-.037	.7	-.048	4
.8	-.058	.9	-.079	1.0	-.097	
1.2	-.134	1.4	-.176	1.6	-.222	
1.8	-.272	2.0	-.319	2.5	-.439	
3.0	-.558	3.5	-.675			

Table 1-V: Airframe Drag Component Inputs (Concluded)

```
*************************************** INPUT GROUP 8 . PROPULSION TABLES ***************************************
         1         2         3         4         5         6         7         8
12345678901234567890123456789012345678901234567890123456789012345678901234567890

AMBIENT TEMPERATURE DEVIATION TABLES
     0.000  10000.000                                                                                              -0
     0.000      0.000

     0.000 100000.000                                                                                              -0
     0.000      0.000

     0.000 100000.000                                                                                              -0
     0.000      0.000

ENGINE WEIGHT TABLES
     0.000       .500      1.000      1.500      2.000      2.500      3.000      3.500      4.000      4.500 -0
     1.000       .902       .820       .745       .675       .612       .560       .511       .468       .430

    20.000     40.000     60.000     80.000    100.000    120.000    150.000    200.000    250.000    400.000 -0
     1.330       .930       .900       .895       .920       .950      1.000      1.060      1.110      1.210

    40.000     50.000     75.000    100.000    125.000    150.000    175.000    200.000    250.000    300.000 -0
      .058       .055       .049       .044       .039       .036       .033       .031       .028       .027

     0.000       .500      1.000      1.500      2.000      2.500      3.000      3.500      4.000      4.500 -0
    15.000     10.300      9.200      8.150      7.600      7.350      7.150      6.950      6.850      6.700

ENGINE LENGTH TABLE
    20.000     40.000     60.000     80.000    100.000    120.000    140.000    180.000    260.000    350.000 -0
     1.182      1.117      1.067      1.029      1.000       .978       .962       .939       .912       .895

REFUEL CAPABILITY OF TANKER
   400.000    800.000   1000.000   1200.000   1400.000   1600.000   2000.000   2400.000   2800.000   3400.000 -0
103865.000  91420.000  85245.000  79450.000  73150.000  67545.000  56440.000  45990.000  36605.000  23210.000

INLET TABLES 1 THROUGH 7 FOLLOW

TABLE NUMBER 1       MACHO = F(MACH)                                                                               -0
     0.000       .400      1.650      2.700
     0.000       .400      1.650      2.700

TABLE NUMBER 24      RF = F(AO/AC,MACHO)
      .200       .400       .550       .700      1.000      1.300      1.500      1.650                            -0
      .200       .600      1.000      1.400      1.800      2.000      2.100      2.160                            -0
      .991       .989       .935       .976       .958       .942       .927       .900
      .400       .530       .743       .935      1.065      1.132      1.173      1.190                            -0
      .983       .983       .991       .976       .968       .959       .947       .923
      .200       .320       .515       .570       .795       .854       .891       .920       .935                 -0
      .983       .993       .992       .979       .974       .970       .964       .954       .920
```

Table 1-VI: Propulsion System Installation Inputs

.200	.382	.532	.665	.742	.778	.806	.819		-0
.983	.957	.931	.976	.971	.965	.955	.949		
.200	.335	.483	.604	.675	.711	.730	.737		-0
.984	.984	.982	.977	.972	.966	.957	.940		
.100	.240	.426	.589	.693	.735	.758	.766		-0
.978	.980	.979	.975	.968	.963	.953	.935		
.100	.214	.424	.637	.743	.790	.812	.818		-0
.963	.967	.965	.962	.957	.951	.942	.919		
.100	.235	.387	.569	.722	.766	.825	.863	.874	-0
.345	.951	.954	.953	.948	.944	.936	.912	.875	

TABLE 2A AS EXPANDED TO 41 POINTS WITH INTERMEDIATE MACH CURVES INTERPOLATED AS DIAGNOSTIC AID

.20											
	.2000	.2980	.3360	.4340	.5920	.6900	.7880	.8860	.9840	1.0820	1.1800
		1.2127	1.2453	1.2780	1.3107	1.3433	1.3760	1.4087	1.4413	1.4740	1.5067
		1.5393	1.5720	1.6047	1.6373	1.6700	1.7027	1.7353	1.7680	1.8007	1.8333
		1.8660	1.8987	1.9313	1.9640	1.9967	2.0293	2.0620	2.0947	2.1273	2.1600
	.9908	.9904	.9900	.9896	.9891	.9881	.9871	.9860	.9850	.9829	.9807
		.9800	.9792	.9785	.9777	.9773	.9762	.9753	.9739	.9724	.9710
		.9695	.9680	.9666	.9651	.9637	.9622	.9608	.9593	.9578	.9553
		.9527	.9501	.9475	.9449	.9424	.9378	.9330	.9283	.9150	.9000
.30											
	.3000	.3687	.4375	.5062	.5750	.6437	.7125	.7812	.8500	.9187	.9875
		1.0104	1.0333	1.0563	1.0792	1.1021	1.1250	1.1479	1.1708	1.1938	1.2167
		1.2396	1.2625	1.2854	1.3083	1.3313	1.3542	1.3771	1.4000	1.4229	1.4458
		1.4688	1.4917	1.5146	1.5375	1.5604	1.5833	1.6063	1.6292	1.6521	1.6750
	.9869	.9867	.9865	.9863	.9859	.9853	.9846	.9839	.9832	.9818	.9802
		.9796	.9791	.9785	.9779	.9774	.9768	.9762	.9757	.9744	.9734
		.9724	.9713	.9702	.9690	.9679	.9667	.9656	.9645	.9633	.9616
		.9597	.9575	.9554	.9533	.9512	.9476	.9434	.9391	.9264	.9115
.40											
	.4000	.4395	.4790	.5185	.5580	.5975	.6370	.6765	.7160	.7555	.7950
		.8082	.8213	.8345	.8477	.8608	.8740	.8872	.9003	.9135	.9267
		.9398	.9530	.9662	.9793	.9925	1.0057	1.0188	1.0320	1.0452	1.0583
		1.0715	1.0847	1.0978	1.1110	1.1242	1.1373	1.1505	1.1637	1.1768	1.1900
	.9830	.9830	.9830	.9830	.9828	.9824	.9820	.9817	.9813	.9807	.9795
		.9793	.9789	.9785	.9782	.9778	.9774	.9770	.9767	.9763	.9759
		.9754	.9745	.9737	.9729	.9721	.9712	.9704	.9696	.9688	.9679
		.9667	.9650	.9633	.9617	.9600	.9575	.9537	.9499	.9417	.9230
.47											
	.7000	.3381	.3762	.4144	.4525	.4906	.5287	.5669	.6050	.6431	.6812
		.6940	.7067	.7194	.7321	.7448	.7575	.7702	.7829	.7956	.8083
		.8210	.8338	.8465	.8592	.8719	.8846	.8973	.9100	.9227	.9354
		.9481	.9608	.9735	.9863	.9990	1.0117	1.0244	1.0371	1.0498	1.0625
	.9830	.9830	.9830	.9830	.9828	.9825	.9822	.9820	.9817	.9812	.9802
		.9799	.9795	.9792	.9789	.9786	.9783	.9780	.9776	.9772	.9768
		.9763	.9756	.9750	.9743	.9737	.9730	.9724	.9717	.9710	.9701
		.9691	.9678	.9666	.9650	.9633	.9612	.9576	.9535	.9446	.9215
.55											
	.2000	.2367	.2735	.3102	.3470	.3837	.4205	.4572	.4940	.5307	.5675
		.5798	.5920	.6043	.6165	.6288	.6410	.6533	.6655	.6778	.6900
		.7023	.7145	.7268	.7390	.7513	.7635	.7758	.7880	.8003	.8125

Table 1-VI: Propulsion System Installation Inputs (Continued)

		.8248	.8370	.8493	.8615	.8738	.8860	.8983	.9105	.9228	.9350
	.9830	.9830	.9830	.9830	.9828	.9826	.9824	.9822	.9820	.9816	.9807
		.9805	.9802	.9799	.9797	.9794	.9791	.9789	.9786	.9782	.9777
		.9772	.9767	.9762	.9758	.9753	.9748	.9743	.9738	.9732	.9724
		.9715	.9707	.9698	.9684	.9667	.9649	.9616	.9571	.9475	.9200
.63											
	.2000	.2336	.2672	.3009	.3345	.3681	.4017	.4354	.4690	.5026	.5362
		.5475	.5587	.5699	.5811	.5923	.6035	.6147	.6259	.6371	.6483
		.6595	.6708	.6820	.6932	.7044	.7156	.7268	.7380	.7492	.7604
		.7716	.7828	.7940	.8053	.8165	.8277	.8389	.8501	.8613	.8725
	.9830	.9830	.9830	.9830	.9829	.9828	.9827	.9824	.9821	.9816	.9810
		.9808	.9806	.9804	.9800	.9797	.9794	.9791	.9788	.9784	.9780
		.9775	.9771	.9767	.9762	.9758	.9753	.9747	.9741	.9735	.9727
		.9719	.9711	.9703	.9690	.9673	.9657	.9629	.9589	.9523	.9300
.70											
	.2000	.2305	.2610	.2915	.3220	.3525	.3830	.4135	.4440	.4745	.5050
		.5152	.5253	.5355	.5457	.5558	.5660	.5762	.5863	.5965	.6067
		[illegible]	.6270	.6372	.6473	.6575	.6677	.6779	.6880	.6982	.7083
		.7185	.7287	.7388	.7490	.7592	.7693	.7795	.7897	.7998	.8100
	.9830	.9830	.9830	.9830	.9830	.9830	.9830	.9826	.9821	.9817	.9813
		[illegible]	.9810	.9808	.9804	.9800	.9797	.9793	.9789	.9786	.9782
		.9778	.9775	.9771	.9767	.9764	.9759	.9752	.9745	.9737	.9730
		.9723	.9716	.9708	.9695	.9680	.9665	.9643	.9607	.9572	.9400
.85											
	.2000	.2287	.2573	.2860	.3147	.3434	.3720	.4007	.4294	.4581	.4867
		[illegible]	.5059	.5154	.5250	.5345	.5441	.5537	.5632	.5728	.5823
		.5919	.6015	.6110	.6206	.6301	.6397	.6492	.6588	.6684	.6779
		.6875	.6970	.7066	.7162	.7257	.7353	.7448	.7544	.7639	.7735
	.9836	.9836	.9836	.9836	.9836	.9836	.9834	.9831	.9825	.9822	.9817
		.9816	.9814	.9812	.9808	.9804	.9801	.9797	.9794	.9790	.9787
		.9783	.9780	.9776	.9773	.9769	.9764	.9756	.9749	.9742	.9735
		.9728	.9721	.9713	.9700	.9685	.9670	.9651	.9613	.9574	.9400
1.00											
	.2000	[illegible]	.2537	.2805	.3074	.3342	.3611	.3879	.4148	.4416	.4685
		.4775	.4864	.4954	.5043	.5133	.5222	.5312	.5401	.5491	.5580
		.5670	.5759	.5849	.5938	.6028	.6117	.6207	.6296	.6386	.6475
		.6565	.6654	.6744	.6833	.6923	.7012	.7102	.7191	.7281	.7370
	.9842	.9842	.9842	.9842	.9842	.9842	.9838	.9834	.9830	.9826	.9822
		.9821	.9813	.9815	.9812	.9808	.9805	.9802	.9798	.9795	.9791
		.9788	.9785	.9781	.9778	.9774	.9768	.9761	.9754	.9747	.9740
		.9733	.9726	.9719	.9704	.9689	.9674	.9659	.9619	.9575	.9400
1.15											
	.1500	.1801	.2101	.2402	.2703	.3004	.3304	.3605	.3906	.4207	.4507
		[illegible]	.4709	.4809	.4909	.5009	.5109	.5209	.5310	.5410	.5510
		.5610	.5711	.5811	.5911	.6011	.6112	.6212	.6312	.6412	.6513
		.6613	.6713	.6813	.6914	.7014	.7114	.7214	.7315	.7415	.7515
	.9813	.9815	.9816	.9818	.9820	.9819	.9817	.9814	.9811	.9809	.9805
		.9803	.9801	.9798	.9796	.9791	.9788	.9785	.9782	.9779	.9776
		.9773	.9770	.9767	.9764	.9759	.9752	.9745	.9738	.9731	.9724
		.9717	.9710	.9703	.9690	.9676	.9661	.9647	.9606	.9561	.9375
1.30											

Table 1-VI: Propulsion System Installation Inputs (Continued)

	.1000	.1333	.1666	.1999	.2332	.2665	.2998	.3331	.3664	.3997	.4330
		.4441	.4552	.4663	.4774	.4885	.4996	.5107	.5218	.5329	.5440
		.5551	.5662	.5773	.5884	.5995	.6106	.6217	.6328	.6439	.6550
		.6661	.6772	.6883	.6994	.7105	.7216	.7327	.7438	.7549	.7660
	.9794	.9787	.9791	.9796	.9797	.9797	.9795	.9796	.9793	.9791	.9788
		.9785	.9783	.9780	.9777	.9774	.9771	.9769	.9766	.9763	.9760
		.9758	.9755	.9752	.9749	.9743	.9736	.9729	.9722	.9715	.9708
		.9702	.9695	.9688	.9677	.9662	.9644	.9634	.9594	.9547	.9350
1.40											
	.1000	.1345	.1690	.2035	.2380	.2725	.3070	.3422	.3768	.4114	.4460
		.4675	.4891	.5106	.5321	.5537	.5152	.5267	.5383	.5498	.5613
		.5728	.5844	.5959	.6075	.6190	.6305	.6421	.6536	.6651	.6767
		.6882	.6997	.7113	.7228	.7343	.7458	.7574	.7689	.7805	.7920
	.9705	.9710	.9715	.9720	.9723	.9724	.9726	.9725	.9726	.9726	.9721
		.9719	.9716	.9713	.9711	.9708	.9706	.9703	.9701	.9698	.9695
		.9691	.9688	.9688	.9685	.9680	.9674	.9668	.9661	.9655	.9649
		.9642	.9636	.9630	.9620	.9605	.9591	.9576	.9543	.9497	.9270
1.50											
	.1000	.1359	.1718	.2077	.2436	.2795	.3154	.3513	.3872	.4231	.4590
		.4713	.4833	.4949	.5059	.5163	.5258	.5428	.5547	.5667	.5787
		.5906	.6025	.6145	.6265	.6385	.6505	.6624	.6744	.6864	.6983
		.7103	.7223	.7342	.7462	.7582	.7701	.7821	.7941	.8060	.8180
	.9626	.9673	.9668	.9666	.9649	.9651	.9654	.9655	.9659	.9661	.9656
		.9652	.9649	.9647	.9645	.9642	.9640	.9638	.9635	.9633	.9631
		.9628	.9626	.9623	.9621	.9618	.9612	.9607	.9601	.9595	.9589
		.9583	.9577	.9571	.9563	.9548	.9533	.9518	.9493	.9448	.9190
1.57											
	.1000	.1373	.1746	.2119	.2492	.2865	.3238	.3611	.3984	.4357	.4730
		.4854	.4978	.5103	.5227	.5352	.5476	.5600	.5725	.5849	.5974
		.6098	.6222	.6346	.6471	.6595	.6719	.6844	.6968	.7092	.7217
		.7341	.7465	.7590	.7714	.7838	.7963	.8087	.8211	.8336	.8460
	.9543	.9654	.9654	.9575	.9582	.9587	.9592	.9597	.9599	.9599	.9595
		.9594	.9592	.9591	.9589	.9588	.9586	.9583	.9580	.9577	.9574
		.9570	.9567	.9564	.9561	.9557	.9552	.9547	.9542	.9535	.9528
		.9520	.9513	.9505	.9490	.9470	.9450	.9407	.9353	.9290	.8970
1.65											
	.1000	.1387	.1774	.2161	.2548	.2935	.3322	.3709	.4095	.4483	.4870
		.4999	.5128	.5257	.5386	.5515	.5644	.5773	.5902	.6031	.6160
		.6289	.6418	.6547	.6676	.6805	.6934	.7063	.7192	.7321	.7450
		.7579	.7708	.7837	.7966	.8095	.8224	.8353	.8482	.8611	.8740
	.9460	.9475	.9489	.9504	.9515	.9523	.9530	.9538	.9540	.9538	.9536
		.9535	.9535	.9534	.9534	.9533	.9532	.9529	.9525	.9521	.9517
		.9513	.9509	.9505	.9500	.9496	.9492	.9488	.9484	.9476	.9467
		.9458	.9449	.9440	.9417	.9392	.9366	.9296	.9214	.9132	.8750

MINIMUM MACH NUMBER FOR INLET DRAG CALCULATIONS .200

TABLE NUMBER 29 DPDPC = F(MACH0)

0.000	.090	.356	.546	1.185	1.470	1.650	1.650	2.415	2.700 -0
.860	.924	.963	.970	.971	.962	.943	.950	.927	.911

TABLE NUMBER 30 (AO/AC)FC = F(MACH0)

.200	.400	.508	.700	.914	1.112	1.365	1.650	1.650	2.700 -0

Table 1-VI: Propulsion System Installation Inputs (Continued)

1.980	1.090	.888	.739	.678	.669	.785	.797	.768	.920	

TABLE NUMBER 2D (AO/AC)BUZZ = F(MACHO)

1.200	1.500	1.500	1.650							-8
0.000	0.000	.387	.440							

TABLE NUMBER 2E (AO/AC)DISTOR = F(MACHO)

.200	.400	.550	.700	1.000	1.300	1.500	1.650			-8
2.120	1.165	.913	.798	.718	.750	.804	.858			

TABLE NUMBER 3 (CD)SPILL = F(AOI/AC,MACHO)

.200	.400	.600	.800	1.000	1.250	1.450	1.650	1.650	1.700	-8
.300	.500	.700								-8
.246	.217	.168								
.287	.203	.133								
.323	.185	.071								
.340	.158	.012								
.367	.158	-.007								
.474	.198	.015								
.575	.242	.066								
.692	.390	.155								
0.000	0.000	0.000								
0.000	0.000	0.000								

TABLE NUMBER 4 (CD)BLEED = F(AOB/AC,MACHO)

.800	1.100	1.650	1.650	2.000	2.400	2.700				-8
0.000	.010	.020	.040	.100						-8
0.000	.011	.014	.026	.067						
0.000	.008	.013	.024	.062						
0.000	.007	.014	.027	.070						
0.000	.008	.015	.031	.079						
0.000	.007	.013	.026	.068						
0.000	.006	.012	.024	.063						
0.000	.006	.012	.023	.059						

TABLE NUMBER 5 (CD)BYPASS = F(AOBY/AC,MACHO)

.900	1.200	1.400	1.800	2.000	2.500	2.700				-8
0.000	.025	.075	.115	.250	.350					-8
0.000	.047	.097	.137	.464	.892					
0.000	.032	.068	.115	.438	.781					
0.000	.018	.043	.080	.409	.830					
0.000	.012	.020	.046	.216	.626					
0.000	.007	.012	.023	.127	.366					
0.000	.003	.006	.012	.055	.130					
0.000	.003	.005	.010	.045	.102					

TABLE NUMBER 6A ACB/AC = F(AO/AC,MACHO)

.600	.700	.800	1.100	1.400	1.650					-8
.600	.700	.800								-8
0.000	0.000	0.000								
0.000	0.000	0.000								
.012	.009	.004								
.041	.031	.018								
.083	.063	.040								
.144	.123	.078								

TABLE NUMBER 6B ACB/AC = F(MACHO)

Table 1 - VI: Propulsion System Installation Inputs (Continued)

1.650	1.900	2.200	2.700							
.069	.065	.072	.080							

TABLE NUMBER 7 ACSY/AC = F(AOE/AC,MACHO)

1.000	1.100	1.200	1.300	1.500	1.650				
0.000	.200	.300	.400	.603	.605	.620	.648	.888	
0.000	0.000	0.000	0.000	0.000	0.000	0.000	0.000	0.000	
0.000	0.000	0.000	0.000	0.000	0.000	0.000	0.000	0.000	
.293	.204	.154	.103	.001	0.000	0.000	0.000	0.000	
.305	.285	.265	.203	0.000	0.000	0.000	0.000	0.000	
.352	.334	.307	.220	.017	.015	0.000	0.000	0.000	
.414	.383	.344	.248	.045	.043	.028	0.000	0.000	

AFTERBODY DRAG TABLE

2.940	2.580	3.050	3.730	4.790						
.500	.700	.800	.860	.900	.940	.960	1.000	1.040	1.100	
1.200	1.300	1.400	1.500	1.600	1.650	2.500	2.300	2.500	2.700	1
.003	.008	.009	.010	.012	.018	.022	.045	.077	.069	
.006	.046	.040	.035	.031	.026	.022	.018	.017	.017	
.011	.011	.012	.014	.018	.025	.032	.061	.096	.084	
.049	.059	.049	.043	.038	.032	.028	.023	.021	.021	
.018	.018	.018	.021	.024	.034	.046	.078	.121	.107	
.047	.077	.062	.054	.048	.040	.035	.029	.026	.026	
.024	.026	.027	.030	.035	.044	.055	.099	.151	.135	
.111	.097	.083	.070	.063	.052	.045	.038	.034	.034	
.036	.036	.038	.041	.044	.056	.073	.141	.203	.179	
.141	.116	.099	.087	.078	.065	.056	.047	.043	.043	

Table 1-VI: Propulsion System Installation Inputs (Concluded)

```
**************************************** INPUT GROUP C , MISSIONS ****************************************
         1         2         3         4         5         6         7         8
12345678901234567890123456789012345678901234567890123456789012345678901234567890

11111111111111111111111111111112                                        100
TAKOFF 0.     0.     0.            .2     0.     0.            1.       1              ( 1)
       0.     .4     0.     0.     6.                                   1A             ( 2)
CLIMB  10.    0.                   35.    1.     0.            0.       2              ( 3)
       0.     0.     0.            0.            0.     0.              2A             ( 4)
0.     4000.  8000.  12000. 16000. 20000. 23000. 27000. 31000. 32000.   2B             ( 5)
.544   .586   .632   .683   .74    .796   .797   .798   .799   .8       2C             ( 6)
CRUISE 30000. .75    250.   2.5    35.    0.     0.            0.       3              ( 7)
2.     0.     0.     0.     1.0    0.     -4.0   0.     0.              3A             ( 8)
ACCEL  25000. .82    2.3    0.     75.    0.     0.            1.       4              ( 9)
       0.     0.     0.            0.            0.     0.              4A             (10)
CRUISE 25000. 2.3    50.    15.    75.    0.     0.            0.       5              (11)
1.0           0.     0.     0.     1.     0.     0.     0.              5A             (12)
CRUISE 25000. 2.3    50.    15.    75.    0.     0.            0.       6              (13)
0.     0.     0.     0.     0.     0.     0.     0.     0.              6A             (14)
SIZE   25000. .9     .9     600.   45.                         1.       7              (15)
                            3.0                                         7A             (16)
SIZE   25000. .9     .9     1.     45.                  1.3    1.       MANEUVER       (17)
                            3.0                                                        (18)
COMBAT 25000. .9     2.     1.     45.    0.     0.            1.       8              (19)
       -540.  0.     0.            0.            0.     0.              8A             (20)
ACCEL  25000. .9     2.7    1.     75.    0.     0.            1.       9              (21)
       0.     0.     0.     2.0    0.            0.     0.              9A             (22)
CLIMB  2.     0.                   75.    1.0    0.            0.       10             (23)
       0.     0.     0.            0.            0.     0.              10A            (24)
29000. 28900.                                                           10B            (25)
2.7    .8                                                               10C            (26)
LOITER 30000. .8     .905   1.     35.                                  DU             (27)
                                                                                       (28)
CRUISE 30000. .75    250.   2.5    35.    0.     0.            0.       11             (29)
3.     0.     0.     0.     1.0    0.     -4.0   0.     0.              11A            (30)
LOITER 0.     .3     20.    4.     35.    0.     0.            0.       12             (31)
       0.     0.     0.     1.0    0.            0.     0.              12A            (32)
        1111112                                                       200
COMBAT 25000. .9     2.     1.     45.    0.     0.            1.                      ( 9)
       -544.  0.     0.            0.            0.     0.                             (10)
CRUISE 30000. .75    250.   2.5    35.                                                 (11)
0.0                         1.0           -4.                                          (12)
LOITER 0.0    .3     20.    4.     35.                                                 (13)
                            1.0                                                        (14)
11112                                                                    11 POLAR
POLAR  0.0    1.1    .1     .9                                                         ( 1)
25000. 45.                                                                             ( 2)
POLAR  0.0    .2     .05    2.3                                                        ( 3)
25000. 75.                                                                             ( 4)
3
```

Table 1-VII: Mission Definitions

```
************************************************  INPUT GROUP D . AIRPLANE DATA  ************************************************
         1         2         3         4         5         6         7         8
12345678901234567890123456789012345678901234567890123456789012345678901234567890

1.0     3.0               1.      1.      3.0                                       1
YF9-129C SAMPLE CASE                                                                2
.005    25.     .005              .006              .031    3.      5.      .05     3
1.      1.      1.      0.        0.      1.        -1.     0.      1.      1.      4
463.    115.    6.      .12       .35     35.       .168            75.     .8449   5
0.      .5587   2.388   .05       60.               0.                              6
60000.  50000.  19500.  .612      209.    866.      713.    1.      6.              7
0.      0.      0.      4.25      0.                325.                            8
2.      .026    13.43             1.072                                             9
        1.34    1.0     .14       .14     1.0       1.0     1.0     1.0     2.5     10
1647.           130.    34.                                         .47     41.5    11
4150.   410.    530.    5350.     1360.   90.       160.    0.      100.    130.    12
870.    390.    380.    590.      5250.   200.      1740.   190.    550.    .05     13
1.0334  .116    .814    .3131     1.3529  .9962     .757    1.0     1.044   .3779   14
.2515   .7679   0.      .4058     .05     2000.     0.      .3216   1260.   570.    15
5.33    9.92    17.00   17.00     23.04   32.65     44.92   50.3    55.5            17L
5.90    11.90   22.40   37.82     45.5    53.5      36.9    27.9    24.7            18A
0.0     2.0     1.0     25000.    0.0                       1.65                    20
1.0     1.068                                       0.0                     2.75    21
0.0     3.52            3.5       3.13              1.93    5.21    .1430   28.04   22
263.5   15238.  3.89    68.3      1973.   .37                                       23
CV MAP                                                                              25
      1.018       1.100       1.200       1.300       1.400       1.500       1.600       2.000       2.800       10.000 -0
      0.000       1.100       1.500       1.750       2.000       3.000       4.000       5.000       8.000       10.000 -0
       .988        .988        .928        .950        .975        .988        .985        .978        .951        .894       1.010
       .988        .988        .835        .940        .956        .986        .987        .987        .960        .907       1.10
       .988        .988        .690        .862        .920        .970        .988        .988        .972        .920       1.20
       .988        .988        .840        .777        .865        .956        .982        .986        .974        .932       1.30
       .988        .988        .823        .768        .848        .938        .968        .982        .976        .942       1.40
       .988        .988        .819        .750        .786        .922        .955        .974        .978        .948       1.50
       .988        .988        .818        .740        .760        .900        .945        .968        .978        .952       1.60
       .988        .988        .813        .740        .760        .840        .900        .935        .975        .970       2.00
       .988        .988        .810        .740        .760        .800        .845        .880        .935        .971       2.90
       .988        .988        .810        .740        .760        .780        .815        .850        .930        .969       10.0
ABMAP           25000.                                                              26                              1
       .800       1.000       1.500       2.500
      1.340       1.170       1.170       1.170
      2.250       2.500       2.750       3.000       3.500       4.500       4.500       5.000                      -0
                                                                                    27
                                                                                    29
100.    1.0     1.0                                                                 30

-.99999

-2.5
            SAMPLE INLET MAP                                                        31

MACH NUMBER ARRAY
            .800        1.000       1.500       2.500                                                               1

CORRECTED AIRFLOW POINTS          INITIAL          DELTA          FINAL
```

Table 1-VIII: Reference Airframe Description

INPUT TO ENGINE LIBRARY PROGRAM

CREATE 1000

END OF INPUTS, BEGIN PROCESSING.

THE ENGINE ROUTINE OPERATING IN THE CREATE MODE WROTE
THE FOLLOWING ENGINES ON TAPE2, IN A MONOTONIC INCREASING ORDER
WITH BLANK RECORDS INSERTED IN THE PROPER POSITIONS.
1001.000
T 1001 SAMPLE ENGINE SAMPLE 16250 3.9 7.8 3.0-0
BOEING ENGINE FOR BEAM DOCUMENT SAMPLE CASE MARCH 1973

ENGINE NO. 1001.00 LOCATED AND TRANSFERRED TO FILE TAPE 2 EITHER TO OR FROM RECORD 1

T 1001 SAMPLE ENGINE SAMPLE 16250 7.00 3.00 3.00-0
BOEING ENGINE FOR BEAM DOCUMENT SAMPLE CASE MARCH 1973

A	T4	PR	WOSYP	WESTR	ENGD	ENGL	ENGW
2.00	3500.0	5.0	260.00	100.00	3.50	7.00	3250.0

YEAR	TYPE	EMVREF	DEXP
1973	4000	19400	4.00

ALT	0	10000	20000	25000	30000	36089	45000

SUPDECK FOR ALTITUDE = 0

MACH	0.00	.20	.30	.40	.60	.80	.90
DTEMP	0.00	20.00					

THRUST LIMITS

MACH	0.00	.20	.30	.40	.60	.80	.90
FN NR	16250	15750	15500	15250	15500	16000	16000
FN NR	16250	15750	15500	15250	15500	16000	16000
FN MIL	16250	15750	15500	15250	15500	16000	16000
FN MIL	16250	15750	15500	15250	15500	16000	16000
FN MA	27500	27750	27750	28250	30750	34000	36000
FN MA	27500	27750	27750	28250	30750	34000	36000

MACH = 0.00 ALT = 0

FN	27500	16250	16000	15250	12000	9250	7250	5250	3250	1000
WF	49750	11000	11000	10500	7750	6000	4750	3500	2500	1000
WC	260.00	260.00	260.00	260.00	230.00	210.00	180.00	150.00	120.00	70.00
PAPA	0.000	0.000	0.000	0.000	0.000	0.000	0.000	0.000	0.000	0.000
A5	0.000	0.000	0.000	0.000	0.000	0.000	0.000	0.000	0.000	0.000
A9	5.500	3.250	3.500	3.500	3.500	3.500	3.250	3.250	3.250	3.250
CV	1.000	1.000	1.000	1.000	1.000	1.000	1.000	1.000	1.000	1.000

10

Table 1-IX: Uninstalled Candidate Engine Data Inputs

MACH = .20		ALT = 0									
FN	27750	15750	14500	13750	10750	8500	6500	4750	3000	1000	10
WF	59750	12750	11000	10250	9000	6250	5000	3750	2750	1250	
WO	260.00	260.00	260.00	260.00	240.00	210.00	180.00	160.00	130.00	80.00	
PAPA	0.000	0.000	0.000	0.000	0.000	0.000	0.000	0.000	0.000	0.000	
A8	0.000	0.000	0.000	0.000	0.000	0.000	0.000	0.000	0.000	0.000	
A9	4.250	3.250	3.500	3.500	3.500	3.500	3.250	3.250	3.250	3.000	
CV	1.000	1.000	1.000	1.000	1.000	1.000	1.000	1.000	1.000	1.000	
MACH = .30		ALT = 0									
FN	27750	15500	14000	12500	10250	8250	6500	4500	3000	1000	16
WF	59500	12750	11000	9750	9750	6500	5000	3750	2750	1500	
WO	260.00	260.00	260.00	260.00	230.00	210.00	180.00	160.00	130.00	90.00	
PAPA	0.000	0.000	0.000	0.000	0.000	0.000	0.000	0.000	0.000	0.000	
A8	0.000	0.000	0.000	0.000	0.000	0.000	0.000	0.000	0.000	0.000	
A9	5.500	3.750	3.500	3.500	3.500	3.500	3.250	3.250	3.250	3.000	
CV	1.000	1.000	1.000	1.000	1.000	1.000	1.000	1.000	1.000	1.000	
MACH = .40		ALT = 0									
FN	28250	15750	13750	12500	10000	8250	6250	4500	2750	1000	18
WF	59750	12750	11250	10000	8750	6750	5250	4000	3000	1500	
WO	260.00	260.00	260.00	260.00	230.00	210.00	180.00	160.00	130.00	90.00	
PAPA	0.000	0.000	0.000	0.000	0.000	0.000	0.000	0.000	0.000	0.000	
A8	0.000	0.000	0.000	0.000	0.000	0.000	0.000	0.000	0.000	0.000	
A9	5.500	3.500	3.500	3.750	3.500	3.500	3.250	3.250	3.250	3.000	
CV	1.000	1.000	1.000	1.000	1.000	1.000	1.000	1.000	1.000	1.000	
MACH = .60		ALT = 0									
FN	28750	15500	13500	12250	10000	8250	6250	4250	2750	1000	18
WF	59500	14500	12250	11000	9000	7500	6000	4500	3250	1750	
WO	260.00	260.00	260.00	250.00	230.00	210.00	190.00	160.00	140.00	100.00	
PAPA	0.000	0.000	0.000	0.000	0.000	0.000	0.000	0.000	0.000	0.000	
A8	0.000	0.000	0.000	0.000	0.000	0.000	0.000	0.000	0.000	0.000	
A9	5.750	3.750	3.750	3.750	3.500	3.500	3.500	3.250	3.250	3.000	
CV	1.000	1.000	1.000	1.000	1.000	1.000	1.000	1.000	1.000	1.000	
MACH = .80		ALT = 0									
FN	34000	16000	12750	11250	9750	7750	6250	4250	2500	1000	18
WF	67750	16000	12750	11250	10000	8250	6500	5000	3750	2250	
WO	260.00	260.00	230.00	220.00	210.00	190.00	170.00	150.00	130.00	110.00	
PAPA	0.000	0.000	0.000	0.000	0.000	0.000	0.000	0.000	0.000	0.000	
A8	0.000	0.000	0.000	0.000	0.000	0.000	0.000	0.000	0.000	0.000	
A9	6.250	4.000	3.750	3.750	3.500	3.500	3.500	3.250	3.250	3.000	
CV	1.000	1.000	1.000	1.000	1.000	1.000	1.000	1.000	1.000	1.000	
MACH = .90		ALT = 0									
FN	36000	16000	13250	11750	10000	8000	5750	4500	2750	1000	18
WF	72250	16250	13250	12000	10000	8250	6750	5500	4000	2250	
WO	250.00	250.00	240.00	230.00	210.00	190.00	170.00	160.00	130.00	110.00	
PAPA	0.000	0.000	0.000	0.000	0.000	0.000	0.000	0.000	0.000	0.000	
A8	0.000	0.000	0.000	0.000	0.000	0.000	0.000	0.000	0.000	0.000	
A9	6.500	4.000	4.000	3.750	3.750	3.500	3.500	3.250	3.250	3.000	
CV	1.000	1.000	1.000	1.000	1.000	1.000	1.000	1.000	1.000	1.000	

SUBDECK FOR ALTITUDE = 10000

MACH	.60	.70	.90	3
DTEMP	0.00			1

Table 1-IX: Uninstalled Candidate Engine Data Inputs (Concluded)

BOEING ENGINE/AIRPLANE MATCHING PROGRAM

MISSION 100		MAR 21, 1973	
PT. DESIGN IOPT=1 IRATIO=1 IFXWNG=0 INOZ=0			
TFM-1290 SAMPLE CASE			
ENGINE DATA		ENGINE DATA	
LIBRARY NO.	1081	SCALE FACTOR	1.353
DESIGNATION	SAMPLE	T/W UNINST MIL	.695
PRESSURE RATIO	5.00	T/W UNINST MAX	1.148
BYPASS RATIO	2.00	T/W INST MIL	.540
T4 DESIGN	3500	T/W INST MAX	.906
T7 DESIGN	4000	NO OF ENGINES	2
PRI AIRFLOW	117.25		
TOTAL AIRFLOW	351.75	WEIGHTS	
DIA FRT FLANGE	4.07	CONTROL	1416
DIA EXHAUST	4.65	HYDRAULICS	494
LENGTH ENG	8.14	AIR COND	649
LENGTH EXH	1.91	K4	5250
TOTAL LENGTH	38.61	FIXED EQUIP	7909
FN SLS DES	21944		

WEIGHTS		WEIGHTS	
WING	5176	UNUS FUEL	256
HOR TAIL	519	K5	550
VERT TAIL	599	PYLONS	0
BODY	6745	OIL	288
LDG GEAR	1726	USEFUL LOAD	1093
ENG SECTION	257	OWE	36339
STRUCTURES	15024	FYF	24841
ENGINES	8744	WT ADDED	-548
EXHAUST SYS	0	RES FUEL	1244
FUEL SYSTEM	1963	MISSION FUEL	23597
K3	130	PAYLOAD	2000
ACCESSORIES	100	EXT STORES	0
DUCT	1228	EXT TANKS	0
VAR GEOM	659	WX	-0
POWER PLANT	12933	GROSS WEIGHT	64227
		AERO DATA	
		BODY AWET	1269
		BODY VOLUME	2069

AERO DATA				TAKEOFF DATA	
WING LOADING			115.0	TAKOFF DIST	1883
SW			558.5	MEAN FN	67917
SW EXPOSED			471.9	MEAN MACH	.197
LE SWEEP			35.0	AUGMENTATION	1.000
AR			6.000	PS MIL	.400
T/C			.170	ALTITUDE	0
MAC			8.764	AMB TEMP	59.00
A CAPT DES			10.254	T/W	1.057
ABL			-0.000	ENG SIZE	0.000
AW NACELLE			0.0	TAKOFF GW	64227
A1 5.90		L1	5.33		
A2 11.90		L2	9.92		
A3 22.40		L3	17.00	MISSION TOTALS	
A4 40.34		L4	17.80	RANGE	600.000
A5 53.45		L5	23.97	HOURS	1.462
A6 67.99		L6	33.50	FUEL	23596.652
A7 47.16		L7	45.66		
A8 40.33		L8	53.80		
A9 35.33		L9	59.00		

	TAKOFF	CLIMB	CRUISE	ACCEL	CRUISE	CRUISE	SIZE	SIZE	COMBAT	ACCEL	CLIMB	LOITER	CRUISE	LOITER
A/P WT	64227	62637	61412	58349	55550	51408	49083	48083	48083	44793	42002	42002	42002	39941
ALT	0	0	37066	25000	25000	25000	25000	25000	25000	25000	29000	30000	44011	0
MACH	.197	.544	.835	2.250	2.300	2.300	.900	.900	.900	2.675	2.700	.800	.835	.300
N MILE	0	22	234	18	37	50	0	0	0	16	12	0	221	0
HOURS	0.0000	.0484	.4769	.0202	.0232	.0361	0.0000	0.0000	.3333	.0165	.0120	.0001	.4617	.3333
D FUEL	1591	1225	3364	2797	2142	3325	0	0	2932	2701	-0	0	2050	1859
NM/KLB	0.000	17.729	74.499	6.397	14.985	15.039	0.000	0.000	0.000	6.083	*470.268	0.000	107.327	0.000
R FACTOR	0	0	4916	0	831	771	0	0	0	0	0	0	4372	0
L/D	13.131	11.270	12.056	9.069	1.146	1.062	7.963	5.353	7.963	7.234	1.526	10.941	11.938	12.969
PSNP	1.677	1.000	.495	2.186	1.991	1.887	2.193	2.193	2.193	2.185	1.000	.268	.471	.079
PSMIL	1.677	1.000	.488	2.188	1.991	1.887	2.193	2.193	2.193	2.185	1.000	.268	.471	.079
PAUG	1.000	0.000	0.000	1.000	.272	.271	1.000	1.000	.000	1.000	0.000	0.000	0.000	0.000
PSOA	1.000	.497	.223	1.000	.442	.441	1.000	1.000	1.000	1.000	.223	.127	.215	.044
TMDOD	0.000	123.095	0.000	1.198	0.000	0.000	5.679	.056	0.000	1.205	-2.312	0.000	0.000	0.000
SFC	2.093	1.041	1.146	2.101	1.309	1.308	2.107	2.107	2.107	2.110	.300	1.510	1.292	1.830
SIZE	0.000	0.000	0.000	0.000	0.000	0.000	1.261	1.249	0.000	1.349	0.000	0.000	0.000	0.000
WC	351.9	306.5	117.1	218.9	687.2	687.2	225.1	225.1	225.1	233.4	461.5	122.8	77.6	151.9
CVTOT	0.000	0.000	0.000	0.000	0.000	0.000	0.000	0.000	0.000	0.000	0.000	0.000	0.000	0.000
CVCELD	0.000	0.000	0.000	0.000	0.000	0.000	0.000	0.000	0.000	0.000	0.000	0.000	0.000	0.000
CV	.979	.987	.993	.995	.973	.973	.985	.985	.985	.985	.983	.975	.997	.942
FN UNYN	0	0	0	0	0	0	0	0	0	0	0	0	0	0
[illegible]	2.711	3.075	2.714	4.412	10.661	13.678	4.508	4.508	4.508	4.595	5.066	2.397	2.597	1.270
ALD/AQ	4.563	6.877	6.707	3.668	2.389	2.389	3.589	3.589	3.589	3.558	7.479	6.956	6.734	8.098
CDAR	.0275	.0544	.0595	.0306	.0327	.0327	.0328	.0328	.0328	.0382	.0502	.0593	.0584	.0655
CDOR	.0201	.0469	.0429	.0130	-.0048	-.0048	.0126	.0125	.0126	.0131	.0136	.0442	.0428	.0525
CDINL	0.0000	.0123	.0757	.0171	.0466	.0466	.0165	.0165	.0165	.0154	.0467	.1476	.0913	.1926
DF	.961	.979	.979	.973	.970	.970	.973	.973	.973	.973	.858	.981	.978	.996
FN	25035	17706	2537	13690	24744	24195	20164	20164	20164	20553	-14930	1919	1759	1540
RAMDRG	0	0	0	0	0	0	0	0	0	0	0	0	0	0
EMDRY	0.00	0.00	69.95	0.00	-961.70	-1334.71	0.00	0.00	652.08	0.00	0.00	0.00	76.05	0.00
EMAUG	0.00	0.00	237.77	0.00	2572.33	2784.03	0.00	0.00	4.35	0.00	0.00	0.00	247.51	0.00
EFF DRY	0	0	191	0	-643	-698	0	0	0	0	0	0	283	0
EFF AUG	0	0	140	0	329	356	0	0	254	0	0	0	292	0

Table 1-X: BEAM Mission Summary Output

DRAG POLAR

FAMILY OF CURVES FOR L.E. SWEEP OF 45.000 DEGREES

MACH= .900 ALTITUDE= 25000

CL	CDYCY	CD	CDFY	CDL	DCDM
0.00000	.02142	.01679	.01538	.00014	.00127
.10000	.02173	.01710	.01538	.00078	.00094
.20000	.02397	.01935	.01538	.00283	.00107
.30000	.02778	.02316	.01538	.00646	.00132
.40000	.03405	.02966	.01538	.01205	.00221
.50000	.04483	.04221	.01538	.02082	.00400
.60000	.06705	.06902	.01538	.03546	.01417
.70000	.10759	.10946	.01538	.05973	.02739
.80000	.14971	.15508	.01538	.09900	.03070
.90000	.19635	.19162	.01538	.14554	.03073
1.00000	.23466	.23002	.01538	.18394	.03078
1.10000	.27771	.27309	.01538	.22701	.03070
1.20000	.32307	.31744	.01538	.27135	.03070

Table 1-XI: Drag Polar Output Map

INLET RECOVERY MAP SAMPLE INLET MAP START MACH 5.658 CAPTURE AREA 3.579

MACH NO	.800	1.000	1.500	2.500
DISTORTION LIMIT				
(WQC/AC)DL	38.28	36.46	35.72	18.46
(PT2/PT0)DL	.9591	.9624	.9455	.9044
BUZZ LIMIT				
(WQC/AC)BL	0.00	0.00	1.64	****
(PT2/PT0)BL	****	****	.9659	****

WQC/AC	PT2/PT0	PT2/PT0	PT2/PT0	PT2/PT0
5.28	.9834	.9842	.9653	.9225
7.92	.9834	.9842	.9642	.9225
10.55	.9834	.9842	.9633	.9225
13.19	.9834	.9842	.9625	.9225
15.83	.9834	.9842	.9623	.9225
18.47	.9832	.9837	.9622	.9040
21.11	.9824	.9829	.9622	.7910
23.75	.9815	.9822	.9622	.7311
26.39	.9802	.9805	.9622	.6328
29.03	.9783	.9785	.9616	.5753
31.66	.9762	.9757	.9577	.5273
34.30	.9724	.9718	.9524	.4868
36.94	.9661	.9619	.9263	.4520
39.58	.9428	.9200	.8642	.4219
42.22	.8856	.8625	.8139	.3956

Table 1 XII: Inlet Recovery Output Map

INLET DRAG MAP SAMPLE INLET MAP START MACH 1.650 CAPTURE AREA 7.579

MACH NO	.800	1.000	1.500	2.500
DISTORTION LIMIT				
(WCC/AC)DL	38.28	36.86	35.72	18.46
(CD)DL	-.0383	-.0253	-.0381	.0468
BUZZ LIMIT				
(WCC/AC)BL	0.00	0.00	1.64	****
(CD)BL	****	****	1.1339	****

WCC/AC	CD	CD	CD	CD
5.28	.5065	.5421	1.0343	.3878
7.92	.4575	.4888	.9621	.2903
10.55	.4086	.4354	.8586	.1929
13.19	.3597	.3820	.7374	.0991
15.83	.3108	.3287	.5101	.0563
18.47	.2619	.2755	.3804	.0468
21.11	.2136	.2226	.2498	.0468
23.75	.1665	.1726	.1717	.0468
26.39	.1280	.1309	.1451	.0468
29.03	.0898	.0897	.0924	.0468
31.66	.0519	.0491	.0374	.0468
34.30	.0141	.0094	-.0139	.0468
36.94	-.0224	-.0263	-.0479	.0468
39.54	-.0479	-.0405	-.0511	.0468
42.22	-.0491	-.0405	-.0511	.0468

Table 1-XLII: Inlet Drag Output Map

AFTERBODY DRAG MAP

ALT 25000 FT WETTED AREA 1259 SQ FT FOREBODY WETTED AREA 826 SQ FT A10 68.8 SQ FT

MACH .800

CDF .01389 CDWAVE 0.32000

A10/A9	CDAB	CDPS	CDABT
2.25000	.00920	-.00583	.02209
2.50000	.01370	-.00333	.02459
2.75000	.01423	0.00000	.02792
3.00000	.01776	.00372	.03164
3.25000	.02412	.01009	.03801
4.00000	.02970	.01567	.04359
4.50000	.03470	.02067	.04859
5.00000	.03970	.02567	.05359

MACH 1.000

CDF .01147 CDWAVE .03684

A10/A9	CDAB	CDPS	CDABT
2.25000	.04547	-.02150	.05694
2.50000	.05724	-.00971	.06870
2.75000	.06687	0.00000	.07844
3.00000	.07574	.00478	.08721
3.25000	.08173	.01076	.09320
4.00000	.10980	.03883	.12127
4.50000	.12940	.05843	.14127
5.00000	.14980	.07883	.16127

MACH 1.500

CDF .00984 CDWAVE .00728

A10/A9	CDAB	CDPS	CDABT
2.25000	.03494	-.01198	.04479
2.50000	.04105	-.00586	.05089
2.75000	.04691	0.00000	.05675
3.00000	.05265	.00574	.06249
3.25000	.06452	.01761	.07436
4.00000	.07450	.02759	.08434
4.50000	.09283	.03593	.09268
5.00000	.09117	.04426	.10101

MACH 2.500

CDF .00719 CDWAVE .00838

A10/A9	CDAB	CDPS	CDABT
2.25000	.01712	-.00580	.02431
2.50000	.02006	-.00286	.02725
2.75000	.02292	0.00000	.03011
3.00000	.02574	.00282	.03243
3.25000	.03140	.00848	.03859
4.00000	.03626	.01335	.04346
4.50000	.04245	.01754	.04765
5.00000	.04464	.02173	.05184

Table 1-XIV: Afterbody Drag Output Map

pressure drag, CDAB; throttle dependent afterbody drag increment, CDPS; and total afterbody drag, CDABT, are listed.

A typical propulsion system element performance summary is presented in Table 1-XV. Uninstalled engine performance characteristics are listed in the upper left corner of the table. Inlet system performance is summarized in the upper right corner. Afterbody performance is summarized in the lower left corner. Finally, installed propulsion system performance characteristics are listed in the lower right tabulation.

Many improvements were made to the BEAM program during ESIP. Provision of interactive installation capability discussed previously, and element performance visibility discussed above, are but two such changes.

A major improvement in body geometry scaling realism was accomplished late in the second phase with conversion of the program to the TEM 129C version. Prior to that time, changes in body volume requirements were distributed homogeneously about the body. Fineness ratio of a scaled, derivative body was the same as that of the reference airplane. Volume required by a larger engine, for instance, would be distributed throughout the body from nose to tail and afterbody closure rate would not be effected. The program had no capability to analytically exploit effect of engine shape changes on airframe configuration. The TEM 129 version of BEAM operated on incremental and total volume relationships primarily.

The TEM 129C version of BEAM was programmed to better define the area distribution of body-buried propulsion system designs. The geometry subroutine of the C version operates on component and total cross-sectional area relationships. Changes in component cross-sectional area requirements are distributed in affected areas only. If size of engines mounted in the aft end changes, then, only the aft end cross-sectional area changes to accommodate the new engine size. Forward portions of the system would not be affected. Airplane length is held constant while the area distribution of the scaled system is adjusted to satisfy cross-sectional area requirements. Airplane length is allowed to change if a minimum diffuser length criteria would be violated otherwise.

Following adjustment of the area distribution, a body length adjustment capability in the TEM 129C version, may be used to optimize body length. Body length can be varied until the structural weight/drag relationship of the scaled system is properly balanced for maximum performance.

BEAM INSTALLED ENGINE PERFORMANCE TABULATION — DATE RUN MAR 21, 1973

ENGINE NO 1001 — YEAR 1973 — SCALE 1.000 — BPR 2.0 — T4 3500 — RP 5 — FNREF 16250
ACAPT 7.58 — A10 50.25 — ACC 12.57 — ACC/A10 .250 — DENG 3.500 — LENG 7.000 — WENG 3258.8

ROPING ENGINE FOR BEAM DOCUMENT SAMPLE CASE MARCH 1973

ALTITUDE 25000 MACH .900

1. UNINSTALLED (INPUT) ENGINE PERFORMANCE

FNU	WF	WQ COR	SFC	FGI	CV	BF
16000	30750	260.0	1.922	20727	1.000	1.000
7750	7750	260.0	1.000	12477	1.000	1.000
7000	6750	260.0	.964	11727	1.000	1.000
6750	6250	260.0	.926	11477	1.000	1.000
5250	5000	250.0	.952	9795	1.000	1.000
4250	4000	220.0	.941	8756	1.000	1.000
3250	3000	200.0	.923	6686	1.000	1.000
2250	2250	170.3	1.000	5341	1.000	1.000
1500	1750	150.0	1.167	4227	1.000	1.000
750	1250	130.0	1.667	3114	1.000	1.000

2. INLET SYSTEM PERFORMANCE

RF	AE/AC	AI/AC	A0/AC	CDSPL	CDBYP	CDBLD	CDINL	DRAG/FN
.973	.681	.698	.681	.0037	0.0000	.0127	.0165	.00373
.973	.681	.698	.681	.0037	0.0000	.0127	.0165	.00818
.973	.681	.698	.681	.0037	0.0000	.0127	.0165	.00915
.973	.681	.698	.681	.0037	0.0000	.0127	.0165	.00952
.975	.656	.675	.656	.0221	0.0000	.0133	.0354	.02789
.979	.580	.603	.590	.0781	0.0000	.0155	.0936	.09754
.981	.528	.554	.528	.1160	0.0000	.0171	.1332	.21828
.982	.450	.480	.450	.1776	0.0000	.0196	.1972	.80912
.983	.397	.430	.397	.2261	0.0000	.0212	.2473	-16.49538
.984	.348	.381	.344	.2748	0.0000	.0229	.2977	-.59202

3. AFTERBODY/EXHAUST SYSTEM PERFORMANCE)

PT8/PA	A8	A9	CVTH	CVCAL	CVTOT	A9/ACC	CDAFT	CDPS	DAF/FN	DPS/FN
4.500	5.514	7.000	.985	1.000	.991	.557	.0328	.0063	.0246	.0095
4.068	3.764	4.000	.986	1.000	.942	.318	.0576	.0187	.0948	.0615
3.797	3.967	4.000	.986	1.000	.936	.318	.0576	.0187	.1060	.0688
3.807	3.771	4.000	.986	1.000	.934	.318	.0576	.0187	.1103	.0716
3.131	4.179	4.250	.988	1.000	.922	.338	.0543	.0171	.1379	.0466
2.989	3.750	4.000	.985	1.000	.835	.318	.0576	.0187	.1991	.1292
2.739	3.539	4.000	.970	1.000	.857	.318	.0576	.0187	.3129	.2030
2.399	3.333	3.750	.959	1.000	.784	.298	.0613	.0205	.8299	.5562
2.076	3.391	3.500	.946	1.000	.637	.279	.0655	.0227	4.4908	0.0199
1.747	3.266	3.250	.953	1.000	-.015	.259	.0704	.0251	-.7782	-.5568

4. INSTALLED PROPULSION SYSTEM PERFORMANCE

PS	FN	SFC	FRAM	FNC	SFCC
2.00	14905	2.007	4727	40164	2.205
1.00	6797	1.109	4727	18317	1.219
.89	6078	1.080	4727	16378	1.187
.86	5843	1.040	4727	15746	1.143
.65	4438	1.105	4545	11879	1.215
.44	3237	1.209	4000	8723	1.329
.30	2058	1.428	3636	5551	1.569
.12	826	2.674	3091	2227	2.939
-.01	-51	-31.997	2727	-136	-37.359
-.15	-1013	-1.214	2364	-2729	-1.334

ALTITUDE 25000 MACH 1.000

1. UNINSTALLED (INPUT) ENGINE PERFORMANCE

FNU	WF	WQ COR	SFC	FGI	CV	BF
17500	37500	260.0	1.914	23295	1.000	1.000
8250	17000	260.0	2.061	14035	1.000	1.000

2. INLET SYSTEM PERFORMANCE

RF	AE/AC	AI/AC	A0/AC	CDSPL	CDBYP	CDBLD	CDINL	DRAG/FN
.972	.675	.700	.675	-.0071	0.0000	.0165	.0094	.00242
.972	.675	.700	.675	-.0071	0.0000	.0165	.0094	.00522

3. AFTERBODY/EXHAUST SYSTEM PERFORMANCE)

PT8/PA	A8	A9	CVTH	CVCAL	CVTOT	A9/ACC	CDAFT	CDPS	DAF/FN	DPS/FN
4.481	5.585	7.250	.985	1.000	.980	.577	.0506	.0118	.0776	.0203
2.397	8.952	9.114	.977	1.000	1.000	.725	.0672	.0001	.1243	.0005

4. INSTALLED PROPULSION SYSTEM PERFORMANCE

PS	FN	SFC	FRAM	FNC	SFCC
2.00	16132	2.018	5785	43474	2.218
1.00	7469	2.212	5785	20126	2.431

Table 1-XV: Installed Propulsion System Performance Output Map

The later approach to body geometry definition is programmed for more accurate and realistic analytical configuration. When a reference airframe has been defined by a designer, it is advantageous to simply exercise alternate engine designs within that airframe. A capability to automatically adjust airframe shape to accommodate the signature of the alternate engine allows this. The earlier version of BEAM had such capability to a degree. Care was required in its use to insure reliable analysis. The later version of BEAM was designed to provide this specific capability. With TEM 129C, alternate engines may be examined in any arbitrary (ESIP fighter/bomber type) fuselage by simply changing reference engine data and inlet size point, if required.

The specific points on the area plot required as inputs to the new program version and the functional relationships for areas and length in the new geometry method are illustrated in Figure 1-35. The two input points on the forebody may be selected arbitrarily. This region contains non-scaled components such as crew and crew space, electronics and avionics, radomes, etc. The other input points are sepcified at stations important to the propulsion system. All of these are monitored in the computational processes and component area requirements are readily established.

Results obtained with the TEM 129C version of BEAM are discussed at the end of the following section. In part, they show that by using TEM 129C a strong effect of engine length on optimum airframe length was established. This result lies at the core of engine/airframe integration and is one of the keys to exploitation of configuring a system to a particular engine signature.

1.2.11 ESIP Phase II Analysis Results

In the second phase of the Exhaust System Interaction Program, initial stages of a system development effort were simulated in order to select proper combinations of engines and airframes which satisfied a set of specified fighter/bomber mission requirements, evaluate effects of various levels of afterbody drag estimates on engine-airplane matching, identify engine company/airframer communications required for system optimization, and evaluate and improve system integration techniques examined in Phase I.

Investigation of systems powered by General Electric engines yielded the results compared graphically in Figure 1-36. These optimum derivative characteristics were obtained using

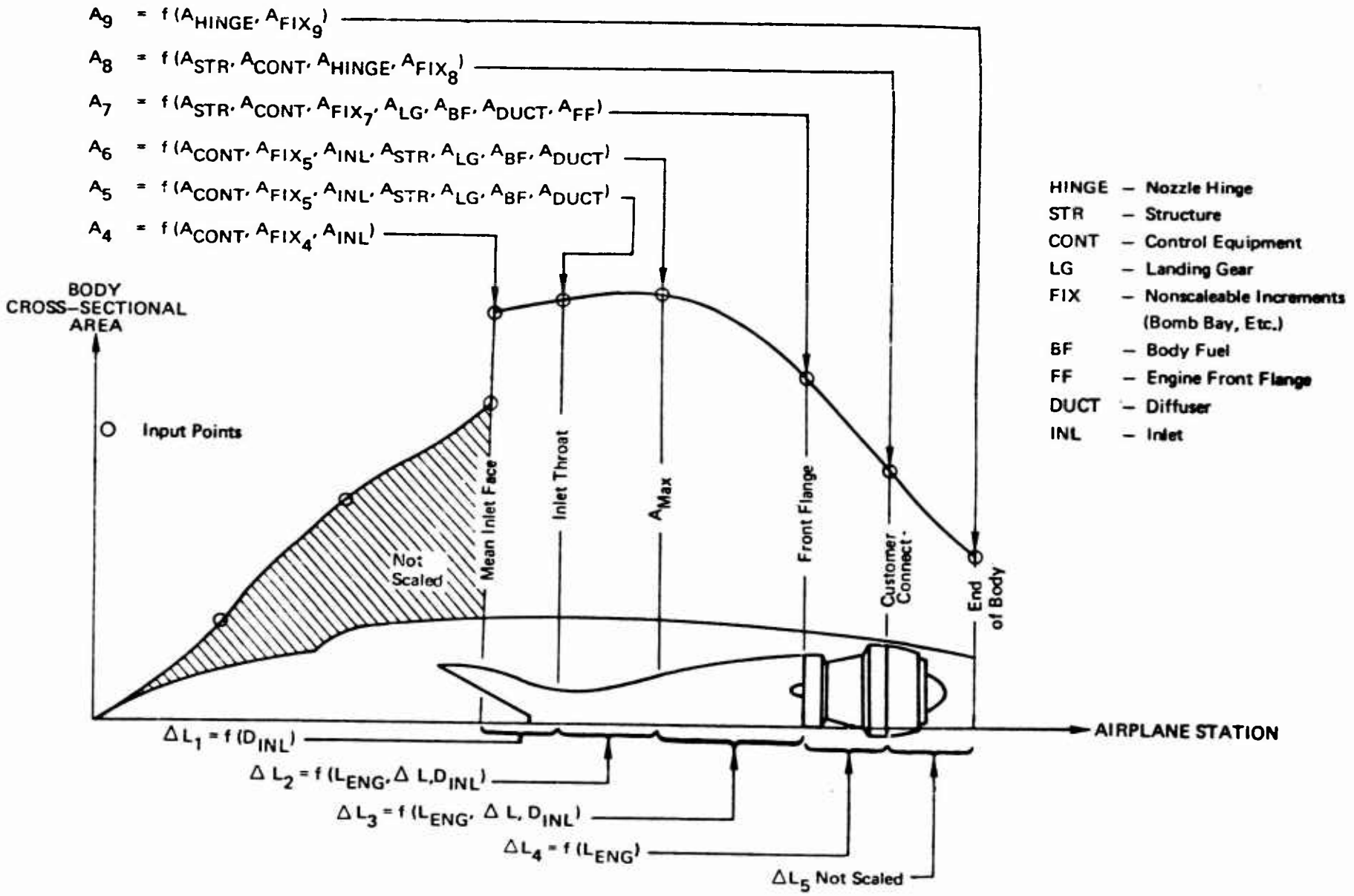

Figure 1-35: Fuselage Geometry Scaling

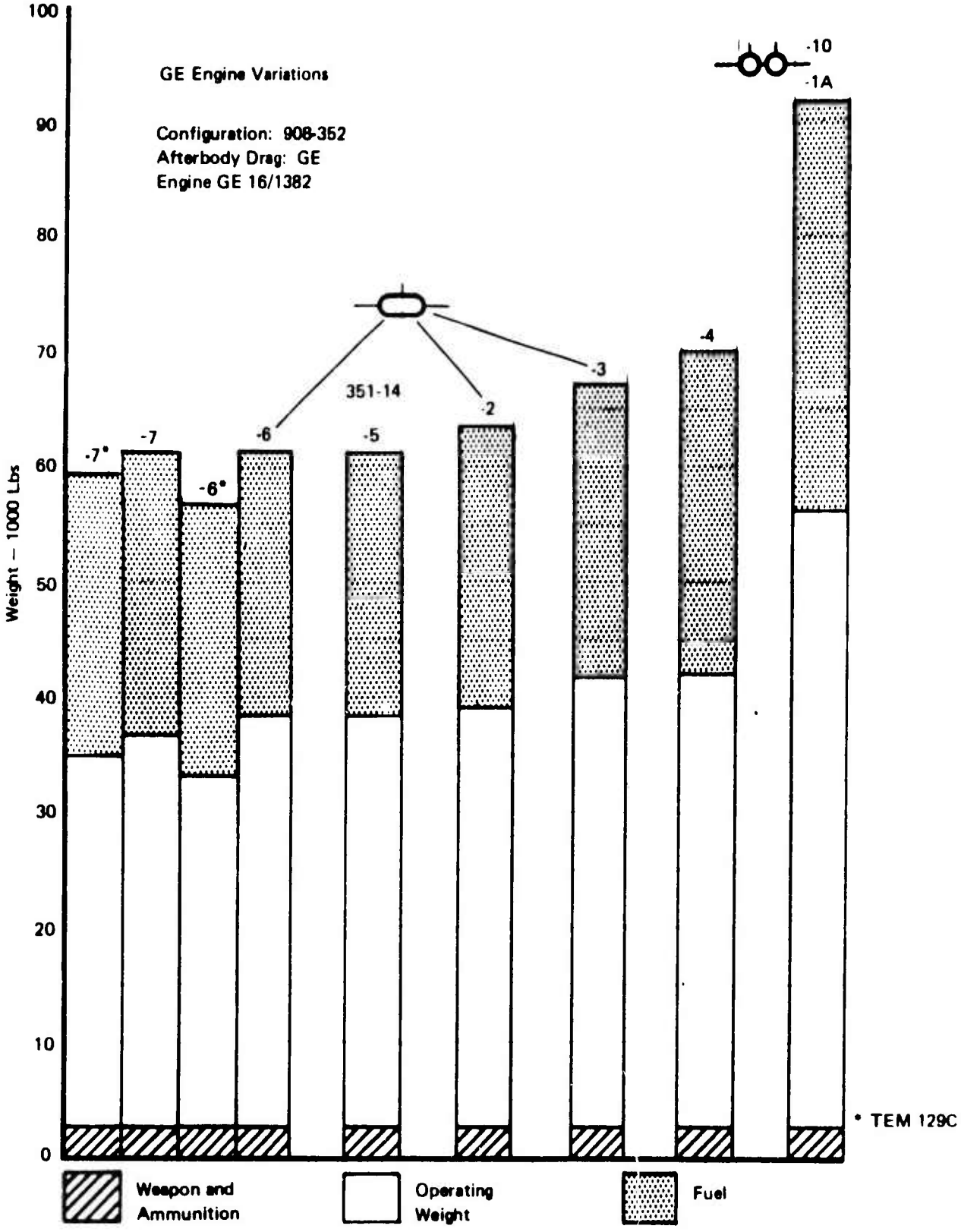

Figure 1-36: Optimum Derivative Airplane Weight Comparison GE Engine Variation

the early, TEM 129, version of BEAM and afterbody drag estimates made by General Electric. The comparison shows the substantial improvement in system figure-of-merit attributable to engine performance characteristics identified by the "derivative approach" to engine cycle determination.

Results of analyses on systems powered by Pratt & Whitney engine offerings are compared on Figures 1-37 and 1-38. System figures-of-merit for both fixed and variable geometry turbine powered designs are included. Note the slight advantage of the variable geometry turbine configurations over the fixed geometry designs.

Figure 1-39 illustrates the relative merit of afterbody arrangements studied in Phase II. The insensitivity of afterbody arrangement to cycle selection for the fighter/bomber requirements is illustrated in Figure 1-40. The results, like those of the previously discussed Pratt & Whitney powered system, were obtained using TEM 129 and Pratt & Whitney afterbody drag estimates.

Effect of afterbody drag level on fighter/bomber system performance is illustrated by the comparison on Figure 1-41. The comparison shows little effect of afterbody drag on system figure-of-merit. This result is believed to be due to both the low levels of afterbody drag estimated for the fighter/bomber and the insensitivity of system performance to afterbody drag for the specified mission requirements.

Several analytical system integration techniques were explored during the Phase II analyses. At first, candidate engines were manually integrated with airframes by a designer. Later, analytical capabilities of the TEM 129 version of the BEAM program were used to assimulate candidate engines into selected reference airframe definitions. A comparison of systems integrated in each of these two ways is presented in Figure 1-42. The results compare favorably.

A later version of BEAM, TEM 129C, incorporated a more realistic body geometry subroutine and the capability to optimize fuselage length and, therefore, affect the system's structural weight/drag relationship. Exploitation of the latter capability yielded the results shown on Figures 1-43 and 1-44.

Both Figures 1-43 and 1-44 show the importance of proper configuration for a particular engine shape. The shorter A1.7 and GE-6 engines integrate more efficiently with shorter airframes. Results of these analyses indicate that the variable geometry engine yields little advantage over the advanced fixed geometry cycle and that the GE-6 engine is

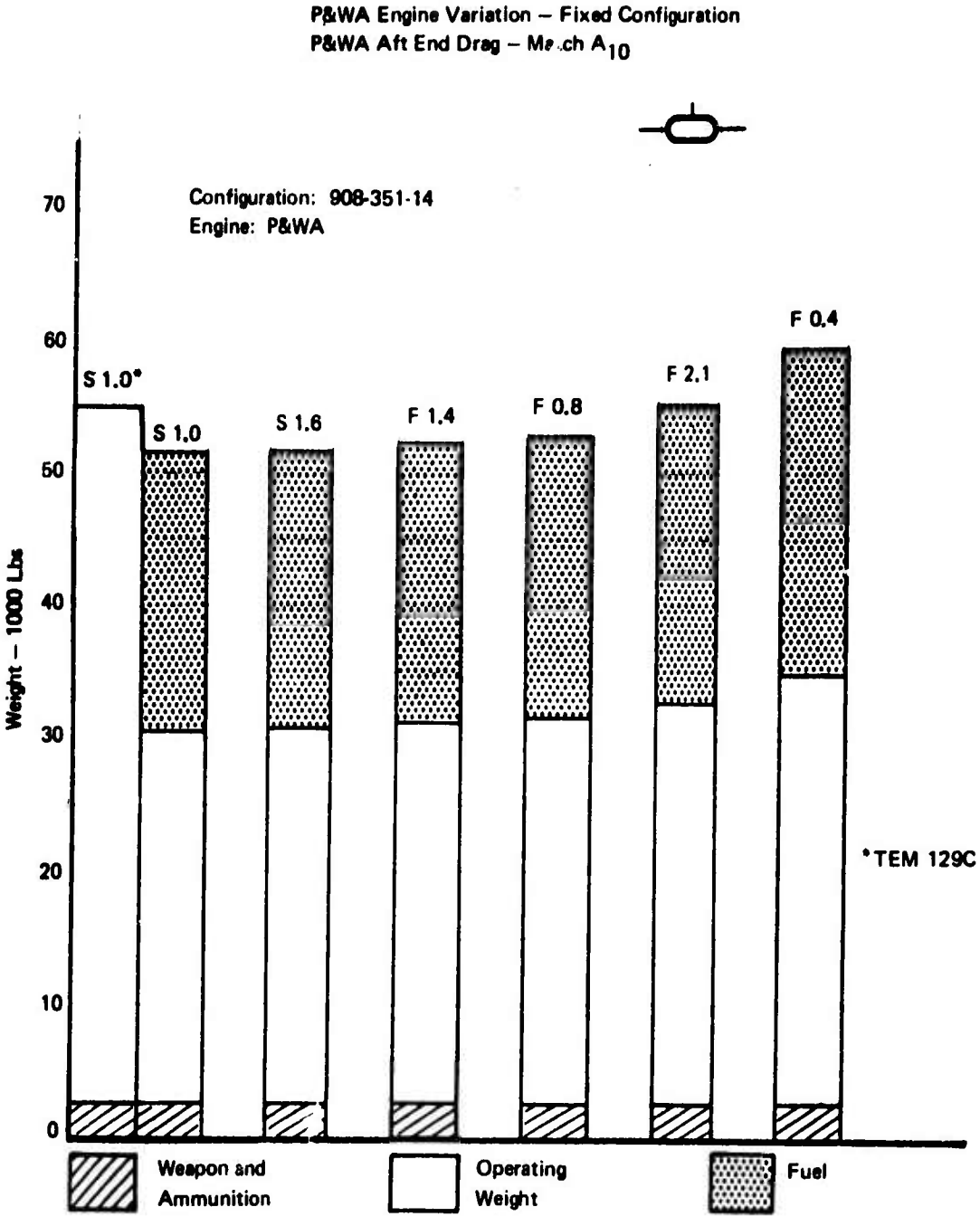

Figure 1-37: Optimum Derivative Airplane Weight Comparison P&WA Engine Variation

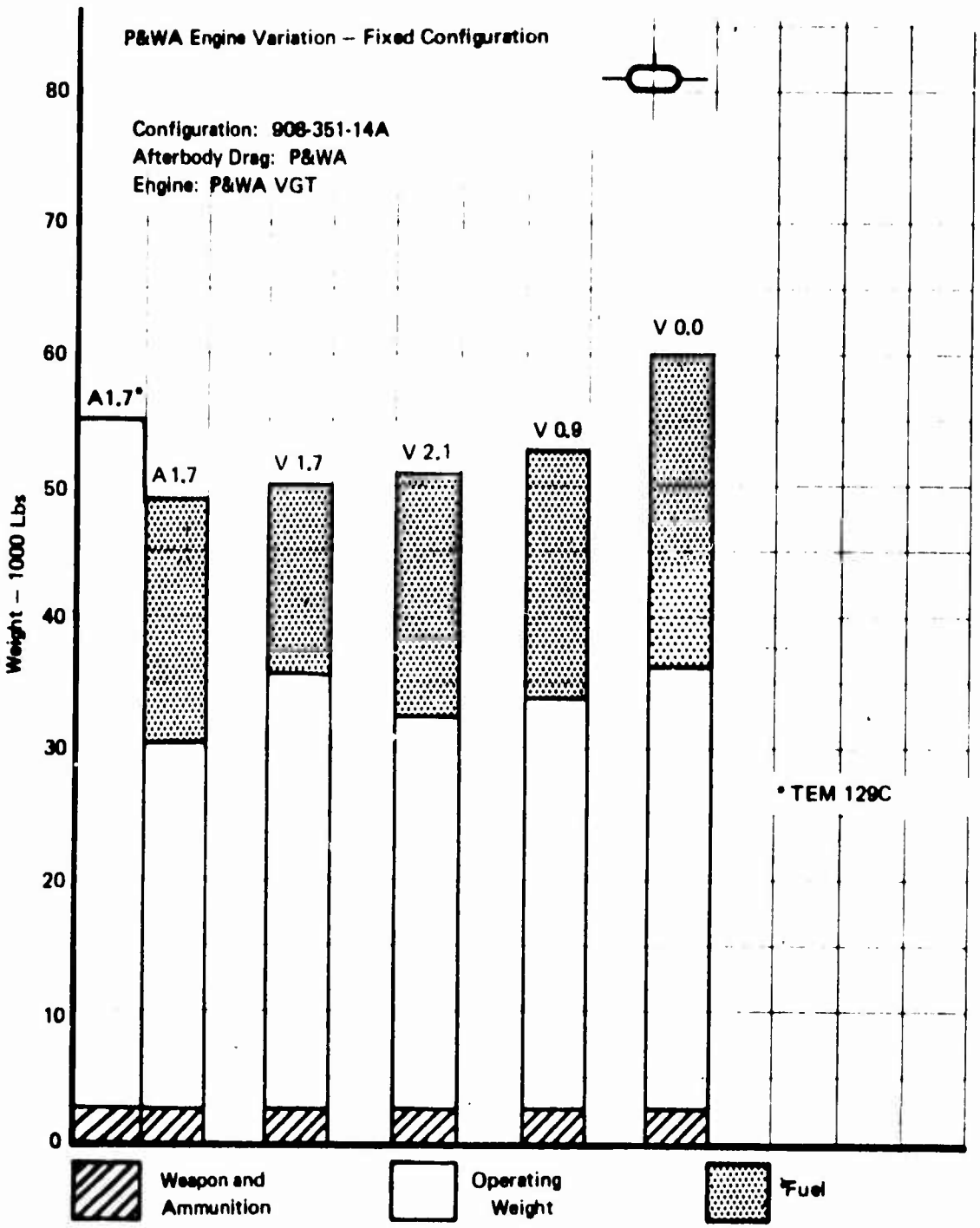

Figure 1-38: Optimum Derivative Airplane Weight Comparison P&WA VGT Engines in 908-351-14A Configuration

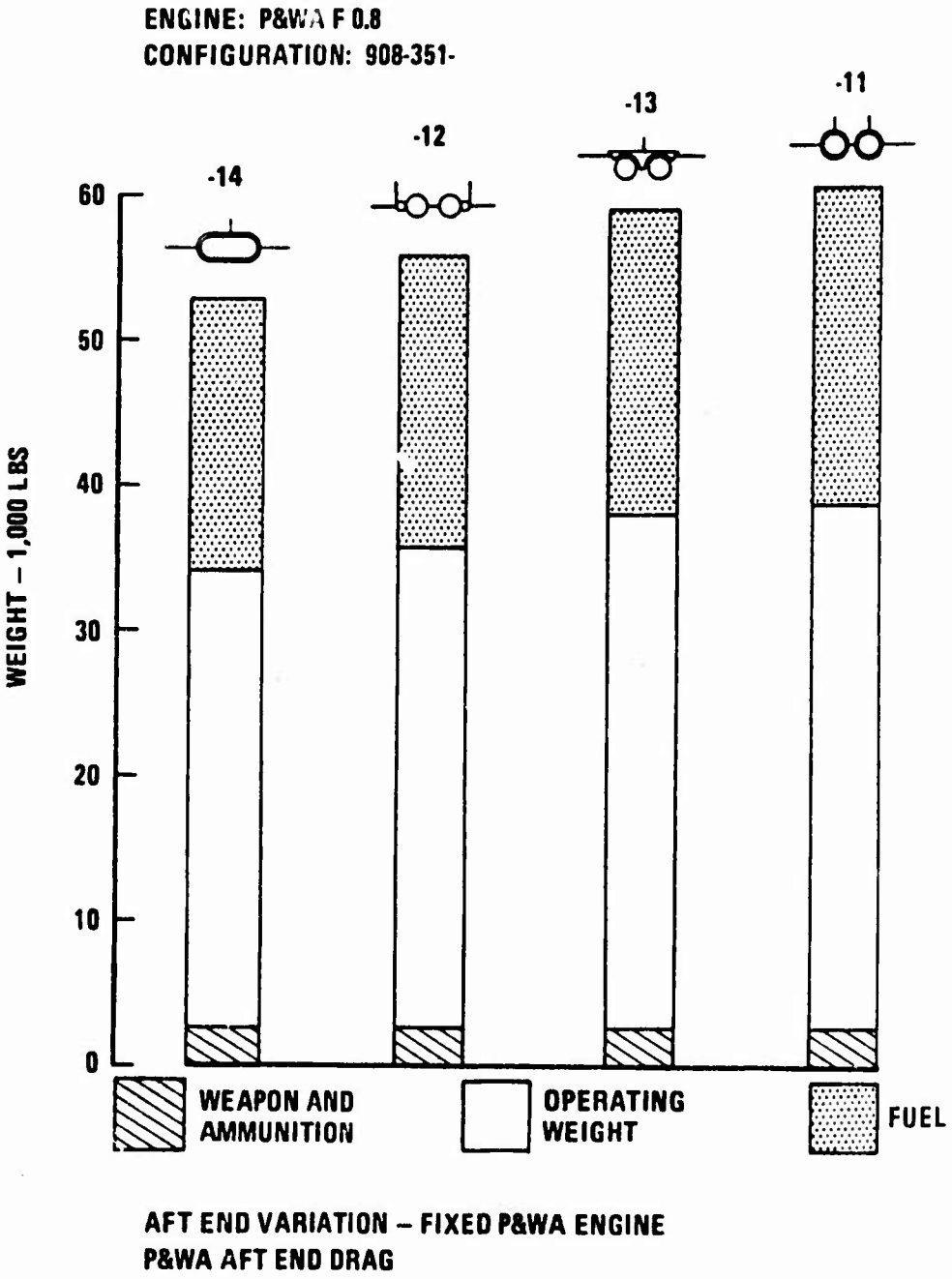

Figure 1-39: Optimum Derivative Airplane Weight Comparison – P&WA Engine Variation

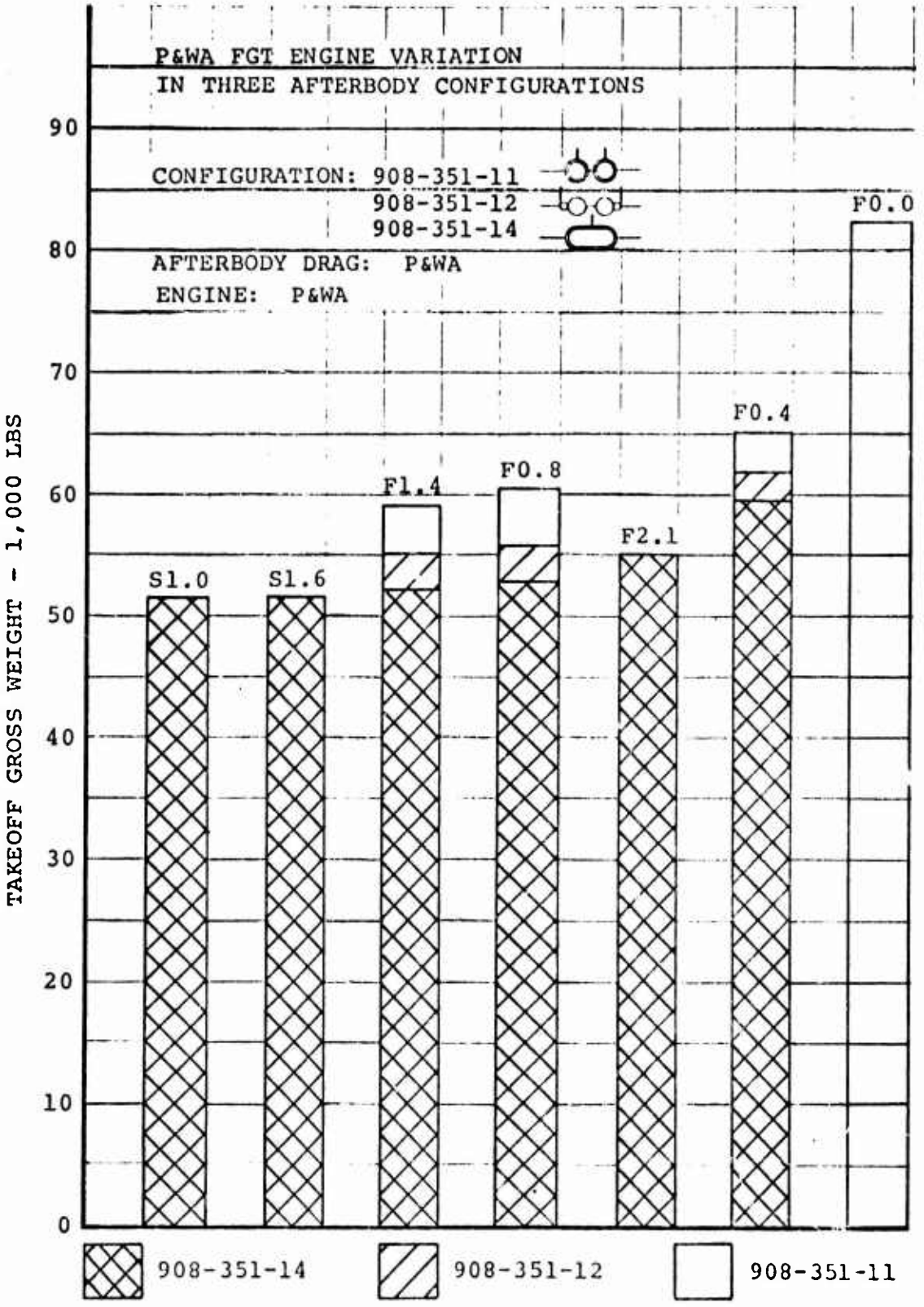

Figure 1-40: Optimum Derivative Airplane Weight Comparison – Effect of Afterbody Type on Engine Rank

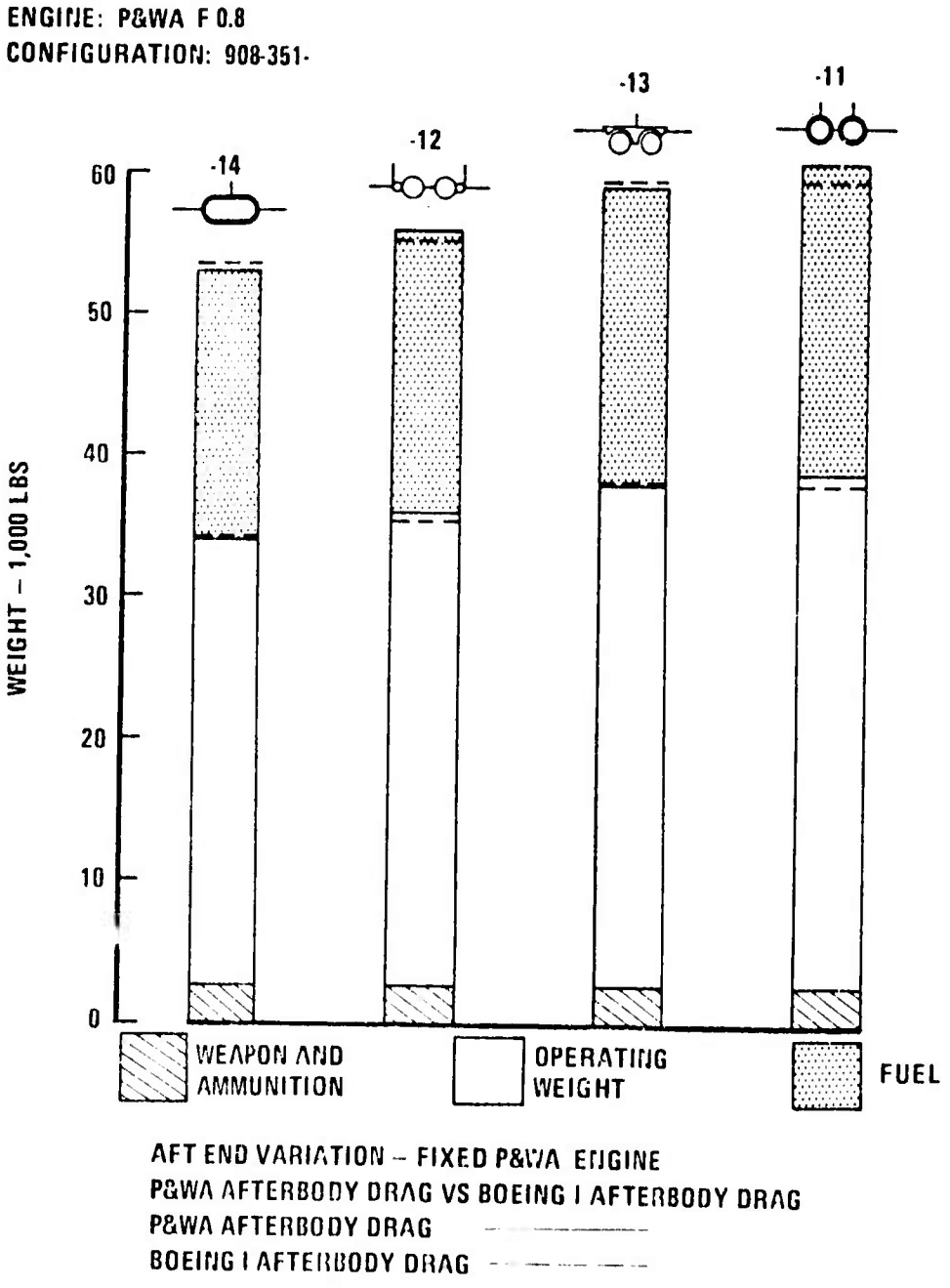

Figure 1-41: Optimum Derivative Airplane Weight Comparison – P&WA Engine Variation

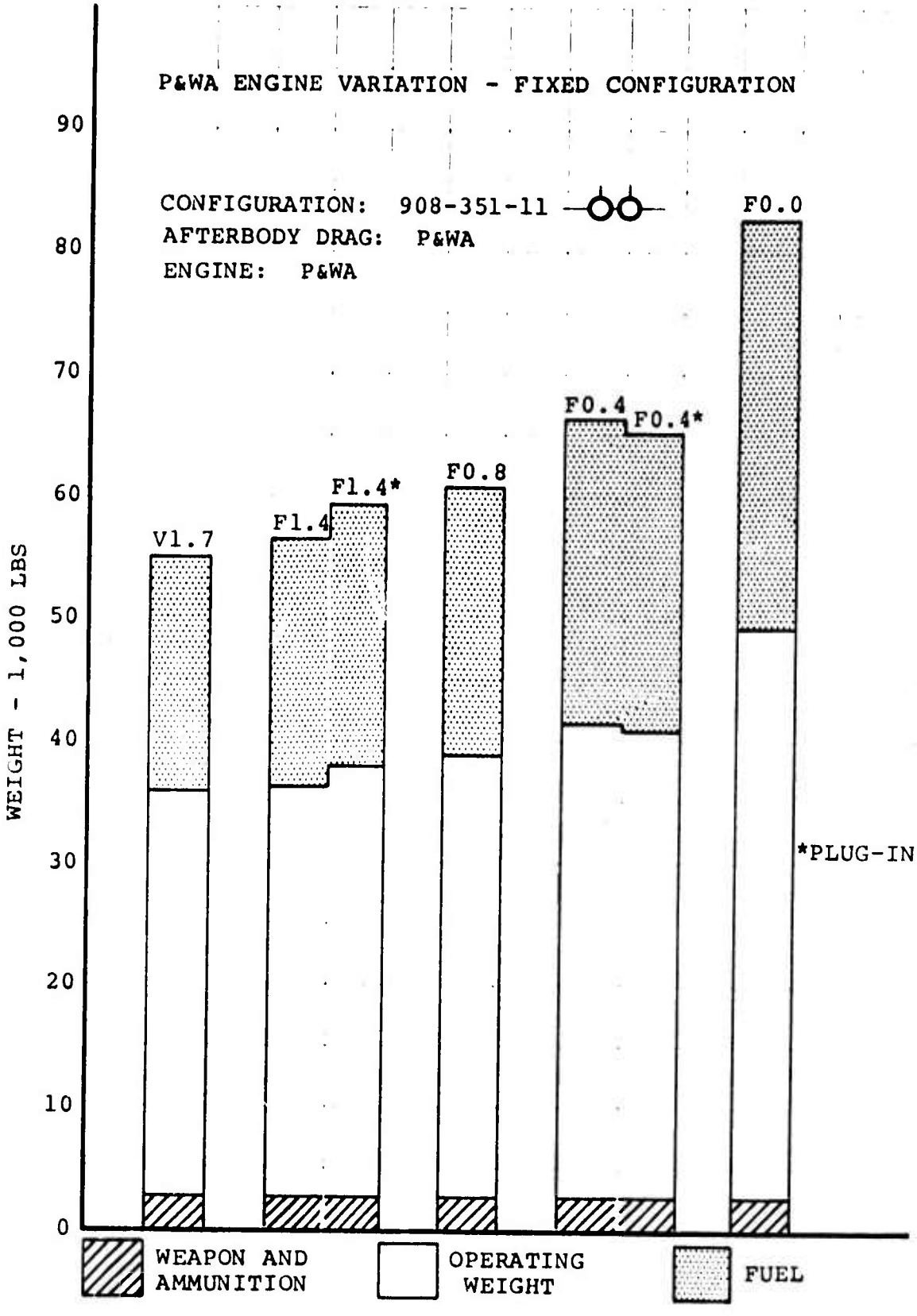

Figure 1-42: Optimum Derivative Airplane Weight Comparison – P&WA Engines in 908-351-11 Type Configuration

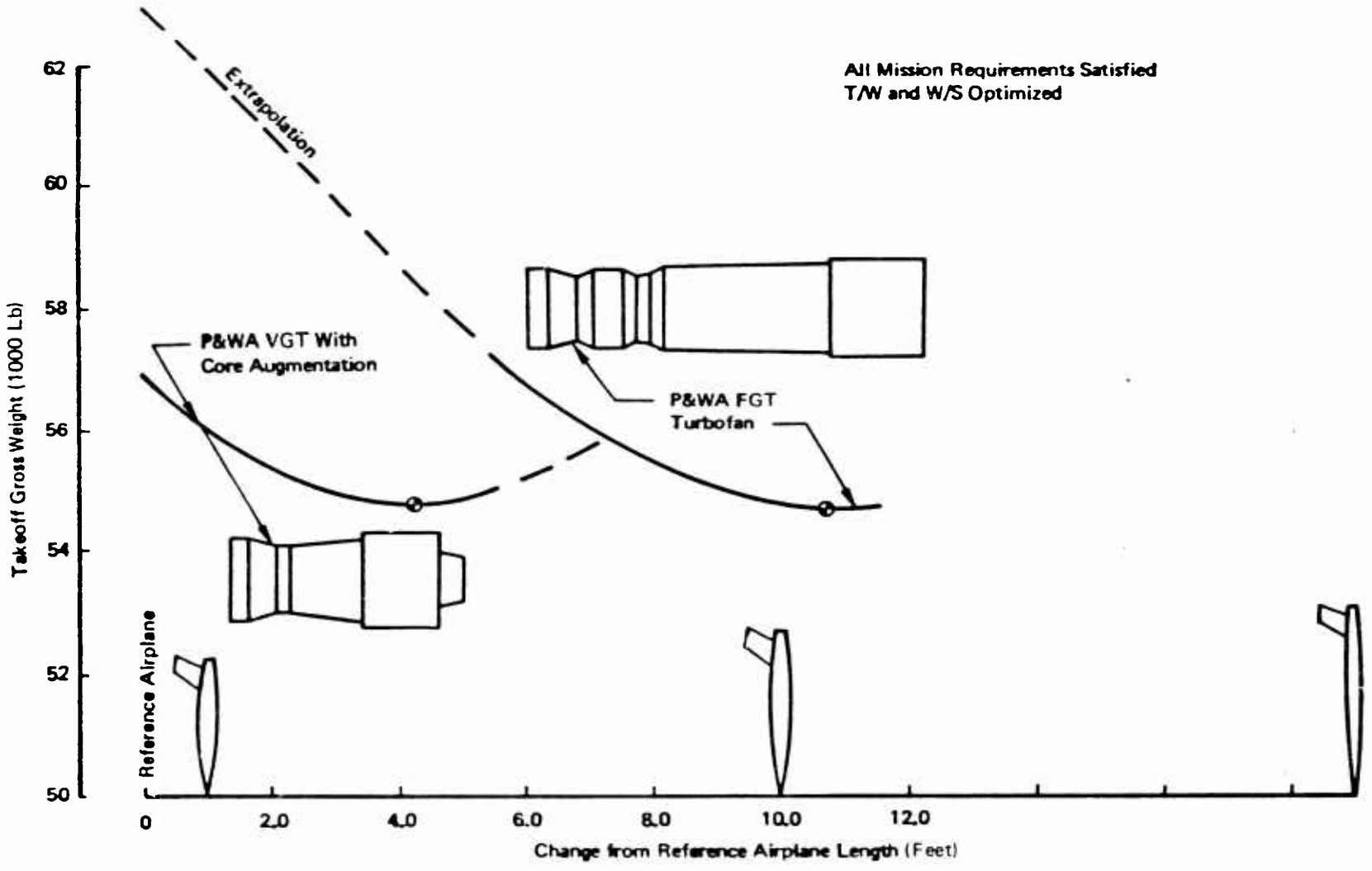

Figure 1-43: Effect of Engine Signature and Airplane Length on Takeoff Gross Weight, TEM 129C

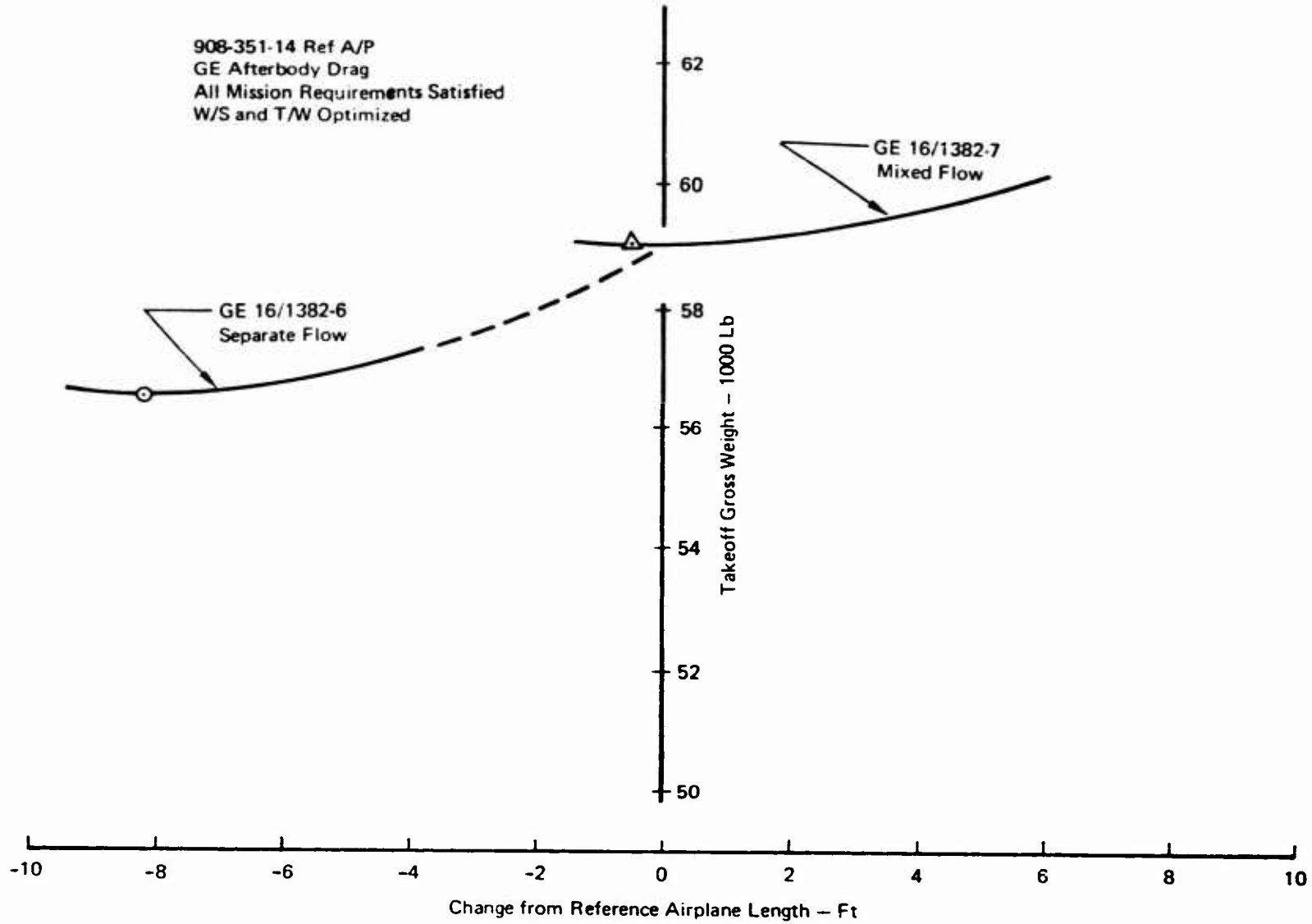

Figure 1-44: Effect of Engine Signature and Airplane Length on Takeoff Gross Weight TEM 129C, GE Engines

superior to the GE-7. The latter result was expected by General Electric and is in opposition to the result obtained with the TEM 129 version of BEAM illustrated on Figure 1-36.

1.2.12 Phase II and III Test Program Description

The wind tunnel model constructed during Phase II and Phase III of the Exhaust System Interaction Program is designed to produce transonic and supersonic data for two-engine multimission aircraft designs. The objectives of the Phase II propulsion tests are to provide experimental data for three candidate airframe-exhaust system combinations to determine the quality of prior predictions and to develop test techniques. The objective of the Phase III aerodynamic tests is to provide detailed experimental data for a single configuration, suitable for final performance predictions. The 0.12 scale model is designed for testing in the AEDC Propulsion Wind Tunnel 16T and 16S facilities. The model is strut-mounted for Phase II tests and is equipped with airblowing nozzles to simulate exhaust plumes. For Phase III testing, the model is sting-mounted and is equipped with flow-through inlets.

The model is divided at A_{MAX} into forebody and afterbody segments. Each is supported from a separate balance to isolate the afterbody and emphasize the exhaust system and its interaction on the airframe, engine, and inlet. A common basic forebody is used for all test configurations. Phase II afterbody exterior contours are true models of three real aircraft designs. Each of the three afterbodies is equipped with three nozzle configurations which provide exit geometry corresponding to cruise, combat, and acceleration segments of the mission profile. The Phase III afterbody is a derivative of one of the Phase II configurations with acceleration nozzles.

The technical approach to the test program requires close coordination between the Phase II and Phase III tests. This approach isolates the incremental aerodynamic effects needed for data correction and application. These increments are power lever effects; nozzle exit geometry effects; inlet fairing interference with and without afterbody boattailing; sting interference; and strut interference. Application of the test results to airplane performance evaluation is based on thrust and drag accounting procedures established in the ESIP program.

Test data are obtained primarily from force and pressure measurements. Two conventional internal balances are installed in tandem to provide separate 6-component measurements of forebody and afterbody forces and moments. External surface drags are measured independently of thrust to improve the quality of drag data by eliminating large thrust tare forces in the drag measurements. Nozzle plug axial forces are measured on one of the Phase II configurations. Pressures are measured with the AEDC P^2B system to provide base and cavity corrections, internal duct flow and blowing nozzle pressure profiles, boundary layer characteristics, and cruise nozzle surface static pressure distributions. Momentum losses in the flow-through duct are subtracted from drag measurements on the forebody balance which supports the entire duct. Oil flow patterns will be observed and photographed during selected runs to show regions of separation on the afterbodies.

Transonic tests are planned for a Mach number range from 0.55 to 1.5. The nominal test conditions correspond to a Reynolds number per foot of 2.5×10^6. The planned Mach number range for the supersonic tests is from 1.6 to 2.7, and the nominal Reynolds number per foot is 0.6×10^6.

Prior to the cancellation of the Phase II and III tests due to AEDC schedule slides, Phase III was intended to demonstrate the methods and achievable accuracy of performance predictions as would be made during the configuration development and design validation phases of airplane development. Phase III was partially accomplished by using available experimental data from associated U. S. Air Force programs.

1.2.12.1 Technical Approach

The technical approach to achieve Phase II and III test objectives is illustrated in Figure 1-45. This approach requires closely integrated propulsion testing and aerodynamic testing. The Phase II propulsion tests with blown nozzles and the Phase III aerodynamic tests with flow-through inlets incorporate variations in model and support combinations from which new test techniques can be developed and verified.

Figure 1-46 shows the test hardware combinations necessary to implement the technical approach. A forward support strut is used for all blowing tests. Flow-through inlet tests are conducted with both the strut and conventional aft sting support systems.

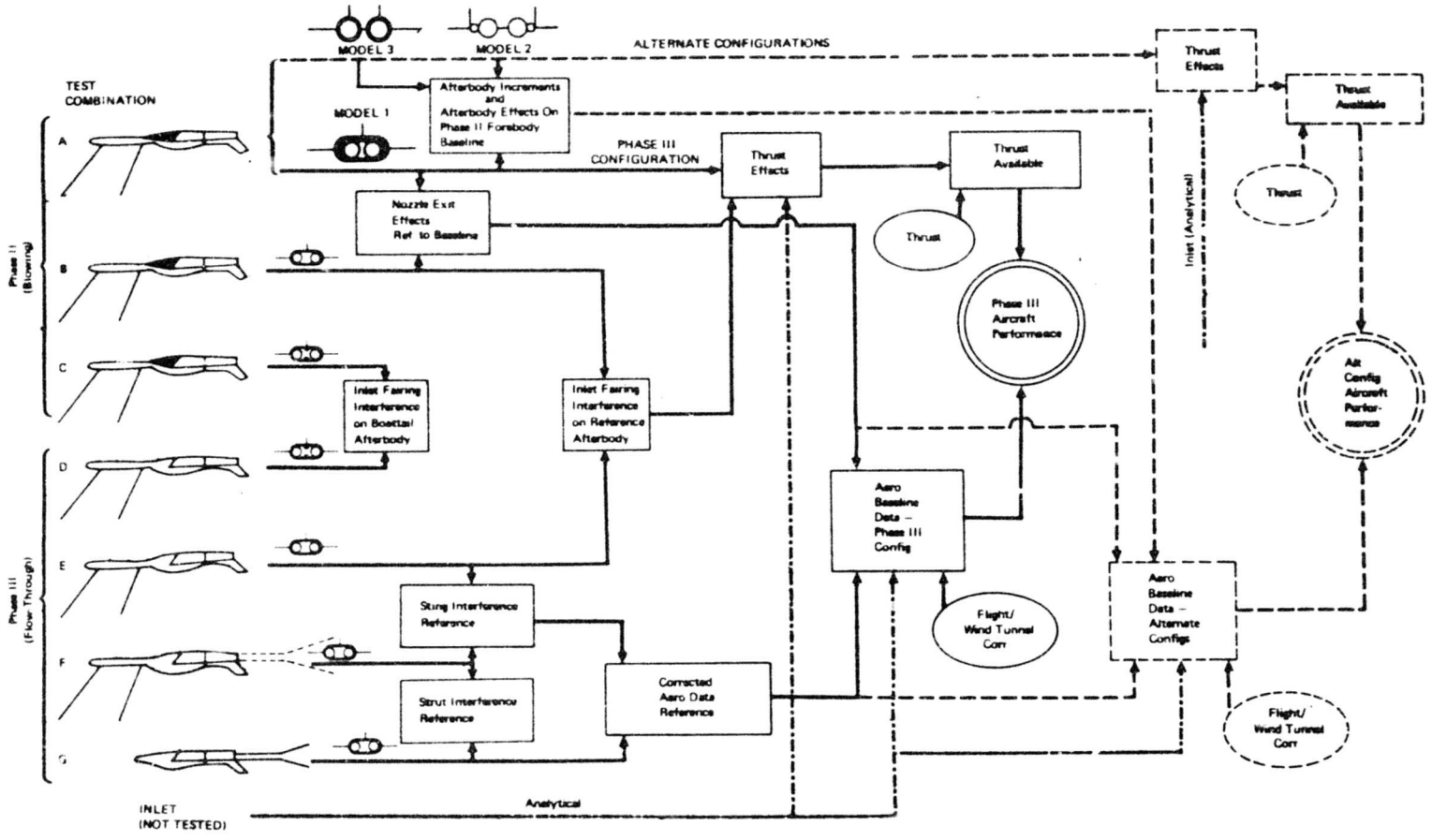

Figure 1-45: Technical Approach

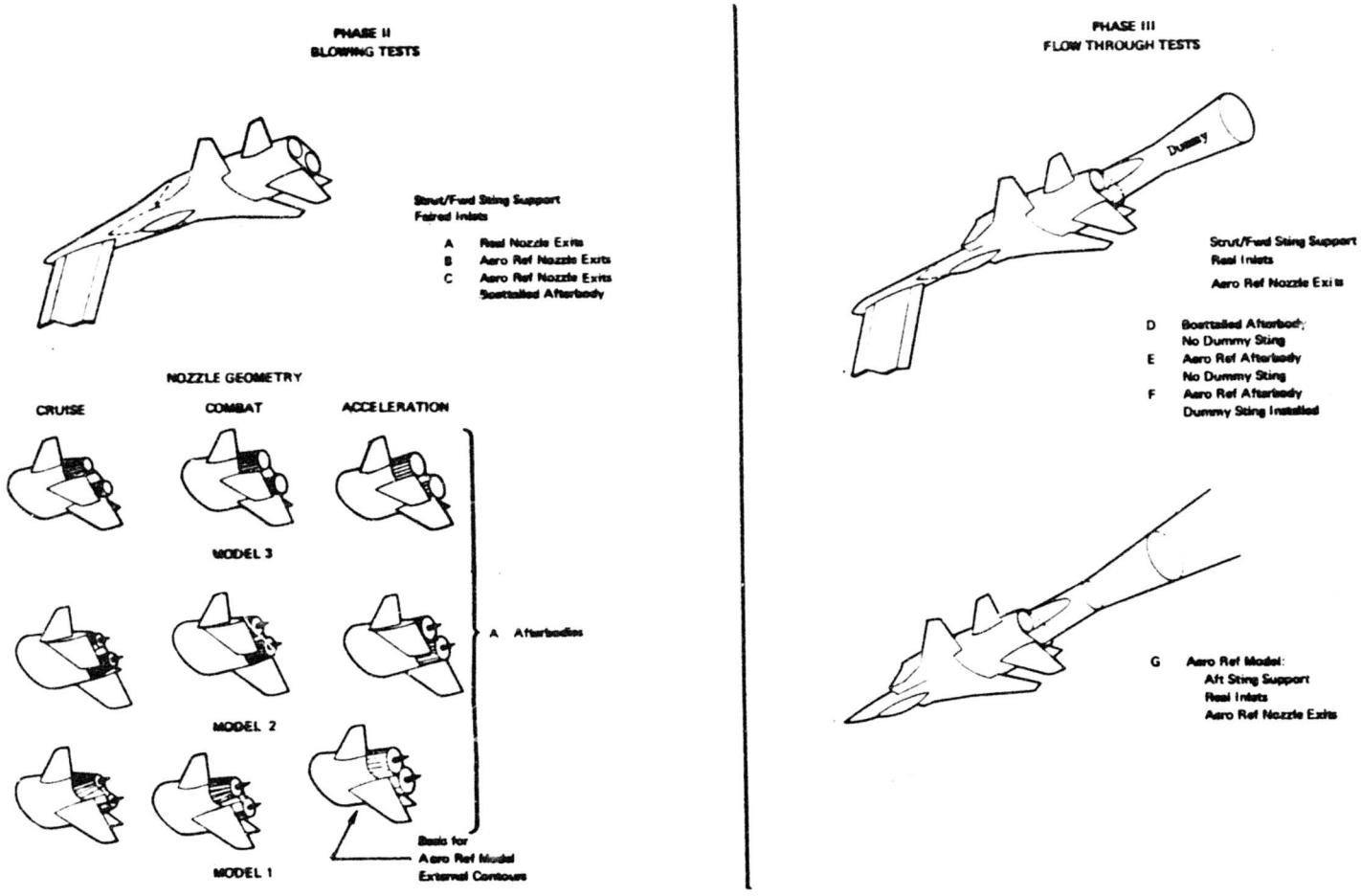

Figure 1-46: Test Combinations

All models are separated into forebodies and afterbodies with the metric break at A_{MAX}. The forebody is common to all configurations. Test Combination A is the basic blowing (propulsion) model, and consists of nine configurations as shown: three afterbody configurations from A_{MAX} to customer connect, each having three nozzle configurations corresponding to cruise, combat, and acceleration segments of the mission profile. The exterior contours of these nine configurations are authentic representations of actual aircraft designs developed during Phase II.

Test Combinations B through G use the Model 1 afterbody from A_{MAX} to customer connect. Test Combination G is the basic flow-through (aerodynamic) model. Its external contours downstream of customer connect are modified Model 1 acceleration nozzle contours. The modifications eliminate the step at customer connect and replace the compound curvature of the real nozzle with straight-line fairings to the acceleration nozzle exit plane cross-section. The purpose of these modifications is to provide the most reliable and repeatable aerodynamic reference data by removing all sources of separation. At the exit plane of this configuration, the flow-through duct exits are located at the outboard limits of the cross-section, thus providing space for a single centerline aft sting support.

External afterbody contours of Test Combinations B, E, and F are identical to the aerodynamic reference model, G. Test Combinations C and D are boattailed aft of customer connect in the region between the airflow exit ducts.

The technical approach illustrated in Figure 1-45 isolates all of the data correction and accounting elements needed for the Phase III configuration:

A	Power lever effects
A - B	Nozzle exit effects
B - E	Inlet fairing interference
C - D	Inlet fairing interference (boattail)
E - F	Sting interference
F - G	Strut interference

The power lever effects from A are measured with realistic exhaust system geometry and account for incremental aerodynamic loads produced by power setting variations from the baseline. The baseline power setting corresponds to the pressure ratio used to normalize thrust and drag data.

Nozzle exit effects from A - B account for incremental aerodynamic loads from reference to baseline conditions. Reference conditions are the flow-through geometry and exit pressure

ratio from the aerodynamic reference model tests. Baseline conditions are realistic exhaust system geometry and pressure ratio used to normalize thrust and drag data.

Inlet fairing effects from B - E may be misleading because of little boattailing on the aerodynamic reference model. C - D will show the sensitivity of inlet fairing effects to boattailing. If C - D differs from B - E, the blowing model test results are not valid because changes in inlet interference would be included in the boattailing effects measured with the three nozzle configurations. In this event, further blowing tests must be postponed until an inlet fairing is devised which produces the same effects on the boattailed and non-boattailed configurations. Two sets of inlet fairings are provided for this contingency.

Sting interference from E - F accounts for aerodynamic effects introduced by the support system used for the aerodynamic reference model.

Strut interference from F - G is not used directly in the data handling procedures, but provides a quantitative evaluation of this particular design for consideration in future test programs.

Complete evaluation of only one configuration is possible because only one flow-through model configuration is available. This Phase III configuration is consistent with Model 1 of Phase II.

1.2.12.2 Alternate Configurations

The two alternate afterbody configurations, Models 2 and 3, provide additional incremental data from Test Combination A as follows:

A	Power lever effects
A	Afterbody effects on Phase II forebody
A	Afterbody configuration effects

The power lever effects of Models 2 and 3 account for power setting variations from their baselines similar to the Model 1 power lever effects.

Afterbody effects on the Phase II forebody account for incremental forebody loads with the Model 1 afterbody replaced with the Model 2 and 3 afterbodies. If signficant effects are found, valuable information is provided on interference phenomena seldom if ever investigated. The

afterbody configuration effects account for afterbody increments due to configuration differences between Model 1 and Models 2 and 3. The forebody plus afterbody increments are applied to the Phase III aerodynamic baseline data as shown in Figure 1-45 to give approximate aerodynamic baseline data for the alternate Model 2 and Model 3 configurations.

The process is subject to probable error because configuration effects and thrust effects are evaluated simultaneously and in the presence of the support strut, forward sting, and inlet fairings, which may have a different influence on different afterbodies. For example, if the strut interference from F - G is large on the Phase III (and, therefore, Model 1) afterbody configuration, it is likely to be different on the Model 2 and 3 afterbodies. Thus, changes in strut interference are misinterpreted as part of the afterbody configuration effects. Also, a single model forebody configuration is used with all three afterbodies, whereas actual designs are tailored with different forebody and wing details. Therefore, if the afterbody effects on the Phase II forebody are large, they may be substantially different on realistic forebodies.

Drag increments applied to available thrust for baseline to power condition effects are completely evaluated in A for the alternate configurations as well as the Phase III (Model 1) configuration. Therefore, the ΔT increments are evaluated in the same manner as given above for the Phase III configuration.

1.2.12.3 Test Model General Characteristics

The aircraft designs were developed, evaluated and selected during ESIP Phase II analytical studies. The test model scale is 0.12. It is designed for transonic and supersonic testing in the AEDC Propulsion Wind Tunnel 16T and 16S facilities. The model is strut-mounted for Phase II tests and is equipped with airblowing nozzles to simulate exhaust plumes. The model is sting-mounted for Phase III tests and is equipped with flow-through inlets.

The model is divided at A_{MAX} into forebody and afterbody segments. Each is supported from a separate balance to isolate the afterbody and emphasize the exhaust system and its interaction on the other configuration elements. The gross body cross-sectional area at A_{MAX}, exclusive of the wing, is 102.43 square inches.

A common forebody, shown in Figures 1-47 and 1-48 is used for all test configurations. The forebody nose is modified with a forward sting fairing when the model is strut-mounted (Figure 1-49). The inlets are capped with fairings for all blown nozzle tests.

The wing is a high performance design using Boeing airfoil sections. Thickness, twist and camber distributions are selected to optimize cruise at M = 0.82. Full consideration is given to anhedral and pivot tilt effects, as well as integration with the strake and body at sweep angle extremes. The wing is attached to the forebody, with provisions for leading edge sweep angles of 35°, 45°, and 75°. The wing also is removable together with its strake. Model wing characteristics are given in Figures 1-47 and 1-50.

The tail surfaces are Boeing symmetrical airfoil sections with 5% thickness ratio, 0.35 taper ratio, 0.8 aspect ratio, and 60° leading edge sweep angle. Horizontal tail surfaces are attached at variable stabilizer angles to determine control effectiveness and trim settings to be used during blowing tests. All tail surfaces are removable.

The following details are included in the model contours:

Aft facing step at body/engine customer connect
Horizontal tail body flats
Wing/strake steps at forward sweep angles
Unsealed horizontal stabilizers at side-of-body
Pivot fairings
Realistic wing bay configuration

1.2.12.4 Phase II Model

The Phase II blowing model is always mounted inverted from the swept strut and forward sting (Figures 1-49 and 1-51). The strut is supported from the tunnel test section pitch table. This strut support system was evaluated in AEDC Tunnel 1T during a strut evaluation test sponsored by the Air Force Aero Propulsion Laboratory. Based on test results, the strut is swept upstream from the model for 16T tests (Figure 1-52). The strut is swept downstream from the model for 16S tests. The strut is built with adjustable pad adapters to the tunnel pitch table to permit reversal between 16T and 16S, and to modify the ±10° pitch table pitch range. The air supply line and instrumentation leads are fed through the strut and sting.

The single air supply passage on the forward sting centerline is divided inside the model and diverted outboard to the

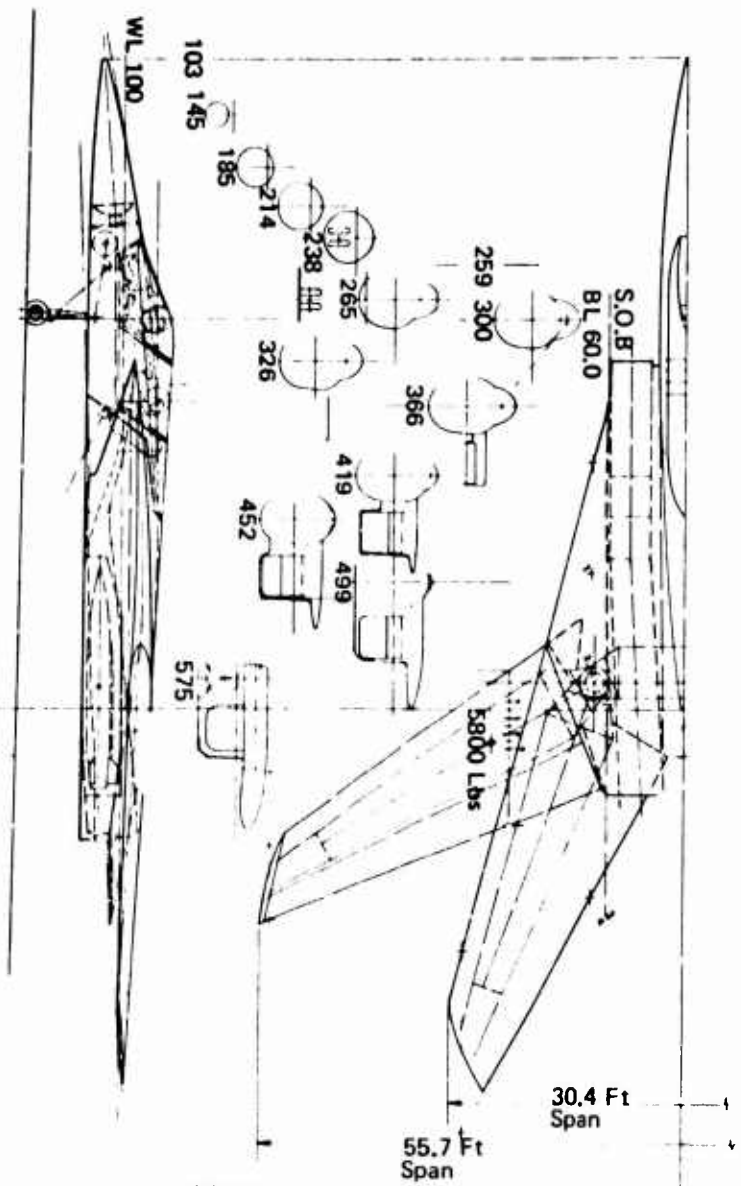

GEOMETRY

		WING	
		35	75
		490	724
		54.22	29.7
		- 8	- 8
		6.0	1.14
		.35	.296
		116.8	333.5

Gross Weight T.O.	55,000
Fuel F.I.F.	20,000
A_{cap} Total	16.28 Sq Ft
Wetted Areas	
Body Structure	921
Body Net	890
Wing 35°	828
Wing 75°	760

Figure 1-47: General Arrangement ESIP Forebody

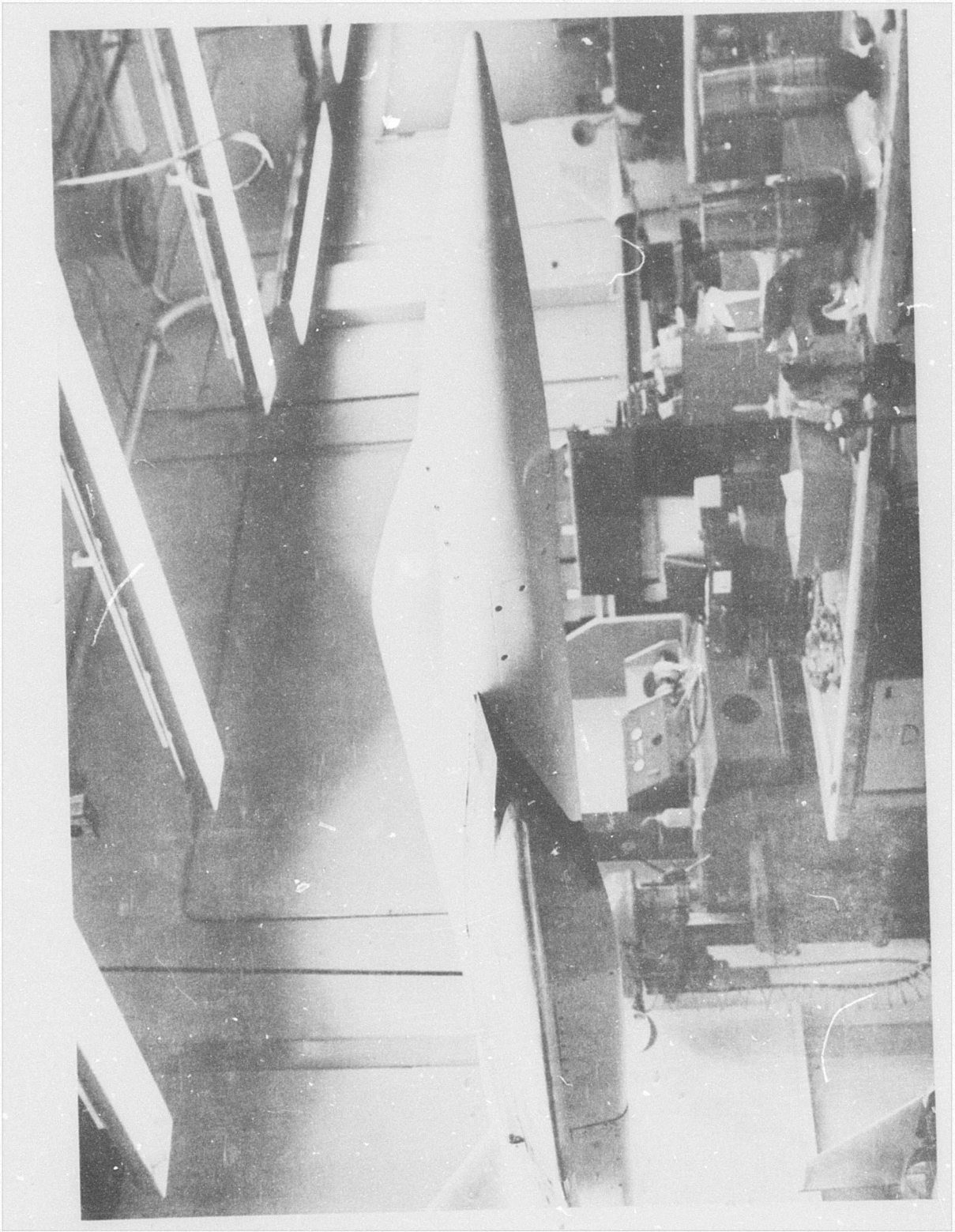

Figure 1-48: Model Forebody

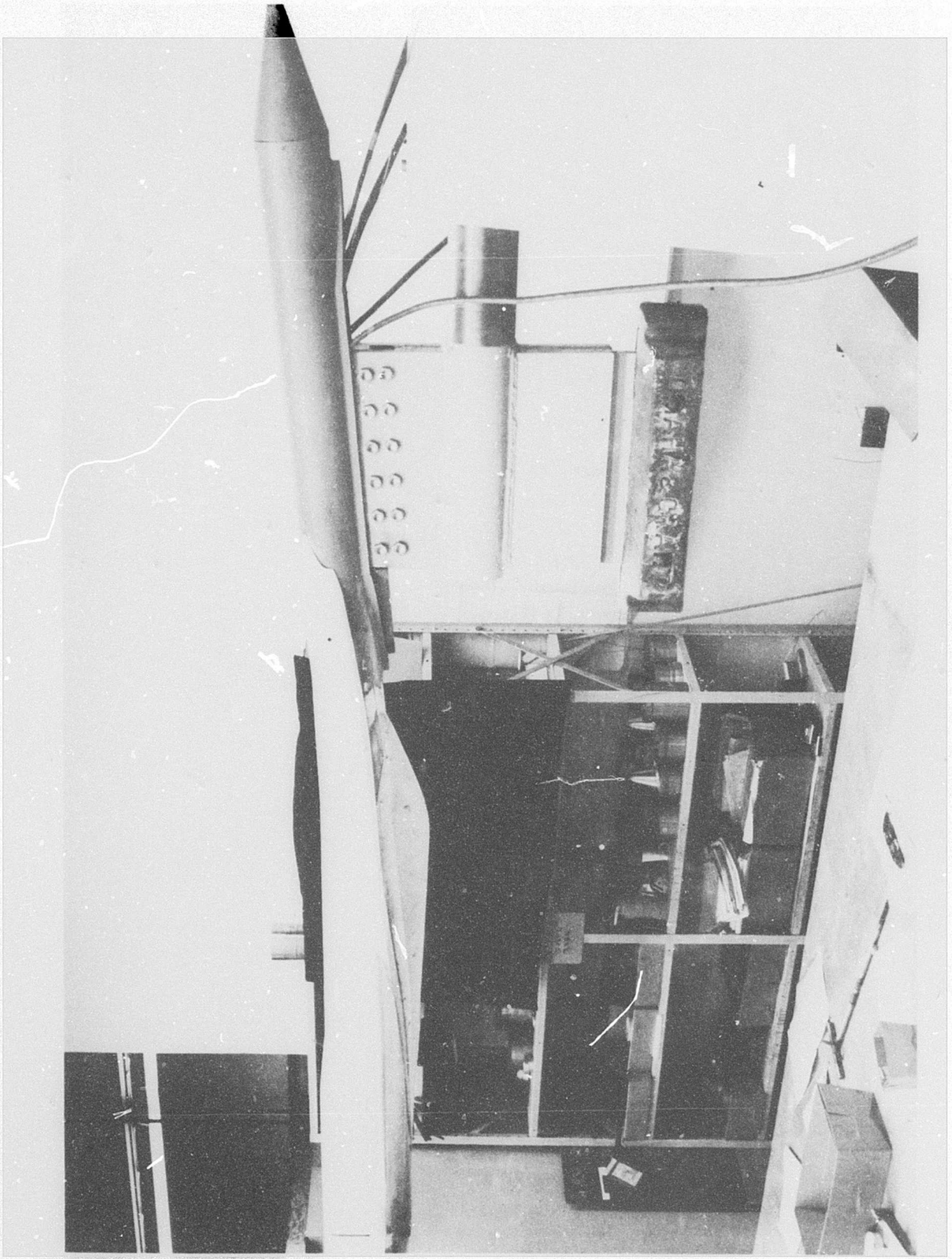

Figure 1-49: Model Forebody With Forward Sting, Strut Mounted

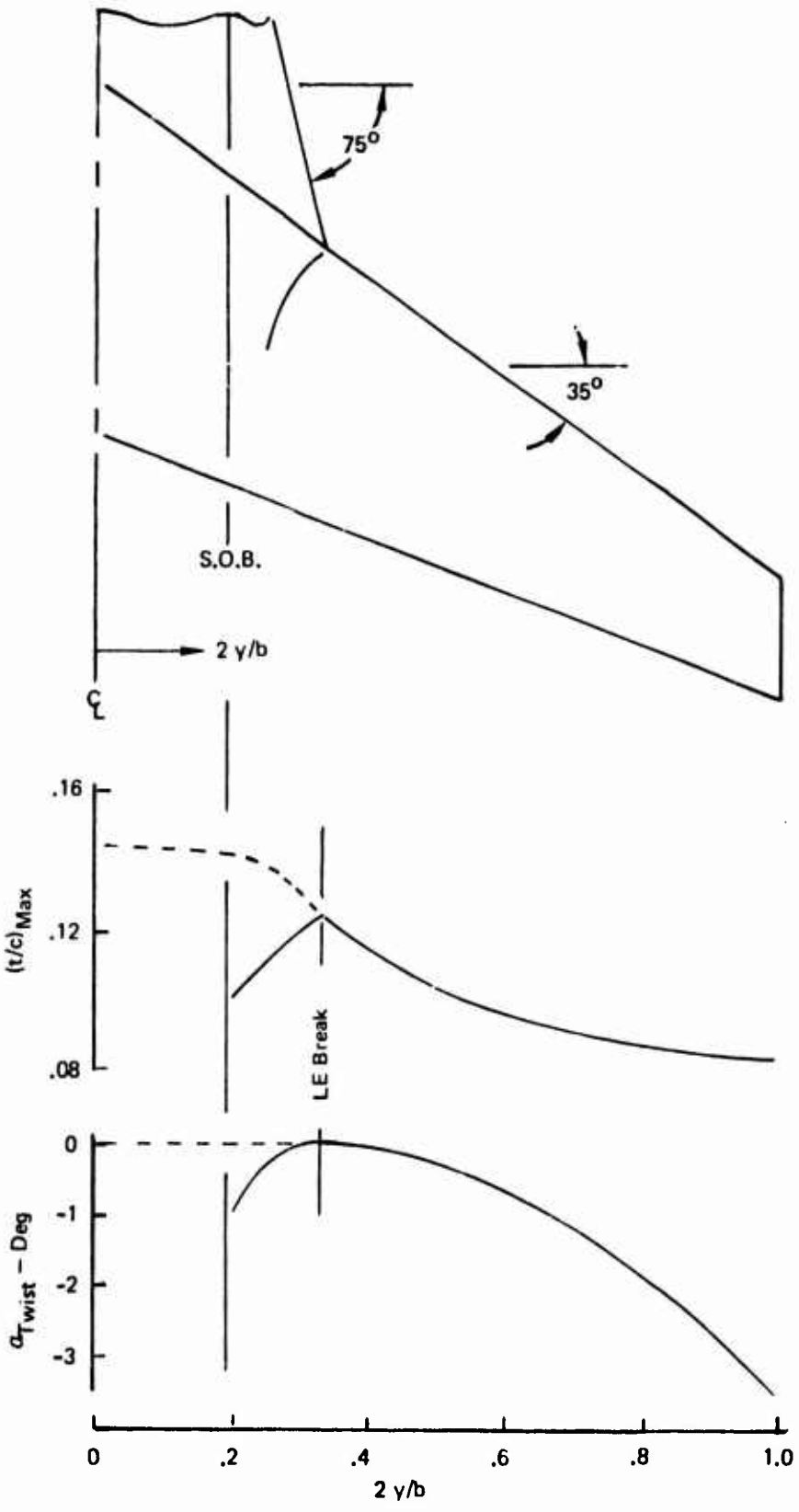

Figure 1-50: Test Model Wing Characteristics

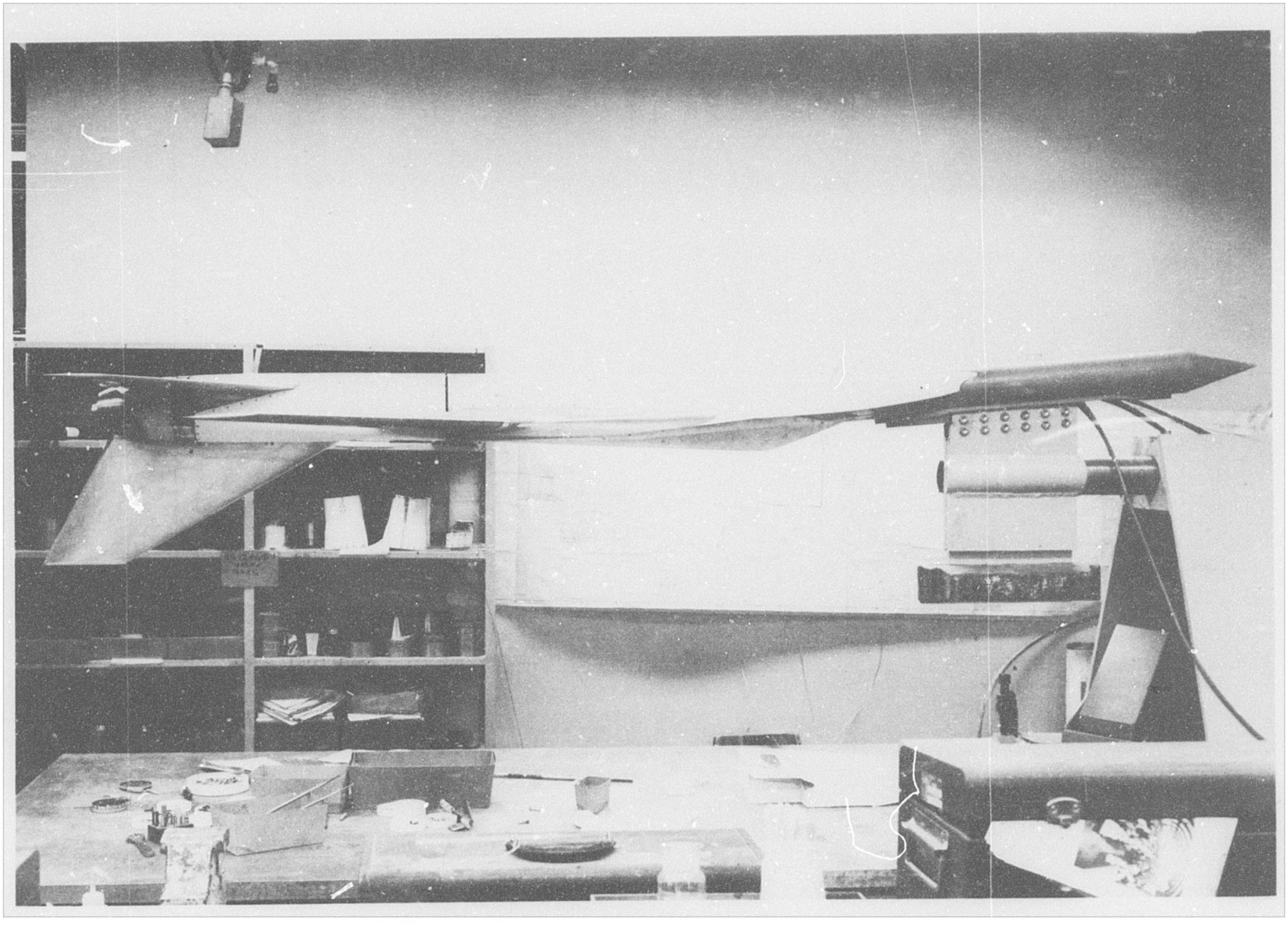

Figure 1-51: Model With Forward Sting, Strut Mounted

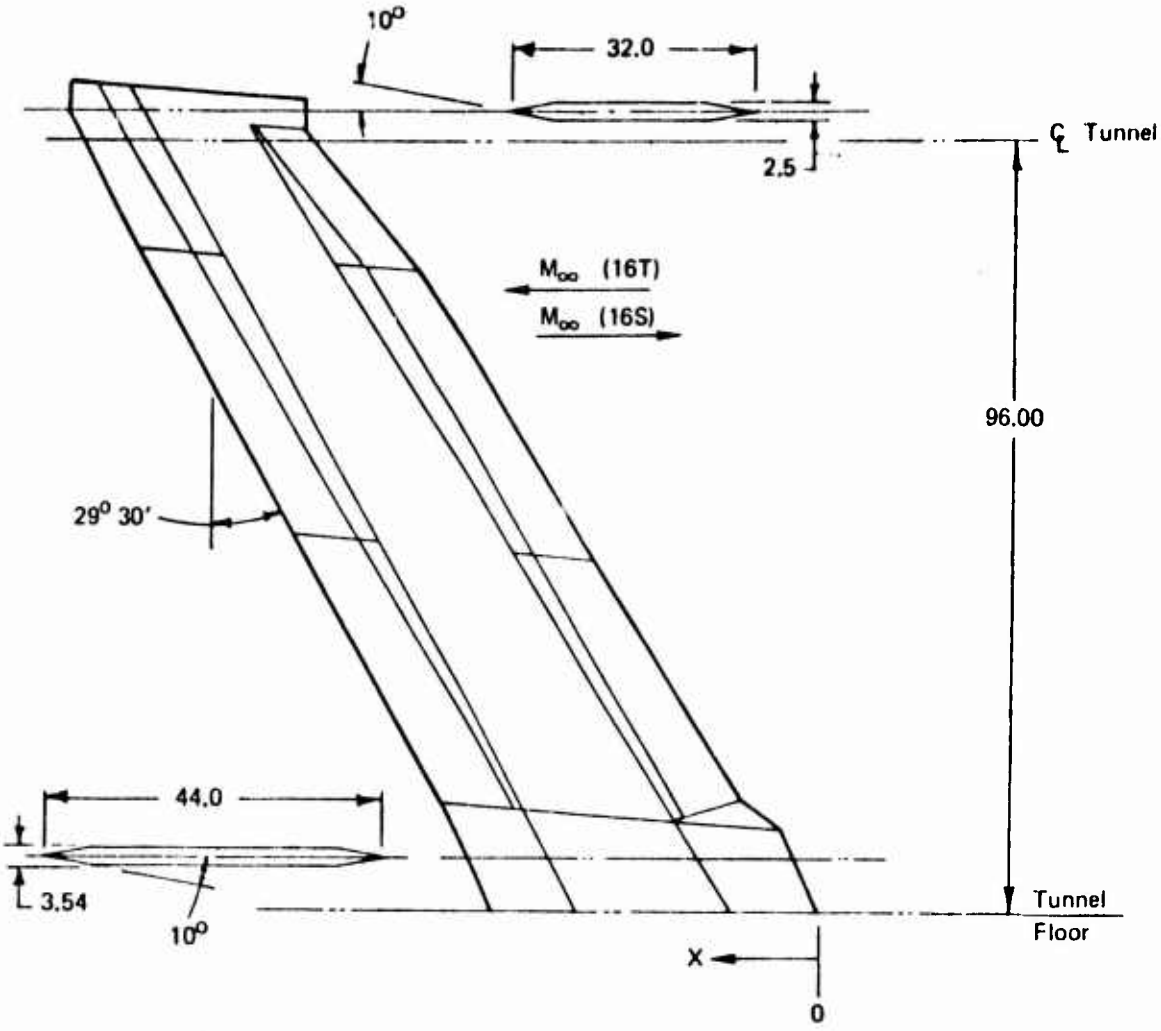

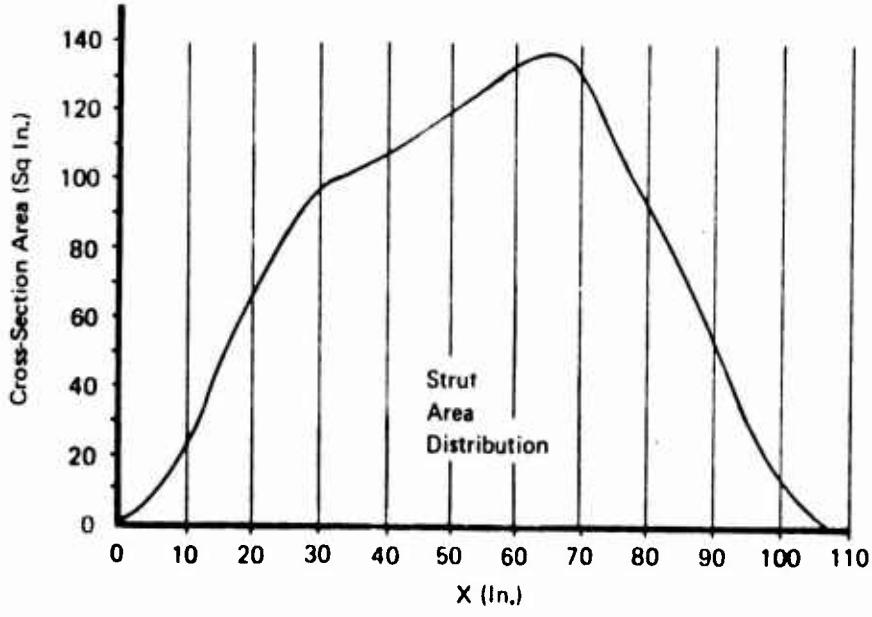

Figure 1-52: Model Support Strut

right and left hand nozzles. A centerline continuation of the forward sting forms the main support structure to which the forebody and afterbody balances are attached in tandem.

The air supply system for the blowing model is continuous from the support strut to the nozzle exits. Nozzle thrust is not recorded by either balance. The forebody and afterbody exterior contours are thin skin shells which attach to their respective balances. The joint between the fore and afterbodies is sealed with a positive flexible seal. The model interior is vented by an opening in this seal at the top body centerline.

The forebody model nose shell is extended to cover the forward sting. The forebody contours also are modified by inlet fairings. The cross-sectional areas of these fairings are designed to duplicate the reference mass flow ratio of the flow-through model inlets. The forward sting actually is an upstream extension of these fairings by a continuation of the cross-sectional area. Thus, except for excessive boundary layer buildup (which any type of inlet fairing will develop), the exterior flow around the inlet should be comparable to that of the flow-through model. Because of the model nose and inlet fairing modifications, forebody data on the blowing model is limited to incremental effects.

A second set of inlet fairings is planned in case the above fairings produce intolerable interference. The additional fairings, for subsonic use only, consist of ellipsoid plugs cantilevered upstream from each inlet.

The afterbody exterior contours are true models of the three real afterbody types. Variable geometry nozzles are simulated by interchangeable cruise, combat, and acceleration nozzles (non-metric) and their corresponding exterior thin skin shells (metric).

A 0.10 inch nozzle exit gap is provided between the metric and non-metric hardware to prevent fouling due to misalignments and relative deflections under aerodynamic load. The gap is sealed with flexible seals. The design of the gap terminates the exterior metric shell from 0.18 to 0.44 inches short of the nozzle exit, because correct exterior contours are maintained up to the gap and the non-metric blowing nozzle exit is maintained at the correct station. All three cruise nozzles are provided with annular gap filler rings which restore the correct exterior contours. Tests with and without the rings show the effects of the modifications to provide the gap. Since the ring installation "hard fouls" the metric afterbodies, the modification effects are interpreted from eight surface static pressure measurements on each cruise nozzle.

Individual downstream air supply systems consisting of adaptors, plenums, choke plates, reservoir total pressure rakes, and nozzles are provided for each of the three multi-mission aircraft configurations. A fourth airblowing system is provided to simulate the flow-through duct exit of the Phase III model.

The three aircraft configurations of Test Combination A, Figure 1-46, are described briefly as follows:

Model 1 (Figure 1-53) is designed with the Pratt & Whitney Aircraft V1.7 variable geometry turbine, separate flow engine. The engines are closely spaced, leading to the selection of a single vertical tail. A separate flow convergent-divergent plug nozzle is used with this engine. The test model uses single flow nozzles designed to duplicate the separate flow exhaust plumes. This is accomplished by increasing the plug size while maintaining external contour and flow exit angles. Plug axial force balances are not required with these nozzles because external flow cannot affect plug forces at nozzle test pressure ratios.

Model 2 (Figure 1-54) is designed with the General Electric Company GE16/1382-6 separate flow fan engine. The engines are moderately spaced, with twin vertical tails mounted on booms outboard of the engines. A separate flow plug nozzle with sliding shroud is used with this engine. The test model nozzles again are designed to duplicate the exhaust plumes with single flow nozzles. The left hand nozzle plug is mounted on a balance to measure the effects of external flow on plug forces.

Model 3 (Figure 1-55) is designed with the Pratt & Whitney Aircraft S1.0 fixed geometry mixed flow engine. The engines are widely spaced, with twin vertical tails mounted at the engine centerlines. A convergent-divergent nozzle is used with this engine and the wind tunnel model duplicates its cruise, combat, and acceleration geometry.

Figures 1-56 shows the blockage distribution of the model installed in the 16T wind tunnel.

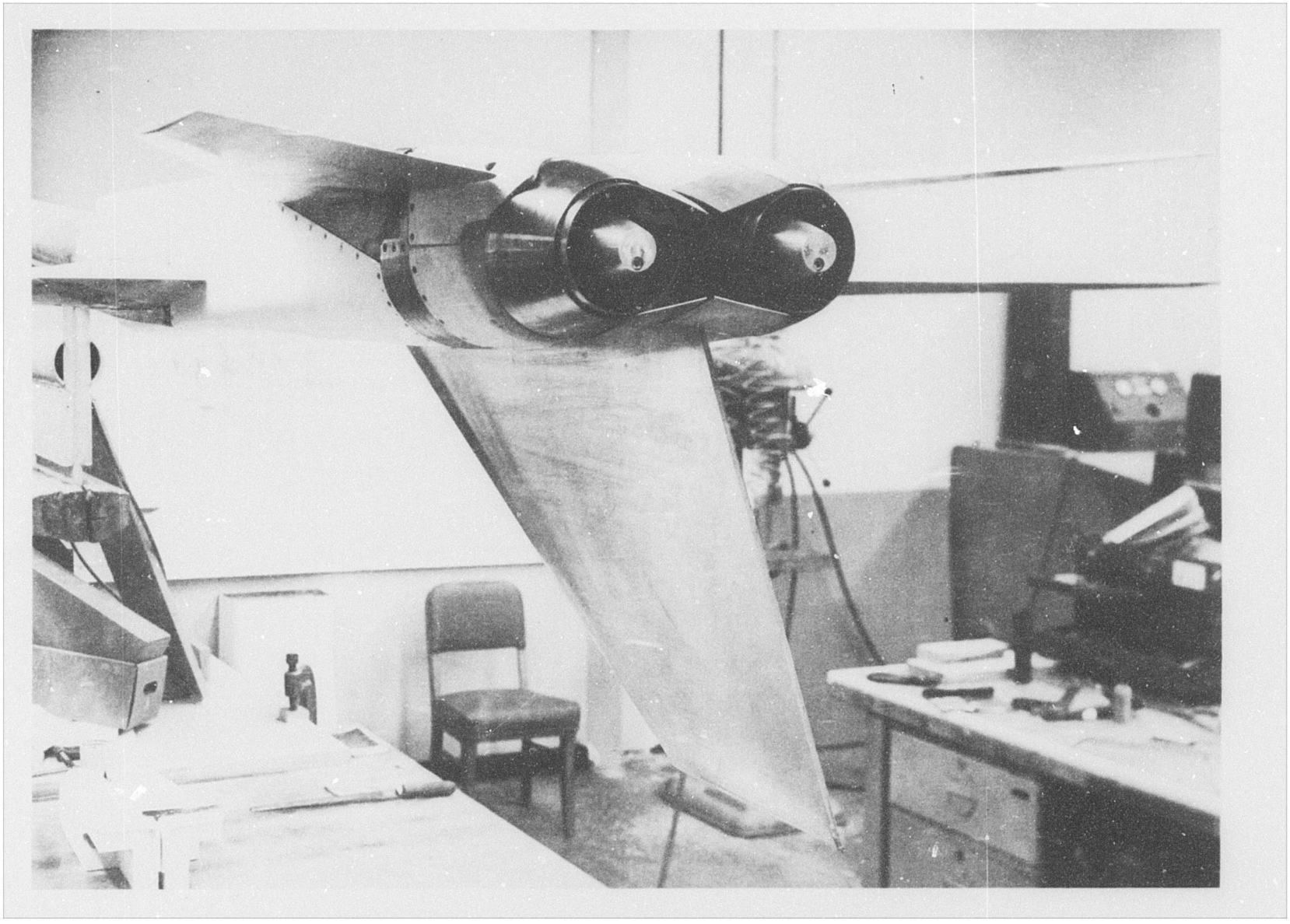

Figure 1-53: Phase II Model 1 Afterbody With Cruise Nozzles

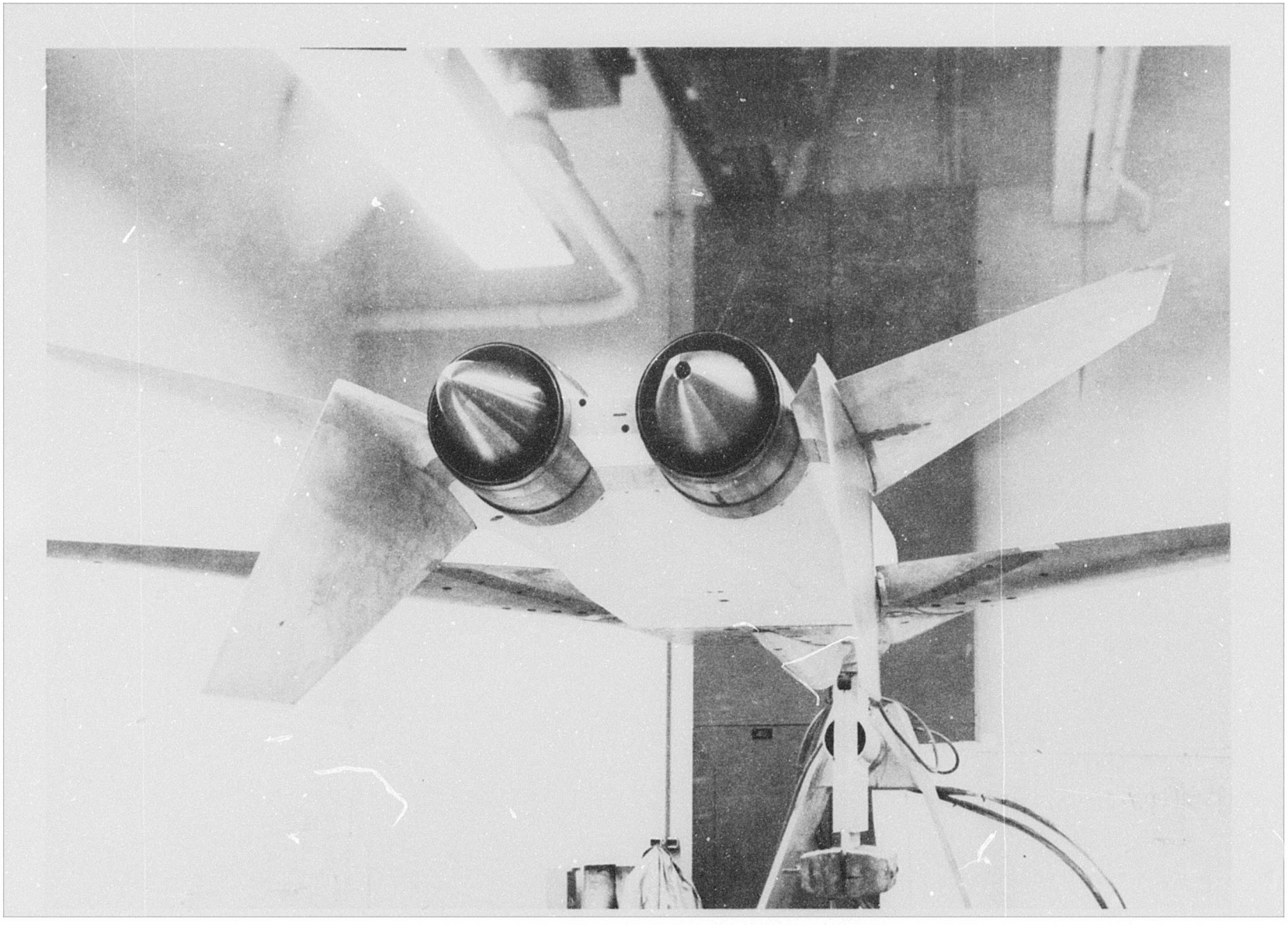

Figure 1-54: Phase II Model 2 Afterbody With Cruise Nozzles

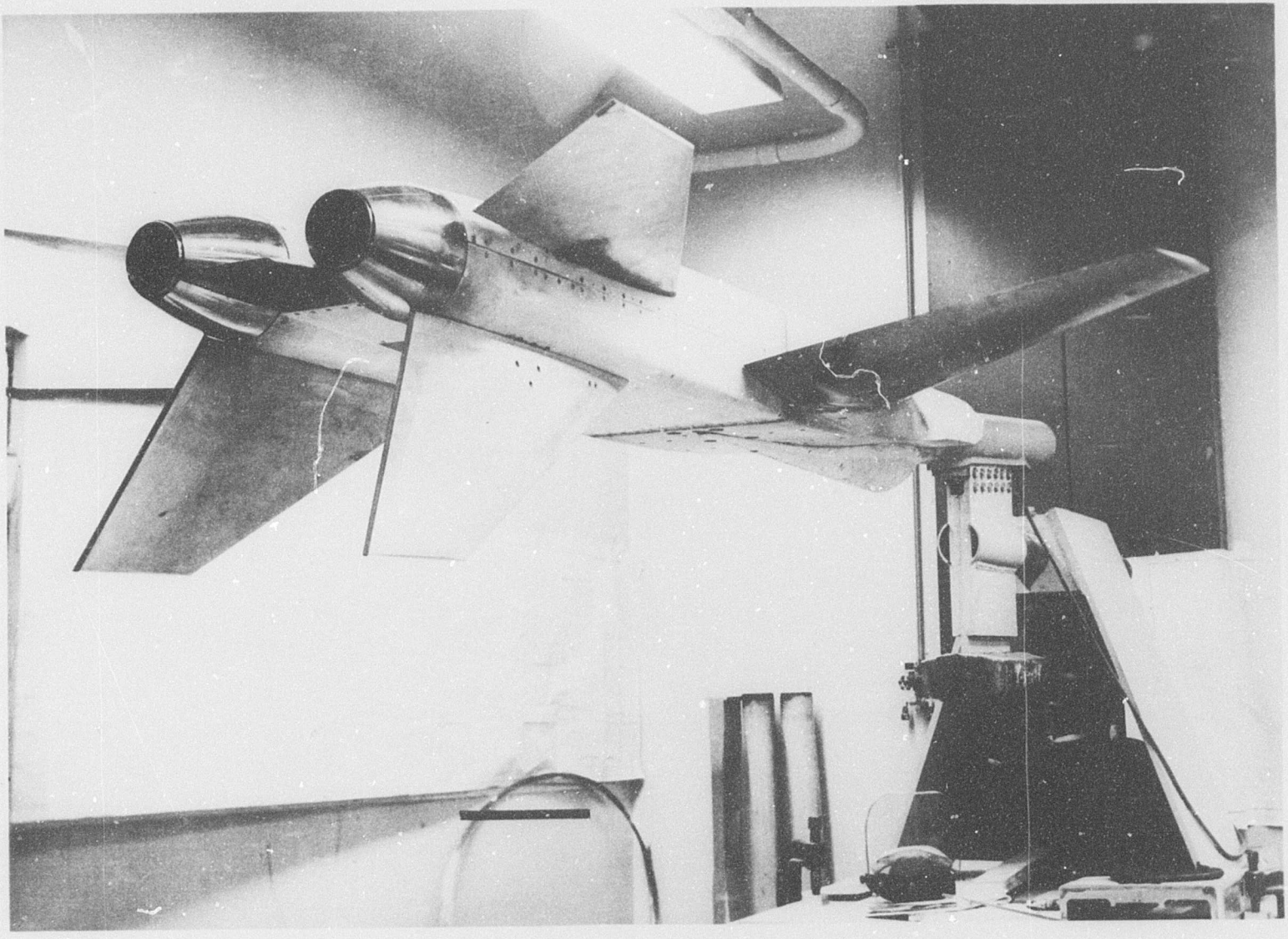

Figure 1-55: Phase II Model 3 Afterbody With Cruise Nozzles

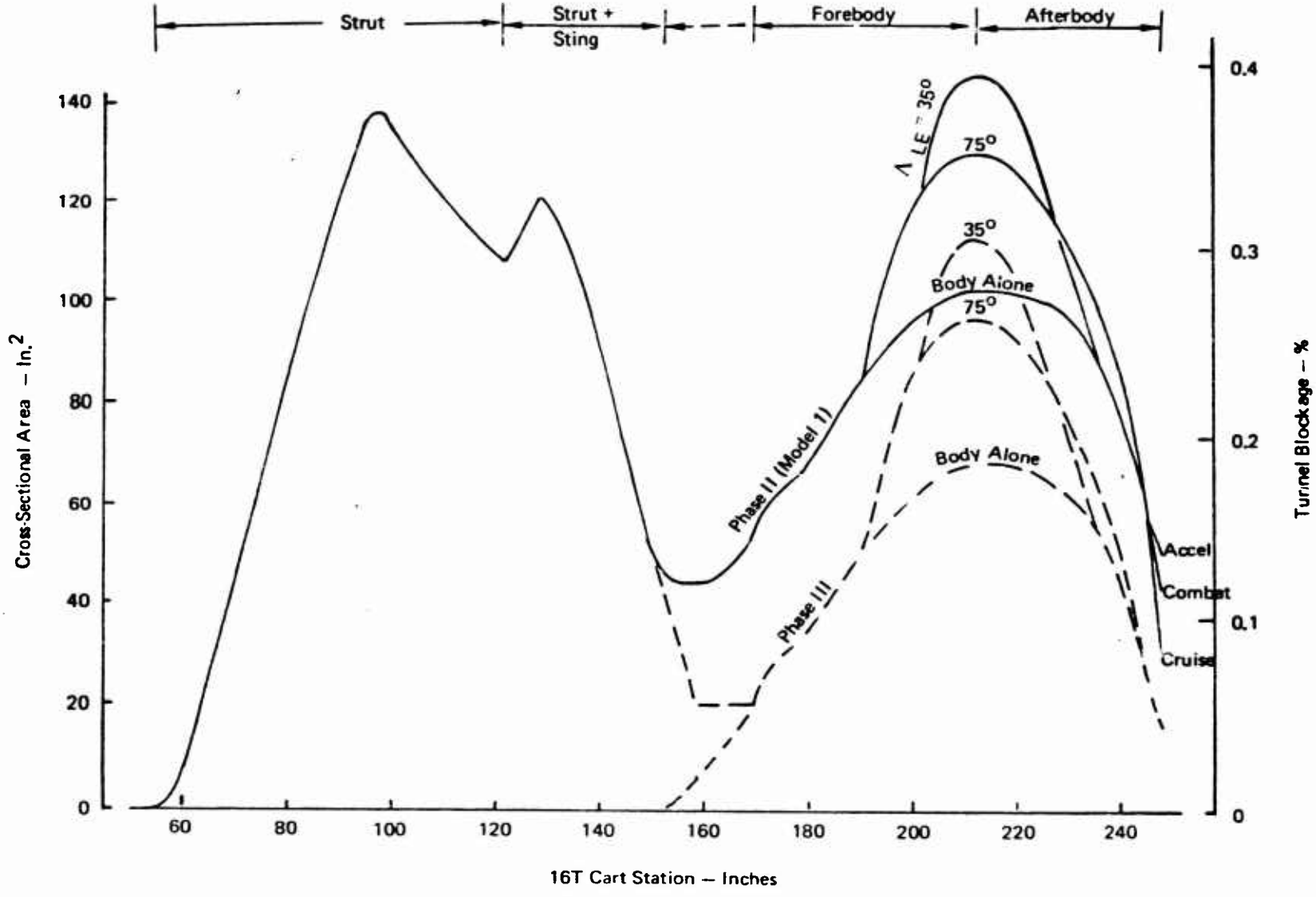

***Figure** 1-56: Model/Support Cross-Sectional Area Distribution in 16T*

1.2.12.5 Phase III Model

The Phase III flow-through model is mounted inverted either from the Phase II strut or from a conventional aft sting. The model is built up using blowing model components. When strut-mounted, the inlet fairings are removed to unplug the real inlets, and the blowing system hardware downstream of the divider is removed and replaced with flow-through ducts. These ducts are continuous to the nozzle exit and are supported from the forebody and forebody balance. The gap at the exit between the interior ducts and afterbody skin is sealed. The balance attachment to the air supply system upstream of the divider is the same as for the blowing installation. Space for the conventional aft sting is provided by outboard placement of the duct exits.

When sting-mounted, all air supply hardware and the forward sting covering are removed, and the correct model nose is attached to the forebody (Figure 1-48). The forebody and afterbody balances are attached to new support structure which is compatible with the aft sting mounting system. The installation beyond the balances is the same as when strut-mounted.

The afterbody hardware for the aerodynamic reference model (Test Combination G of Figure 1-45) also is used to construct Phase III Test Combinations E and F and Phase II Test Combination B. The dummy sting of Test Combination F is attached to the afterbody balance support structure and is non-metric.

Phase III Test Combination D of Figure 1-45 is strut-mounted and the afterbody fairing from customer connect to the base is not constrained by the need for sting entry space. The afterbody hardware for this configuration utilizes this space for boattailing. This boattailed hardware also is used to construct Phase II Test Combination C of Figure 1-45.

1.2.12.6 Test Program

The Phase II and III test programs are correlated with mission profile segments. Tests are planned in PWT 16T at Mach numbers of 0.55 and 0.82 for climb and cruise data; at 0.90 Mach number for combat and acceleration data; and at Mach numbers of 0.925, 0.95, 1.2, and 1.5 for acceleration data. Tests are planned in PWT 16S at Mach numbers of 1.6, 2.0, and 2.7 for acceleration data, and at 2.3 Mach number for acceleration, penetration, and recovery data.

The nominal transonic test Reynolds number per foot is 2.5×10^6. Reynolds number variations are planned with the Phase II Model 1 configuration and the Phase III aerodynamic reference model. These variations are made within the 16T operating envelope and within the balance limits.

The nominal supersonic test Reynolds number per foot is 0.6×10^6. This test condition coincides with balance limits.

Angles-of-attack from 0° to 10° are planned at Mach numbers of 0.55, 0.82, and 0.90. At higher Mach numbers the angle range is reduced to 0° to 4°. Sideslip angles are always 0°.

Phase II blowing tests require airflow rates up to 37 pounds per second with 80 psia at the reservoir total pressure rake. This corresponds to approximately 1000 psia supply pressure to the model. The blowing test procedure is to run through the angle-of-attack sweep with continuous airflow at the desired conditions. This procedure makes most efficient use of the facility occupancy. Exhaust plume effects are varied by testing over a range of nozzle exit pressure ratios. Jet boundary simulation parameters from available research are used to predict pressure ratios which provide the desired plume shape. Effects of the specific plume shape are then determined by interpolation.

The Phase III tests are run prior to Phase II to provide inputs necessary for the blowing tests. These inputs are control effectiveness for setting up trimmed blowing configurations, and reference data for evaluating inlet fairing interference on boattailed afterbodies. Thus, the anticipated test sequence is the reverse order of Test Combinations shown in Figure 1-45; i.e., G, F, E . . . A. Interruptions in the test sequence are required between G and F in both 16T and 16S to change from the sting mount to the strut mount, and between the 16T and 16S tests to change test carts. An additional interruption may be advisable during the course of the 16T Phase II blowing tests (C, B, and A).

Estimated occupancy times required to conduct the Phase II and Phase III test programs are:

	Phase II	Phase III
16T	305 hrs.	180 hrs.
16S	130 hrs.	80 hrs.

1.2.13 Phase I Data Correlation

Afterbody drag data obtained during the Phase I parametric afterbody drag test were correlated during Phase II and a simple, fast prediction method for twin, faired afterbodies was developed.

The experimental data and, therefore, the correlation cover a range of jet-to-maximum area ratios and afterbody length-to-equivalent diameter ratios and several types of area plots. Convergent and convergent-divergent nozzles over a range of pressure ratios were represented. A correlation at design pressure ratios was obtained for single vertical tails and twin tails centered on nacelles. Twin outboard tail data could not be correlated; trends are reported in the Phase II report.

Jet effects for afterbodies with mostly attached flow were correlated by Pratt & Whitney using ESIP data and data from NASA-Langley test programs.

1.2.13.1 Twin Faired Afterbody Drag Correlation

Initial attempts to correlate data on the basis of the IMS parameter failed when applied to long afterbodies with steep slopes near the trailing edge. Examples are shown on Figure 1-57. The longer afterbodies tend to fall on the lower line at M = 0.9 and 0.95. Oil flow photographs showed separation near the trailing edge on these afterbodies (see Figure 1-58). It appeared reasonable that actual body slopes beyond the point of separation should not be permitted to influence the correlation parameter, as it was felt they would not influence the pressure drag. A "truncated" IMS parameter, called IMS_T, was developed by limiting the maximum local slope in the area plot when calculating the IMS_T. The calculation is illustrated on Figure 1-59. The effect of limiting the effective slope to a maximum value of 1.4 on Figure 1-59(a) is to truncate the upper portion of the area under the curve on Figure 1-59(b). Since the area under the curve represents IMS, it is seen that IMS_T is reduced significantly compared to IMS. However, if the area distribution were such that the slope rose rapidly but did not exceed the maximum value, as shown by the deshed line on Figure 1-59(b), truncation would not occur and the values of IMS and IMS_T would be identical and remain high.

The correlation using the IMS_T parameter is shown on Figure 1-60. The maximum local slope was varied versus Mach number so as not to upset the already good correlation

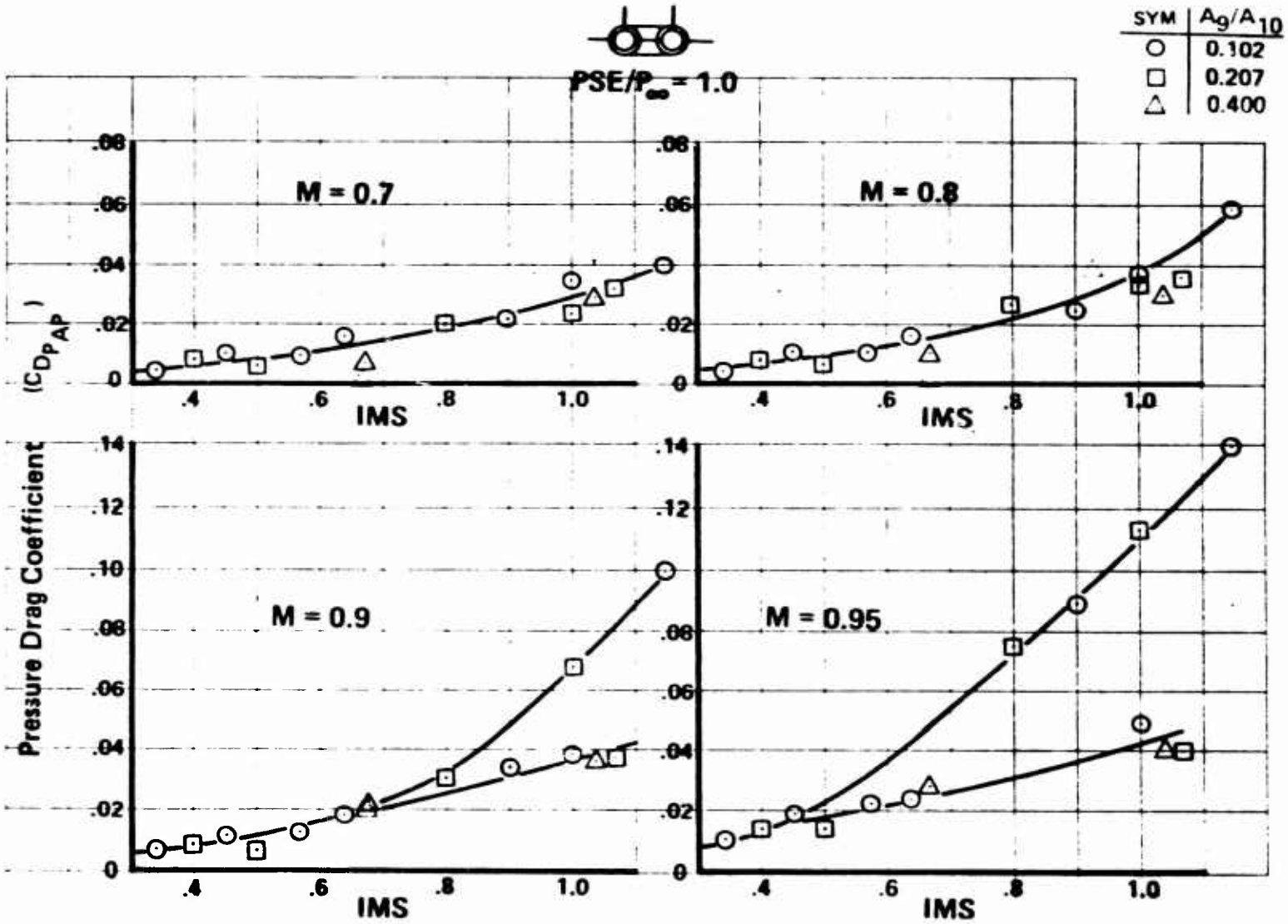

Figure 1-57: Drag Correlation for Twin Vertical Configurations

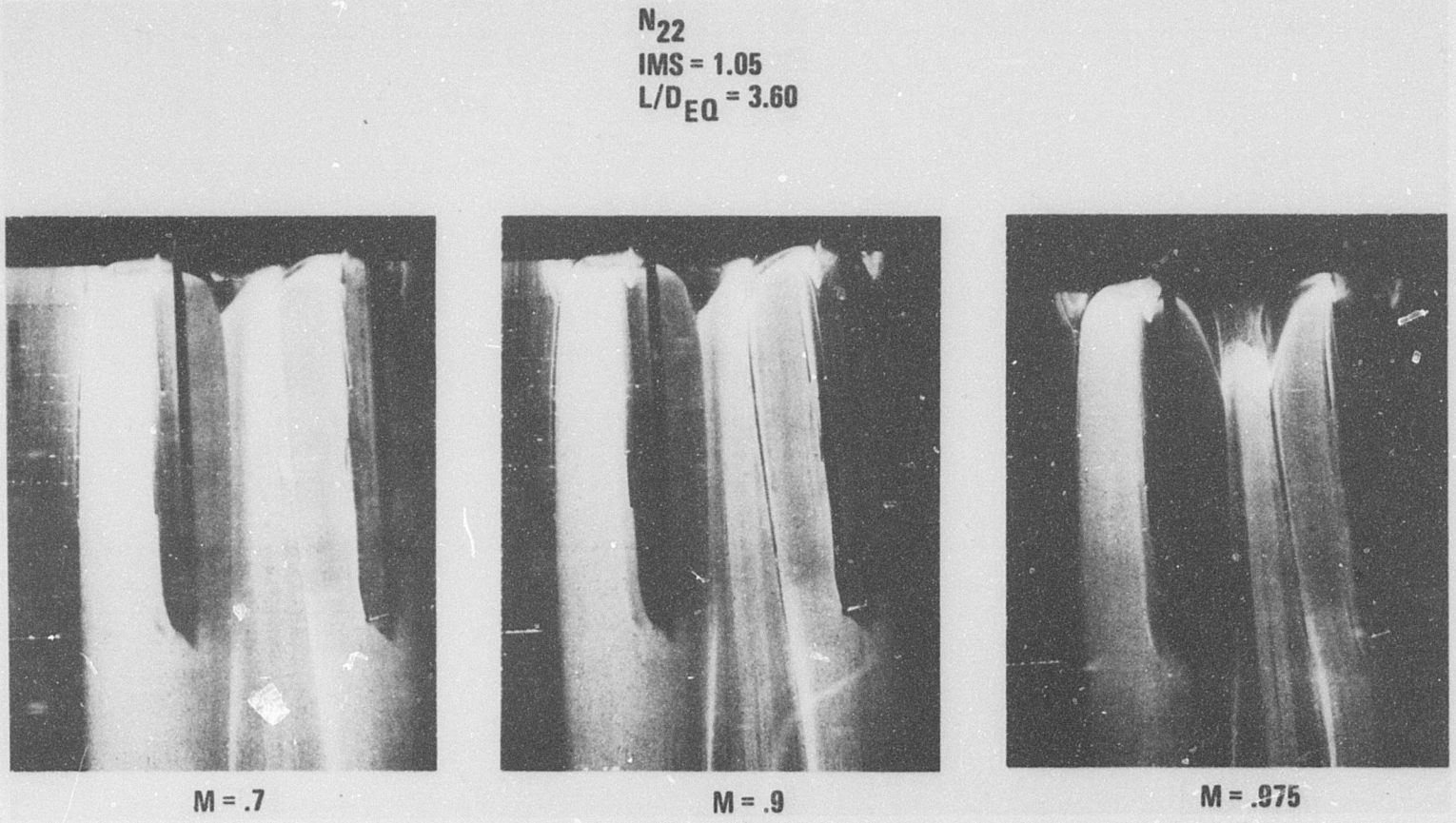

Figure i-58: Separation Region on N_{22} Afterbody

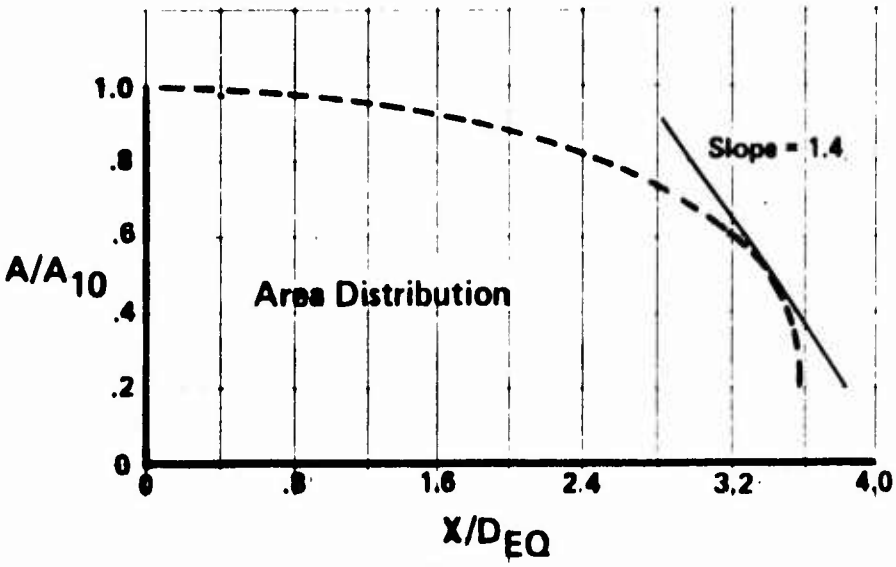

Figure A

$$IMS_T = -\frac{1}{(1 - A_s/A_{10})} \int_{A_s/A_{10}}^{1.0} \frac{d\ (A/A_{10})}{d\ (L/D_{eq})}\ d\ (A/A_{10})$$

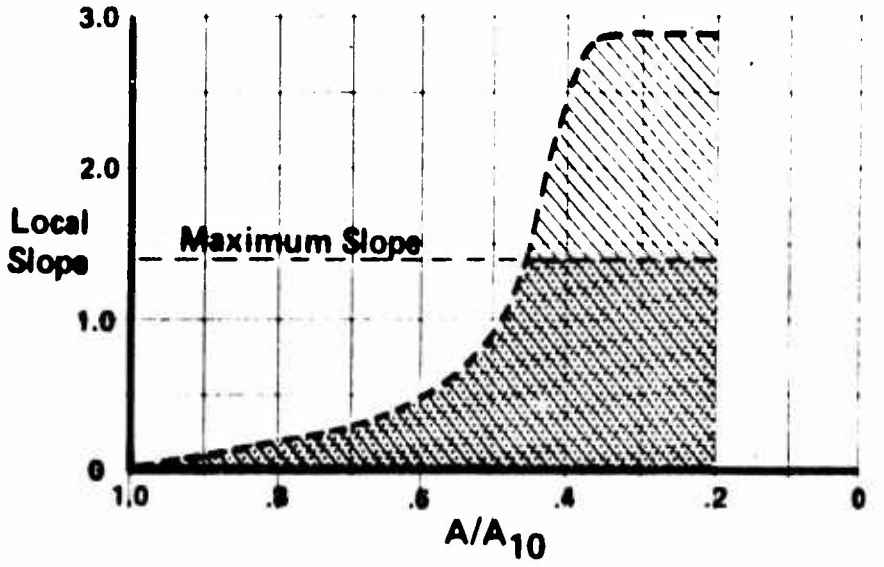

Figure B

Figure1-59: IMS Truncation Method

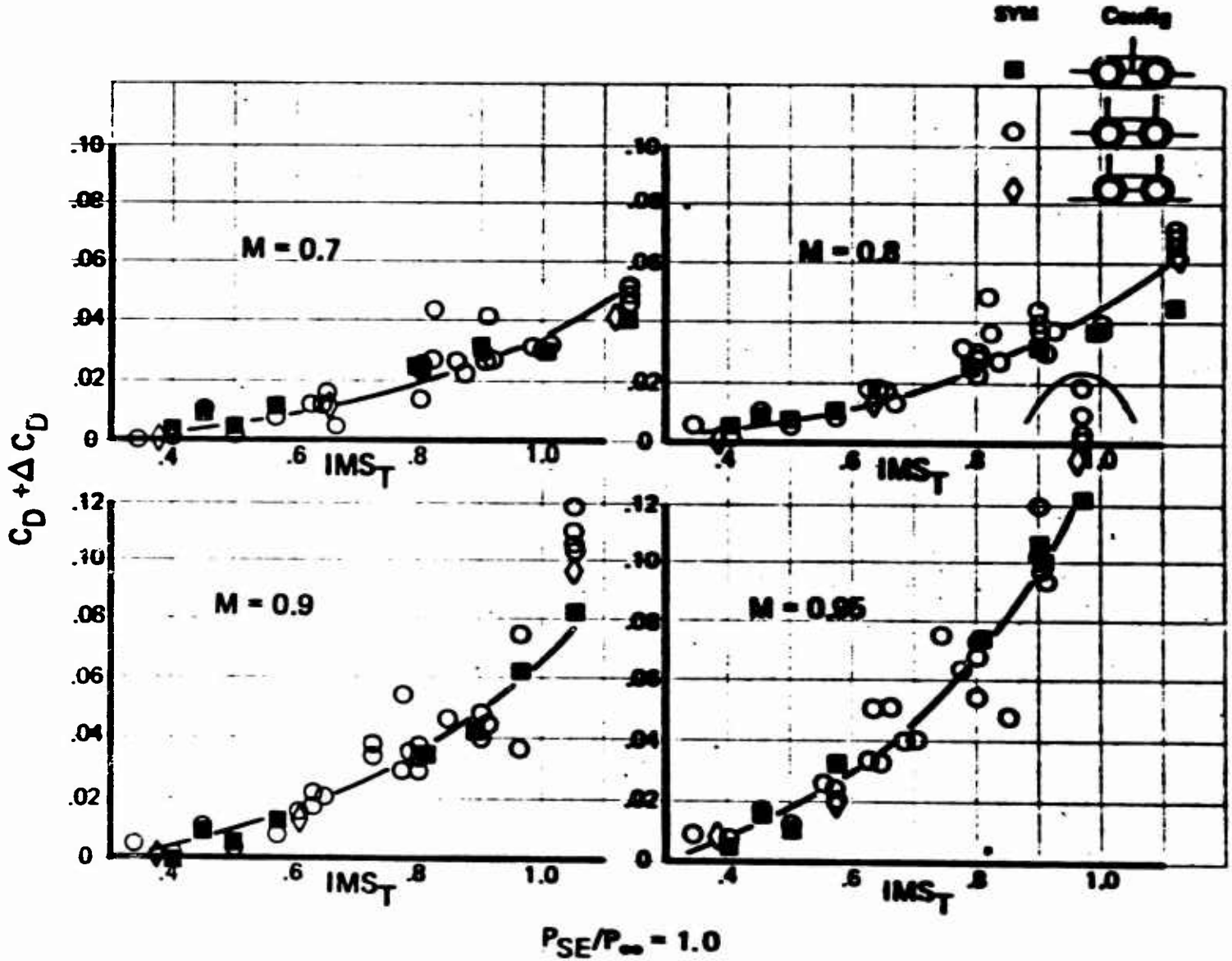

Figure 1-60: Combined Drag Correlation for Single & Twin Vertical Configurations

at M = 0.7 and M = 0.9. The schedule of maximum slope versus Mach number thus developed is shown on Figure 1-61. This schedule was confirmed by observation of the way the point of separation moves as a function of Mach number on oil flow photographs.

It was further found that the IMS_T curves at all four Mach numbers varied almost precisely as IMS_T to the 2.77 power This trend is shown on Figure 1-62, where single vertical tail data were raised to the twin level by the addition of a constant increment of $\Delta C_D = 0.006$. This second correlation means that only two curves are needed to predict the pressure drag of a given afterbody: the maximum slope (Figure 1-61) and the correlation parameter $C_D + \Delta C_D/(IMS_T)^{2.77}$ (Figure 1-62); both plotted against Mach number. The prediction process is illustrated on Figure 1-63, suitable for either manual or computerized calculation. The result is pressure drag at fully expanded jet conditions.

1.2.13.2 Nozzle Plume Parameter Correlation

A plume correlation parameter has been derived from ESIP and NASA-Langley data which approximates the twin jet aftbody drag change with nozzle pressure ratio from M = 0.7 to M = 1.2. The drag variation was determined to be a function of nozzle type, nozzle area ratio, and aftbody geometry. The drag correlating parameter (given below) describes the afterbody drag with changing P_{S9}/P_{SO} ratios.

$$C_{D_{A_{10}-A_9}} = \left(C_{D_{A_{10}-A_9}}\right)_{P_{S9}=P_{SO}} - \left[4.5e^{-M_o^2}\left(1-\frac{P_{S9}}{P_{SO}}\right)\left(1.1\frac{A_9}{A_{10}}-1.0\right)\left(\frac{A_9}{A_{10}}\right)^{3/2} IMS_T\right]$$

Where:

$$0 \leq IMS_T \leq 0.9,\ 1.0 \leq \frac{A_9}{A_8} \leq 1.4,\ 0.1 \leq \frac{A_9}{A_{10}} \leq 0.4,\ 0.7 \geq M \leq 1.2$$

Comparison of the correlation to data are found in Figures 1-64, 1-65, 1-66, and 1-67. Figures 1-64 and 1-65 compare the correlation to convergent and convergent-divergent nozzle data. Convergent and C-D nozzle data agrees well.

The correlation above was developed so that it could also be applied to plug nozzles. It was found that if the plug nozzle is treated like a convergent nozzle (i.e., substitute

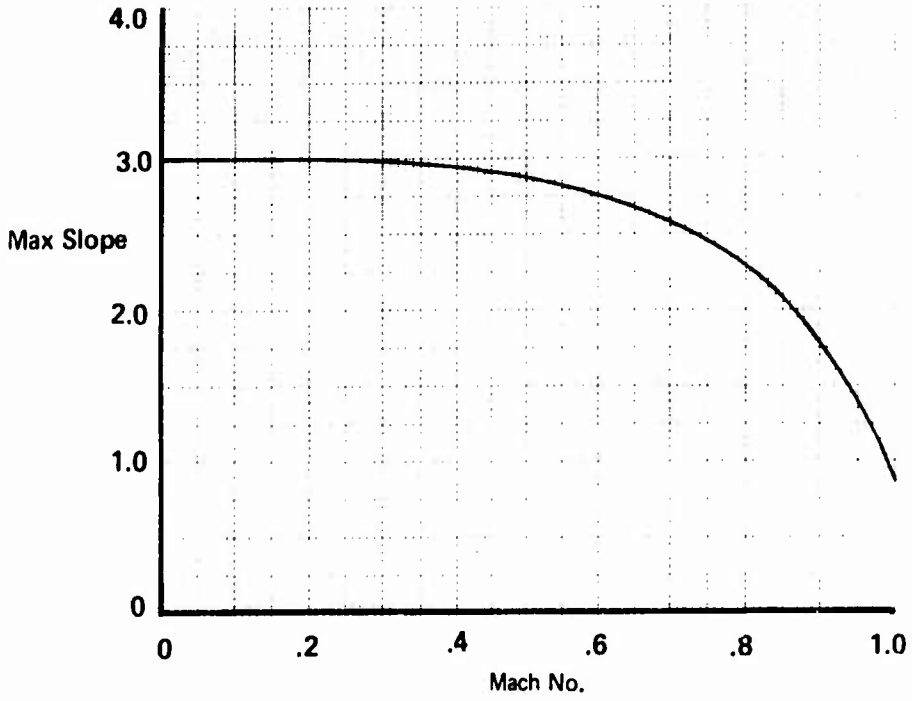

Figure 1-61: Maximum Local Slope for IMS_T Calculations

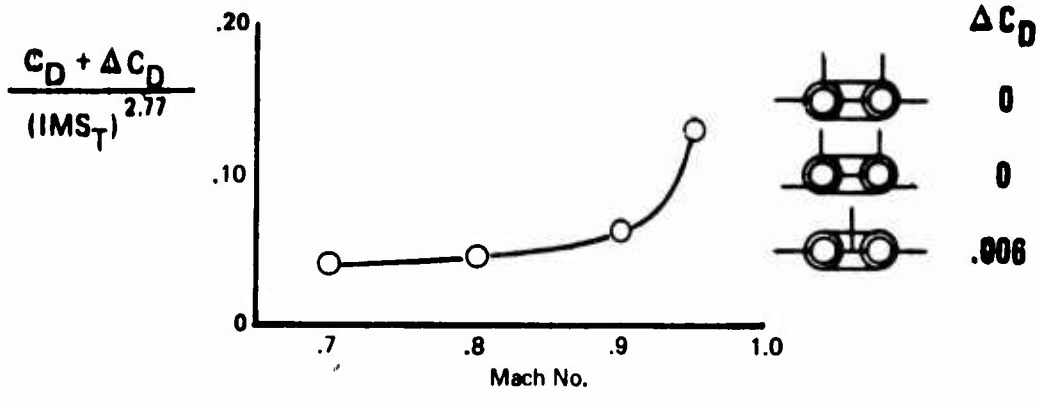

Figure 1-62: IMS_T Parametric Correlation Curves

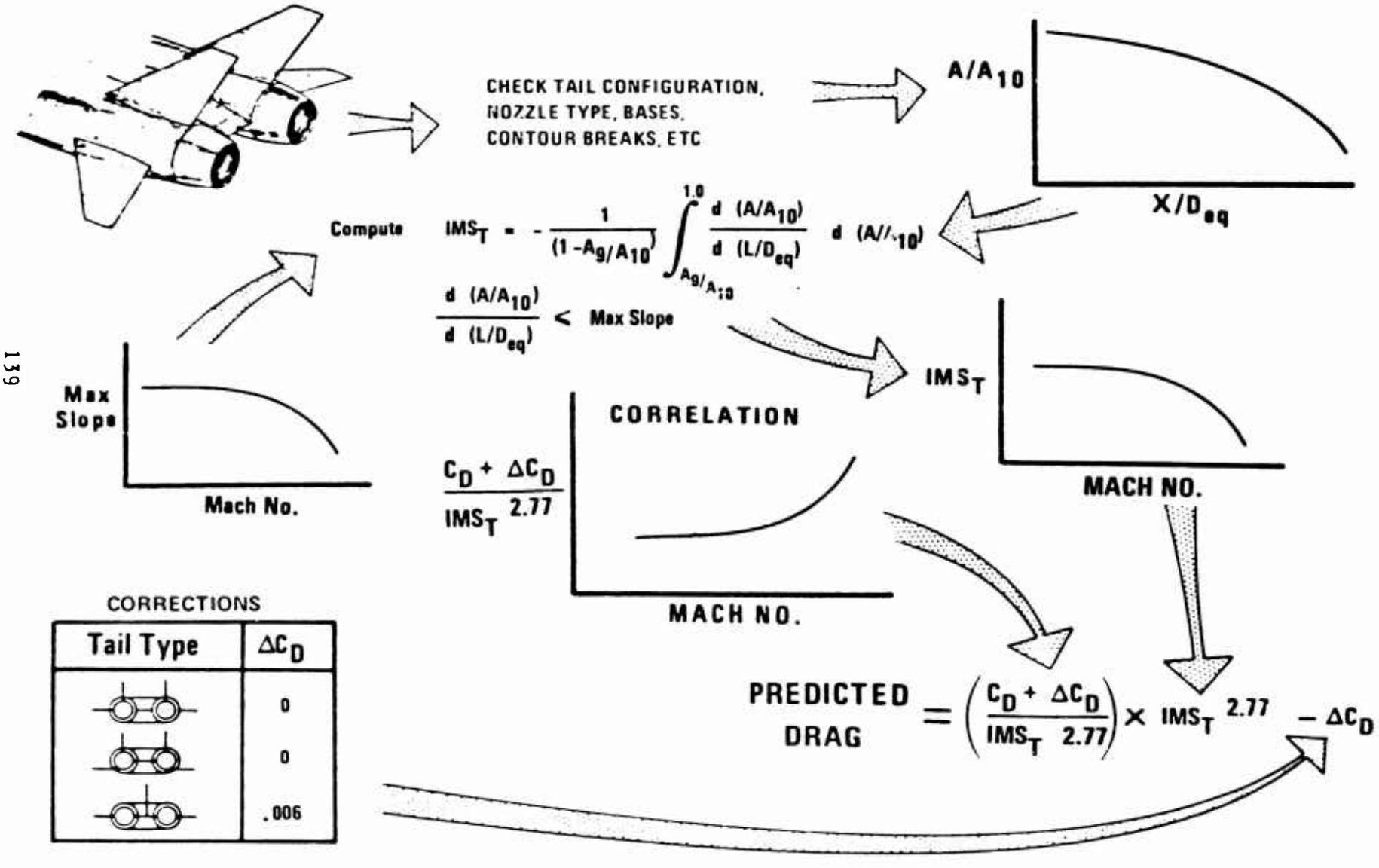

Figure 1-63: Drag Prediction Method

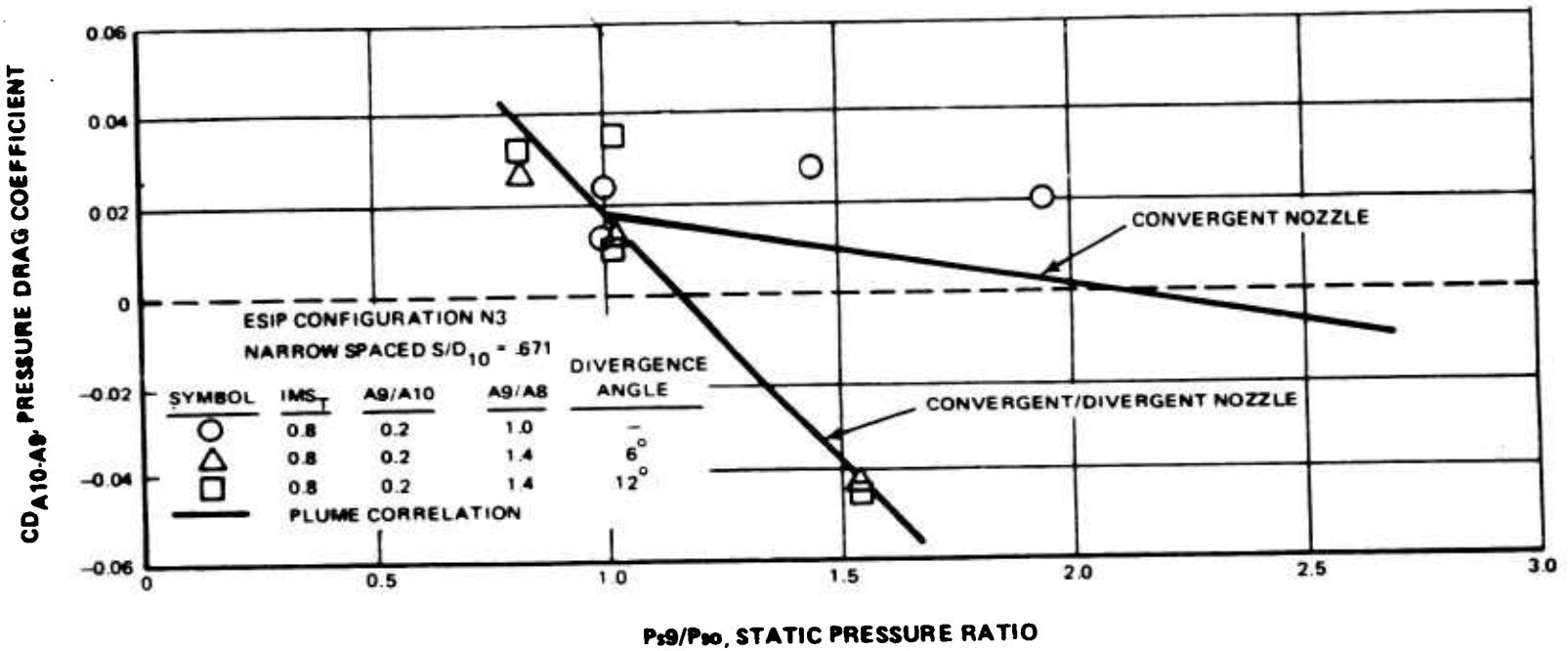

Figure 1-64: ESIP Data: M_0 = 0.7 Twin Jet Plume Correlation

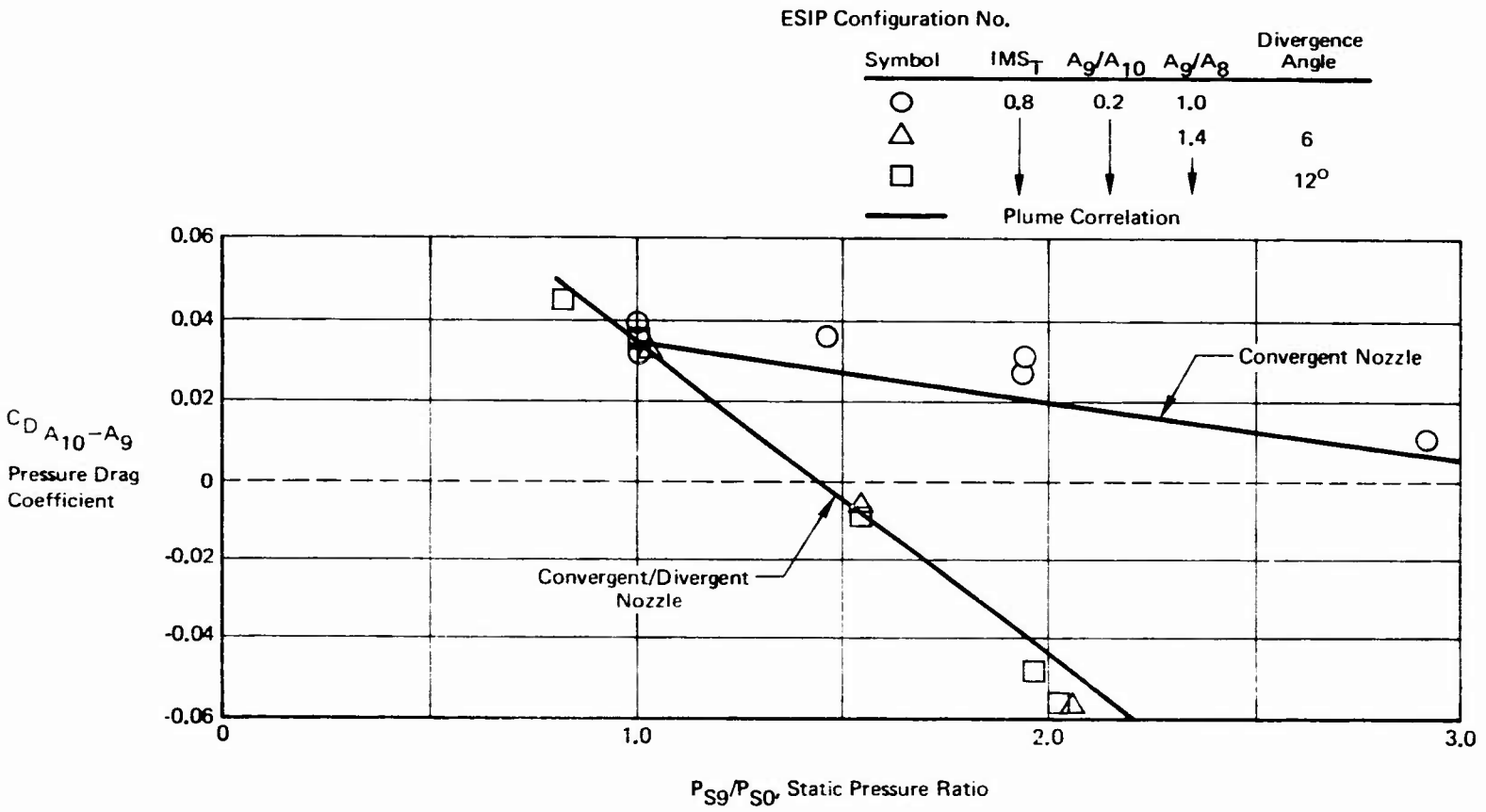

Figure 1-65: ESIP Data, M_o= 0.9 Twin Jet Plume Correlation

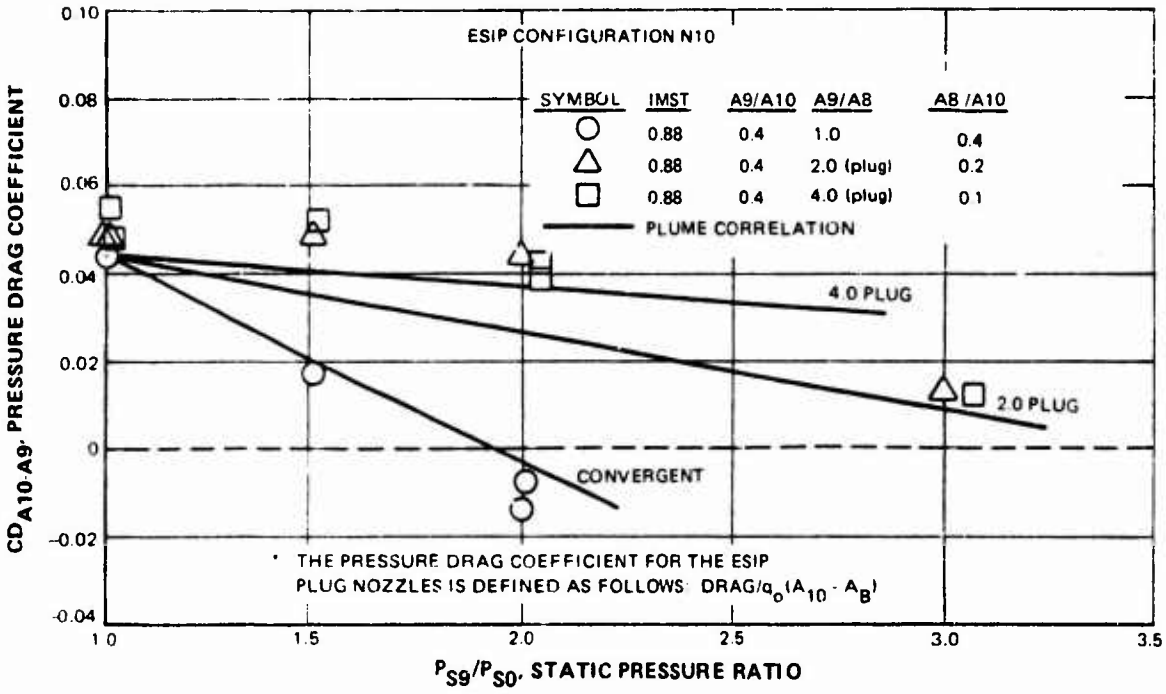

Figure 1-66: ESIP Data, M_0 = 0.9 Twin Jet Plume Correlation -- Plug Nozzles

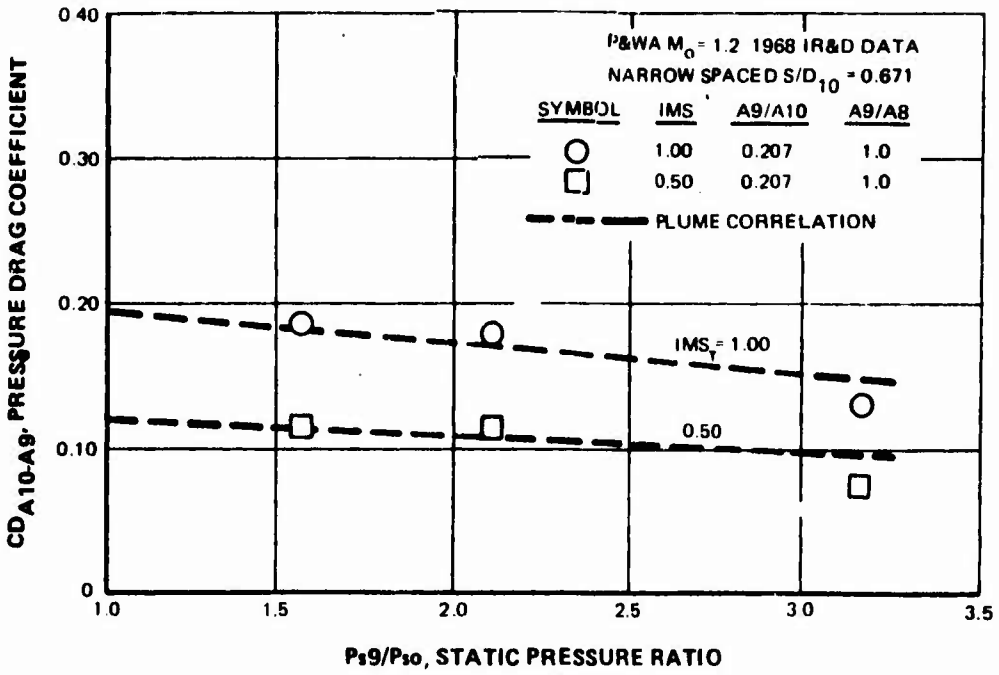

Figure 1-67: P&WA Data: M_0 = 1.2 Twin Jet Plume Correlation

A_8 for A_9 in the equation above) and the IMS_T is only calculated over the afterbody to the throat station, the plume correlating parameter will again approximate the drag/plume pressure ratio variation quite well. The agreement between the plug nozzle "drag vs P_{S9}/P_{SO}" variation and the equation prediction is presented in Figure 1-66.

1.2.14 ESIP Phase II Model Strut Suction Evaluation - Pre-Test Report and Test Plan

A mounting strut interference study was proposed for the AEDC 1T facility. The primary purpose of the test program is to determine in a qualitative manner the effects on model afterbody pressure data of boundary layer removal (suction) along the trailing edge of a mounting strut similar to the strut for the Phase II model for the 16-foot tunnel. The intent of the proposed 1T program is to determine the gross effects of strut suction and whether future detailed larger scale tests are justified.

To minimize costs for this test, existing hardware was to be utilized as far as possible. The basic model was to be an existing axisymmetric cylindrical body with a blunt base and an ogive nose. This model is instrumented for afterbody surface and base pressures and is sting mounted. Strut effects were to be determined by using dummy struts under the model. The primary strut simulates the ESIP configuration and is equipped for suction along the entire (perforated) trailing edge (see Figure 1-68). A second strut simulates a more conventional forebody strut configuration but is not equipped for suction.

The suction strut was to be run with two amounts of suction, zero suction, and with the perforated trailing edge sealed and faired (simulating a solid strut).

This test, like the ESIP 16T and 16S tests, had to be cancelled because the AEDC 1T tunnel schedule slid beyond the end date of the ESIP contract.

1.2.15 Airframe Performance Maps

1.2.15.1 Drag Polar Methodology

Airframe performance maps of drag polars, typical of those used in ESIP engine-airplane performance calculations are

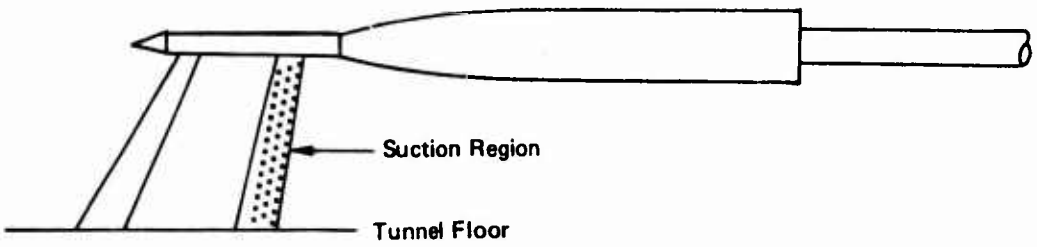

SUCTION STRUT

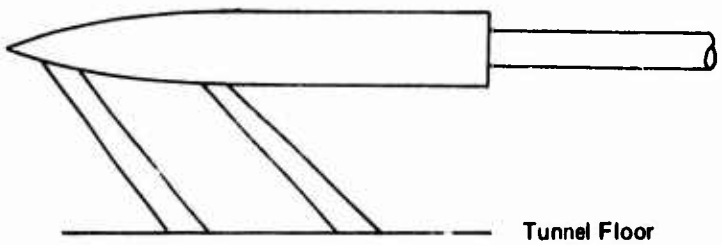

SOLID STRUT

Figure 1-68: ESIP Strut Evaluation Models

shown on Figures 1-69 and 1-70. The drag build-up is accomplished using the Boeing Engine-Airframe Matching (BEAM) computer program which consists of a series of equations utilizing empirical relationships which are input in tabular form. Tables typical of those used for ESIP mission analyses include: wing geometry ratios, non-axisymmetric drag increments, drag-due-to-lift, critical Mach number increments for wing camber, compressibility effects, wave drag corrections and body wave drag constants.

The BEAM program builds airplane drag polars at any set of operating conditions by summing the appropriate drag components from the input tables. Examples of polars developed by the BEAM drag subroutine are presented in Table 1-XI.

1.2.15.2 Inlet Selection and Performance Maps

A two-dimensional horizontal ramp, mixed compression inlet was selected as the primary inlet for the ESIP fighter/bomber mission. At the time of inlet type selection, it was thought that the mission acceleration requirement would size the engine. Since the mixed-compression design would provide high performance during both the supersonic cruise leg, $M_\infty = 2.3$, and the acceleration to $M_\infty = 2.7$, it appeared the obvious choice. The design is one for which sufficient background data is available to provide Level II performance estimates. A side-mounted inlet location ahead of the strake was selected to provide a good inlet flow field (assuming appropriate forebody tailoring), free of both bomb bay door interference and ingestion problems associated with the landing gear.

Detailed performance maps, suitable for inputting directly into the new inlet subroutines in the BEAM program were developed for an inlet of this type. These maps include the local inlet Mach number, inlet recovery at various mass flow ratios, maximum mass flow ratios, buzz and distortion limits, bleed and bypass characteristics and the inlet spillage drag increment at the reference mass flow ratio, required for the drag polar build-up.

1.2.15.2 Inlet/Engine Airflow Matching

The fighter/bomber inlet has been sized for operation over the trial mission with all engine offerings. Typical resulting airflow matching characteristics are given in Figures 1-71 through 1-73. Maximum airflows over the mission and a typical

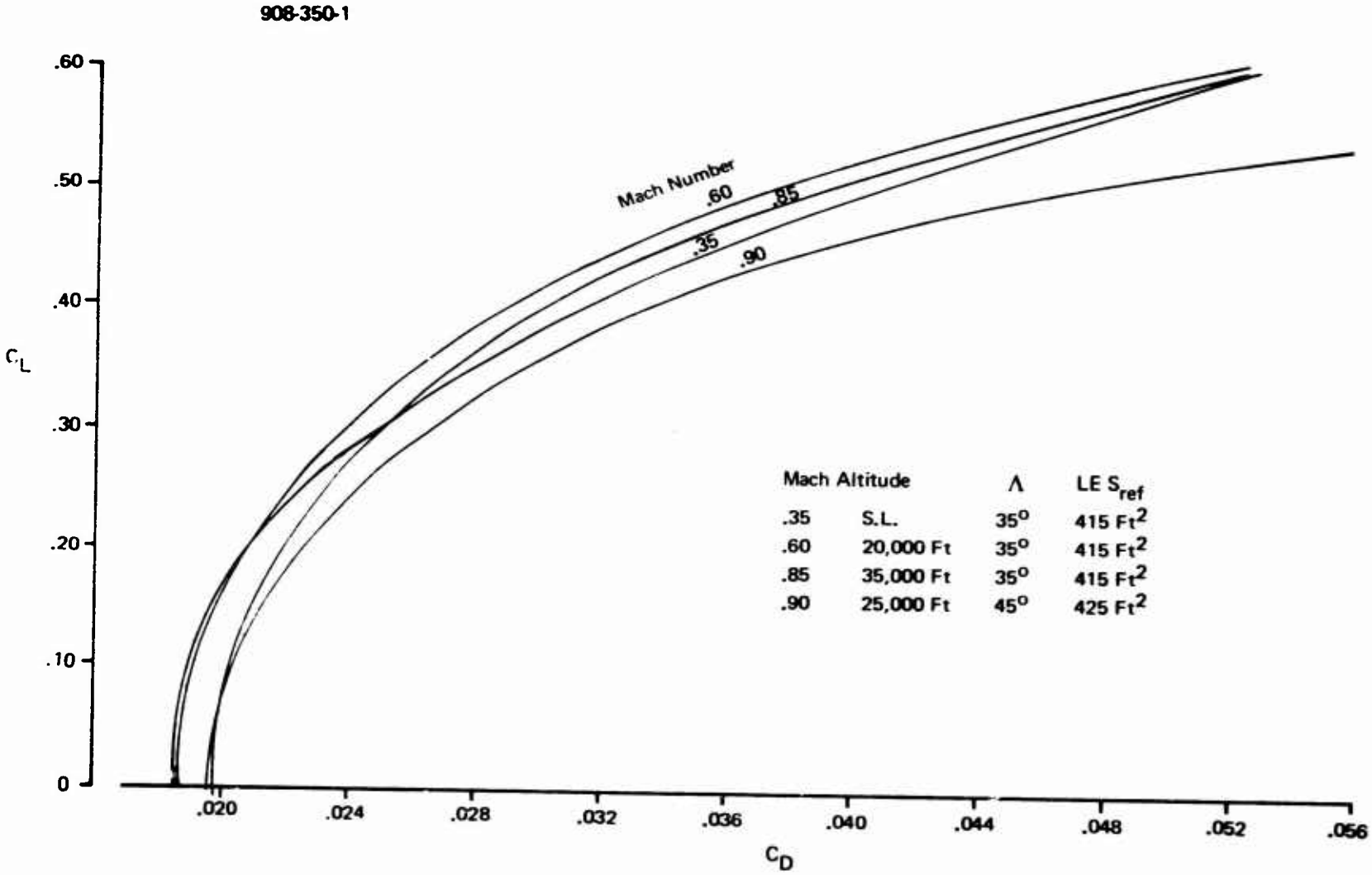

Figure 1-69: Subsonic Drag Polars

908-350-1

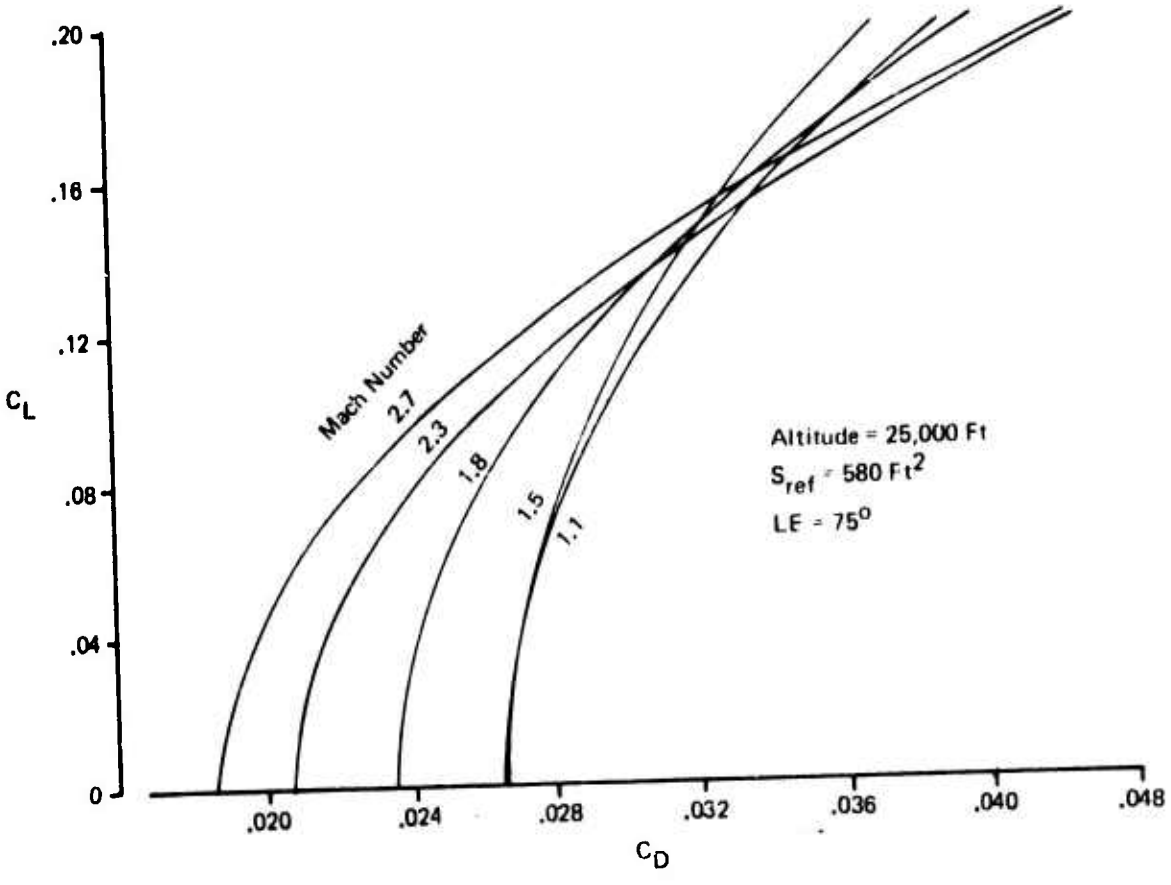

Figure 1-70: Supersonic Drag Polars

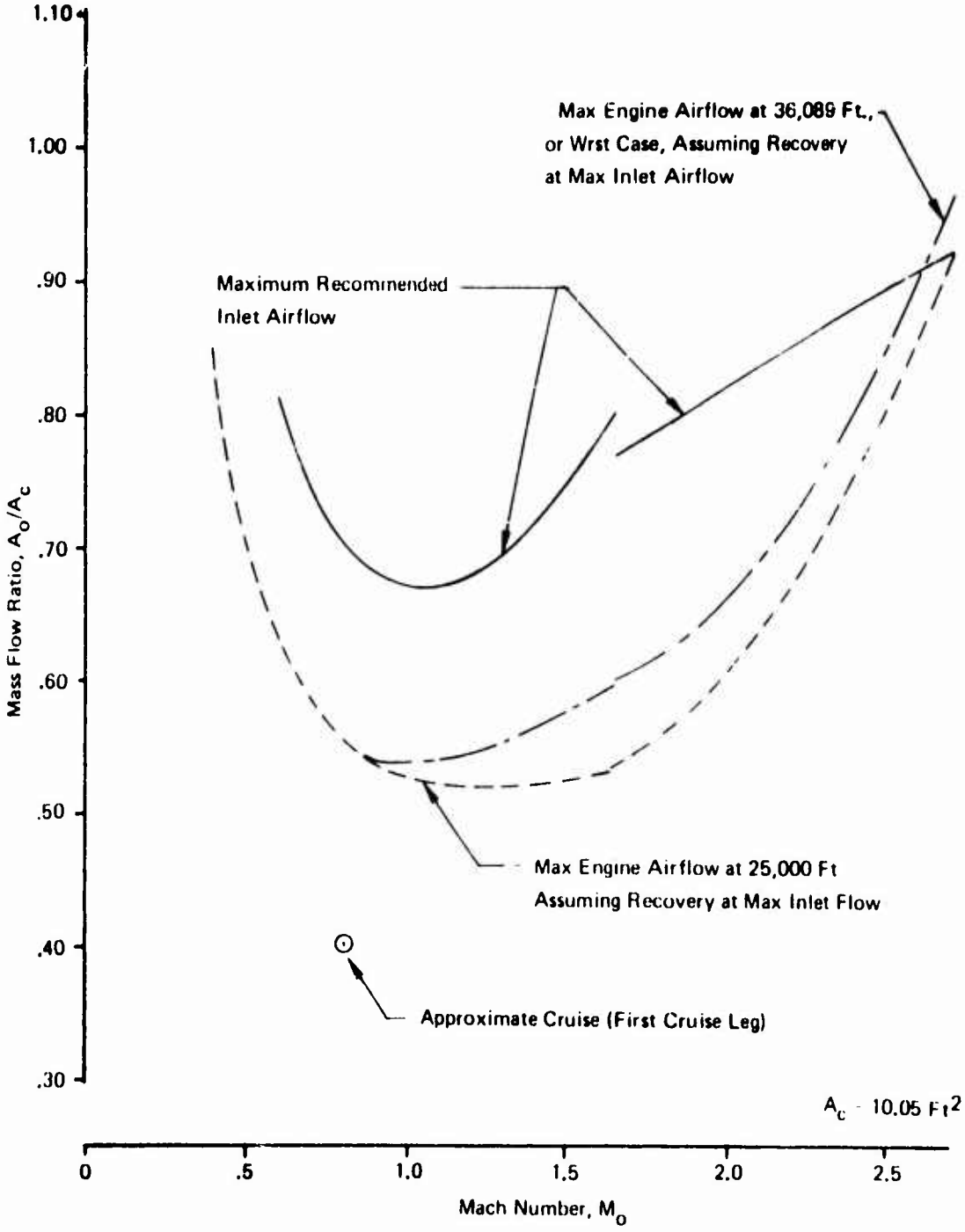

Figure 1-71: Airflow Characteristics of Engine GE 16 F2/A2
(Inlet Sized at 25,000 Ft, Mach 2.7)

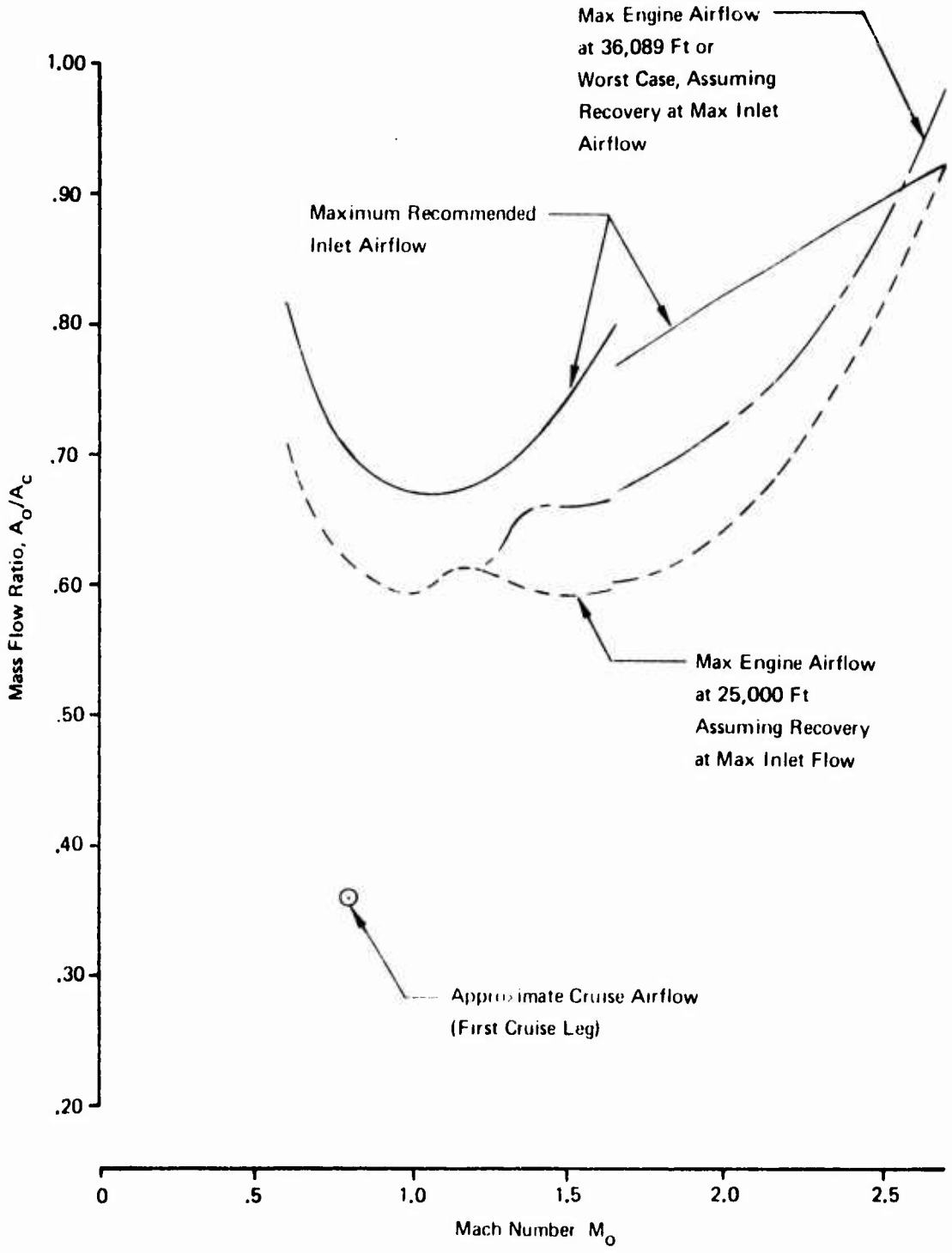

Figure 1-72: Airflow Characteristics of Engine P&WA Turbojet (Inlet Sized at 25,000 Ft Mach 2.7)

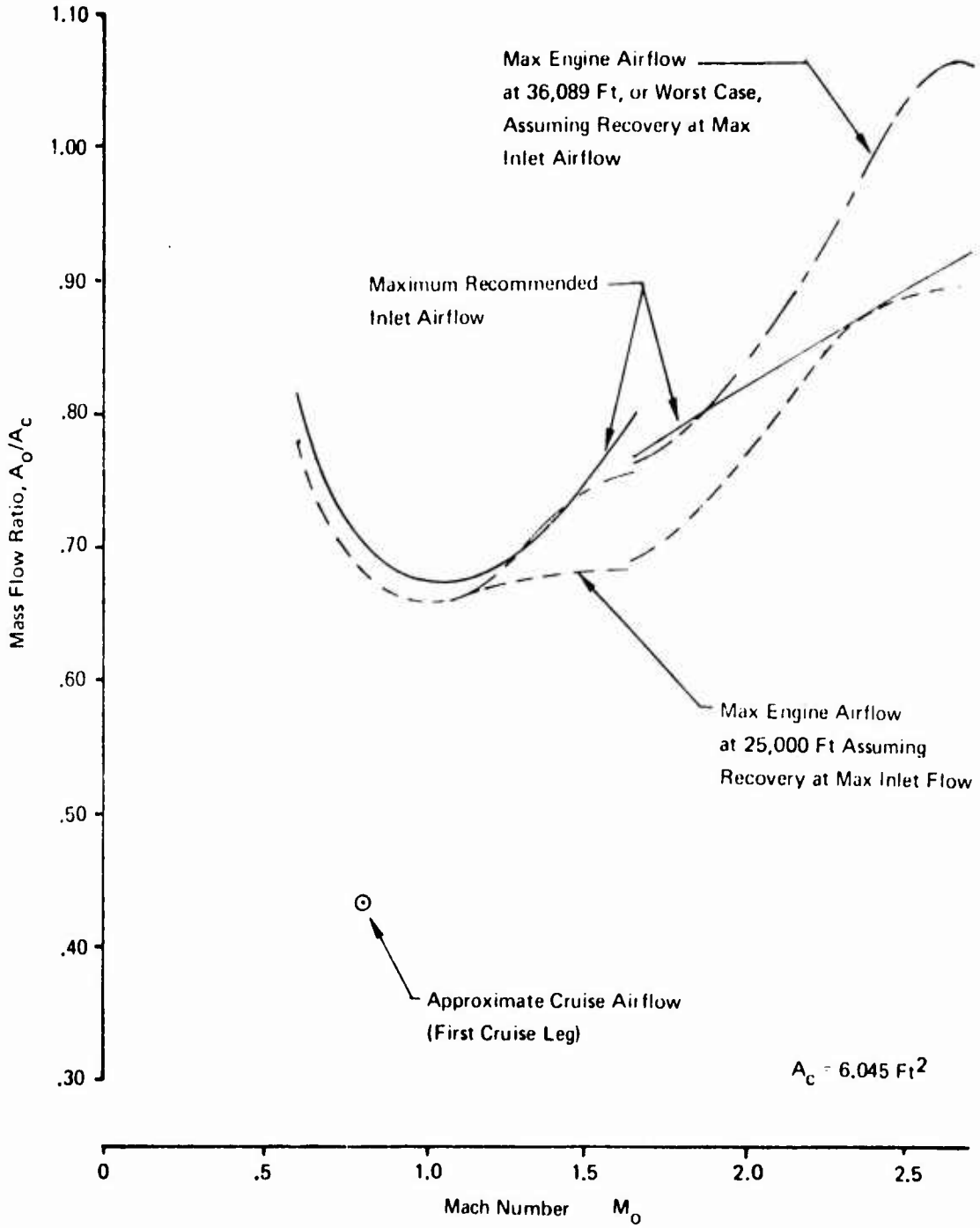

Figure 1-73: Airflow Characteristics of P&WA F 0.4 Turbofan (Inlet Sized at 25,000 Ft, Mach 2.3)

cruise airflow condition are indicated on each figure. The inlet sizes indicated in the figures correspond to a 50,000 lb takeoff gross weight airplane.

In addition, maximum airflow conditions found in the complete matrix of engine data, without regard for any required airplane operating envelope, are also given. As indicated in the figures, airflow matching problems would arise if operation above 25,000 feet were attempted at high Mach numbers.

The inlet size selected for each engine is the smallest size that permits operation at or below the maximum recommended inlet mass flow ratio at all operating points required to fly the given mission. The "maximum recommended inlet mass flow ratio" is the mass flow ratio above which distortion is likely to become excessive.

1.2.15.4 Weights and Weight Scaling

The operating weight of each baseline airplane is calculated using parametric/statistical weight estimating methods developed by Boeing and recorded in Boeing document number D6-15095TN, Rev. "C," vendor quotations and engine manufacturers data. These methods are continually updated to reflect new materials, construction techniques, design criteria and environmental conditions.

A group weight statement is prepared for each baseline airplane as general arrangement drawings become available. The weight of each major structural item is based upon prediction methods which utilize pertinent weight influence parameters. The wing weight, for example, is a function of the following parameters: planform area, leading edge sweep, aspect ratio, taper ratio, thickness ratio, wing loading at basic flight design gross weight, ultimate load factor, wing relieving loads, pivot location and diameter, temperature and material considerations, control surface type and area, and high lift requirements. The weight of other structures is similarly estimated using the appropriate parameters. The group weight statements for baseline ESIP airplanes, broken down by basic components, is shown in Table 1-XVI.

Parametric weight scaling data for each baseline airplane are prepared upon completion of group weight statements. These data are presented graphically as operating weight available versus maximum takeoff gross weight, and as delta operating weight versus engine scale and tabularly as BEAM input data.

Table 1-XVI: Group Weight Statements for ESIP Fighter/Bomber

CONFIGURATION 908-		352-10	351-11	-11	-11
	SYMBOLS	GE-1	FO.0	FO.4	FO.8
WING	W_w	4110	4150	4150	4150
HORIZONTAL TAIL	W_{HT}	270	430	420	420
VERTICAL TAIL	W_{VT}	700	700	730	730
BODY AND STRAKE	W_R	7290	6610	6600	6740
LANDING GEAR	W_{LG}	2270	1360	1380	1380
NACELLE OR ENG SECTION	$W_{NAC}+W_M$	220	280	300	330
AIR INDUCTION	W_D+W_{VG}	2340	1430	1530	1520
STRUCTURE		(17200)	(14960)	(15110)	(15270)
PROPULSION		8220	8570	7370	7190
INSTRUMENTS & NAV EQUIP	ΔK_{FE}	170	170	170	170
SURFACE CONTROLS	$W_{CONT}+W_{SWP}$	1320	1290	1290	1290
HYDRAULIC/PNEUMATIC	W_{HYD}	380	380	380	380
ELECTRICAL	ΔK_{FE}	800	800	800	800
AVIONICS	ΔK_{FE}	2490	2490	2490	2490
ARMAMENT	ΔK_{FE}	490	490	490	490
FURNISHINGS & EQUIP	ΔK_{FE}	800	800	800	800
AIR COND & ANTI-ICING	W_{AC}	590	590	590	590
AUXILIARY GEAR	ΔK_{FE}	80	80	80	80
GUN AND PROVISIONS	ΔK_{FE}	420	420	420	420
FIXED EQUIPMENT		(7540)	(7510)	(7510)	(7510)
WEIGHT EMPTY		32960	31040	29990	29970
CREW	ΔK_{UL}	400	400	400	400
CREW PROVISIONS	ΔK_{UL}	40	40	40	40
OIL & TRAPPED OIL	W_{OIL}	190	190	170	170
UNAVAILABLE FUEL	W_{UNFU}	190	190	190	190
PAYLOAD PROVISIONS	ΔK_{UL}	110	110	110	110
NON-EXP USEFUL LOAD		(930)	(930)	(910)	(910)
OPERATING WEIGHT		33890	31970	30900	30880
PAYLOAD (INCL EXP PEN AIDS)		2540	2540	2540	2540
FUEL-WING		5000	5000	5000	5000
FUEL-BODY		8570	10490	11560	11580
MAX TO GROSS WEIGHT		50000	50000	50000	50000
BASIC FLIGHT DESIGN WT.		38210	38210	38210	38210
FULL INTERNAL FUEL (EST.)		18500	18500	18500	18500
DESIGN LANDING WEIGHT		36360	36360	36360	36360

Table 1-XVI: Group Weight Statements for ESIP Fighter/Bomber (Concluded)

-11	-11A	-12	-13	-14	-14A	-14B	-14C	-15
F1.4	V1.7	F0.8	F0.8	F0.8	V1.7	GE-4	GE-3	F0.8
4150	4150	4150	4150	4150	4150	4150	4150	4150
420	410	250	270	300	410	290	290	760
730	760	640	530	530	530	570	600	620
6670	6500	6250	6600	5960	5350	6560	6650	6270
1380	1380	1670	1760	1470	1360	1470	1470	2220
330	250	330	330	330	250	270	220	330
1540	1900	1410	1580	1540	1803	1460	1830	1290
(15220)	(15350)	(14700)	(15220)	(14280)	(13920)	(14770)	(15210)	(15640)
6970	7550	7190	7190	7190	7550	8710	8670	7190
170	170	170	170	170	170	170	170	170
1290	1280	1320	1270	1280	1260	1290	1290	1270
380	380	380	380	380	380	380	380	380
800	800	800	800	800	800	800	800	800
2490	2490	2490	2490	2490	2490	2490	2490	2490
490	490	490	490	490	490	490	490	490
800	800	800	800	800	800	800	800	800
590	590	590	590	590	590	590	590	590
80	80	80	80	80	80	80	80	80
420	420	420	420	420	420	420	420	420
(7510)	(7500)	(7540)	(7490)	(7500)	(7480)	(7510)	(7510)	(7490)
29700	30400	29430	29900	28970	28910	30990	31390	30320
400	400	400	400	400	400	400	400	400
40	40	40	40	40	40	40	40	40
190	200	170	170	170	200	200	210	170
190	190	190	190	190	190	190	190	190
110	110	110	110	110	110	110	110	110
(930)	(940)	(910)	(910)	(910)	(940)	(940)	(950)	(910)
30630	31340	30340	30810	29880	29850	31930	32340	31230
2540	2540	2540	2540	2540	2540	2540	2540	2540
5000	5000	5000	5000	5000	5000	5000	5000	5000
11830	11120	12120	11650	12580	12610	10530	10120	11230
50000	50000	50000	50000	50000	50000	50000	50000	50000
38210	38210	38210	38210	38210	38210	38210	38210	38210
18500	18500	18500	18500	18500	18500	18500	18500	18500
36360	36360	36360	36360	36360	36360	36360	36360	36360

These methods have been used to predict the operating weight of 41 existing military and commercial airplanes within ±10% of measured weight.

1.2.15.5 Afterbody Drag Estimates

Afterbody drag estimates used in the Phase II analyses were mapped in terms of gross body maximum cross-sectional area, A_{10}; nozzle exit area, A_9; and Mach number. The maps were derived from estimates made by Boeing at Levels I and II and the subcontracting engine companies at Level I. The Level I estimates are based, in part, on test data gathered on blown models of side-by-side twin engine installations. Little supersonic test data supports the Level I estimates. Level II, subsonic estimates are based on correlations of a large amount of Phase I parametric test data. No test data supports the supersonic afterbody drag levels used with the subsonic Level II estimates.

A comparison of subsonic and supersonic reference afterbody drag levels, calculated at Level I for several of the Phase II configurations, is illustrated in Figure 1-74.

1.2.16 Conclusions

The Phase II development simulation concluded with identification of three candidate engine cycles and an afterbody arrangement with which the engines might be properly integrated. All three of the engines are high temperature, advanced technology turbofan cycles. Two of these were supplied by Pratt & Whitney Aircraft, and the third was provided by General Electric. The Pratt & Whitney engines were a conventionally shaped, mixed flow fan and a characteristically short, separate flow, variable geometry turbine with both fan and core flow augmentation. The General Electric engine was also a short, separate flow design. However, it used a fixed geometry turbine and fan flow augmentation only. Figure 1-75 summarizes the ESIP engine optimization results.

The best afterbody arrangement of those examined in Phase II used a structural ring or single cowl to support both engines, the horizontal tail surfaces, and a single vertical fin. A base area separated the engines at the end of the body. Isolation of this design depended solely on its basic drag/structural weight relationship. Installed propulsion system characteristics do not appear to affect the relative merit relationships between afterbody arrangements.

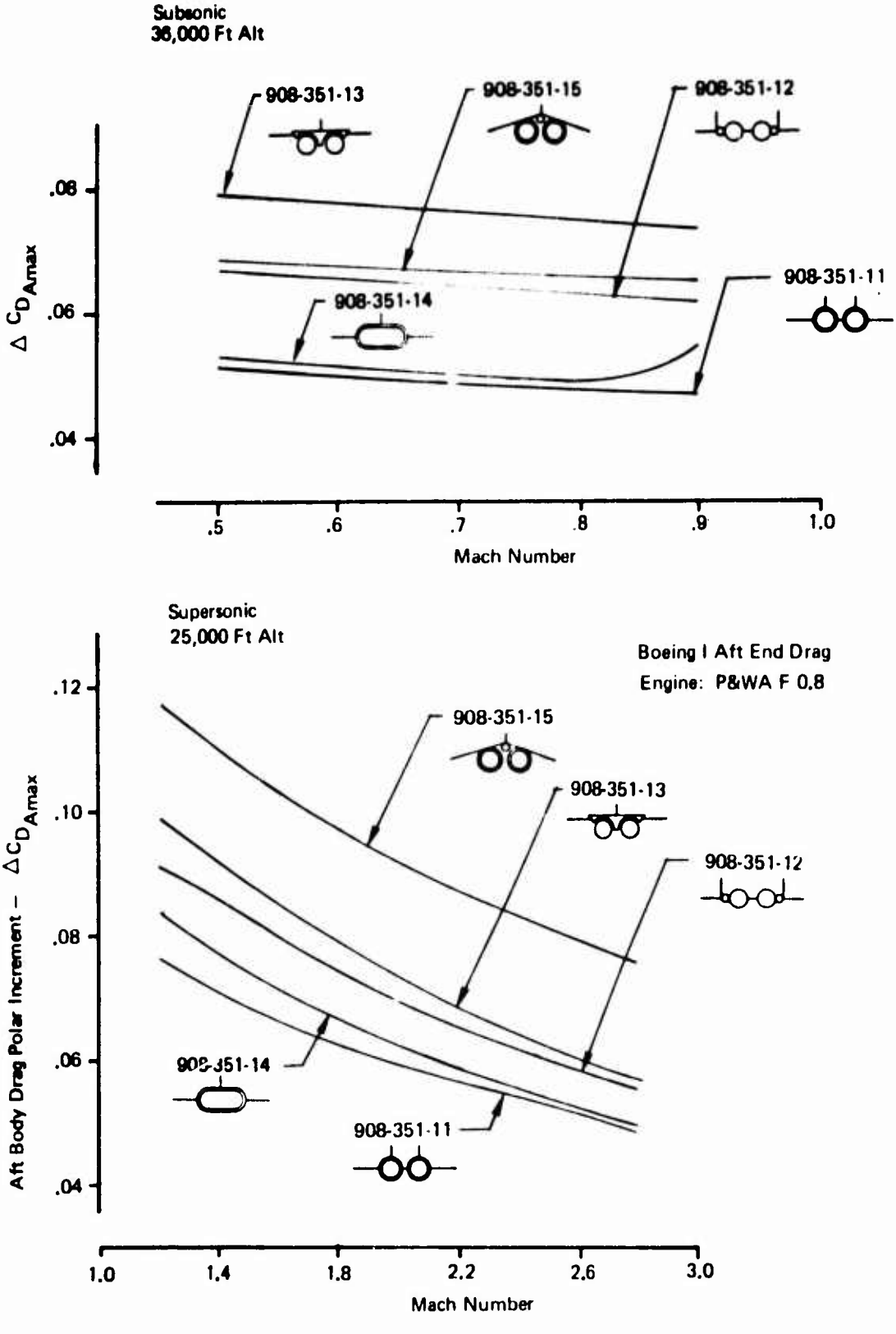

Figure 1-74: Optimum Derivative Airplane Non-Throttle Dependent Aft Body Drag Comparison

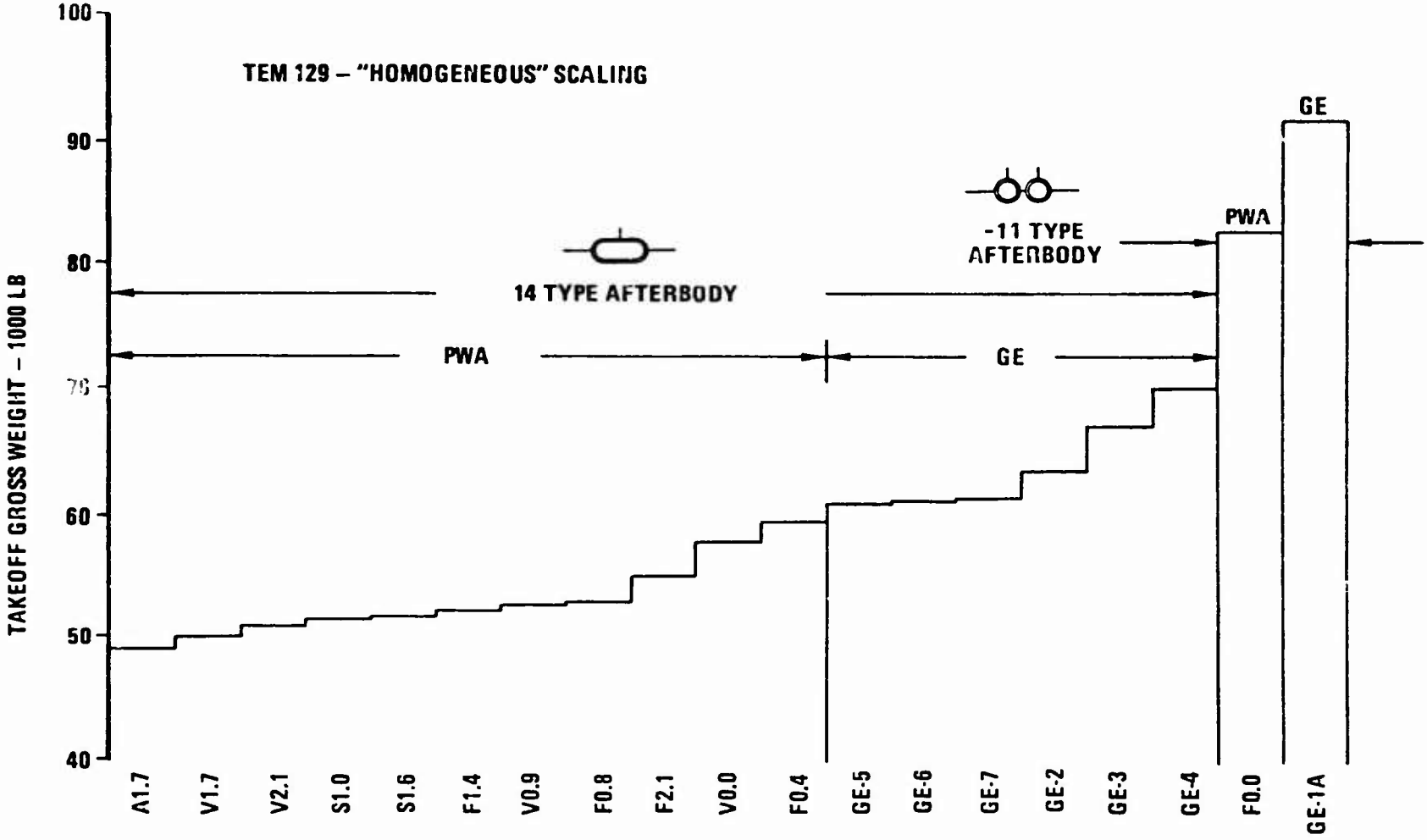

Figure 1-75: ESIP Engine Optimization

A new analytical integration technique was used to positively identify optimum engine/airframe combinations at Level I. Development of the new methodology was directed by early Phase II results. The later analytical processes lent additional realism to engine/airplane matching and allowed a greater degree of freedom in optimization of an engine/airframe combination. The fuselage length of a few engine/airframe combinations was adjusted to optimize structural weight/drag relationships in the final stages of Phase II.

Configurations were investigated with afterbody drags estimated at three levels of validity. Both Boeing and the subcontracting engine companies made Level I estimates. Boeing also made subsonic afterbody drag estimates at Level II using correlations of Phase I parametric afterbody test data.

Phase II development simulation engine/airframe matching was insensitive to the differences in subsonic afterbody drag level estimated at Levels I and II. This result is felt to be due to (1) the low levels of afterbody drag estimated for the fighter/bomber, and (2) insensitivity of fighter/bomber performance to afterbody drag for the specified mission requirements.

Substantial amounts of manual and analytical system integration, engine company/airframer data exchange and element and system performance analysis led to final definition of optimum engine/airframe combinations for the fighter/bomber. Development simulation results also led to identification of good combinations of engines and airframes for Phase II/III test models. Artist's concepts of these configurations are presented in Figures 1-76, 1-77, and 1-78.

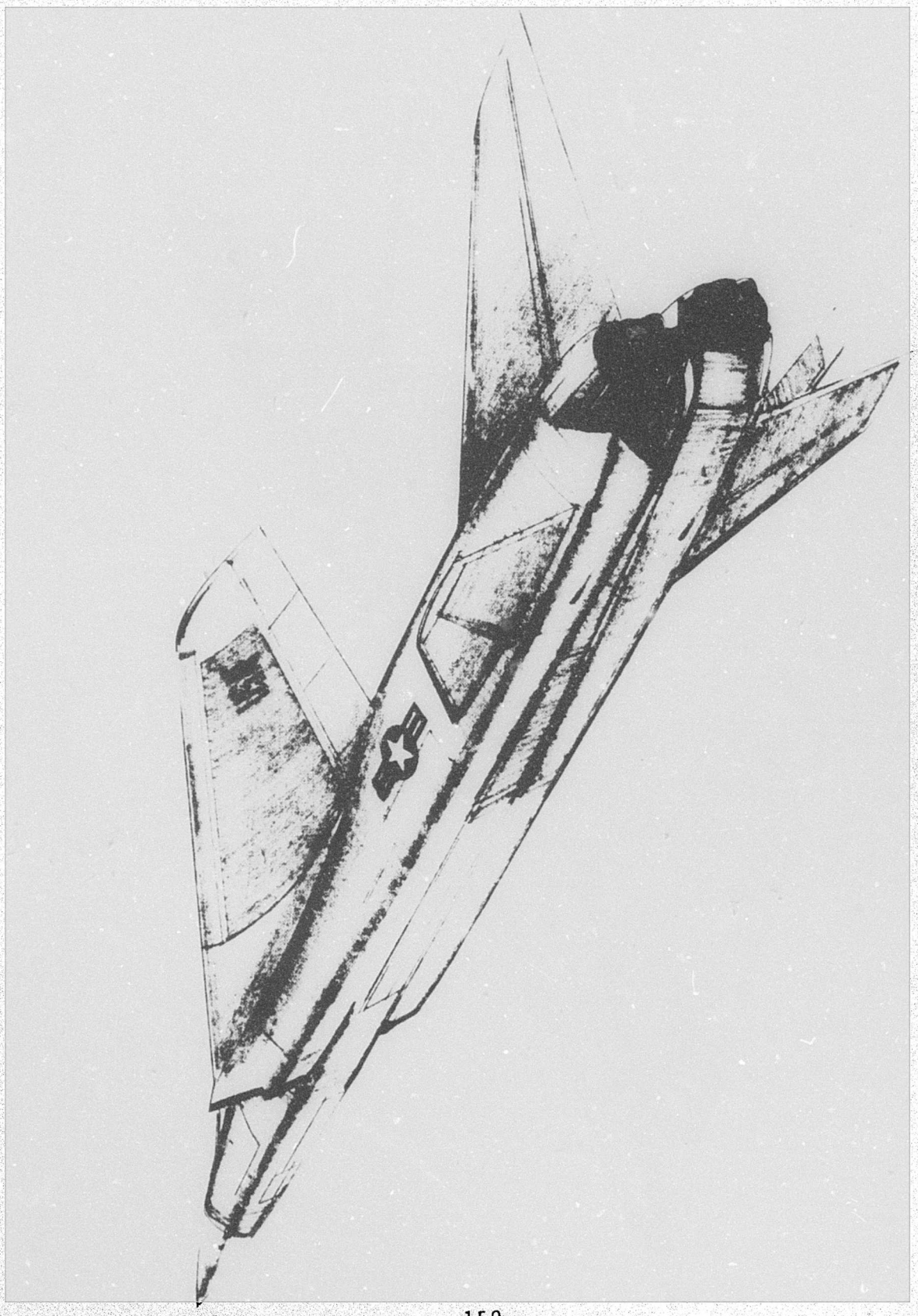

Figure 1-75: Single Vertical Base

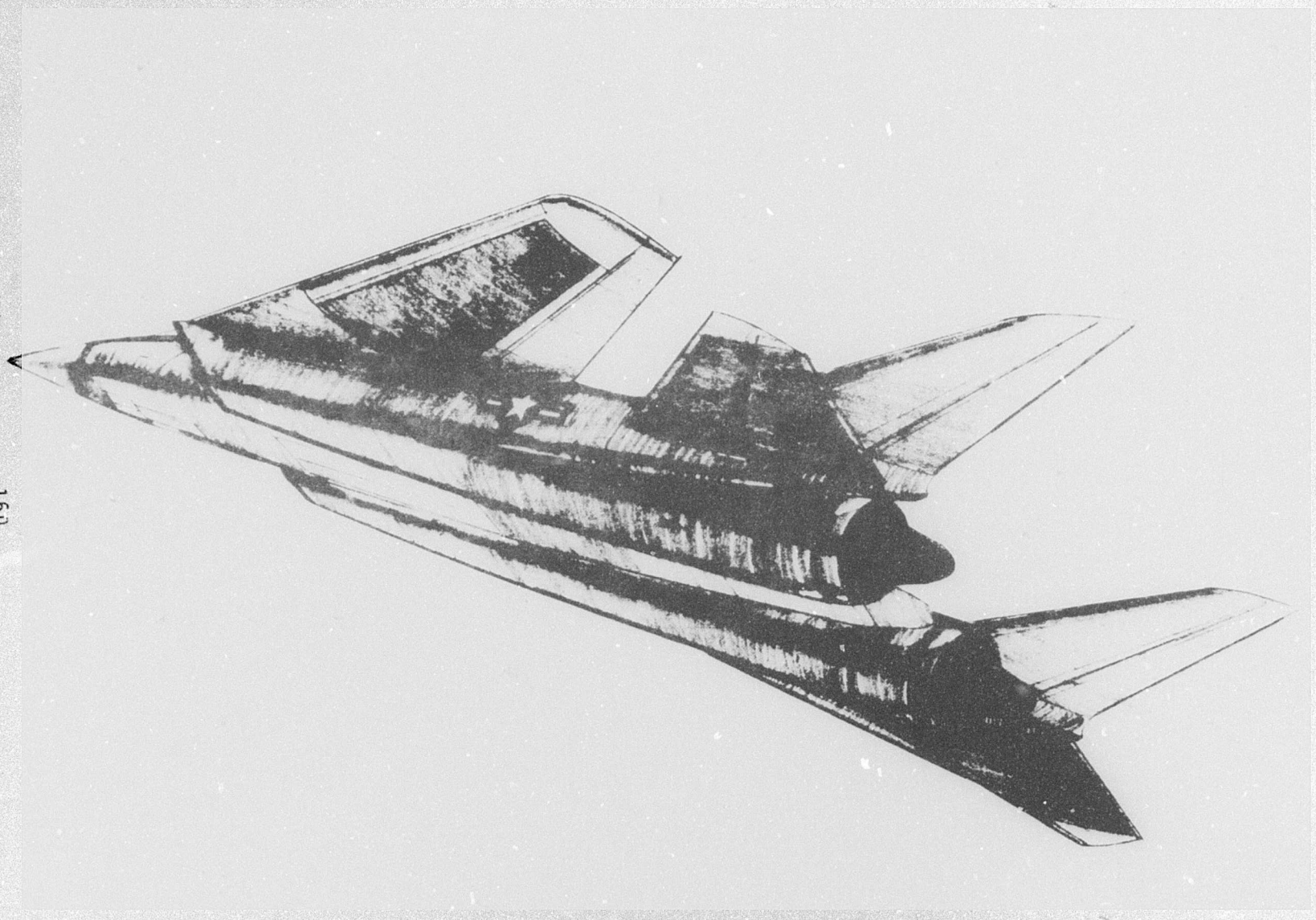

Figure 1-77: Twin Vertical Booms

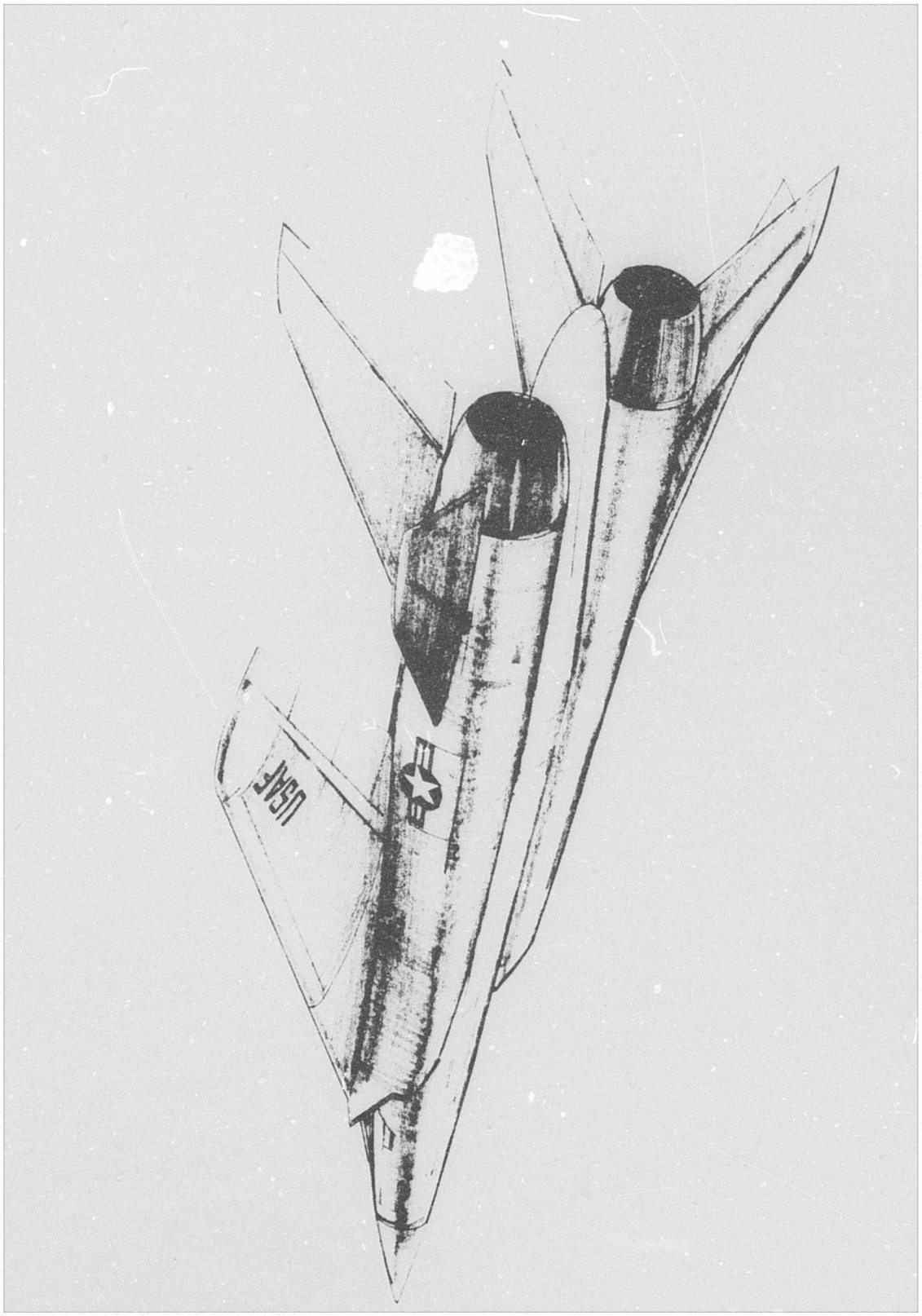

Figure 1-78: Twin Vertical Nacelle